NOVEL METALLO-ORGANIC CORROSION INHIBITORS FOR MILD STEEL AND ALUMINUM ALLOYS IN AQUEOUS SOLUTIONS AND SOL-GEL COATINGS

By

VOLKAN CICEK

Bachelor of Science in Chemistry
Bogazici University
Istanbul, Turkey
2001

Submitted to the Faculty of the
Graduate College of the
Oklahoma State University
In partial fulfillment of
The requirements for
The degree of
DOCTOR OF PHILOSOPHY
July, 2008

NOVEL METALLO-ORGANIC CORROSION INHIBITORS FOR MILD STEEL AND ALUMINUM ALLOYS IN AQUEOUS SOLUTIONS AND SOL-GEL COATINGS

Dissertation Approved:

_____Dr. Allen Apblett_____

Dissertation Adviser

_____Dr. Nicholas Materer_____

_____Dr. LeGrande Slaughter_____

_____Dr. Martin High_____

_____Dr. A. Gordon Emslie_____

Dean of the Graduate College

ACKNOWLEDGEMENTS

I would like to express my sincere appreciation and gratefulness to my dissertation advisor, Dr. Allen W. Apblett for his guidance, motivation, financial support, and inspiration. His valuable advice, criticism, and encouragement have greatly helped me in the materialization of this dissertation. I have benefited much from his broad range of knowledge, and his scientific approach.

My deep appreciation extends to my committee members, Dr. Nicholas Materer, Dr. LeGrande Slaughter, and Dr. Martin High, for their extensive assistance, valuable advice, gracious guidance, and constructive comments throughout the years.

I am deeply grateful to my colleagues, all former and present members of Dr. Apblett's research group, for their valuable discussions, support, continuous encouragement, and for all the help they extended during the course of my study.

I am also thankful to Department of Chemistry at Oklahoma State University for their financial support and help throughout my graduate education.

Thanks are also due to my father, my mom, my sister, my relatives, and friends for their moral support, and encouragement throughout the years.

Finally, I am deeply indebted to my wife, Mine Cicek, for her unconditional love, patience, care, and sacrifice. Your moral support during this time was invaluable to me.

THANK YOU ALL

TABLE OF CONTENTS

CHAPTER **PAGE**

CHAPTER **PAGE**

CHAPTER **PAGE**

CHAPTER **PAGE**

CHAPTER **PAGE**

CHAPTER **PAGE**

CHAPTER **PAGE**

CHAPTER **PAGE**

LIST OF TABLES

TABLE **PAGE**

LIST OF FIGURES

FIGURE **PAGE**

FIGURE **PAGE**

FIGURE **PAGE**

FIGURE **PAGE**

FIGURE **PAGE**

FIGURE **PAGE**

FIGURE **PAGE**

FIGURE **PAGE**

FIGURE **PAGE**

FIGURE **PAGE**

FIGURE **PAGE**

CHAPTER I

1. INTRODUCTION

1.1 Corrosion and Its Definition

According to American Society for Testing and Materials corrosion glossary, corrosion is defined as "the chemical or electrochemical reaction between a material, usually a metal, and its environment that produces a deterioration of the material and its properties".[1]

Other definitions include Fontana's description that corrosion is the extractive metallurgy in reverse[2], which is expected since metals thermodynamically are less stable in their elemental forms than in their compound forms as ores. Fontana states that it is not possible to reverse fundamental laws of thermodynamics to avoid corrosion process, however he also states that much can be done to reduce its rate to acceptable levels as long as it is done in an environmentally safe and cost-effective manner.

In today's world, a stronger demand for corrosion knowledge arises due to several reasons. Among them the application of new materials requires extensive information concerning corrosion behavior of t\hese particular materials. Also the corrosivity of water and atmosphere have increased due to pollution and acidification caused by industrial

production. The trend in technology to produce stronger materials with decreasing size makes it relatively more expensive to add a corrosion allowance to thickness. Particularly in application where accurate dimensions are required widespread use of welding due to developing construction sector has increased the number of corrosion problems.[3] Developments in other sectors such as off shore oil and gas extraction, nuclear power production, and medicinal health have also required stricter rules and control. More specifically, reduced allowance of chromate based corrosion inhibitors due to their toxicity constitutes one of the major motivations of this study to replace chromate inhibitors with the environmentally benign and efficient ones.

1.2 The Corrosion Process and Affecting Factors

There are four basic requirements for corrosion to occur. Among them is the *anode*, where dissolution of metal occurs generating metal ions and electrons. These electrons generated at the anode travel to the cathode via an *electronic path* through the metal and eventually they are used up at the *cathode* for the reduction of positively charged ions. These positively charged ions move from the anode to the cathode by an *ionic current path*. Thus, the current flows from the anode to the cathode by an ionic current path and from the cathode to the anode by an electronic path, thereby completing the associated electrical circuit. Anode and cathode reactions occur simultaneously and at the same rate for this electrical circuit to function.[4] The rate of anode and cathode reactions, that is the corrosion rate is defined by American Society for Testing and Materials as material loss per area unit and time unit.[1]

In addition to the four essentials for corrosion to occur; there are secondary factors affecting the outcome of the corrosion reaction, among them there is temperature, pH, associated fluid dynamics, concentrations of dissolved oxygen, and dissolved salt. Based on pH of the media, for instance, several different cathodic reactions are possible. The most common ones are:

Hydrogen evolution in acid solutions,

$$2H^+ + 2e^- \longrightarrow H_2 \qquad \text{(Eq. 1.1)}$$

Oxygen reduction in acid solutions,

$$O_2 + 4H^+ 4e^- \longrightarrow 2H_2O \qquad \text{(Eq. 1.2)}$$

Hydrogen evolution in neutral or basic solutions,

$$2H_2O + 2e^- \longrightarrow H_2 + 2OH^- \qquad \text{(Eq. 1.3)}$$

Oxygen reduction in neutral or basic solutions,

$$O_2 + 2H_2O + 4e^- \longrightarrow 4OH^- \qquad \text{(Eq. 1.4)}$$

The metal oxidation is also a complex process, and includes hydration of resulted metal cations among other subsequent reactions.

$$M^0 \longrightarrow M^{n+} + ne^-, \qquad \text{(Eq. 1.5)}$$

In terms of pH conditions, near neutral conditions are chosen as the media for the purposes of this study, therefore hydrogen evolution and oxygen reduction reactions in acidic conditions will not be considered within the scope of this research. And among

cathode reactions in neutral or basic solutions, oxygen reduction is the primary cathodic reaction due to the difference in electrode potentials. Thus, oxygen supply to the system, in which corrosion takes place, is of utmost importance for the outcome of corrosion reaction. In addition to choosing neutral pH conditions, inhibitors are tested in stagnant solutions, thus effects of varying fluid dynamics on corrosion are ruled out. Weight-loss tests are performed at ambient conditions, thus effects of temperature and dissolved oxygen amounts are not tested, while for salt-fog chamber tests, temperature is increased for accelerated corrosion testing of sol-gel coated Al 2024 alloy samples. For both weight-loss tests and salt fog chamber tests, however, dissolved salt concentrations were kept high for accelerated testing to be possible.

Despite the fact that dissolved oxygen was not a tested parameter in this study, when corrosion products such as hydroxides are deposited on a metal surface, a reduction in oxygen supply occurs since the oxygen has to diffuse through deposits. Since the rate of metal dissolution is equal to the rate of oxygen reduction, a limited supply and limited reduction rate of oxygen will also reduce the corrosion rate. In this case the corrosion is said to be under cathodic control.[5] In other cases corrosion products form a dense and continuous surface film of oxide closely related to the crystalline structure of metal. Films of this type prevent primarily the conduction of metal ions from metal-oxide interface to the oxide-liquid interface, resulting in a corrosion reaction that is under anodic control.[5] When this happens, passivation occurs and metal is referred as a passivated metal. Passivation is typical for stainless steels and aluminum.

1.3 Corrosion Types Based on Mechanism

Brief definitions of major types of corrosion will be given in this section in the order of commonalities and importance of these corrosion types for the metal alloys investigated in this study, which are mild steel, Aluminum 2024, 6061, and 7075 alloys.

1.3.1 Uniform Corrosion

Uniform corrosion occurs when corrosion is quite evenly distributed over the surface leading to a relatively uniform thickness reduction.[6-7] Metals without a significant passivation tendency in the actual environment, such as iron, are liable to this form. Uniform corrosion is assumed to be the most common form of corrosion and responsible for most of the material loss.[6] However it is not a dangerous form of corrosion because prediction of thickness reduction rate can be done by means of simple tests.[7] Therefore, corresponding corrosion allowance can be added, taking into account strength requirements and lifetime.

1.3.2 Pitting Corrosion

Pitting corrosion is one of the most observed corrosion types for aluminum and steel and it is the most troublesome one in near neutral pH conditions with corrosive anions such as Cl^-, or SO_4^{2-} present in the media.[8-11] It is characterized by narrow pits with a radius of equal or less magnitude than the depth. Pitting is initiated by adsorption of aggressive anions such as halides and sulfates that penetrate through the passive film at irregularities in the oxide structure to the metal-oxide interface. It is not clear why the breakdown event occurs locally.[9] In the highly disordered structure of a metal surface,

aggressive anions enhance dissolution of the passivating oxide. Also, absorption of halide ions causes a strong increase of ion conductivity in the oxide film so that the metal ions from the metal surface can migrate through the film.

Thus, locally high concentrations of aggressive anions along with low solution pH values strongly favor the process of pitting initiation. In time, local thinning of the passive layer leads to its complete breakdown, which results in the formation of a pit. Pits can grow from a few nanometers to the micrometer range. In the propogation stage, metal cations from the dissolution reaction diffuse towards the mouth of the pit or crevice (in the case of crevice corrosion) where they react with OH^- ions produced by the cathodic reaction, forming metal hydroxide deposits that may cover the pit to a varying extent. Corrosion products covering the pits facilitate faster corrosion because they prevent exchange of the interior and the exterior electrolytes leading to very acidic and aggressive conditions in the pit.[9-11] Stainless steels have high resistance to initation of pitting. Therefore rather few pits are formed, but when a pit has been formed it may grow very fast due to large cathodic areas and a thin oxide film that has considerable electrical conductance.[12] Conversely for several aluminum alloys, pit initiation can be accepted under many circumstances. This is so because numerous pits are formed, and the oxide is insulating and has therefore low cathodic activity, thus corrosion rate is under cathodic control. However, if the cathodic reaction can occur on a different metal because of galvanic connection as for deposition of Cu on the aluminum surface, pitting rate may be very high. Therefore the nature of alloying elements is very important.[13]

1.3.3 Crevice Corrosion

Crevice corrosion occurs underneath deposits and in narrow crevices that obstruct oxygen supply.[14-16] This oxygen is initially required for the formation of the passive film and later for repassivation and repair. Crevice corrosion is a localized corrosion concentrated in crevices in which the gap is wide enough for liquid to penetrate into the crevice but too narrow for the liquid to flow. A special form of crevice corrosion that occurs on steel and aluminum beneath a protecting film of metal or phosphate such as in cans exposed to atmosphere is called *filiform corrosion*.[14] Provided that crevice is sufficiently narrow and deep, oxygen is more slowly transported into the crevice than it is consumed inside it. When oxygen has been completely consumed, OH^- can no longer be produced there. Conversely dissolution of the metal inside the crevice continues, driven by the oxygen reduction outside of the crevice. Thus, the concentration of metal ions increase and with missing OH^- production in the crevice, electrical neutrality is maintained by migration of negative ions such as Cl^- into the crevice.[15] This way, an increasing amount of metal chlorides or other metal salts are produced in the crevice. Metal salts react with water and form metal hydroxides, which are deposited, and acids such as hydrochloric acid, which cause a gradual reduction of pH down to values between 0-4 in the crevice, while outside of crevice it is 9-10, where oxygen reduction takes place. This autocatalytic process leads to a critical corrosion state. Since pH has been reduced strongly

$$2H^+ + 2e^- \longrightarrow H_2 \quad [16] \qquad \text{(Eq. 1.1)}$$

reduction of hydronium ions takes place in addition to the primary cathodic reaction of

$$O_2 + 2H_2O + 4e^- \longrightarrow 4OH^-.$$[16] (Eq. 1.4)

1.3.4 Galvanic Corrosion

Galvanic corrosion occurs, when a metallic contact is made between a more noble and a less noble one.[17-19] A necessary condition is that there is also an electrolytic condition between the metals, so that a closed circuit is established. The area ratios between cathode and anode is very important. For instance, if the more noble cathodic metal has a large surface area and the less noble metal has a relatively small area, a large cathodic reaction must be balanced by a correspondingly large anodic reaction concentrated in a small area resulting in a higher anodic reaction rate[17]. This leads to a higher metal dissolution rate or corrosion rate. Therefore, the ratio of cathodic to anodic area should be kept as low as possible. Galvanic corrosion is one of the major practical corrosion problems of aluminum and aluminum alloys[18] since aluminum is thermodynamically more active than most of the other common structural materials, and the passive oxide which protects aluminum may easily be broken down locally when the potential is raised due to contact with a more noble material. This is particularly the case when aluminum and its alloys are exposed in waters containing chlorides or other aggressive species.[19]

The series of standard reduction potentials of various metals can be used to explain the risk of galvanic corrosion; however these potentials express thermodynamic properties, which do not take into account the kinetic aspects.[20] Also, if the potential difference between two metals in a galvanic couple is too large, the more noble metal does not take part in corrosion process with its own ions. Thus, under this condition, the reduction potential of the more noble metal does not play any role. Therefore establishing

a galvanic series for specific conditions becomes crucial. For example a new galvanic series of different materials in seawater at 10 ˚C and at 40 ˚C has been established by University of Delaware Sea Grant Advisory Grant Program[18], and a more detailed one by the Army Missile Command[21]. According to these galvanic series Aluminum 6061-T6 alloy is more active than 7075-T6 alloy, which is more active than 2024-T4 alloy. In this scheme, mild steel ranks lower than the aluminum alloys. This order may be opposite to the order of corrosion affinity in different circumstances such as in the case for aircrafts.[21]

1.3.5 Intergranular Corrosion

Intergranular corrosion is the localized attack with propagation into the material structure with no major corrosion on other parts of the surface.[6,22-25] The main cause of this type of corrosion is the presence of galvanic elements due to differences in concentration of impurities or alloying elements.[6] In most cases, there is a zone of less noble metal at or in the grain boundaries which acts as an anode, while other parts of the surface form the cathode.[22] The area ratio between the cathode and anode is very large and therefore the corrosion rate can be high. The most familiar example of intergranular corrosion is associated with austenitic steels.[23] A special form of intergranular corrosion in aluminum alloys is *exfoliation corrosion*.[24] It is most common in AlCuMg alloys, but also observed in other aluminum alloys with no copper present. Both exfoliation corrosion and other types of intergranular corrosion are efficiently prevented with a coating of a more resistant aluminum alloy such as an alclad alloy or commercially pure aluminum, which is the reason in most modern aircrafts alclad 2024-T3 alloy is used[25].

1.3.6 Selective Corrosion

Selective corrosion or *selective leaching* occurs in alloys in which one element is clearly less noble than the others.[26] As a result of this form of corrosion the less noble metal is removed from the material leading to a porous material with very low strength and ductility. However, regions that are selectively corroded are sometimes covered with corrosion products or other deposits. Thus the component keeps exactly the same shape making the corrosion difficult to discover.[26]

1.3.7 Erosion or Abrasion Corrosion

Erosion or abrasion corrosion occurs when there is a relative movement between a corrosive fluid and a metallic material immersed in it.[6,27] In such cases, the material surface is exposed to mechanical wear leading to metallically clean surfaces, which results in a more active metal. Most sensitive materials are those normally protected by passive oxide layers with inferior strength and adhesion to the substrate, such as lead, copper, steel, and some aluminum alloys. When wearing particles move parallel to the material surface, the corrosion is called *abrasion corrosion.* On the other hand, erosion corrosion occurs when the wearing particles move with an angle to the substrate surface.[27]

1.3.8 Cavitation Corrosion

Cavitation corrosion occurs at fluid dynamic conditions causing large pressure variations due to high velocities, as often is the case for water turbines, propellers, pump

rotors and external surfaces of wet cylinder linings in diesel engines.[6,22-23] While erosion corrosion has a pattern reflecting flow direction, cavitation attacks are deep pits grown perpendicularly to the surface. Pits are often localized close to each other or grown together over smaller or larger areas, making a rough, spongy surface.[23]

1.3.9 Fretting Corrosion

Fretting corrosion occurs at the interface between two closely fitting components when they are subjected to repeated slight relative motion.[23,28] The relative motion may vary from less than a nanometer to several micrometers in amplitude. Vulnerable objects are fits, bolted joints, and other assemblies where the interface is under load.[28]

1.3.10 Stress Corrosion Cracking

Stress Corrosion Cracking is defined as crack formation due simultaneous effects of static tensile strength and corrosion.[23,29] Tensile stress may originate from an external load, centrifugal forces, temperature changes or internal stress induced by cold working, welding or heat treatment. The cracks are normally formed in planes normal to the tensile stress, and they propogate intergranularly or transgranularly and maybe branched.[29]

Corrosion fatigue is crack formation due to varying stresses combined with corrosion.[23,30] This is different from stress corrosion cracking because stress corrosion cracking develops under static stress while corrosion fatigue develops under varying stresses.[30]

1.4 Corrosion Types of Based on the Media

Corrosion types can also be categorized based on what type of environment they take place in. Accordingly, major corrosion types are atmospheric corrosion, corrosion in fresh water, corrosion in seawater, corrosion in soils, corrosion in concrete, and corrosion in the petroleum industry.

1.4.1 Atmospheric Corrosion

Atmospheric corrosion can be categorized further such as atmospheric corrosion in rural or inland areas, in dry environments with little or no pollution, in marine environments on or by the sea with more humidity and salts, in urban areas with pollution due to exhaust and smoke, or in industrial areas with high pollution due to industry smoke and precipitates.[31-33]

In general for atmospheric corrosion, dusts and solid precipitates are hygroscopic and attract moisture from air. Salts can cause high conductivity and carbon particles can lead to a large number of small galvanic elements since they act as efficient cathodes after deposition on the surface.[32-33] The most significant pollutant is SO_2, which forms H_2SO_4 with water.[34-35] Water, that is present as humidity, bonds in molecular form to even the most clean and well-characterized metal surfaces.[32-33] Through the oxygen atom it bonds to the metal surface or to metal clusters and acts as a Lewis base by adsorbing on e^--deficient adsorption sites. Water may also bond in dissociated form, in which case the driving force is the formation of metal-oxygen or metal-hydroxyl bonds. The end products resulting from water adsorption are then hydroxyl and atomic hydrogen groups adsorbed on the substrate surface.[36] Atmospheric corrosion rate is influenced by the

formation and protective ability of the corrosion products formed. The composition of corrosion products depends on participating dissolved metal ions and anions dissolved in the aqueous layer. According to HSAB theory hard metal ions such as Al^{3+} and Fe^{3+} prefer H_2O, OH^-, O^{-2}, SO_4^{-2}, NO_3^-, CO_3^{-2} while intermediate metals such as Fe^{2+}, Zn^{2+}, Ni^{2+}, Cu^{2+}, Pb^{2+} prefer softer bases such as SO_3^{-2} or NO_2^- while soft metals such as Cu^+ or Ag^+ prefer soft bases as R_2S, RSH or RS^-.[34-35]

In the specific case of iron or steel exposed to dry or humid air, a very thin oxide film composed of an inner layer of magnetite (Fe_3O_4) forms, covered by an outer layer of FeOOH (rust).[37-38] Atmospheric corrosion rates for iron are relatively high and exceed those of other structural metals. They range (in μm/year) from 4 to 65 (rural), 26 to 104 (marine), 23 to 71 (urban) and 26 to 175 (industrial).[39]

In the case of aluminum, the metal initially forms a few nm thick layer of aluminum oxide, γ-Al_2O_3, which in humidified air is covered by aluminum oxyhydroxide, γ-AlOOH, eventually resulting in a double-layer structure.[40-42] The probable composition of the outer layer is a mixture of Al_2O_3 and hydrated Al_2O_3, mostly in the form of $Al(OH)_3$. However, the inner layer is mostly composed of Al_2O_3 and small amounts of hydrated aluminum oxide mostly in the form of AlOOH.[43-45] This oxide layer is insoluble in the pH interval of 4 to 9.[46] Lower pH values results in the dissolution of Al^{3+}. Rates of atmospheric corrosion of aluminum outdoors (in μm/year) are substantially lower than for most other structural metals and are from 0.0 to 0.1 (rural), from 0.4 to 0.6 (marine), and ~1 urban.[47,48]

In general, anodic passivity of metals, regardless of type of corrosion, is associated with the formation of a thin oxide film, which isolates the metal surface from

the corrosive environment. Films with semiconducting properties such as Fe, Ni, Cu oxides provide inferior protection compared to metals as Al, which has an insulating oxide layer.[49]

An alternative explanation of differences between oxide films of different metals based on their conducting properties, is the *network-forming* oxide theory in which covalent bonds connect the atoms in a three dimensional structure. Due to nature of covalent bonding, there is short range order on the atomic scale but no long-range order. These networks of oxides can be broken up by the introduction of a *network-modifier*.[50] When a network-modifier is added to a network-forming oxide, they break the covalent bonds in the network introducing ionic bonds, which can change the properties of mixed oxides such as Cu/Cu_2O or Al/Al_2O_3 where rate of diffusion of Cu in Cu_2O is 10000 times larger than Al in Al_2O_3.[51] Depending on single oxide bond strengths, metal oxides can be classified as network formers, intermediates, or modifiers. Network formers tend to have single oxide strengths greater than 75 kcal/mol, intermediates lie between 75 and 50 and modifiers lie below this value.[52-53] Iron is covered by a thin film of cubic oxide of γ-Fe_2O_3/Fe_3O_4 in the passive region. The consensus is that the γ-Fe_2O_3 layer, as a network former, is responsible for passivity while Fe_3O_4, as a network modifier, provides the basis for formation of higher oxidation states but does not directly contribute toward passivity.[54] The most probable reason that iron is more difficult to passivate is that it is not possible to go directly to the passivating species of γ-Fe_2O_3. Instead a lower oxidation state film of Fe_3O_4 is required and this film is highly susceptible to chemical dissolution. Until the conditions are established whereby the Fe_3O_4 phase can exist on the surface for a reasonable period of time, the γ-Fe_2O_3 layer will not form and iron dissolution will

continue.[55-56] Impurities such as water also modify the structure of oxide films. Water acts as a modifying oxide when added to network-forming oxides and thus weakens the structure.[57-58] In conclusion metals, which fall into network-forming or intermediate classes, tend to grow protective oxides, such as Al or Zn. Network formers are non-crystalline, while the intermediates tend to be microcrystalline at low temperatures. The metals, which are in the modifier class, have been observed to grow crystalline oxides, which are thicker and less protective.[59] A partial solution is to alloy the metal with one that forms a network-forming oxide in which the alloying metal tends to oxidize preferentially and segregates to the surface as a glassy oxide film[60]. This protects the alloy from corrosion. For example, the addition of chromium to iron causes the oxide film to change from polycrystalline to noncrystalline as the amount of chromium increases making it possible to produce stainless steel.[61-63]

Alloying is important such that pure Al has a high resistance to atmospheric uniform corrosion, while the aerospace alloy Al 2024, containing 5% Cu among others, is very sensitive to selective aluminum leaching in aqueous environments. It is, on the other hand, less sensitive to pitting. In the case of steel, the addition of chromium as an alloying element substantially decreases the amount of pitting corrosion in addition to other corrosion types.[64]

1.4.2 Corrosion in Water

Second to atmospheric corrosion is corrosion in water. The rate of attack is greatest if water is soft and acidic and the corrosion products form bulky mounds on the surface as in the case of iron.[23] The areas where localized attack is occurring can

seriously reduce the carrying capacity of pipes. In severe cases iron oxide can cause contamination leading to complaints of 'red water'.[65] In seawater the bulk pH is 8 to 8.3, however due to cathodic production of OH^- the pH value at the metal surface increases sufficiently for deposition of $CaCO_3$ and a small extent of $Mg(OH)_2$ together with iron hydroxides. These deposits form a surface layer that reduces oxygen diffusion. Due to this and other corrosion inhibiting compounds as phosphates, boric acid, organic salts that are present the average corrosion rate in seawater is usually less than that in soft fresh water. However the rate is higher than it is for hard waters due their higher Ca and Mg content.[66] An exception occurs when a material is in the splash zone in seawater, where a thin water film exists on the surface a majority of the time that frequently washes away the layer of corrosion deposits resulting in the highest oxygen supply and leading to the highest corrosion rate.[65] In slowly flowing seawater, the corrosion rate of aluminum is 1 to 5 μm/year, whereas for carbon steel it is 100 to 160 μm/year.[67] Additionally, even when the oxygen supply is limited, corrosion can occur in waters where SRB (sulfate-reducing bacteria) are active.[68] Other surface contamination such as oil, mill scale (a surface layer of ferrous oxides of FeO and Fe_2O_3 that forms on steel or iron during hot rolling)[69] or deposits may not increase the overall rate of corrosion, but can lead to pitting and pinhole corrosion in the presence of aggressive anions.[70,71]

Cooling Water Systems

Cooling water systems are employed to expel heat from an extensive variety of applications ranging from large power stations down to a small air conditioning units associated with hospitals and office blocks.[82] Corrosion inhibitors extend the life of these

systems by minimizing corrosion of heat exchange, receiving vessels, and pipework that would otherwise possess a safety risk, reduce plant life and impair process efficiency.[83] Based on the type of system present, that is, either open or closed, once-through or recirculated systems, different amounts and types of corrosion inhibitors are employed. In potable waters for example, since the systems are non-recirculating, use of corrosion inhibitors is limited by toxicity and cost. The inhibitors used must be inexpensive and still can only be added in low quantities. Calcium carbonate, silicates, polyphosphates, phosphate and zinc salts are commonly used inhibitors in potable water. Once-through cooling waters have the similar limitation of cost. Inhibitors with sulfate, silicate, nitrite and molybdate are oftenly used in the closed-water systems, such as steam boiler systems. [84] However, the hardness in the system may precipitate the molybdate, thus resulting in increased inhibitor demand and corrosion of the iron material in the system.[85]

Oil/Petroleum Industry

In oil/petroleum industry, corrosion of steel and other metals is a common problem in gas and oil well equipment, in refining operations, and in pipeline and storage equipment.[73-77] Production tubing that carries oil/gas up from the well has the most corrosion.[78] Petroleum has water and CO_2 in water forms carbonic acid, which in turn forms $FeCO_3$. Deposits of $FeCO_3$ are cathodic relative to steel leading to galvanic and pitting corrosion.[79] Besides water content, the salt content is also similar to seawater and with pressures bigger than 2 bars; oil and gasses become corrosive.[80] High flow rates, high flow temperatures, and H_2S ratio in petroleum are other major factors causing corrosion.[81]

Mine waters

Mine waters occupy a special place in corrosion studies considering their widely varying composition from mine to mine. Because of its low cost, availability, and ease of fabrication, mild steel is widely used as a structural material in mining equipment, although it can experience rapid and catastrophic corrosion failure when in contact with polluted acid mine waters. Specifically in coal mines corrosion is known to be a serious problem.[86]

1.4.3 Corrosion in Soil

Particle size of soils is an important factor on corrosion in addition to the apparent effect of acidity levels. Gravel contains the coarsest and clay contains the finest particles, with 2 mm. diameter for the former and 0.002 mm. diameter for the latter. Sizes of sand and silt are in between gravel and clay. While clay prevents the supply of oxygen but not water, gravels allow oxygen supply as well.[72]

In *concrete*, carbonation of concrete reduces the pH of solution and leads to general breakdown of passivity.[31]

1.5 Nature of Protective Metal Oxide Films

Regardless of the corrosion type, the major product of iron and steel corrosion is FeOOH, which is referred to as rust.[87] Rust can occur in 4 different crystalline modifications based on the type of corrosion and the environment that the corrosion takes

place: α-FeOOH (goethite), β-FeOOH (akaganeite), γ-FeOOH (lepidocrocite), and δ-FeOOH (feroxyhite).[88-89]

α-FeOOH seems to be the most stable modification of the ferric oxide hydroxides. Solubility of α-FeOOH is approximately 10^5 times lower than that of γ-FeOOH. The relative amounts of α-FeOOH and γ-FeOOH depend on the type of atmosphere and the length of exposure.[89] In freshly formed rust in SO_2 polluted atmospheres γ-FeOOH is usually slightly dominant. On prolonged exposure the ratio of γ-FeOOH to α-FeOOH decreases.[90] Also in weakly acidic conditions in general γ-FeOOH is transformed into α-FeOOH depending on the sulfate concentration and temperature.[91] In marine atmospheres, where the surface electrolyte contains chlorides, β-FeOOH is found. β-FeOOH has been shown to contain up to 5% chloride ions by weight in marine locations.[92] δ-FeOOH has not been reported in rust created under atmospheric conditions on carbon steel.[93] Magnetite, Fe_3O_4, may form by oxidation of $Fe(OH)_2$ or intermediate ferrous-ferric species such as green-rust.[94] It may also be formed by reduction of FeOOH in the presence of a limited oxygen supply according to[95]

$$8FeOOH + Fe \longrightarrow 3Fe_3O_4 + 4H_2O \qquad \text{(Eq. 1.6)}$$

The rust layer formed on unalloyed steel generally consists of two regions: an inner region, next to the steel/rust interface often consisting primarily of dense, amorphous FeOOH with some crystalline Fe_3O_4; and an outer region consisting of loose crystalline α-FeOOH and γ-FeOOH.[37-38,96]

Aluminum initially forms a few nm thick layer of aluminum oxide, mainly γ-Al_2O_3 (boehmite), which in humidified air is covered by aluminum oxyhydroxide, γ-

AlOOH due to hydrolysis, resulting in a double-layer structure.[40-42] Related reactions that occur within the passive film when in contact with humidity or water are as follows;

$$Al^{3+} + 3OH^{-} \longrightarrow AlOOH + H_2O \quad \text{(Eq. 1.7)}$$

$$Al_2O_3 + H_2O \longrightarrow 2AlOOH \quad \text{(Eq. 1.8)}$$

$$AlOOH + H_2O \longrightarrow Al(OH)_3 \quad \text{(Eq. 1.9)}$$

The probable composition of the outer layer is a mixture of Al_2O_3 and hydrated Al_2O_3, mostly in the form of amorphous $Al(OH)_3$ or α-$Al(OH)_3$ (bayerite). This outer coating of AlOOH-$Al(OH)_3$ is colloidal and porous with poor corrosion resistance and cohesive properties. The inner layer on the other hand is mostly composed of Al_2O_3 and small amounts of hydrated aluminum oxide mostly in the form of AlOOH. This inner coating of Al_2O_3-AlOOH is continuous, resistant to corrosion and is a good base for paints and lacquers [43-45] Altogether, this passive layer is insoluble in the pH interval of 4 to 9.[46] Lower pH values results in the dissolution of Al^{3+}.[97]

1.6 Effect of Aggressive Anions on Corrosion

Both weight-loss and salt-fog chamber tests in this study have been performed under circumstances, where high salt concentrations were present. For weight-loss tests, high salt concentrations were applied for accelerated corrosion testing purposes in addition to simulating the actual highly corrosive environments such as marine environments, seawater, and industrial areas. In the case of salt-fog chamber tests, chemical stress in accelerated testing primarily refers to chloride containing salts in solution because airborne contaminants are believed to play a very minor role in paint aging.[461] Other chemical stress factors such as UV effect was not tested in this

investigation since any coating, such as a sol-gel coating, can be protected from UV exposure by simply painting over it with a paint that does not transmit light.

Many mechanisms have been proposed for the suppression or acceleration of metallic dissolution by the action of aggressive anions in general.[462,463] The simple most common theory on the accelerated corrosion due to aggressive anions is the concept of competitive adsorption. Aggressive anions, such as Cl^-, compete with adsorption of OH^- or the inhibitor ion depending on pH. Thus, aggressive anions increase the concentrations of inhibitors required to prevent corrosion. This must be taken into account; since the application of less than the adequate inhibitor concentration leads to pitting corrosion.[81] Competitive adsorption of aggressive anions can lead to corrosion in two different ways. Cl^-, for instance, may either cause the initial local breakdown of the passive oxide film or simply interfere with the repassivation process after the film has been broken down locally. In one study, no indication was found that Cl^- is incorporated into the anodic film on iron when the passive oxide film was initially formed in a Cl^- containing solution suggesting that Cl^- ions cause local film thinning by interfering with the film repair.[464-466]

In the case of aluminum adsorbed aggressive anions such as chloride can undergo a chemical reaction with the passive film and produce soluble transient compounds such as $Al(OH)_2Cl$, $AlOHCl_2$, and AlOCl, which are easily dissolved into the solution once they are formed.[12] Similarly, soluble $FeSO_4$ complex forms in presence of another aggressive anion, that is SO_4^{2-}.[10] Thus as a result of these adsorption-dissolution processes, the protective oxide film is thinned locally, small pits are made and the corrosion rate of aluminum is greatly enhanced.[98]

When aggressive anions have to be compared with one another, the stability of the intermediate complexes of substrate metal and aggressive anions must be considered. In the specific case of steel corrosion, if an anion, X^-, is first adsorbed on the steel surface, a surface complex forms in the anodic process, and then the complex is desorbed from the surface[11,467]

$$Fe + X^- \longleftrightarrow (Fe\ X^-)_s \quad \text{(Eq. 1.10)}$$

$$(Fe\ X^-)_s \longleftrightarrow (Fe\ X)_s + e^- \quad \text{(Eq. 1.11)}$$

$$(FeX)_s \longrightarrow FeX^+ + e^- \quad \text{(Eq. 1.12)}$$

$$FeX^+ \longleftrightarrow Fe^{2+} + X^- \quad \text{(Eq. 1.13)}$$

s represents ion or compound at the surface. In general, if the adsorbed anion or the surface complex is stable, the corrosion of steel is suppressed. Therefore, the order of tested anions in terms of the stability of the surface complex based on the corrosion rates would be[467] $ClO_4^- > SO_4^{2-} > Cl^-$

Due to the stability of intermediate complexes between the metal substrate and the aggressive anions, pitting corrosion does not occur for chromium metal. Stability constants of CrX^{2+} complexes are smaller than 1, for instance it is 1 when X is Cl^- and 10^{-5} when it is I^-.[8] In addition, exchange of Cl^- and H_2O ligands between the inner and outer sphere of chromium halide complexes is extremely slow.[8] Together these factors causes insolubility of $CrCl_3$ in cold water due to very low dissolution rate of Cr^{3+}. Therefore the presence of a Cr-Cl complex at the surface will not increase the dissolution rate because it will dissolve very slowly by itself. In the case of Fe^{3+} this exchange is very rapid. Similarly Fe-Cr alloys are more resistant to pitting in Cl^- solution than is pure Fe.

1.7 Corrosion Prevention Methods

With such variety in types of corrosion comes many different prevention methods. Among these is selecting a material which does not corrode in the actual environment. When changing the material is not possible, changing the environment to prevent transport of essential reactants of corrosion often using corrosion inhibitors seems to be the second most reasonable prevention method. Using chemical inhibitors to lower molecular oxygen activity at the metal surface is one example of this type of prevention technique. Also, applying coatings on the metal surface in the form of paint, providing a barrier between the metal surface and the corrosive environment is another very commonly used prevention technique. Other prevention techniques include but are not limited to using special designs to prevent water accumulation on the metal surfaces or changing the potential, which results in a more negative metal and thus prevents transfer of positive metal ions from the metal to the environment.[101]

The objective of the proposed research was the development of novel chemical inhibitors for mild steel and aluminum alloys. Inhibitors that could be employed in water or as a component of a protective coating were targeted. Mild steel alloy was chosen due to the fact that it finds extensive use in various structural applications due to its physical characteristics, such as stiffness and high strength to weight ratios. The aluminum and aluminum alloys are widely used in engineering applications because of their combination of lightness with strength, their high corrosion resistance, their thermal and electrical conductivity, heat and light reflectivity, and their hygienic and non-toxic qualities.[102] In addition to their mechanical properties, the low residual radioactivity is another unique property of aluminum leading to its use as the first wall in thermonuclear

reactors. However the long and safe exploitation of aluminum alloys in nuclear power production greatly depends on its corrosion stability, which is why the type of the alloy and corrosion protection measures is important.[103] This investigation was focused on the 2024, 6061, and 7075 alloys.

1.8 Alloys Used In This Study and Their Properties

The composition of alloying elements of mild steel samples used in this study was 0.02-0.03 % S, 0.03-0.08 % P, 0.4-0.5 % Mn, and 0.1-0.2 % C.

The aluminum alloys are usually divided into two major groups; cast alloys and wrought alloys. While the term wrought aluminum may not be as familiar as wrought iron, it basically refers to aluminum material that is constructed using wrought iron techniques. Essentially, this means that the aluminum is "shaped" to produce the desired material. The term "wrought iron" is slightly ambiguous as it refers not only to the method of construction but also to the type of metal used. In other words, wrought iron is a specific type of iron and also a style of metal work, while wrought aluminum simply refers to the metalworking method-not the type of aluminum. Cast aluminum on the other hand is made from literally pouring molten aluminum into a cast and allowing it to harden. Each wrought and cast aluminum alloy is designated by a four digit number by the Aluminum Association of U.S[104-105] with slight differences between wrought and cast alloys (See Table 1-1). The first digit indicates the alloy group according to the major alloying element. The second digit indicates the modification of the alloy or impurity limits. Original (basic) alloy is designated by “0” as the second digit. Numbers 1…9 indicate various alloy modifications with slight differences in the compositions.

The last two digits identify the aluminum alloy or indicate the alloy purity. In the alloys of the 1xxx series the last two digits indicate the level of purity of the alloy: 1070 or 1170 mean minimum 99.70% of aluminum in the alloys, 1050 or 1250 mean 99.50% of aluminum in the alloys, 1100 or 1200 means a minimum 99.00% of aluminum in the alloys. In all other groups of aluminum alloys (2xxx through 8xxx) the last two digits signify different alloys in the group. For the purposes of this study, only wrought aluminum 2024, 6061, and 7075 alloys are used.

Table 1-1 Designations for alloyed wrought and cast aluminium alloys

Wrought Alloy		**Cast Alloy**	
Name	Major Alloy Element	**Name**	Major Alloy Element
1xxx	More than 99% pure Al	**1xx.x**	More than 99% pure Al
2xxx	Cu, small amount of Mg	**2xx.x**	Cu
3xxx	Mn	**3xx.x**	Si with Cu and/or Mg
4xxx	Si	**4xx.x**	Si
5xxx	Mg	**5xx.x**	Mg
6xxx	Mg, Si	**6xx.x**	Unused
7xxx	Zn, small amount of Cu, Mg, Cr, Zr	**7xx.x**	Zn with Cu and/or Mg
8xxx	Other elements (Li, Ni)	**8xx.x**	Sn

1.8.1 Aluminum 2024 alloy

The 2xxx (aluminum-copper) alloy series started to be used frequently with the development of 24S (2024) in 1933 for maximum solubility of alloying elements in the solid phase. Due to their high strength, toughness, and fatigue resistance, modifications of 24S are widely used today for aircraft applications.[106] However the alloys of these series, in which the copper is major alloying element, are less corrosion resistant than the alloys of other series. Copper increases the efficiency of the cathodic counter reaction of the corrosion such as O_2 and H^+ reduction reaction and, thus, the presence of copper increases the corrosion rate.[107]

1.8.2 Aluminum 7075 Alloy

Alloy 75S (7075), developed during World War II, provided the high-strength capability not available with aluminum-magnesium-copper alloys. This type of alloy contains major additions of Zn, along with Mg or both Mg and Cu. The Cu containing alloys have the highest strength and therefore have been used as construction materials, especially in aircraft applications. The Cu-free alloys, which have good workability, weldability as well as moderate strength, have increased in their applications in automotive industry.[107] The first commercial aluminum-magnesium-silicon alloy (51S) was developed and brought to market by 1921.

1.8.3 Aluminum 6061 Alloy

The introduction of alloy 61S (6061) in 1935 filled the need for medium-strength, heat-treatable products with good corrosion resistance that could be welded or anodized. The corrosion resistance of alloy 6061 even after welding made it popular in early railroad and marine applications. Alloy (62S) 6062, a low-chromium version of similar magnesium and silicon, was introduced in 1947 to provide finer grain size in some cold-worked products. Unlike the harder aluminum-copper alloys, this 61S and 62S alloy series of Al-Mg-Si could be easily fabricated by extrusion, rolling, or forging. These alloys'mechanical properties were adequate (mid 40-45 ksi range) even with a less-than-optimum quench, enabling them to replace mild steel in many markets. The moderate high strength and very good corrosion resistant properties of this alloy series of Al-Mg-Si make them highly suitable in various structural building, marine and machinery applications. The ease of hot working and low quench sensitivity are advantages in forged automotive and truck wheels. Also made from alloy 6061 are structural sheet and tooling plate produced for the flat-rolled products market, extruded structural shapes, rod and bar, tubing, and automotive drive shafts.[108]

Detailed composition of the alloys used in this study is given in Table 1-2;

Despite its inferior corrosion resistant properties, Al 2024 was chosen for this study for both aqueous and sol-gel coating applications due to the characteristics of the binder, that is sol-gel coating, which was designed primarily for Al 2024 in prior research. The reason why the sol-gel coating was initially designed for Al 2024 alloy is due to the fact that it is a peculiar alloy used in the fuselage structures of aircrafts where the corrosion resistance properties are compromised for the sake of mechanical strength.

The nominal composition of Al 2024-T3 alloy is 4.4% Cu, 1.5% Mg, 0.6%Mn, and lesser amounts of Fe, Si, and impurity element allowable.[109-111] The "T3" designation indicates that the alloy was solution-annealed, quenched, and aged at ambient temperatures to a substantially stable condition.[112]

Table 1-2 Chemical Composition of Aluminum Alloys

Composition of Alloys	**2024**	**6061**	**7075**
Al	**91.5-92.8**	**96.8-97.2**	**86.85-89.55**
Cu	**3.8-4.9**	0.15-0.4	1.2-2.0
Mg	1.2-1.8	0.8-1.2	2.1-2.9
Mn	0.3-0.9	≤ 0.15	≤ 0.30
Fe	≤ 0.50	≤ 0.7	≤ 0.50
Si	≤ 0.50	0.4-0.8	≤ 0.40
Zn	≤ 0.25	≤ 0.25	**5.1-6.1**
Zr+Ti	≤ 0.20	-	≤ 0.25
Ti	≤ 0.15	≤ 0.15	≤ 0.20
Cr	≤ 0.10	0.04-0.35	0.18-0.28

It is important to recognize that in most modern aircraft an “alclad” variant of the 2024-T3 is used. Alclad 2024-T3 has a thin layer of commercially pure Al applied to enhance corrosion resistance.[25]

However, alclad layer is easily removed exposing the underlying 2024-T3 core in maintenance operations where grinding-out of cosmetic corrosion surfaces is routine. Thus, corrosion protection of the Al 2024-T3 core then becomes an issue, especially for older aircraft that have experienced many depot maintenance cycles.[113]

1.9 Cost of Corrosion and Use of Corrosion Inhibitors

In a study, entitled “Corrosion Costs and Preventive Strategies in the United States,” conducted from 1999 to 2001 by CC Technologies Laboratories, the total annual estimated direct cost of corrosion in the U.S. is a staggering $276 billion—approximately 3.1% of the nation’s Gross Domestic Product (GDP).[114] This cost includes the application of protective coatings (paint, surface treatment, etc), inspection and repair of corroded surfaces and structures, and disposal of hazardous waste materials. The study reveals that, although corrosion management has improved over the past several decades, the U.S. must find more and better ways to encourage, support, and implement optimal corrosion control practices. Due to reasons such as economics and ease of application, corrosion inhibitors continue to be the most common corrosion prevention technique. Compared to other techniques corrosion inhibitors are very convenient since they can be employed alone or within a protective coating, such as paint. Also, among many developed corrosion inhibitors it is possible to find a working one for any specific demand.[115]

The definition of corrosion inhibitor favored by the National Association of Corrosion Engineers (NACE) is: a substance which retards corrosion when added to an environment in small concentrations.[116] Alternatively, according to the American Society for Testing and Materials Corrosion Glossary, a corrosion inhibitor is defined as a chemical substance or combination of substances that, when present in the proper concentration and forms in the environment, prevents or reduces corrosion.[1]

Available references in corrosion phenomena in the technical literature appeared by the end of the 18th century. The first patent in corrosion inhibition was given to Baldwin, British patent 2327.[117]

Corrosion inhibition is reversible, and a minimum concentration of the inhibiting compound must be present to maintain the inhibiting surface film. Good circulation and the absence of any stagnant areas are necessary to maintain inhibitor concentration.[118]

Inhibitors function in one or more ways to control corrosion; namely by adsorption of a thin film onto the surface of a corroding material, or by inducing the formation of a thick corrosion product, or by changing the characteristics of the environment resulting in reduced aggressiveness. Some remove oxygen in the aqueous media to reduce the cathodic reaction. Though there are lots of chemicals that can function as inhibitors, some may be too expensive and not economical. Chemicals that are toxic or not environmentally friendly are also of limited use. Moreover, inhibitors for one metal may or may not work for another or even may cause corrosion. In addition, the effectiveness of inhibitors is affected by the pH, temperature and water chemistry of the system.[119]

Generally, inhibitors efficient in acid solutions have little or no effect in near-neutral aqueous solutions since in acidic media the main cathodic process is hydrogen evolution, and inhibitor action is due to adsorption on oxide-free metal surfaces.[120] In alkaline conditions, most metals are inclined to be passive, and are protected from most of the corrosion damage.[121] In near-neutral solutions however corrosion processes result in the formation of sparingly soluble surface products such as oxides, hydroxides, salts and cathodic half-reaction is oxygen reduction. Therefore the inhibitor action must be exerted on the oxide-covered surface by increasing or maintaining the protective characteristics of the oxide or surface layers in aggressive solutions.[122-123]

1.10 Types of Corrosion Inhibitors

While there are various inhibitor classifications listed in the literature, there is no completely satisfactory way to categorize. One of the common ways is to classify them according to their reaction at the metal surface.[1, 124]

1. *Anodic inhibitors* reduce the actual rates of the metal dissolution that is the anodic reaction.

2. *Cathodic inhibitors* reduce the rates of the cathodic reactions such as the hydrogen evolution or oxygen reduction reactions.

3. *Mixed inhibitors* retard the anodic and cathodic corrosion processes simultaneously by general adsorption covering the entire surface, sometimes with a polymer.

1.10.1 Anodic Inhibitors

Anodic or passivating inhibitors slow down corrosion by either stabilizing or repassivating the damaged passive film by forming insoluble compounds or by preventing adsorption of aggressive anions via competitive adsorption. They are used in the neutral pH range to treat cooling water systems, cooling system metals, and steel-concrete composites.[125] Passivating inhibitors can be further divided into two types: direct passivating inhibitors which are oxidizers themselves and indirect passivating inhibitors which are non-oxidizers and require the presence of oxygen.[126] Direct passivating inhibitors react with metals directly and become incorporated into the passive film to strengthen it, complete it and repair it.[127] Chromate (CrO_4^{2-}) and nitrites (NO_2^-) are the best oxidizers which can passivate steel in deaerated solutions; however both inhibitors have limited uses due to toxicity.[128] In open systems, oxygen is abundant enough; while in closed systems the addition of oxidizing salts is needed for indirect passivating inhibitiors such as analogues of chromate such as molybdates to function.[129-130] Indirect passivators may develop a protective film in the form of a salt. It is proposed for example that ferrous ions at the solution/metal interface react with molybdate ions to form a complex which is further oxidized to an insulative ferric-molybdate and covers the metal surface with a thin, adherent protective film.[131-132]

1.10.2 Cathodic Inhibitors

Cathodic Inhibitors slow down corrosion by reducing the rate of the cathodic reaction in the corrosion system. They may form precipitates in the cathodic locations to

limit access of the cathodic reaction species, and are also called precipitation inhibitors.[133] Zinc salts are cathodic inhibitors that form precipitates of zinc hydroxide at the cathode.[134] Magnesium salts also work in similar way.[135] Bicarbonate (HCO_3^-) forms insoluble metal carbonates in alkaline solution.[136] Phosphates, the most widely used corrosion inhibitors of steel, precipitate as ferrous and ferric phosphates on the substrate surface.[137] Oxygen scavengers, react with the dissolved oxygen to limit the supply of oxygen for the cathodic reaction. Sodium sulfite is an oxygen scavenger commonly used at room temperatures. It reacts with oxygen to form sulfate. However, since oxygen scavengers remove oxygen only, they are not effective in acidic media.[138] Cathodic poisons make discharges of hydrogen gas difficult.[139] Cathodic inhibitors are generally not as effective as anodic inhibitors (passivators), but on the other hand they are not likely to cause pitting.[140]

As for organic inhibitors, chelating agents, which contain at least two functional polar groups, such as acidic –COOH, -SH or basic $–NH_2$ groups, those able to form coordinate bonds with metal cations are good examples.[141] Gluconate is such a complexing agent with two carboxylic groups and have been extensively studied in this research.

1.11 Chromates: Best Corrosion Inhibitors to Date

Overall, chromates as inhibitors and in chromate conversion coatings as protective coatings continue to be the most efficient corrosion prevention method for the most commonly used metals such as steel, aluminum, zinc, and magnesium among

others. [142] The term conversion coating here refers to the traditional surface passivation treatment for steel and aluminum which produces a layer of corrosion product, by means of dissolution of the base metal through reaction with the passivating solution and precipitation of insoluble compounds, capable of resisting further chemical attack.[115,143] Chromate conversion coatings used for aluminum, typically generated from mixtures of soluble hexavalent chromium salts and chromic acid, participate in oxidation-reduction reactions with aluminum surfaces[144], precipitating a continuous layer of insoluble trivalent compounds.[145] The use of chromate conversion coatings to increase the corrosion resistance and paintability of aluminum alloys can be traced to the early part of the twentieth century.[146] The protection of many aluminum alloys, such as those used in aerospace components, depends heavily on chromates. Of particular interest to the Navy is the use of chromate conversion coatings on aircraft aluminum alloys owing to excellent corrosion resistance and the ability to serve as an effective base for paint. [147-149]

Only films formed in chromate solutions meet the stringent corrosion resistance requirements of the military specifications MIL-C81706.[150] It is estimated that about 100,000 tonnes of aluminum per year in the UK are chromate treated. An anodized film may be substituted for chromate conversion coatings on certain aluminum products but only at greater operating and capital costs.[97]

Among advantages of the chromate conversion coatings are good paint adhesion, low cost, quick and simple application process by immersion, spray, or rolling, the capability to resist forming operations, and excellent corrosion resistance, including a self-healing ability.[151]

Results from exposure corrosion testing show that aluminum surfaces prepared with a chromate conversion coating and a chromate-free primer perform much better than a chromate-free sol-gel type of conversion coating with the same chromate-free primer[152], which gives rise to the second part of this study, the necessity for enriching the sol-gel coating with efficient inhibitors.

1.11.1 Limitations on the Use of Chromates due to Toxicity

The mobility of aqueous Cr^{6+} within biological systems and its reactivity with biochemical oxidation mediators make it both highly toxic and carcinogenic and generally regarded as a very hazardous soil and groundwater pollutant.[102,143,153-156]

More rigid environmental regulations have been introduced about the use of chromates, mandating the elimination of hexavalent chromium as the active ingredient in corrosion inhibition packages for the protection of aluminum-skinned aircraft.[157-158] The harmful effects of chromates on human tissue have been well documented. Dermatitis and skin cancer have been reported among workers merely handling components protected by a chromate film.[97] Many reviews in the literature points out to toxicity of chromates, such an association of Cr^{6+} with lung cancer. Although there is no general agreement on the details for the Cr^{6+} induced damage to DNA resulting in cancers, it is clear that Cr^{6+} is highly water soluble and passes through cell membranes and highly reactive intermediates such as Cr^{5+} stabilized by alpha hydroxyl carboxylates and Cr^{4+} are genotoxic and react either directly or through free radical intermediates to damage DNA.[159-164] Also, adverse toxicity of chromates to aquatic life has always been a

problem. Chromate is quoted on the EU Red List of the EU Dangerous Substances Directive No 76/464/EEC and Groundwater Directive No 80/68/EEC.[81]

National Primary Drinking Water Regulations prepared by EPA (Environmental Protection Agency) states that chromium is a naturally occurring element found as chrome iron ore, primarily as chromite ($FeOCr_2O_3$), in rocks, animals, plants, soil, and in volcanic dust and gases.[165-168] In air, chromium compounds are present mostly as fine dust particles which eventually settle over land and water. Chromium can strongly attach to soil and only a small amount can dissolve in water and move deeper in the soil to underground water. There is also a high potential for accumulation of chromium in aquatic life. [165,167]

Chromium is present in the environment in several different forms. The most common forms are chromium(0), chromium(III), and chromium(VI). No taste or odor is associated with chromium compounds. Chromium(III) occurs naturally in the environment and is an essential nutrient. Chromium(VI) and chromium(0) are generally produced by industrial processes. The metal chromium, which is the chromium(0) form, is used for making steel. Chromium(VI) and chromium(III) are used for chrome plating, dyes and pigments, leather tanning by means of chromic sulfate, wood preserving by means of copper dichromate, treating cooling tower water, magnetic tapes, cement, paper, rubber, composition floor covering, automobile brake lining and catalytic converters and other materials. Smaller amounts are used in drilling muds, textiles, and toner for copying machines. [165-168] Production of the most water soluble forms of chromium, the chromate and dichromates, was in the range of 250,000 tons in 1992. [165,167] The two largest sources of chromium emission in the atmosphere are from the chemical manufacturing industry

and combustion of natural gas, oil, and coal. The following treatment methods have been approved by EPA for removing chromium: Coagulation/Filtration, Ion Exchange, Reverse Osmosis, Lime Softening. [165] From 1987 to 1993, according to the Toxics Release Inventory, chromium compound releases to land and water totaled nearly 200 million pounds. These releases were primarily from industrial organic chemical industries. The largest releases occurred in Texas and North Carolina. The largest direct releases to water occurred in Georgia and Pennsylvania. In 1974, Congress passed the Safe Drinking Water Act Law, which requires EPA to determine safe levels of chemicals in drinking water which do or may cause health problems. [165,167] The MCLG (Maximum Contaminant Level Goal) for chromium has been set at 0.1 ppm (parts per million) because EPA believes this level of protection would not cause any of the potential health problems described below. Based on this MCLG, EPA has set an enforceable standard called a Maximum Contaminant Level (MCL). MCLs are set as close to the MCLGs as possible, considering the ability of public water systems to detect and remove contaminants using suitable treatment technologies. The MCL has also been set at 0.1 ppm because EPA believes, given present technology and resources, this is the lowest level to which water systems can reasonably be required to remove this contaminant should it occur in drinking water. The Reference Concentration (RfC) for chromium (VI) (particulates) is 0.0001 mg/m^3 based on respiratory effects in rats. The Reference Concentration (RfC) for chromium (VI) (chromic acid mists and dissolved Cr (VI) aerosols) is 0.000008 mg/m^3 based on respiratory effects in humans. EPA has not established an RfC for chromium (III). The RfD for chromium (III) is 1.5 mg/kg/d based

on the exposure level at which no effects were observed in rats exposed to chromium (III) in the diet. [165-168]

The general population is exposed to chromate by eating food, drinking water, and inhaling air that contains the chemical. The average daily intake of chromium, generally in the form of chromium(III), from air, water, and food is estimated to be less than 0.2 to 0.4 micrograms (µg), 2.0 µg, and 60 µg, respectively.[166,168]

EPA reports hexavalent chromium to cause shortness of breath, coughing, wheezing(mostly with inhalation of chromium trioxide), and skin irritation or ulceration, when people are exposed to it at levels above the MCL for relatively short periods of time, while damage to circulatory and nerve tissues, stomach upsets and ulcers, convulsions, kidney and liver damage, perforations and ulcerations of the septum, bronchitis, asthma, decreased pulmonary function, pneumonia, skin irritation and even death are potential results of a long-term or a lifetime exposure. Some people are extremely sensitive to chromium(VI) or chromium(III). Allergic reactions consisting of severe redness and swelling of the skin have been noted. Long-term exposure to chromium(VI) has been associated with lung cancer as in the case of workers exposed to levels in air that were 100 to 1,000 times higher than those found in the natural environment. Lung cancer may occur long after exposure to chromium has ended. Limited information on the reproductive effects of chromium (VI) in humans exposed by inhalation suggest that exposure to chromium (VI) may result in complications during pregnancy and childbirth. [165,167]

On the contrary, chromium(III) is an essential nutrient, with a daily intake of 50 to 200 µg/d recommended for adults. This ion helps the body use sugar, protein, and fat. Without chromium(III) in the diet, the body loses its ability to use sugars, proteins, and fat properly, which may result in weight loss or decreased growth, improper function of the nervous system, and a diabetic-like condition. With too much intake, chromium (III) can also cause health problems but is considered about 100 to 1000 times less toxic than chromium (VI). Although each form can be converted to the other form under certain conditions, chromium (III) is not oxidized to chromium (VI) in the natural soil environment. [166,168]

Cr(III) compounds are one of the major candidates to replace chromium(VI) based corrosion inhibitors and protective coatings if the required corrosion resistance and adhesion of organic coatings can be obtained.[153] Thus, Cr(III) compounds were investigated in this project as chromate replacements. Cr(III) is not an oxidizing agent but it will form the mixed oxides/hydroxides with the substrate in the presence of a primary passivator/oxidizing agent such as dissolved oxygen. When a primary oxidizing agent is present, the substrate can oxidize to its higher oxidation state cations producing hydroxide and the existing Cr(III) ions can react with the produced hydroxides to form a conversion coating composed of mixed oxides/hydroxides of the substrate and Cr(III).[97] The metal, chromium(0), is less common and does not occur naturally. It is not clear how much it affects health, but it is not currently believed to cause a serious health risk.[169]

The International Agency for Research on Cancer (IARC) has determined that chromium(VI) is carcinogenic to humans. IARC has also determined that chromium(0) and chromium(III) compounds are not classifiable as to their carcinogenicity to

humans.[170,171] The World Health Organization (WHO) has determined that chromium(VI) is a human carcinogen.[171] The Department of Health and Human Services (DHHS) has determined that certain chromium(VI) compounds (calcium chromate, chromium trioxide, lead chromate, strontium chromate, and zinc chromate) are known human carcinogens.[172] Finally, the EPA has classified chromium (VI) as a Group A, known human carcinogen by the inhalation route of exposure.[165-168, 173-176]

In the light of given negative effects of hexavalent chromium compounds, stricter environmental regulations have already mandated their removal from water and general waste effluents, and have mandated their near term removal from corrosion inhibiting packages used for the protection of aluminum-skinned aircraft.[149,157,177-180] Strict regulations already exist for chromate residues which require the use of expensive effluent treatments to achieve the desired residual concentrations by precipitating hexavalent chromium compounds.[97,181] Despite their negative aspects, to date, no replacements exist in the market for carcinogenic chromates with the same efficiency for a range of aluminum alloys and steel, neither as pigment, nor as a metal pretreatment.[110,182]

For perhaps the last 20+ years, a considerable effort has focused on discovering nonchromate corrosion-inhibiting compounds for protection of aluminum alloys. A number of reviews focusing on this subject alone have been written in the past several years.[183,184,185]

Given the toxicity and carcinogenity of chromates; the purpose of this study is not only to synthesize *efficient corrosion inhibitors* for certain alloys of certain metals to be applied in different environments, but also to find *environmentally friendly corrosion*

inhibitors for successful chromate replacements. In this regard, the standard for an environmentally friendly inhibitor is considered as having acceptable or no toxicity compared to chromate inhibitors. Studying the reasons underlying the success of chromate inhibitiors seems as the first reasonable approach one might take before formulating chromate replacements.

1.11.2 Corrosion Inhibition Mechanism of Chromates

Chromates are very effective inhibitors of Fe, Al, Cu, Zn corrosion. The unique chemical and electronic properties of the oxo-compounds of chromium give rise to a unique ability to inhibit corrosion in ferrous and nonferrous materials.[186] They are both anodic and cathodic inhibitors due to their abilities to form precipitates with the dissolving metal ions such as iron, aluminum, and zinc ions, at anodic sites and by reducing to trivalent chromium to form composite inert compounds at cathodic sites.[187] The tetrahedral, d^0, hexavalent Cr^{6+} oxoanion compounds of chromium, which are chromate, dichromate, bichromate, and chromic acid, dissolve as stable and mobile complexes in water. Thus, they are easily transported to sites of localized corrosion where they are reduced to very stable, kinetically inert refractory oxide compounds of Cr^{3+}.[188] These octahedral, trivalent, d^3, compounds of Cr^{3+} are irreversibly adsorb at metal and metal oxide surfaces to form a protective film of a near monolayer thickness.[189] As one of these irreversibly adsorbed compounds, $Cr(OH)_3$ provides a good, hydrophobic barrier with good adhesion properties.[190] The concentration of the transported or leached chromate is sufficient to be active as an inhibitor for the metal under the paint, at defects or at cut edges. These hexavalent oxoanion compounds of chromium also have optimum

solubilities enabling them to be used as efficient paint pigments, in which blistering of the paint does not occur.[147] Also, possibly the most crucial property of the barrier film of trivalent chromium compounds is its ability to store Cr^{6+} oxoanions that can be slowly released into a solution when attacked by aggressive anions. These released Cr^{6+} oxoanions can migrate to and interact at defects to interrupt corrosion, which gives rise to the unique "self-healing" ability of chromate conversion coatings in general. There is a good agreement that chromate conversion coatings not only contain but also release hexavalent chromium to repair defects and damage of the conversion coating.[190-199]

Specifically for aluminum corrosion; released Cr^{6+} oxoanions inhibit pit initiation by adsorbing onto aluminum oxides, thereby discouraging adsorption of anions such as chloride and sulfate, which promote dissolution and destabilization of the protective oxides.[200-201] Thus, competitive adsorption of chromates with regard to aggressive anions such as chloride and sulfate appears as another major property of chromate conversion coatings.[202]

Along with nitrites, chromates passivate independent of dissolved oxygen in contrast to molybdates and vanadates, which require the presence of dissolved oxygen as a primary passivator.[203]

In general, following steps of reactions occur;[204]

$$Cr^{6+} \longrightarrow Cr^{3+} + 3H_2O \longrightarrow Cr(OH)_3 + 3H^+ \longrightarrow Cr_2O_3.3H_2O \qquad \text{(Eq. 1.14)}$$

The hydrolysis reactions generate H^+, which are consumed by redox reactions.

In alkaline conditions,[205]

$$CrO_4^{2-} + 4H_2O + 3e^- \longrightarrow Cr(OH)_3 + 5OH^- \qquad \text{(Eq. 1.15)}$$

In case of iron corrosion in near neutral conditions,[206]

$$6FeO + 2CrO_4^{2-} + 2H_2O \longrightarrow Cr_2O_3 + 2Fe_2O_3 + 4OH^- \quad \text{(Eq. 1.16)}$$

Mixed chromium/iron hydroxides also form such as,[207]

$$3Fe^{2+} + HCrO_4^{2-} + 8H_2O \longrightarrow Fe_3Cr(OH)_{12} + 5H^+ \quad \text{(Eq. 1.17)}$$

In contrast to nitrites, molybdates, vanadates and other inhibitors, chromates are also effective in moderately acidic conditions. In an acidic medium, CrO_4^{2-} converts to $Cr_2O_7^{2-}$, which is a very strong oxidant, according to

$$Cr_2O_7^{2-} + 14H^+ + 6e^- \longrightarrow 2Cr^{3+} + 7H_2O, \quad \text{(Eq. 1.18)}$$[208]

The following reaction takes place with the metal substrates[209]

$$6/n\ M^0 + Cr_2O_7^{2-} + 7H^+ \longrightarrow 6/n\ M^{n+} + 2Cr^{3+} + 7H_2O \quad \text{(Eq. 1.19)}$$

where M^0 can be Al, Fe, Zn.

For the specific case of chromium conversion coating formation on Al, the following overall formation reactions are given;[210,211]

$$Cr_2O_7^{2-} + 2Al + 2H^+ + H_2O \longrightarrow CrOOH + 2AlOOH \quad \text{(Eq. 1.20)}$$

or[212]

$$Cr_2O_7^{2-} + 2Al + 2H^+ + 2H_2O \longrightarrow 2Cr(OH)_3 + Al_2O_3 \quad \text{(Eq. 1.21)}$$

The chromate conversion coating process is aided by fluoride, which prevents rapid passivation of the Al surface, thus allowing Cr^{6+} to Cr^{3+} reduction and is also aided by ferricyanide, which functions as a mediator between Al oxidation and chromate reduction and accelerates the redox reaction.[213]

As a result of these multiple redox reactions, while hexavalent chromium(VI) is reduced to its lower oxidation state oxides and hydroxides, the substrate metal is oxidized to its oxides and hydroxides. The pH also rises to the point where trivalent chromium and other oxide/hydroxide compounds are insoluble.[214] Consequently, a protective conversion

coating of adherent composite oxide/hydroxides[215] form with the general formula of M_2O_3/Cr_2O_3 and/or $M(OH)_3/Cr(OH)_3$, where M^0 = Fe, Al.[216]

Another reason for protective ability of chromium oxide and hydroxide film over aluminum surfaces is their stability over a wider range of pH. Based on Pourbaix-diagrams, the approximate stability limit of the Al oxide is at pH 9, while it is up to pH 15 for chromium (III) oxide.[217]

1.12 Chromate Inhibitor Replacements:Current and Potential Applications

Given some basic information about the corrosion inhibition mechanisms of chromates; many studies have been conducted for chromate replacements. For effective replacement of hexavalent Cr, however, an inhibitor has to inhibit the oxygen reduction reaction as well as anodic dissolution/pitting and several studies indicate that hybrid formulations seem to be the best way to do just that. Typically, in these hybrid formulations an organic oxygen reduction reaction inhibitor is included with environmentally benign anodic inhibiting anions.

1.12.1 Nitrites

Another commonly used inhibitor that passivates independent of dissolved oxygen is nitrites. Nitrites are the established inhibitors for rusting machinery tooling, and workpieces, and are often used with alkanolamines. However, like chromates they are also being replaced because of the risk of carcinogenic nitrosamine formation.[218]

Nitrites' MCL (Maximum Contaminant Level) and MCLG (Maximum Contaminant Level Goal) limits have been determined as 1 mg/L each by EPA (Environmental Protection Agency). Infants below the age of six who drink water containing nitrite in excess of the MCL could become seriously ill and, if untreated, may die. Symptoms include shortness of breath and blue-baby syndrome. Major nitrite sources are listed as runoffs from fertilizer uses, leaches from septic tanks, and sewages.[219]

1.12.2 Trivalent Chromium Compounds

Cr(III) compounds arise as one of the potential replacements for Cr(VI) compounds given its much lower toxicity. Cr(III) is not an oxidizing agent but it will form the mixed oxides/hydroxides with the substrate. Therefore, in the presence of a primary passivator/oxidizing agent such as dissolved oxygen, the substrate can oxidize to its higher oxidation state cations producing hydroxide and the existing Cr(III) ions would react with the produced hydroxides to form a conversion coating composed of mixed oxides/hydroxides of the substrate and Cr(III).[149,220-221] Despite this there are limited successful applications of trivalent chromium coatings. The corrosion resistance of trivalent chromium coatings was found considerably less effective than that of hexavalent chromium conversion coatings, as significant concentrations of localized pitting were observed after a 168-hr salt spray test.[179] Thus, rather than using trivalent chromium coatings alone, incorporation of corrosion inhibitors based on trivalent chromium compounds into coatings that have better mechanical properties seems to be a more reasonable prevention method.

Formation of trivalent chromium hydroxides is based on their ability to form coordination compounds of coordination number six. The hydrolysis of coordination complexes is accelerated by addition of alkali and the hydroxides may form successively in the following manner;[222]

$$[Cr(H_2O)_6]Cl_3 \longrightarrow [Cr(OH)(H_2O)_5]Cl_2 + HCl \quad \text{(Eq. 1.22)}$$

$$[Cr(OH)(H_2O)_5]Cl_2 \longrightarrow [Cr(OH)_2(H_2O)_4]Cl + HCl \quad \text{(Eq. 1.23)}$$

$$[Cr(OH)_2(H_2O)_4]Cl \longrightarrow [Cr(OH)_3(H_2O)_3] + HCl \quad \text{(Eq. 1.24)}$$

These species can polymerize as shown in eq. 1.25.

$$2[Cr(OH)(H_2O)_5]Cl_2 \longrightarrow [(H_2O)_4Cr\begin{matrix}OH\\OH\end{matrix}Cr(H_2O)_4]Cl_4 + 2H_2O \quad \text{(Eq. 1.25)}$$

One concern is that Cr(III) and Al(III) compounds are both capable of forming octahedral complexes and the introduction of these ions into an aqueous electrolyte will interfere with conversion of the hydrous alumina into the aluminum hydroxide film by bonding to the active film sites. Therefore, similar to their application in hexavalent chromate conversion coatings, flouride ions are used to remove aluminum oxide and hydroxide films on the substrate surface before forming trivalent chromium conversion coatings.[223]

$$Al_2O_3 + 12F^- + 3H_2O \longrightarrow 2AlF_6^{3-} + 6OH^- \quad \text{(Eq. 1.26)}$$

1.12.3 Oxyanions Analogous to Chromate

Other likely candidates to replace chromates are reducible hypervalent transition metals similar to chromium, which are compounds of Mo, V, Mn, and Tc. The high-

valent oxoanions of these elements exist in aqueous solution and they reduce to form insoluble oxides, which exhibit high resistance to dissolution in an alkaline environment in the same way as Cr.[224-227] Other anodic inhibitors might include oxo-compounds of P and B as well.[228] Among these analogous metals, however, the oxoanion of hypervalent Mn, permanganate, is thermodynamically unstable with respect to the oxidation of water unless the solution is sufficiently alkaline and all technecium isotopes are radioactive.[229-230] Vanadium oxide is relatively more stable toward high pH and Mo oxide is stable toward lower pH values.[231] Solely as oxides, the elements of Mo and V will never give the same stability as seen in analogous Cr^{3+} oxide.[232] On the other hand, the oxo-compounds of these elements can form very stable polyoxometallates with each other, or phosphates and tungstates, providing significant inhibition for aluminum corrosion, particularly when combined with other compounds.[233-234]

The inhibition mechanism of aluminum corrosion by molybdates, vanadates and similar oxyanions is primarily due to the competitive adsorption of these anions with aggressive anions such as chloride and sulfate anions. As a result of adsorption of oxyanions in the place of aggressive anions, oxygen bridged complexes with the metal substrates form. Such complexes were found in catalyst systems such as MoO_3 + Al_2O_3 and WO_3 + Al_2O_3.[235-239] These compounds are expected to have a low solubility in the electrolyte hindering the dissolution of the passive film and retarding pit initiation and propogation of pitting corrosion.

Oxides of heavier elements such as Nb, Hf, Ti, Zr, and Ta are very stable in their highest oxidation state. The mechanism for rare-earth inhibition seems to originate from the alkaline precipitation of protective oxide films at active cathodes. However, soluble

and mobile precursors of these oxides remain difficult to stabilize in aqueous solution with the slight exception of Ce, which is the only lanthanide element that exhibits a tetravalent oxidation state that is stable as a complex in aqueous solution.[335-336] Ce^{4+} behaves somewhat like Cr^{6+}. The reduction product, Ce^{3+}, however, is not nearly as stable as compared to Cr^{3+}.[337]

Molybdates

The molybdates have been the most investigated metal oxyanion analogues. Although Mo compounds are not totally harmless they are rapidly excreted by the body.[240] Unlike many other transition metals, molybdenum has been described as having an extremely low or even negligible toxicity.[241] In a review it is stated that in spite of considerable use of molybdenum in industry, no incidences have been reported yet due to industrial poisoning by molybdenum.[242] Molybdenum compounds are listed in the lowest potentially carcinogenic category.[243-245]

The most recent TLV (Threshold Limit Value) published by the American Conference of Government Industrial Hygienists 1984-1985 show the time-weighted average TLV for soluble molybdenum particulates to be 5 mg/m^3 and for insoluble particulates to be 10 mg/m^3. For comparison, the TLV for total particulates in the nuisance dust category is 10 mg/m^3.[246] Molybdenum has long been identified as a micronutrient essential to plant life,[247-248] and as playing a major biochemical role in animal health as a constituent of several important enzyme systems.[249-250] Several studies have indicated that molybdenum-deficient diets may be associated with the incidence of various forms of cancer.[251-255]

From an environmental perspective, five statutes, and their associated regulations, govern the use and disposal of chemicals within the United States. These are Safe Drinking Water Act,[256] the Resource Conservation and Recovery Act (RCRA), [257] the Clean Water Act (CWA), [258] the Comprehensive Environmental Response Liability Act, [259] and the Toxic Substances Control Act (TSCA). [260] Molydenum is not a regulated parameter under any of these statutes. The TSCA requires all existing chemical substances be registered. Sodium molybdate has been assigned the Chemical Abstract Service number of 7631-95-0 for instance but has not been selected for toxicity testing. Under RCRA, molybdenum is neither listed as a hazardous waste nor a hazardous constituent. Section 311 of the CWA lists 299 substances as hazardous if spilled in waterways, no molybdenum compound is included. In summary, sodium molybdate and other molybdates are free of accompanying toxic elements or compounds; and exhibit an environmental compatibility within the framework of their commercial utilization as a corrosion inhibitor.

Furthermore, molybdate inhibitors are recommended by the UK Health and Safety Executive Guideline (HSG70) as part of a complete water treatment program designed to minimize the risk of infecting cooling systems with the pathogen Legionella Pneumophila.[81]

Molybdenum (Mo) occurs naturally in various ores; the principal source being molybdenite (MoS_2). Molybdenum compounds are used primarily in the production of metal alloys. Molybdenum is also considered an essential trace element with the provisional recommended dietary intake of 75-250 µg/day for adults and older children (NRC, 1989).[261] There is no information available on the acute or subchronic oral toxicity

of molybdenum in humans. Subchronic and chronic Reference Concentrations (RfC) for molybdenum are not available. Information on the inhalation toxicity of molybdenum in humans following acute and subchronic exposures is also not available. The chronic oral Reference Dose (RfD) for molybdenum and molybdenum compounds is 0.005 mg/kg/day, based on biochemical indices in humans (U.S. EPA, 1992). The subchronic RfD is also 0.005 mg/kg/day (U.S. EPA, 1992). Molybdenum is placed in EPA Group D, not classifiable as to carcinogenicity in humans (U.S. EPA, 1990).[261]

Corrosion-inhibiting behavior was first attributed to the molybdates in 1939.[262] First they were used as pigments;[263]and in a wide variety of applications as corrosion inhibitors.[264-275, 285-298] Specifically, they are utilized in alcohol-water antifreezes to protect automobile cooling systems from corrosion since 1939.[283-284] Molybdate allows the partial[276-278], or in complex formulations, the complete replacement of nitrite.[279-281] In addition to being efficient, molybdate inhibitior replacements for nitrites and others were found to be cost effective.[282] Typically, a molybdenum concentration of 50-150 ppm is maintained in the closed cooling water systems and the pH level is maintained within the range of 9.0-10.5.[299-302] Even with concentrations insufficient to produce a layer, Mo(VI) is effective in improving the barrier properties of oxide or other films.[103-303]

In addition to the general competitive adsorption of oxyanion analogues with those of aggressive anions as in the case of chromates, the protective effect for steel by MoO_4^{2-} may also be due to oxygen atoms produced via the reduction of the Mo^{6+} to Mo^{4+} (or MoO_2) during film formation,

$$MoO_4^{2-} \longrightarrow MoO_2 + 2O^- \qquad \text{(Eq. 1.27)}$$

These oxygen atoms interfere with the ability of Cl^- like anions to reach the metal/film interface. The formation of MoO_2 in neutral medium is predicted by the Pourbaix diagram for Mo [304]. Also, the inhibitive nature of molybdate anions may be due to the formation of a thin film of molybdate in a range of reducible valency states, resulting in a passivating effect at anodic sites on the metal surface like other oxyanion analogues of chromate. [305]

In the case of molydate assisted inhibition of aluminum corrosion, it is believed that a layer of boehmite, $Al_2O_3.H_2O$, is formed on the surface of the aluminum specimen accompanied by a closure of the cavities with the alkali molybdate that is adsorbed on the surface. The oxidation state of molybdenum on the aluminum surface greatly depends on the type of molybdate that is used. It is Mo^{4+} when simple MoO_4^{2-} is used, and it is Mo^{5+} when polymolybdates are used.[306] Other theories on molybdate inhibition in the literature are widely available.[310]

Vanadates

Vanadium is a metallic element that occurs in six oxidation states and numerous inorganic compounds. Some of the more important compounds are vanadium pentoxide (V_2O_5), sodium metavanadate ($NaVO_3$), sodium orthovanadate (Na_3VO_4), vanadyl sulfate ($VOSO_4$), and ammonium vanadate (NH_4VO_3). Vanadium is used primarily as an alloying agent in steels and non-ferrous metals (ATSDR, 1990).[364] Vanadium compounds are also used as catalysts and in chemical, ceramic or specialty applications. An inhalation reference concentration has not been derived for vanadium or its compounds (U.S. EPA, 1992).[364] There is no information available on the acute or subchronic oral toxicity of vanadium in humans. Subchronic and chronic Reference Concentrations (RfC)

for vanadium are not available. Reference Doses (RfD) for chronic oral exposures are: 0.007 mg/kg/day for vanadium; 0.009 mg/kg/day for vanadium pentoxide; 0.02 mg/kg/day for vanadyl sulfate; and 0.001 mg/kg/day for sodium metavanadate (U.S. EPA, 1987, 1991a,b). The subchronic RfDs for these compounds are the same as the chronic RfDs, except for sodium metavanadate, which is 0.01 mg/kg/day (U.S. EPA, 1987, 1991a,b). There is little evidence that vanadium or vanadium compounds are reproductive toxins or teratogens. There is also no evidence that any vanadium compound is carcinogenic; however, very few adequate studies are available for evaluation. Vanadium has not been classified as to carcinogenicity by the U.S. EPA (1991a).[364]

Like molybdates and other oxyanion analogues of chromates, the inhibitive action of monovanadate anions are attributed to their competitive adsorption on the metal surface, the formation of an adsorbed layer on the oxide film, and the formation of a highly insoluble salt with dissolved metal ions which prevents the penetration of Cl^- ions and consequently decreases the rate of corrosion.[81]

It is proposed that vanadates undergo a reduction to a four-valent state upon incorporation into the surface coating of aluminum similar to MnO_2, and MoO_2.[365] Therefore, the protective ability of the four-valent oxides is a pure barrier protection, while hexavalent state compounds work as passivators.

Salts of Polyhydroxycarboxylic Acids

Non-toxic organic chemicals that are efficient as corrosion inhibitors include sodium, calcium and zinc salts of polyhydroxycarboxylic acids. The gluconic acid

derivatives were found to hinder general corrosion of carbon steel in near neutral media.[180] Many studies have been carried out on the use and the mechanism of action of sodium, calcium, zinc and borogluconates as corrosion inhibitors for metals, particularly for carbon steel in the neutral environment.[340-357] In other studies gluconate salts were tested as non-toxic environmentally friendly inhibitors to replace the currently used inhibitors in cooling water systems.[358-362] There are other applications of gluconates in addition to cooling waters, such as their use to improve the corrosion resistance of medical instruments in sterilizing solutions[363] and structures in marine environments[66] Calcium and zinc gluconates are used as dietary supplements and as first-aid treatments while iron gluconate is used for the treatment of iron deficiencies. However, zinc appears on the list of Environmental Protection Agency as a pollutant, but the permissible content in potable water, declared by the WHO (World Health Organization) is 5.0 mg/L as opposed to 0.1 mg/L of hexavalent chromium.[366]

Since it is listed as a secondary pollutant of drinking water some basic information about its uses and toxicity levels are produced herein. Zinc is used primarily in galvanized metals and metal alloys, but zinc compounds also have wide commercial applications as chemical intermediates, catalysts, pigments, vulcanization activators and accelerators in the rubber industry, UV stabilizers, and supplements in animal feeds and fertilizers. They are also used in rayon manufacture, smoke bombs, soldering fluxes, mordants for printing and dyeing, wood preservatives, mildew inhibitors, deodorants, antiseptics, astringents, and as rodenticides (Lloyd, 1984; ATSDR, 1989). [367] Zinc is an essential element with recommended daily allowances ranging from 5 mg for infants to 15 mg for adult males (NRC, 1989). In some medical treatment it is recommended 50 mg

of zinc to be taken per day as zinc gluconate.[181] The upper limit of zinc in drinking waters is given as 5 mg/L. An inhalation reference concentration has not been derived for zinc or zinc compounds (U.S. EPA, 1992). There is no information available on the acute or subchronic oral toxicity of zinc in humans. Subchronic and chronic Reference Concentrations (RfC) for zinc are not available. The currently accepted RfD for both subchronic and chronic exposures is 0.2 mg/kg/day based on clinical data demonstrating zinc-induced copper deficiency and anemia in patients taking zinc sulfate for the treatment of sickle cell anemia (U.S. EPA, 1992). No case studies or epidemiologic evidence has been presented to suggest that zinc is carcinogenic in humans by the oral or inhalation route (U.S. EPA, 1991a). Zinc is placed in weight-of-evidence Group D, not classifiable as to human carcinogenicity due to inadequate evidence in humans and animals (U.S. EPA, 1991a).[367]

1.12.4 Synergistic Use of Oxyanions Analogues of Chromate

Despite many similarities, oxyanion analogues of chromate are not strong oxidants like chromate and only in the presence of a primary passivator can they inhibit corrosion as anodic inhibitors. Therefore, their combined use with those of synergistic constituents in formulations seems to be a reasonable approach for obtaining sufficient efficiency for replacement of chromates.[368-371] Among synergistic constituents, cathodic inhibitors are synergists of molybdate inhibition.[311] In neutral or alkaline solutions, these cations can interrupt the cathodic reaction of the corrosion process by forming an adherent, insoluble oxide, hydroxide or carbonate film, which is not provided by the oxyanion analogues of chromate. Zn^{2+} most efficiently synergizes molybdate inhibition

of steel in aerated, neutral and alkaline cooling tower water.[312] Ca^{2+}, another cathodic inhibitor usually present as hardness in cooling water, significantly increased the corrosion protection of steel already synergistically inhibited with MoO_4^{2-}-Zn^{2+}.[311,313] An amount of 10% of calcium or zinc gluconate was found to considerably reduce the amount of molybdate required for the same inhibition effect as observed in molybdate alone.[180] In a comparative study it was found that permanganate increased the corrosion resistance more than molybdate and molybdate more than cerium(III) nitrate for 6061-T6. However, the order was opposite for 2024-T3.[338-339] Many examples of inhibitors that are synergistic with oxyanion analogues of chromate for the protection of ferrous and nonferrous metals are available in the literature.[314-334]

1.13 Sol-Gels (Ormosils): Properties and Uses

As mentioned earlier, conversion coatings are applied to metal surfaces to promote both adhesion of organic finishes such as paints and for corrosion protection of the metal substrate. As an alternative to chromate conversion coatings, sol-gel processing grew out of the ceramics field. In this method, soluble metal salts and/or metal organic materials are used to produce a wide variety of mixed metal oxide and metal-oxide-organic composites.[372-375] It is proposed that the only universal process for treating several Al alloys that is effective in various corrosion environments, is environmentally compliant, are coatings consisting of organofunctional and nonorganofunctional silanes.[109,179,376-382] These coatings are a promising solution for the corrosion protection of aluminum alloys, which is a key requirement for aircraft as the US Air Force extends the

lifetime of its fleet.[383] The downside of epoxy silicate sol-gel coatings when compared to chromate conversion coatings is that the sol-gel films cannot passivate a damaged area.[378]

In 1985, Wilkes et al[384] first reported successful preparation of a new type of organic-inorganic hybrid material by the reaction of TEOS (tetraethyl ortho-silicate) and PDMS (polydimethyl siloxane), which he named "c*eramers*". At approximately the same time, Schmidt independently reported the successful preparation of new organic-inorganic hybrid materials which he termed "*ormosils*" (organically bonded or modified silicates).[385] Ormosils are hybrid organic-inorganic materials formed through the hydrolysis and condensation of organically modified silanes with traditional alkoxide precursors.[386-387] Later on, after other oxides such as ZrO_2 were also bonded to organic groups, Schmidt has also used the term "*ormocers*".[388]

The sol-gel process, which is mainly based on inorganic polymerization reactions, is a chemical synthesis method initially used for the preparation of inorganic materials such as glasses and ceramics. Instead of using metal alkoxides as the precursor for the sol-gel reaction, alkoxysilanes are used as the only or one of the precursors and the organic groups are introduced into the inorganic network through the silicon-carbon bond in an alkoxysilane.[391,424,434]

One of the attractive features of the sol-gel process is that it enables the preparation of numerous types of new organic-inorganic materials with improved thermal, mechanical, optical, and electrical properties such as host oxide materials which are either impossible or extremely difficult to synthesize by any other process.[384-385,387,389-391] The numerous applications of these materials include scratch and abrasive-resistant hard coatings and special coatings for polymeric materials, metal, and glass

surfaces.[391-402] Specifically for mild steel[403] and aluminum 2024 alloys[387,404] widespread uses of these ormosil materials have been reported.

1.13.1 Types of Sol-Gels

Silanes used for ormosil manufacture are a family of organo-silicon monomers with the general formula R-Si(OR')$_3$, where R is an organofunctional group and R' is usually a methyl or ethyl group. In an aqueous environment, the alkoxy group hydrolyzes to form a silanol R-Si(OH)$_3$, which in turn forms a chemical bond with the hydrated oxide film.[408,415] The other functional group on the silane molecule, R, may bond strongly with the polymer resin base of the paint coating. Introduction of these covalently bonded Si-R groups allows chemical modification of the resulting material's properties. The inorganic components tend to impart durability, scratch resistance, and improved adhesion to the metal substrates, while the organic components contribute to increased flexibility, density, and functional compatibility with organic polymer paint systems.[390]

Precursors, which generally are di- and tri-functional silanes, span a wide range of sizes, chemical reactivities, and functionalities. The use of precursors containing non-hydrolyzable Si-C bonds, such as bifunctional or/and trifunctional alkoxysilanes (R'$_n$Si(OR)$_{4-n}$, n = 1-3, R = alkyl, R' = organic group), allows introduction of organic groups directly bonded to the polymer-like silica network.[385,404,416-419] Trifunctional alkoxysilanes are more commonly used as precursors than other alkoxysilane precursors because a variety of such silanes are commercially available, while bifunctional alkoxysilanes have to be used in the presence of higher functionality precursors in order to form a three-dimensional network.[391,420]

Ormosils can be divided into three categories based on their preparation methods. In type A, the organic such as a dye, is mixed into the sol-gel liquid solution, such as triethanolamine (TEOA) in alcohol. On gelation, the organic is trapped in the porous silica matrix. It is assumed that no chemical reactions have occurred between the two constituents.[420,421] In type B, a porous oxide gel is first formed, in which the porosity and pore size is controlled by heating. An organic solution is then impregnated into the pores of the gel. The organic phase is then solidified via polymerization, and a nanocomposite is formed such as para-methoxy-methamphetamine (PMMA) in silica. Still, no chemical bonds usually exist between the organic and inorganic phases.[420,422] In type C, the organic solution is added to the oxide gel liquid solution but unlike type A, a chemical bond is formed between two phases or the inorganic oxide precursor may already have a chemically bonded organic group, such as $CH_3Si(OCH_3)_3$ prior to the reaction. Types A, B, and C can further be mixed. The most common system in this class of hybrids is that of PDMS (polydimethylsiloxane) and tetraethoxysilane (TEOS). Together, these various types of Ormosils offer a very wide spectrum of chemistry, structures, and applications.[423,425]

1.13.2 Corrosion Inhibition Mechanism of Sol-Gel Coatings

Other than versatile coating formulations and ease of application under normal conditions, ormosil coatings exhibit increased thickness as compared to their inorganic counterparts.[405-406] Thus, sol-gel derived coatings provide good corrosion protection for various metal substrates, such as Fe, Al, and Zn, due to their ability to form a dense barrier to the penetration of water and corrosion initiators to go along with their good

adhesion properties, and chemical interness.[407] It should be noted however, when adsorbed initially, the silane actually is highly hydrophilic. It becomes hydrophobic by loss of water molecules only after the cure of the paint. This hydrophilicity/hydrophobocity dual nature is a unique property of silanes, not shown by any other existing interface modifiers. Interfaces modified by silane perform well even under paints which are poor in terms of permeability, porosity or barrier properties, since the hydrophobic nature of organo-functional groups limits the degree of hydration, and reduces the degree of adhesion loss.[408] The reduction in adhesion of paints on non-silane treated aluminum surfaces after exposure to an aqueous environment is associated with the transformation of the aluminum oxide film beneath the paint coating to a hydrated oxide, which adheres poorly to the aluminum.[409] Thus the silane processes do not require the same high-cost paint systems as chromates do, which is another advantage of these novel treatments.[410-411]

Another important aspect of corrosion protective coatings is that these coatings should be barriers between the coatings and their environment, but no known coating system stops completely the transport of oxygen, water and corrosive ions to the coatings/metal interface.[412,446-452] Therefore, most corrosion control coating systems are at least two-coat systems, sometimes even three-coat systems so that the topcoat layer with its hydrophobic polymer composition has the greatest resistance to UV, and the primer and midcoat adhere to the substrate and each other due to the high crosslink density and wet adhesion properties of the polymers that exist therein. However, the main reason for multiple-layer coating systems overall is the substantial decline in the probability of one defect area overlying another, thus preventing localized corrosion.

Therefore, the same final thickness of coating applied by multiple layers will give a significantly better performance than that of a single layer of this thickness.[383]

Despite the fact that sol-gel coatings do not have the self-healing ability of chromate conversion coatings, they still effectively inhibit certain types of corrosion, such as uniform corrosion, provided that there is no coating failure, since coating failures may lead to excessive pitting corrosion for aluminum alloys in particular.[182] Corrosion resistance behavior of sol-gels is related to the crosslinking of the polysiloxane to the metal alkoxide with the formation of M-O-Si bridges and to the formation of polymetallosiloxane-Al interfacial chemical bonds.[402] Thus it is desirable to improve the chemical interaction between the first monolayer of the coating and the substrate such that electrochemical reactions like the reduction of oxygen are inhibited and bonds may withstand the attack of water and other aggressive species like OH^-.[421,426]

The adsorption of organic compounds on metal substrates is generally achieved by two ways. Organic compounds are either adsorb from the the electrolyte similar to other conventional inhibitors or adsorb onto the metal surface by condensation from the vapor phase similar to that of volatile corrosion inhibitors, such as morpholine, hydrazine or hexylamine salts. With no significant e-transfer between the substrate and the adsorbed molecule, this pure electrostatic adsorption process is called physisorption, which is fast and reversible due to low activation energy.[427,428] However provided that e^- transfer occurs due to orbital overlap between a single pair of electrons of the adsorbed molecule and empty bonds of the solid, physisorption becomes chemisorption, which is highly irreversible. Chemisorption is slower than physisorption and it requires higher activation energy. In contrast to physisorption, it is specific for certain metals. On the other hand,

the inhibitor should have free single e^- pairs, or π-electrons for chemisorptions to occur. Based on Lewis acid-base concept, higher polarizability of the involved heteroatom leads to stronger chemisorption. The inhibitor is then e^--donor and the metal is e^--acceptor in agreement with the soft and hard acid and base theory (HSAB).[429-431]

Silane coupling is adherence of the organosiloxane-modified natural polymer to the aluminum surface in the form of chemisorption. As a result of this coupling, sol-gel derived thin films highly adhere to metal surfaces, which is confirmed by bond strength measurements in the literature.[109] Chemisorption of silanes is provided by their hydrolysis in humid atmospheres to silanols R_4-n$Si(OH)_n$. Following hydrolysis, condensation occurs through reactions between –OH or –COOH groups on the polymer precursor, the silanol groups from organosiloxane side-chains, and hydroxyl species present on the aluminum surface. The hydrolysis of the silane is expected to be the rate-determining step and polymerization begins when hydrolysis is nearly finished.[432] The commonly used silane coupling agents have the structure $X_3Si(CH_2)_nY$, where X represents a group that can hydrolyze, such as methoxy or ethoxy, and Y an organofunctional group such as chlorine, amine, epoxy, or mercapto-substituted alkyl groups. Non-functional silanes are very similar to functional silanes in their structure, except that they have hydrolyzable Si-O-C bonds on both ends, and are better known as cross-linking agents.[110]

1.13.3 Synthesis of Sol-Gels

Synthesis is typically described by two steps; first hydrolysis of metal alkoxides to produce hydroxyl groups, followed by polycondensation of the hydroxyl groups and

residual alkoxyl groups to form a three-dimensional network. These reactions are as follows;[434-442]

Hydrolysis Reactions

$$Si(OR)_4 + H_2O \longleftrightarrow (HO)Si(OR)_3 + ROH \quad \text{(Eq. 1.28)}$$

$$(OH)Si(OR)_3 + H_2O \longleftrightarrow (HO)_2Si(OR)_2 + ROH \quad \text{(Eq. 1.29)}$$

$$(HO)_2Si(OR)_2 + H_2O \longleftrightarrow (HO)_3Si(OR) + ROH \quad \text{(Eq. 1.30)}$$

$$(HO)_3Si(OR) + H_2O \longleftrightarrow Si(OH)_4 + ROH \quad \text{(Eq. 1.31)}$$

General Hydrolysis Reaction:

$$M(OR)_x + xH_2O \longrightarrow M(OH)_x + xROH \quad \text{(Eq. 1.32)}$$

Alcohol Condensation (Alcoxolation)

$$\equiv Si\text{-}OR + HO\text{-}Si\equiv \longleftrightarrow \equiv Si\text{-}O\text{-}Si\equiv + ROH \quad \text{(Eq. 1.33)}$$

Water Condensation (Oxolation)

$$\equiv Si\text{-}OH + HO\text{-}Si\equiv \longleftrightarrow \equiv Si\text{-}O\text{-}Si\equiv + HOH \quad \text{(Eq. 1.34)}$$

General Condensation Reaction:

$$2M(OH)_x \longrightarrow (OH)_{x-1}M\text{-}O\text{-}M(OH)_{x-1} + H_2O \quad \text{(Eq. 1.35)}$$

The hydrolysis rate is high under an acidic environment relative to that of condensation, and acid catalysts promote the development of more linear or polymer-like molecules in the initial stages. In addition to the pH of the reaction, the concentration of reagents and the size of the alkoxy group can also influence the hydrolysis and condensation reactions through a steric or leaving-group stability effect. As a result, species such as tetramethoxysilane (TMOS) tends to be more reactive than tetraethoxysilane (TEOS).[372,388]

Gelation

The condensation reaction leads to the formation of a sol, which can be cast into films, fibers, or blocks and then gelled through continued condensation. The gel phase in sol-gel processing is defined and characterized as a three-dimensional solid "skeleton" enclosing a liquid phase. Both liquid and solid phases are continuous and of colloidal dimensions. The solid phase is typically a condensed polymeric sol where the particles have cross-linked between themselves to form a three-dimensional network. [388]

Drying

When the gelled materials dry, capillary forces cause shrinkage of the flexible skeleton. The skeleton stiffens as it shrinks until the gel can withstand capillary pressures at which point the pores empty leaving a microporous solid xerogel. Gel films can be formed on a substrate by two methods, immersion and non-immersion (spray, dip, spin-on, etc.) Sol-gel based coatings must be designed to contain and deliver soluble non-chrome inhibitors at a rate to maintain effective concentrations in the coating system. [388] Highly organic films do not adhere to the metal surface well, presumably due to the low inorganic content and insufficient concentrations of Si-OH groups to produce covalent Si-O-Al bonds with the underlying metal surface. In addition, high viscosity Ormosils produced using low hydrolysis water content do not flow evenly over the substrate surface, producing differences in texture at regions where gelation occurred. On the other hand, ormosils prepared from high water content do not wet the aluminum surface well due to high surface tension of the mainly aqueous sol, resulting in very thin, unevenly coated films. Therefore, appropriate inorganic/organic ratio and water content are very

important for the formation of good quality, corrosion resistant, barrier films highly adherent to the underlying metal substrate.[443]

1.13.4 Incorporation of Corrosion Inhibitive Pigments into Sol-Gel Coatings

The main protection mechanisms of coatings in general are;[444]

1. Creating a path of extremely high electrical resistance, thus inhibiting anode-cathode reactions.
2. Creating an effective barrier against the corrosion reactants; primarily water and oxygen.
3. Providing an alternative anode for the dissolution process.
4. Passivating the metal surface with soluble pigments.

The first corrosion protection mechanism of organic coatings, that is to create a path of extremely high electrical resistance between anodes and cathodes, is probably the most important one also.[452] This electrical resistance reduces the flow of current available for anode-cathode corrosion reactions. One way to achieve this is to incorporate corrosion protective pigments into the coatings. Inhibitor pigments can increase the electrical resistance in the coating due to their unique physical properties or due to the physical properties of their products they form in the coating.

In addition to the inhibitive pigments, which contain the anodic/cathodic and mixed inhibitor types, those described earlier, there are two more classes of inhibitors commonly incorporated into protective coatings. These two inhibitor pigment types are barrier and sacrificial pigments.

Barrier Pigments

Barrier pigments are chemically inert, flake or plate-like shaped particles, such as MIO (micaceous iron oxide) particles.[453] The term micaceous refers to its particle shape, which is flake-like or lamellar shape. In addition to providing a barrier against diffusion of aggressive species through the coating, barrier pigments also provide mechanical reinforcement to the paint film and when present in the topcoat they can also block ultraviolet light, thus shielding the binder from this destructive form of radiation.[454-455] As a result, barrier pigments can be incorporated into primer, intermediate coat, or topcoat since they are chemically inert and do not react with the metal unlike inhibitive or sacrificial pigments.[454]

Sacrificial Pigments

Sacrificial pigments usually contain zinc in the form of zinc dust in large amounts. When in electrical contact with the steel surface, the zinc film acts as the anode of a large corrosion cell and protects the steel cathode. In other words, znc sacrificially corrodes instead of steel.[456] In addition to sacrificially corroding, zinc dust also provides barrier action due to formation of its insoluble corrosion products.[457-459]

Inhibitive Pigments

Inhibitive pigments are soluble species, such as molybdates or phosphates, which are carried to the metal surface, where they inhibit corrosion by passivating the substrate surface mostly by forming protective films.[453] Solubility and reactivity are critical

parameters for inhibitive pigments with too much of both parameters, coating degradation occur due to blistering and delamination.

Prior to this investigation, a sol-gel coating for Al 2024-T3 alloy has been developed and found successful.[414] Therefore, the purpose of this study has been to enhance the corrosion inhibitive properties of this particular sol-gel coating by incorporating inhibitor pigments into its structure. For the purpose of this study, only inhibitive pigments are put into test, although inhibitive pigments or their reaction products can act like barrier or sacrificial pigments as well.

1.14 References

1. *Terminology Relating to Corrosion and Corrosion Testing*, ASTM (American Society for Testing and Materials) Designation G 15 – 99b (Revised), **2000**, 03.02.
2. Fontana, M.G.; *Corrosion Engineering*, McGraw-Hill, New York, **1986**.
3. Bardal, E.; *Corrosion and Protection*, Springer, **2003**, 2.
4. Davis, J. R.; *Corrosion: Understanding the Basics*, ASM International, **2000**, p.25.
5. Bardal, E.; *Corrosion and Protection*, Springer, **2003**, 6.
6. Fontana, M. G.; Greene, N. D.; *Corrosion Engineering*, New York-Singapore, McGraw-Hill, **1967, 1978, 1986**.
7. Bardal, E.; *Corrosion and Protection*, Springer, **2003**, 92.
8. Kruger, J.; Long, G. G.; Kuriyama, M.; Goldman, A. J.; *Passivity of Metals and Semiconductors*, Elsevier Science Publishers, Amsterdam, **1983**, 163.
9. Strehblow, H. H.; *Mechanisms of Pitting Corrosion in Corrosion Mechanisms in Theory and Practice*, 2nd ed., New York-Basel: Marcel Dekker, **2002**.

10. Pou, T. E.; Murphy, O. J.; Bockris, J. O. M.; Tongson, L. L.; Monkowski, M.; *Proceedings, 9th International Congress on Metallic Corrosion*, Toronto, **1984**, 2, 141.
11. Bertocci, U.; *Advances in Localized Corrosion*, NACE (National Association of Corrosion Engineers), Proceedings of 2nd International Conf. on Localized Corrosion, Orlando, FL, **1987**, 127.
12. Smith, E.; Nabarro, F. R. N. (Ed.); *Dislocations in Solids*, North Holland Publishing Co., New York, **1979**, 4, 365.
13. Kaesche, H.; The Corrosion of Metals; *Physico-Chemical Principles and Actual Problems*, Springer-Verlag, Berlin, **1966**, 374.
14. Combrade, P.; *Crevice Corrosion of Metallic Materials in Corrosion Mechanisms in Theory and Practice*, 2nd ed., New York-Basel: Marcel Dekker, **2002**.
15. Leidheiser, H.; *Coatings in Corrosion Mechanisms*, New York-Basel: Marcel Dekker, **1987**, 183-186.
16. Ijsseling, F.P.; *Survey of Literature on Crevice Corrosion*, The Institute of Materials, London, **2000**.
17. Wallen, B.; Anderson, T.; *Galvanic Corrosion of Copper Alloys in Contact with a Highly Alloyed Stainless Steel in Seawater*, 10th Scandinavian Corrosion Congress, **1986**.
18. Dexter, S. C.; *Galvanic Corrosion*, University of Delaware Sea Grant College Program, November, **1999**.
19. Bardal, E.; Drugli, J. M.; Gartland, P. O.; A Review-The Behavior of Corrosion Resistant Steels in Seawater, *Corrosion Science*, **1974**, 30, 343-353.

20. Valen, S.; Bardal, E.; Rogne, T.; Drugli, J. M.; *New Galvanic Series Based Upon Long Duration Testing in Flowing Seawater*, 11th Scandinavian Corrosion Congress, **1989**.
21. Practical Galvanic Series, *Army Missile Command, Report RS-TR-67-11*, **1997**.
22. *Annual Book of ASTM Standards*, Part 10, Philadelphia: ASTM.
23. Uhlig, H. H.; *Corrosion and Corrosion Control*, New York-London:John Wiley&Sons, **1971**.
24. Bardal, E.; *Corrosion and Protection*, Springer, **2003**, 131-132.
25. Hatch, J.E.; *Aluminum: Properties and Physical Metallurgy*, Materials Park, OH: ASM International, **1984**, 301.
26. Bardal, E.; *Corrosion and Protection*, Springer, **2003**, 135-136.
27. Hutchings, I. M.; *The Erosion of Materials by Liquid Flow*, MTI Publ., Materials Technological Institute of the Chemical Processing Industry, **1986**, 25.
28. Bardal, E.; *Corrosion and Protection*, Springer, **2003**, 154.
29. Lees, D. J.; *Characteristics of Stress Corrosion Fracture Initiation and Propagation*, Metallurgist and Materials Technology, **1982**, 14-1, 29-38.
30. Bardal, E.; *Corrosion and Protection*, Springer, **2003**, 170.
31. Roberge, P. R.; *Handbook of Corrosion Engineering*, New York: McGraw-Hill, **1999**.
32. Leygraf, C.; *Atmospheric Corrosion in Corrosion Mechanisms in Theory and Practice*, Marcel Dekker, New York-Basel-Hong Kong, **1995**, 441.
33. Kucera, V.; Mattson, E., *Atmospheric Corrosion in Corrosion Mechanisms*, New York: Marcel Dekker, **1987**.

34. Henriksen, J. F.; *Norwegian Inst. Of Air Research Communications*, **1985**.

35. *Effects of Sulphur Compounds on Materials, Including Historical and Cultural Monuments, in Airborne Sulphur Pollution: Effects and Control*, United Nations, New York, **1984**.

36. Thiel, P. A.; Madey, T. E.; *Surf. Sci. Rep.* **1987**, 7, 1.

37. Fehlner, F. P.; Graham, M. J.; *Thin Oxide Film Formation on Metals in Corrosion Mechanisms in Theory and Practice*, Marcel Dekker, New York-Basel-Hong Kong, **1995**, 123.

38. Alwitt, R. S. in Diggle, J. W.; Vijh, A. K. (Eds.), *Oxides and Oxide Films*, Marcel Dekker, New York, **1976**, 4, 169.

39. Knotkova, D. et al.; *in Atmospheric Corrosion of Metals*, ASTM STP 767, Philadelphia, **1982**, p.7

40. Barr, T. L.; *J. Vac. Sci. Technol.*, **1977**, 14, 828.

41. Marcus, P.; Hinnen, C.; Olefijord, I.; *Surf. Interface Anal.*, **1993**, 20-11, 923-929

42. Nylund, A, Olefijord, I.; *Surf. Interface Anal.*, **1994**, 21-5, 283-289.

43. Bernard, W.J.; Florio, S.M.; *J. Electrochem. Soc.*, **1985**, 132, 2319.

44. Kobayashi, M.; Niioka, Y.; *Corro. Sci.*, **1990**, 31, 237.

45. Robinson, J.; Thomson, G. E.; Shimizu, K.; in Herbert, K. R.; Thompson, G. E. (Eds.), *Oxide Films on Metals and Alloys*, Electrochemical Society, Pennington, NJ, **1994**, 1.

46. Pourbaix, M.; *Atlas of Electrochemical Equilibria in Aqueous Solutions*, NACE (National Association of Corrosion Engineers), Houston, Texas, **1974**.

47. Mattson, E.; Lindgren, S.; *Metal Corrosion in the Atmosphere*, ASTM STP 435, American Society for Testing and Materials, Philadelphia, **1968**, 240.

48. Mattson, E.; *Tek. Tidskr.*, **1968**, 98, 767.

49. Strehblow, H. H.; *Korros*, **1976**, 27, 792.

50. Kingery, W. D.; Bowen, H. K.; Uhlmann, D. R.; *Introduction to Ceramics*, 2nd Ed. Wiley, New York, **1976**, 91 ff.

51. Fehlner, F. P.; Mott, N. F.; *Oxid. Metals*, **1970**, 2, 59.

52. Sun, K. H.; *J. Am. Chem. Soc.*, **1947**, 30, 277.

53. Nagayama, M.; Cohen, M.; *J. Electrochem. Soc.*, **1962**, 109, 781; **1963**, 110, 670.

54. Okamoto, G.; Proceedings, *5th International Congress of Metal Corrosion*, National Association of Corrosion Engineers, Houston, **1974**, 8.

55. Bloom, M. C.; Goldenberg, M.; *Corros. Sci.*, **1965**, 5, 623.

56. Foley, C. L.; Kruger, J.; Bechtold, C. J.; *J. Electrochem. Soc.*, **1967**, 14, 994.

57. Grimblot, J.; Eldridge, J.M.; *J. Electrochem. Soc.*, **1981**, 128, 729.

58. Kubaschewski, O.; Hopkins, B. E.; *Oxidation of Metals and Alloys*, 2nd Ed. Butterworths, London, **1962**, 266 ff.

59. Jolly, W. L.; *Modern Inorganic Chemistry*, 2nd Ed., McGraw-Hill, New York, **1991**, 238.

60. McBee, C. L.; Kruger, J.; *Electrochem. Acta.*, **1972**, 17, 1337.

61. Keller, F.; Edwards, J. D.; *Met. Prog.*, **1948**, 54, 195-200.

62. Dignam, M. J.; *The Kinetics of Growth of Oxides, Comprehensive Treatise of Electrochemistry*, Electrochemical Materials Science, Plenum, New York, **1981**, 4, 247.

63. Wagner, C.; Models for Lattice Defects in Oxide Layers on Passivated Iron and Nickel:, *Ber. Bunsenges, Phys. Chem.*, **1973**, 77, 1090.

64. Blecher, B.; *Aluminum Materials Technology for Automobile Construction*, Ed. W. J. Bartz, Mechanical Engineering Publications, London, England, **1993**, 43-51

65. Rogers, T. H.; *Marine Corrosion*, London: George Newnes, **1969**.

66. Mor, E.; Bonino, G.; *Proc. 5th Europ. Symp. Corr. Inhibitors*, Ferrara, Italy, **1971**, 659-70.

67. *Metals Handbook*, 9th Ed., Corrosion of Metals, Park, Ohio: ASM International, **1987**, 13.

68. Iverson, W. P.; *An Overview of the Anaerobic Corrosion of Underground Metallic Structures, Evidence for a New Mechanism, Underground Corrosion*. ASTM STP 741. American Society for Testing and Materials, **1981**.

69. *NACE (National Association of Corrosion Engineers) International 2007 Glossary of Corrosion*, Houston, TX, **2007**.

70. Dismuke, T.; Coburn, S.K.; Hirsch, C.M.; *Handbook of Corrosion Protection for Steel Pile Structures in Marine Environments*,1st Ed., American Iron and Steel Institute, Washington, D.C., **1981**.

71. Klöppel, H.; Fliedner, A.; Kördel, W.; Behaviour And ecotoxicology of Aluminium in Soil and Water, *Chemosphere*, **1997**, 35-1, 353-363

72. Romanoff, M.; *Underground Corrosion*, National Bureau of Standard, US, **1957**, 579.

73. Wilson, J.; *Petroleum Engineering*, **1983**, 6, 25.

74. Craig, D.; *Petroleum Engineering*, **1987**, 10, 35.

75. Wu, Y.; *Corrosion*, NACE (National Association of Corrosion Engineers) International, Houston, TX, **1987**, 87, 36.

76. Sharp, S. P.; Yarborough, L.; US Patent: US 4350600, **1982**.

77. Stanford, J. R.; Campbell, G. D.; US Patent: US 3959158, **1976**.

78. Sutanto, H.; Smerad, V.A.W.; *SPE Production Engineering*, **1990**, 8, 295.

79. Houghton, C. J.; Westmark, R. V.; *Downhole Corrosion Mitigation in Ekofisk (North Sea) field in CO_2 Corrosion in Oil and Gas Production,* Selected Papers, Abstracts, and References; Houston: NACE (National Association of Corrosion Engineers) Task Group T-1-3, **1984**.

80. Duncan, R. N.; Materials Performance in Khuff Gas Service, *Materials Performance*, **1980**, 45-53.

81. Vukasovich, M.S.; Farr, J.P.G.; Molybdate in Corrosion Inhibition-A Review, *Polyherdon*, **1986**, 5½, 551-559

82. Brown, J. M.; Roberts, H. A.; Herrold, J. J.; *Methods for Inhibiting Corrosion in Cooling Water Systems*, U. S. Patent 5425914, **1995**.

83. Bradbury, D.; Swan, T.; Segal, M. G.; *Application Technique for the Descaling of Surfaces*, **1988**.

84. Schauhoff, S.; Kissel, C.L.; New Corrosion Inhibitors for High Temperature Applications, *Materials and Corrosion*, **2000**, 51, 141-146.

85. Fivizzani, K. P.; *Use of Molybdate as Corrosion Inhibitor in a Zinc/Phosphonate Cooling Water Treatment*, U. S. Patent 5320779, **1994**.

86. Singh, G.; Inhibition of Mild Steel Corrosion in Acid Mine Waters Containing Ferric Ions, *Br. Corros. J.*, **1988**, 23, 4250-253.

87. Hiller, J. E.; *Korros.*, **1966**, 20, 943.

88. Karaivanov, S.; Gawrilov, G.; *Korros.*, **1973**, 24, 30.

89. *Clays and Clay Minerals*, **1980**, 28-4, 272-280.

90. Engelhardt, R. et al.; *Neue Huette*, **1971**, 16, 593.

91. Misawa, T.; *Corros. Sci.*, 1973, 13, 659.

92. Keller, P.; *Korros.*, **1971**, 22, 32.

93. Schwarz, H.; *Korros.*, **1972**, 23, 648.

94. Baum, H. et al.; *Neue Huette*, **1974**, 19, 423.

95. Keller, P.; *Korros.*, **1969**, 20, 102.

96. Misawa, T. et al.; *Corros. Sci.*, **1971**, 11, 35.

97. Becker, G. et al.; *Arch. Eisenhuettenwes.*, **1969**, 40, 341.

98. Sehmbhi, T. S.; Barnes, C.; Ward, J.J.B.; *Alternatives to Chromate Conversion Coatings for Aluminum*, BNF Metals Technology Centre, Wantage, Oxon

99. Rozenfeld, L.; *Atmospheric Corrosion of Metals*, National Association of Corrosion Engineers, Houston, **1972**.

100. Kaesche, H.; *Localized Corrosion*, National Association of Corrosion Engineers, Houston, **1974**, 516.

101. Bird, C. E.; Strauss, F. J.; *Mater. Perform.*, **1976**, 15-11, 27.

102. Bardal, E.; *Corrosion and Protection*, Springer, **2003**, 154.

103. Wernick, S.; Pinner, R.; Sheasbay, P.G.; *The Surface Treatment and Finishing of Aluminum and Its Alloys*, 5th edn., ASM International Pub. Ltd., England, **1987**, 1, 269-276.

104. Lomakina, S. V.; Shatova, T. S.; Kazansky, L. P.; *Heteropoly Anions As Corrosion Inhibitors For Aluminum In High Temperature Water*, Inst. Of Physical Chemistry, Russian Acedemy of Sciences, Moscow, Russia, **1993**, 1645-1655.

105. *Aluminum Statistical Review for 1999*, The Aluminum Association, Inc., Washington, D.C., **2000**.

106. Sanders, R. E.; Technology Innovation in Aluminium Products, *The Journal of The Minerals*, **2001**, 53-2, 21–25.

107. Staley, J. T.; Liu, J.; Hunt, W.H., Jr.; *Advanced Materials and Processes*, **1997**, 152-4, 17–20.

108. Kang, Y.; *Studies on the Corrosion Protection of Metal by Alloying and Organic Inhibitors*, **1997**, 51.

109. Edwards, J. D.; Frary, F. C.; Jeffries, Z.; *The Aluminum Industry*, New York: McGraw-Hill, **1930**, 2, 245.

110. Metroke, T.L.; Parkhill, R.L.; Knobbe, E.T.; Passivation of Metal Alloys Using Sol-Gel Derived Materials-a Review, *Progress in Organic Coatings*, **2001**, 41, 233-238.

111. van Ooij, W. J.; Song, J.; Subramanian, V.; Silane-Based Pretreatments of Aluminum and Its Alloys As Chromate Alternatives, *Applied Surface Science*, **2005**, 246-1, 82-89.

112. Hatch, J. E.; *Aluminum: Properties and Physical Metallurgy*, Materials Park, OH, ASM International, **1984**, 354.

113. Hatch, J. E.; Aluminum: Properties and Physical Metallurgy, Materials Park, OH:, ASM International, **1984**, 136.

114. Kending, M. W.; Buchelt, R. G.; Corrosion Inhibition of Aluminum and Aluminum Alloys by Soluble Chromates, Chromate Coatings, and Chromate-Free Coatings, *Corrosion*, **2003**, 59-5, 383.

115. *Corrosion Costs and Preventive Strategies in the United States*, CC Technologies Laboratories, Inc. in Dublin, Ohio with support from the FHWA (Federal Highway Administration) and NACE (National Association of Corrosion Engineers), **2001**.

116. West, J. M.; *Basic Corrosion and Oxidation*, Halsted Press, New York, **1980**.

117. NACE (National Association of Corrosion Engineers) Glossary of Corrosion Terms, *Mat. Pro.*, **1965**, 4-1, 79.

118. Pictilova, N.; Balezin, S. A.; Baranek, V. P.; *Metallic Corrosion Inhibitors*, Pergamon Press, New York, **1960**.

119. Jones, D. A.; *Principles and Prevention of Corrosion*, Prentice-Hall, Upper Saddle River, NJ, **1996**.

120. Hackermann, N.; *Fundamentals of Inhibitors*, NACE (National Association of Corrosion Engineers) Basic Corrosion Course, Houston, TX, **1965**.

121. Trabanelli, G.; Carassiti, V.; *in Advances in Corrosion Science and Technology*, Plenum, New York, **1970**, 1, 147.

122. Thomas, J. G.; *Corrosion*, Newnesbutterworths, London, **1976**, 2, 183.

123. McCafferty, E.; *Corrosion Control by Coatings*, Science Press, Princeton, **1979**, 279.

124. Rosenfeld, L.; *Corrosion Inhibitors*, McGraw-Hill, New York, **1981**.

125. Nathan, C. C.; *Corrosion Inhibitors*, NACE National (National Association of Corrosion Engineers) Publications, Houston, TX, **1973**.

126. Wilcox, G. D.; Babe, D. R.; Warwick, M. E.; The Role of Molybdates in Corrosion Prevention, *Corrosion Reviews,* **1986**, 6-3, 336.

127. Batchelor, A. W.; Lam, N. L.; Chandrasekaran, M.; *Materials Degradation and Its Control by Surface Engineering*, 2nd Ed., Imperial College Press, **2002**, 119 ff.

128. Lumsden, J.; Szklarska-Smialowska, Z.; *Corrosion*, **1978**, 34-5, 169.

129. Federal Register, *Proposed Prohibition Of Hexavalent Chromium Chemicals In Comfort Cooling Towers*, Part V, 40 CFR, Part 749, **1988**.

130. Roti, J.; Saeder, K.; *A Comprehensive Evaluation of Molybdate Based Cooling Water Treatment Technology*, Cooling Tower Institute, Paper TP-88-03, **1988**.

131. Stranick, M. A.; Weber, T. R.; Molybdate *Corrosion Inhibition in Waters of Low Oxygen Content*, Amax Report, L-312-60, **1983**.

132. *AWT Technical Reference and Training Manual*, Association of Water Technologies Inc., McLean, VA, **2001**.

133. Koch, G. H.; Brongers, M. P. H.; Thompson, N. G.; Virmani, Y. P.; Payer, J. H.; *Corrosion Costs and Preventative Strategies in the United States*, NACE (National Association of Corrosion Engineers) Publications, Houston, TX, **2004**.

134. Heiyantuduwa, R.; Alexander, M. G.; Mackechnie, J. R.; Performance of a Penetrating Corrosion Inhibitor in Concrete Affected by Carbonation-Induced Corrosion, *J. Mat. in Civ. Engrg.*, 2006, 18-6, 842-850.

135. Baiqing, Z.; Xiaowei, W.; Qin, L.; Yisheng, P.; Performance and Mechanism of a Water Stabilizer for Low Hardness Cooling Water, *Anti-Corrosion Methods and Materials*, **2003**, 50-5, 347-351.

136. Whittemore, M.; LaCosse, G.; Riley, J.; Composition and Method for Inhibiting Chloride-Induced Corrosion and Limescale Formation on Ferrous Metals and Alloys, U.S. Patents 5948267, **1999**.

137. Gallant, D.; Simard, S.; A Study on the Localized Corrosion of Cobalt in Bicarbonate Solutions Containing Halide Ions, *Corrosion Science*, 2005, 47, 1810-1838.

138. Narayanan, T. S. N.; Jegannathan, S.; Ravichandran, K.; Corrosion Resistance of Phosphate Coatings Obtained By Cathodic Electrochemical Treatment: Role of Anode–Graphite Versus Steel, *Progress in Organic Coatings*, **2006**, 55-4, 355-362.

139. Shimura, Y.; Taya, S.; Oxygen Scavenger and Boiler Water Treatment Chemical, U.S. Patent 6861032, **2002**.

140. Davis, J. R.; *Corrosion: Understanding the Basics*, ASM International, **2000**, 182.

141. Ozdemir, L.; North American Tunneling:2004, *Proceedings of the North American Tunneling Conference*, Atlanta, GA, **2004**, 350.

142. Harrop, D. in Clubley, B. G. (Ed.), *Chemical Inhibitors for Corrosion Control*, Royal Society of Chemistry, Cambridge, **1991**, 2.

143. Clark, W. J.; McCreery, R. L.; *J. Electrochem. Soc.*, **2002**, 149, B379.

144. *ASM Handbook*, 10^{th} edition, ASM Inter., Metals Park, Ohio, **1994**, 5, 405-411.

145. Suzuki, Y.; *Corrosion-Resistant Coatings Technology*, Marcel Dekker, New York, **1989**, 5.

146. Zhao, J.; Frankel, G.; McCreery, R. I.; *J. Electrochem. Soc.*, **1998**, 45, 2258.

147. Wernick, S.; Pinner, R.; Sheasby, P. G.; *Chemical Conversion Coatings, In the Surface Treatment and Finishing of Aluminum and Its Alloys,* Materials Park, OH, ASM International, **1987**, 220.

148. Ooij, W. J.; Corrosion Protection of Aluminum Alloys by Conversion Systems and Organic Coatings, *Chemtech*, **1998**, 26-63

149. Smith, C. J. E.; Baldwin, K. R.; Garette, S.A.; Gibson, M. C.; Hewins, M. A. H.; Lane, P. L.; Proceedings International Symposium on Aluminum Surfaces Science and Technology, Antwerp, Belgium, *ATB Metallurgie,* 1997, XXXVII, 266.

150. Agarwala, V. S.; *Trivalent Chromium Solutions for Applying Chemical Conversion Coatings to Aluminum Alloys,* Naval Air Warfare Center, **1996**.

151. *Chemical Conversion Materials for Coating Aluminum and Aluminum Alloys,* Military Specification MIL-C-81706.

152. Camprestrini, P.; van Westing, E. P. M.; de Wit, J. H. W.; Influence of Surface Preparation on Performance of Chromate Conversion Coatings on Alclad 2024 Aluminum Alloy Part I: Nucleation and Growth, *Electrochimica Acta*, **2001**, 2553-2571.

153. Osborne, J. H.; Du, J.; Nercissiantz, A.; Taylor, S. R.; Bernard, D.; Bierwagen, G. P.; *Advanced Corrosion-Resistant Aircraft Coatings,* prepared under contract no. F33615-96-C-5078, Wright-Patterson AFB, OH, Air Force Material Command, **2000**.

154. Kending, M. W.; Buchelt, R. G.; Corrosion Inhibition of Aluminum and Aluminum Alloys by Soluble Chromates, Chromate Coatings, and Chromate-Free Coatings, Corrosion, 59, 379-400

155. Lunn, G.; Sansone, E. B.; *Destruction of Hazardous Chemicals in the Laboratory*, John Wiley&Sons, Toronto, Canada, **1990**, 63-66.

156. Sax, N. I.; Lewis, R. J. Sr.; *Dangerous Properties of Industrial Materials*, 7th edn., Van Nostrand Reinhold, New York, **1989**, 2, 912-913.

157. Cohen, S. M.; *Corr.*, **1995**, 51-1, 71-78.

158. *Blue Ribbon Advisory Report*, Wright Laboratory, Wright Patterson Airforce Base, Dayton, OH, **1995**.

159. Metroke, T. L.; Gandhi, J. S.; Apblett, A.; Corrosion Resistance of Ormosil Coatings on 2024-T3 Aluminum Alloy, *Progress In Organic Coatings*, **2004**, 50-4, 231-246.

160. O'Brien, P. O.; Kortenkamp, A.; *Transit. Metal Chem.*, **1995**, 20, 636.

161. *Chromium and Nickel Welding in Monographs on the Evaluation of Carcinogenic Risks to Humans*, Lyon, France, International Agency for the Research on Cancer, **1990**, 49.

162. Suzuki, Y.; *Ind. Health*, **1990**, 28, 9.

163. Suzuki, Y.; Fukuda, K.; *Arch. Toxicol.*, **1990**, 64, 169.

164. Stearns, D.; Wetterhahn, K.; *Chem. Res. Toxicol.*, **1994**, 7, 219.

165. Lay, P.; Levina, A.; *J. Am. Chem. Soc.*, **1998**, 120, 6704.

166. U.S. Environmental Protection Agency. *Integrated Risk Information System (IRIS) on Chromium, VI*. National Center for Environmental Assessment, Office of Research and Development, Washington, DC., **1999**.

167. U.S. Environmental Protection Agency. *Integrated Risk Information System (IRIS) on Chromium, III*. National Center for Environmental Assessment, Office of Research and Development, Washington, DC., **1999**.

168. U.S. Environmental Protection Agency. *Toxicological Review of Hexavalent Chromium*, National Center for Environmental Assessment, Office of Research and Development, Washington, DC., **1998**.

169. U.S. Environmental Protection Agency. *Toxicological Review of Trivalent Chromium*, National Center for Environmental Assessment, Office of Research and Development, Washington, DC., **1998**.

170. Agency for Toxic Substances and Disease Registry (ATSDR), *Toxicological Profile for Chromium*, U.S. Public Health Service, U.S. Department of Health and Human Services, Atlanta, GA, **1998**.

171. Occupational Safety and Health Administration (OSHA). Occupational Safety and Health Standards, Toxic and Hazardous Substances. *Code of Federal Regulations.* 29 CFR 1910.1000., **1998**.

172. World Health Organization. Chromium. *Environmental Health Criteria 61*. Geneva, Switzerland, **1988**.

173. U.S. Department of Health and Human Services. Registry of Toxic Effects of Chemical Substances (RTECS, online database), National Toxicology Information Program, National Library of Medicine, Bethesda, MD, **1993**.

174. SAIC. *PM/Toxics Integration: Addressing Co-Control Benefits*. Submitted to U.S. Environmental Protection Agency, Office of Air Quality Planning and Standards, Research Triangle Park, NC. 1998.

175. American Conference of Governmental Industrial Hygienists (ACGIH), *1999 TLVs and BEI,. Threshold Limit Values for Chemical Substances and Physical Agents, Biological Exposure Indices,* Cincinnati, OH, **1999**.

176. National Institute for Occupational Safety and Health (NIOSH), *Pocket Guide to Chemical Hazards*, U.S. Department of Health and Human Services, Public Health Service, Centers for Disease Control and Prevention. Cincinnati, OH, **1997**.

177. Daugherty, M. L.; *Chemical Hazard Evaluation and Communication Group, Biomedical and Environmental Information Analysis Section*, Health and Safety Research Division, by Martin Marietta Energy Systems, Inc., for the U.S. Department of Energy under Contract No. DE-AC05-84OR21400, Oak Ridge, Tennessee, **1992**.

178. Hughes, A. E.; Taylor, R. J.; Hinton, B. R.; Chromate Conversion Coatings on 2024 Al Alloy, *Surf. Interface Anal.*, **1997**, 25, 223.

179. Friberg, L.; Nordberg, G. F.; Vouk, V. B.; *Handbook of Toxicology of Metals*, Elsevier, Amsterdam, **1986**, 2.

180. Metroke, T. L.; Kachurina, O.; Knobbe, E. T.; Spectroscopic and Corrosion Resistance Characterization of GLYMO-TEOS Ormosil Coatings for Aluminum Alloy Corrosion Inhibition, *Progress in Organic Coatings*, **2002**, 44, 295-305.

181. Sarc, O. L.; Kapor, F.; Halle, R.; Corrosion Inhibition of Carbon Steel in Chloride Solutions by Blends of Calcium Gluconate and Sodium Benzoate, *Materials and Corrosion*, **2000**, 51, 147-151.

182. A New Class of Corrosion Inhibitor, *Specialty Chemicals Magazine*, Bricorr 288, **2001**.

183. Metroke, T. L.; Kachurina, O.; Knobbe, E. T.; Electrochemical and Salt Spray Analysis of Multilayer Ormosil/Conversion Coating Systems for the Corrosion Resistance of 2024-T3 Aluminum Alloys, *Journal of Coatings Technology*, **2002**, 74-927, 53-61.

184. Twite, R. L.; Bierwagen, G. P.; *Prog. Org. Coat.*, **1998**, 33, 91.

185. Cohen, S. M.; *Corrosion*, **1995**, 51, 71.

186. Hinton, B. W. R.; *Met. Finish.*, **1991**, 89, 15-55

187. Kending, M. W.; Buchelt, R. G.; Corrosion Inhibition of Aluminum and Aluminum Alloys by Soluble Chromates, Chromate Coatings, and Chromate-Free Coatings, *Corrosion*, **2003**, 59-5, 379.

188. Cotton, F.A.; Wilkinson, G.; *Advanced Inorganic Chemistry*, 2nd ed., New York, NY, Wiley Interscience, **1966**, 818.

189. Frankel, G. S.; *Mechanism of Alloy Corrosion and the Role of Chromate Inhibitors*, First Annual Report, Contract no. F49620-961-0479, Columbus, OH, **1997**.

190. Clark, W. J.; McCreery, R. L.; *J. Electrochem. Soc.*, **2002**, 149, B379.

191. Pearlstein, F.; Agarwala, V. S.; *Non-Chromate Conversion Coatings for Aluminum Alloys in Corrosion Protection by Coatings and Surface Modification*, The Electrochemical Society, PV 93-28 Pennington, NJ, **1993**, 199.

192. Katzman, H. A.; Malouf, G. M.; Bauer, R.; Stupian, G. W.; *Appl. Surf. Sci.*, **1979**, 2-3, 416-432.

193. Asami, K.; Oki, Thompson, G. E.; Wood, G. C.; Ashworth, V.; *Electrochim. Acta*, **1987**, 32, 337.

194. Drozda, T.; Maleczki, E.; *Radioanal. Nucl. Chem. Lett.*, **1985**, 95, 339.

195. Hagans, P. L.; Haas, C. M.; *Surf. Interf. Anal.*, **1994**, 21, 65.

196. Kending, M. W.; Davenport, A. J.; Isaacs, H. S.; *Corros. Sci.*, **1993**, 43, 41.

197. Yu, H.; Zhang, G.; Wang, Y.; *Appl. Surf. Sci.*, **1992**, 62, 217.

198. Kending, M. W.; Davenport, A. J.; Isaacs, H. S.; *Corros. Sci.*, **1993**, 43.

199. Xia, L.; Akiyama, E.; Frankel, G.; McCreery, R.; *J. Electrochem. Soc.*, **2000**, 147, 2,556.

200. Zhao, J.; Frankel, G. S.; McCreery, R. L.; *J. Electrochem. Soc.*, **1998**, 145, 2258.

201. Ramsey, J.; McCreery, R. L.; *J. Electrochem. Soc.*, **1999**, 146, 4076.

202. Kendig, M.; Addison, R.; Jeanjaquet, S.; *J. Electrochem. Soc.*, **1999**, 146, 4419.

203. Sato, N.; *Corrosion*, **1989**, 5, 354.

204. Cotton, F.; Wilkinson, G.; *Advanced Inorganic Chemistry*, 5th Ed., Wiley, New York, 694.

205. Sinko, J.; US Patents, 5,378,446; 5,176,894.

206. *The Handbook of Chemistry and Physics*, 70th Ed., CRC Press, Boca Raton, FL, 1997, 187 ff.

207. Uhlig, H. H.; *Corrosion and Corrosion Control*, 2nd Ed, Wiley/Interscience, New York, **1971**.

208. Jones, D. A.; *Principles and Prevention of Corrosion*, MacMillan, New York, **1992**, pp. 49, 116, 489, 506.

209. Weisberg, H. E.; *Chromate and Molybdate Pigments*, Paint and Varnish Production, **1968**.

210. Piens, M.; *Importance of Diffusion in the Electrochemical Action of Oxidizing Pigments*, JCT 51, **1979**, 655.

211. Hagans, P. L.; Haas, C. M.; *Chromate Conversion Coatings*, in surface Engineering Materials Park, OH, ASM International, **1987**, 405

212. Hughes, E.; Taylor, R. J.; Hinton, B. W. R.; *Surf. Interf. Anal.*, **1997**, 25, 405.

213. Ilevbare, G. O.; Scully, J. R.; Yuan, Y.; Kelly, R. G.; Inhibiting of Pitting Corrosion on Aluminum Alloy 2024-T3: Effect of Soluble Chromate Additions vs. Chromate Conversion Coating, *Corrosion*, **2000**, 56, 227.

214. Wernick, S.; Pinner, R.; Sheasby, P. G.; *Chemical Conversion Coatings*, in the Surface Treatment and Finishing of Aluminum and Its Alloys, Materials Park, OH, ASM International, **1987**, 220.

215. Blecher, B.; *Aluminum Materials Technology for Automobile Construction*, Ed. W. J. Bartz, Mechanical Engineering Publications, London, England, **1993**, 43-51

216. Seo, M.; Sato, N.; *Inhibition in the Context of Passivation*, I-7-1, in Reviews on Corrosion Inhibitor Science and Technology, NACE, Houston, TX, **1993**.

217. Sinko, J.; Challenges of Chromate Inhibitor Pigments Replacement In Organic Coatings, *Progress In Organic Coatings*, **2001**, 42, 273-274.

218. Pourbaix, M.; *Atlas of Electrochemical Equilibria in Aqueous Solutions*, NACE, Houston, Texas, **1974**.

219. Bennett, E. O.; Bennett, D. L.; *Tribol. Int.*, **1984**, 17, 341.

220. *Consumer Factsheet on: nitrates/nitrites*, U.S. EPA (Environmental Protection Agency), **2006**.

221. Pearlstein, F.; Agarwala, V. S.; Trivalent Chromium Solutions for Applying Chemical Conversion Coatings to Aluminum Alloys or for Sealing Anodized Aluminum, *Plating and Surface Finishing*, **1994**, 50-55.

222. Pearlstein, F.; Agarwala, V. S.; U.S. Patent 5,304,257, **1994**.

223. Udy, M. J.; *Chromium: Chemistry of Chromium and Its Compounds*, ACS Monograph Series, Reinhold Publishers, New York, NY, **1956**, 177-178.

224. Barnes, C.; Ward, J. J. B.; Sehmbhi, T. S.; Carter, V. E.; *Trans IMF*, **1982**, 60, 45.

225. Haaksma, R.; Weir, J. A.; *Proc. The 27th International SAMPE Tech. Conf.*, Albuquerque, New Mexico, **1995**, 1074-1082.

226. J. Sinko; *Prog. Org. Coat.*, **2002**, 42-3, 267-282.

227. J. Sinko; *Considerations on the Chemistry and Action Mechanism of Corrosion Inhibitor Pigments in Organic Coatings* in 6th Biennial Conf. Organic Coatings, New Paltz, NY, Institute of Material Science, **2000**.

228. Mikhailovski, Y. N.; Berdzenishvili, G. A.; *Prot. Met.*, **1986**, 21, 6, 704-711.

229. Kendig, M.; Cunningham, M.; Jeanjaquet, S.; Hardwick, D.; *J. Electrochem. Soc.*, **1997**, 11, 3721.

230. Frey, C. U.; Richens, D. T.; Merbach, A. E.; *J. Am. Chem. Soc.*, **1996**, 118, 5265.

231. Pepper, S. E.; Bunker, D. J.; Bryan, N. D.; Livens, F. R.; Charnock, J. M.; Pattrick, R. A. D.; Collison, D.; Treatment of radioactive wastes: An X-ray Absorption Spectroscopy Study Of The Reaction Of Technetium With Green Rust, *J. of Colloid and Interface Science*, **2003**, 268, 2, 408-412

232. Yamamato, T.; *A Novel Anti-Corrosion Pigment Containing Vanadate/Phosphate, in Proc. Advances* in Corrosion Protection by Organic Coatings, PV 89-13 Pennington, NJ, The Eletrochem. Soc., **1989**, 476.

233. Cook, R. L.; Taylor, S. R.; *Corrosion*, **2000**, 56, 321

234. Zein, S.; *J. Appl. Electrochem.*, **2001**, 31, 711.

235. Moutarlier, V.; Gigandet, M. P.; Ricq, L.; Pagetti, J.; *Appl. Surf. Sci.*, **2001**, 1-2.

236. Mitchell, P. C. H.; Wass, S. A.; Complexes of Molybdenum And Tungsten, *Annu. Rep. Prog. Chem., Sect. A: Inorg. Chem.* , **1991**, 88, 127 – 145.

237. Giordano, N.; Castellam, A.; Bart, J. C. J.; Vaghi, A.; Campadelli, F.; *J. Catal.*, **1975**, 37, 204.

238. Zingg, D. S.; Makovsky, L. E.; Tischer, R. E.; Brown, F. R.; Hercules, D. M.; *J. Phys. Chem.*, **1980**, 84, 2898.

239. Grunert, W.; Shpiro, E. S.; Feldhaus, R.; Anders, K.; Antoshin, G. V.; Minachev, K. M.; *J. Catl.*, **1987**, 107, 522.

240. Chappell, P. J. C.; Kibel, M. H.; Baker, B. G.; *J. Catal.*, **1988**, 110, 139.

241. Sax, N. I.; Lewis, R. J., Sr.; *Dangerous Properties of Industrial Materials*, 7th edn., Van Nostrand Reinhold, New York, **1989**, 3, 2424.

242. Ashmead, H. J.; *J. Appl. Nutr.*, **1972**, 24, 8.

243. Sax, N. I.; *Dangerous Properties of Industrial Materials*, 5th Edition, Reinhold, New York, **1979**, 836.

244. Sigel, H.; (Ed.), *Metal Ions in Biological Systems*, Carcinogenicity and Metal Ions. Marcel Dekker, New York, **1980**, 10.

245. Occupational Safety and Health Act, Public Law 91-596, 84 Stat. 1593; 29 U.S.C. 655 et seq., as amended, **1970**.

246. Federal Mine Safety Health Act of 1977; 86 U.S.C. 801 et seq., as amended, **1977**.

247. ISBN 0-936712-54-6, American Conference of Governmental Industrial Hygienists, 6500 Glenway Avenue, Building D-5, Cincinnati, OH 45211.

248. Anderson, J.; *J. Aust. Inst. Agric. Sci.*, **1942**, 873.

249. Neenan, M.; *Proc. Soil Sci. Soc.*, Fla, **1953**, 13, 178.

250. DeRenzo, E. C.; Kaleita, E.; Heytler, P. G.; Oleson, J. J.; Hutchings, B. L.; Williams, J. H.; *Arch. Biochem. Biophys*, **1953**, 45, 247.

251. Richert, D. A.; Westerfield, W. W.; *J. Biol. Chem.*, **1953**, 203, 915.

252. Burell, R. J.; Roach, W. A.; Shadwell, A.; *J. Nat. Cancer Inst.*, **1966**, 35, 201.

253. Nemenko, B. A.; Moldakulova, M. M.; Borina, S.N.; *Vopr. Onkol.*, **1976**, 22, 75.

254. Department of Chemical Etiology and Carcinogenesis, Cancer Inst., Chinese Academy of Medical Sciences, Henan Hydrogeological Team, Lab. Of Henan Geo. Bureau, Health Bureau of Anyang District and Linxian Office of Esophagel Cancer Prevention and Treatment, Chin. J. Oncol. **1980**, 2, 29.

255. Luo, X. M.; Lu, S. M.; Liu, Y. Y.; *Chin. J. Epidemiol.*, **1982**, 3, 91.

256. Luo, X. M.; Trace Substances in Environmental Health-XVI, University of Missouri, **1983**, 357.

257. Safe Water Drinking Act, Public Law 93-523, 88 Stat. 1660; 42 U.S.C. 300 et seq., as amended, **1974**.

258. Resource Conservation and Recovery Act, Public Law 94-580, 90 Stat. 95; 42 U.S.C. 3251 et seq., as amended, **1976**.

259. Federal Water Pollution Control Act, as amended by the Clean Water Act, Public Law 92-500, 86 Stat. 816, 33 U.S.C. 1251 et seq., as amended, **1972.**

260. Comprehensive Environmental Response Compensation and Liability Act of (1980), Public Law 96-510, 94 Stat. 2767; 42 U.S.C. 9601 et seq., as amended, **1980**.

261. Toxic Substances Control Act, Public Law 94-469, 90 Stat. 2003; 15 U.S.C. 2601 et seq., as amended, **1976**.

262. Opresko, D. M.; Ph.D., Chemical Hazard Evaluation Group, Biomedical and Environmental Information Analysis Section, Health and Safety Research Division, by Martin Marietta Energy Systems, Inc., for the U.S. Department of Energy under Contract No. DE-AC05-84OR21400, Oak Ridge, Tennessee, **1993**.

263. NACE Glossary of Corrosion Terms, *Mater. Perform.*, **1968**, 7, 10, 68.

264. Killefer, D. H.; Linz, A.; *Molybdenum Compounds: Their Chemistry and Technology*, Interscience, New York, **1952**, 163.

265. Robertson, W. D.; *Chem. Eng.*, **1950**, 57, 290.

266. Killefer, D. H.; Paint, *Oil Chem. Rev.*, **1954**, 117, 24.

267. Robertson, W. D.; *J. Electrochem. Soc.*, **1951**, 98, 94.

268. Choudhury, A. K.; Shome, S. C.; *J. Sci. Ind. Res.*, **1958**, 17A, 30.

269. Choudhury, A. K.; Shome, S. C.; *J. Sci. Ind. Res.*, **1959**, 18A, 568.

270. Shoen, H. O.; Brand, B. G.; *Off. Dig. Fed. Soc. Paint Technol.*, **1960**, 32, 1522.

271. Weisbergy, H. E.; *Paint Varn. Prod.*, **1968**, 58,3, 32.

272. Kronstein, M.; von Burgsdorff, W. A.; Hanan, N.; Weir, D. L.; *Aust. Finish. Rev.*, **1966**, 12, 13.

273. Kronstein, M.; U.S. Patent 3,272,663, **1966**.

274. Chisolm, S. L.; U.S. Patent 3,311,529, **1967**.

275. Kronstein, M.; U.S. Patent 3,528,860, **1970**.

276. Schnake, P.; Jensen, D. P.; Albrecht, R. H.; NASA Contract NAS 8-11788, Final Report, **1964**.

277. Noda, M.; Nakal, H.; Sasaki, M.; Kanno, Z.; Japanese Patent 79116338, **1979**.

278. Vukasovich, M. S.; *Lubr. Eng.*, **1980**, 36, 708.

279. Vukasovich, M. S.; Robitaille, D. R.; U.S. Patent 4,313,837, **1982**.

280. Koh, K. W.; U.S. Patent 4,218,329, **1980**.

281. Fette, C. J.; *Lubr. Eng.*, **1979**, 35, 625.

282. Vukasovich, M. S.; In *Proceedings of the 3rd Inter. Colloqium on Lubrication in Metal Working*, Machining and Metal Forming Processes, Technishe Akademie Esslingen, Nellingen, **1982**.

283. Vukasovich, M. S.; *Lubr. Eng.*, **1984**, 40, 456.

284. Bayes, A. L.; US Patent 2,147,395, **1939**.

285. Lamprey, H.; US Patent 2,147,409, **1939**.

286. Lewis, G.W. Jr.; *Research Project No 37*, Climax Molybdenum Company of Michigan, Ann Arbor, MI, **1961**.

287. Wiggle, R. R.; Hospadaruk, V.; Styloglu, E. A.; *Mater. Perform.*, **1981**, 20, 6, 13.

288. Rowe, L.C. in *Corrosion Inhibitors*, Ed: C.C. Nathan, National Assoc. of Corrosion Engineers, Houston, TX, **1973**, 173.

289. Vukasovich, M. S.; Sullivan, F. J.; *Mater. Perform.*, **1983**, 22, 8, 25.

290. Wilson, J. C.; Hirozawa, S. T.; Conville, J. J.; U.S. Patent 4,440,721, **1984**.

291. Rao, P. V.; Seetharamaiah, K.; Rama Char, T. L.; *J. Electrochem. Soc.* India, **1974**, 23, 1, 7.

292. Wiggle, R. R.; Hospadaruk, V.; Tibaudo, F. M.; Paper No. 810038, *Society of Automotive Engineers*, Detroit, MI, **1981**.

293. Vukasovich, M. S.; Sullivan, F. J. (Eds); *Inhibitors and Coolant Corrosivity*, 2nd International Symposium on Engine Coolants and Their Testing, American Society for Testing and Materials, Philedelphia, PA, **1984**.

294. Hirozawa, S. T.; European Patent Application 0,042,937A1, **1982**.

295. Yoshioka, T.; Japanese Patent 8217472, **1982**.

296. Engelhardt, P. R.; Ventura, E. M.; British Patent Application 8409522, **1984**.

297. Vukasovich, M. S.; Sullivan, F. J.; *Mater. Perform.*, **1983**, 22, 8, 25.

298. Rowe, L. C.; Chance, R. L.; Walker, M. S.; *Mater. Perform.*, **1983**, 22, 6, 17.

299. Potter, N. M.; Loranger, R. B.; Vergosen III, H. E.; *American Laboratory*, **1984**, 104.

300. Robertson, W. D.; *Chem. Eng.*, **1950**, 57, 290.

301. Bregman, J. I.; U.S. Patent 3,024,301, **1962**.

302. Hatch, G. B.; *Corrosion*, **1965**, 21, 129.

303. Robertson, W. D.; *Chem. Eng.*, **1950**, 57, 291.

304. Wilcox, G. D.; Gab, D. R.; Warwick, M. E.; *Corr. Rev.*, **1986**, 6, 4, 327-365.

305. Pourbaix, M.; *Atlas of Electrochemical Equilibria*, Pergamon Press, Oxford, **1966**, 272.

306. Abdallah, M.; El-Etre, A. Y.; Soliman, M. G.; Mabrouk, E. M.; Some Organic and Inorganic Compounds as Inhibitors for Carbon Steel Corrosion in 3.5 Percent NaCl Solution, *Anti-Corrosion Methods and Materials*, **2006**, 53/2, 118-123.

307. Zimin, P. A.; Kazansky, L. P.; Izvest.AN SSSR, *Ser.Khim.*, **1983**, 1943.

308. Pryor, M. J.; Cohen, M.; *J. Electrochem. Soc.*, **1953**, 100, 203.

309. Stern, M.; *J. Electrochem. Soc.*, **1958**, 105, 638.

310. Cartledge, G. H.; *Corrosion*, **1962**, 18, 3166.

311. Keddman, M.; Pallotta, C.; *J. Electrochem. Soc.*, **1985**, 132, 781.

312. Leidheiser, H.; *J. Corrosion*, **1980**, 36, 339.

313. Vukasovich, M. S.; Robitaille, D. R.; *J. Less-Common Met.*, **1977**, 54, 437.

314. Robitaille, D. R.; Bilek, J. G.; *Chem. Eng.*, **1976**, 83, 12, 79.

315. Mansfeld, F.; Wang, V.; Shih, H.; *J. Electrochem. Soc.*, **1991**, 138, 12, 174-175.

316. Hughes, E.; Gorman, J. D.; Paterson, P. J. K.; *Corr. Sci.*, **1996**, 38, 11, 1957-1976.

317. Gorman, J. D.; Johnson, S. T.; Johnston, P. N.; Paterson, P. J. K.; Hughes, A. E.; *Corr. Sci.*, **1996**, 38, 11, 1977-1990

318. Fedrizzi, L.; Deflorian, F.; Canteri, R.; Fedrizzi, M.; Bonora, P. L.; *Proc. Prog. In the Understanding and Prevention of Corrosion*, Barcelona, Spain, **1993**, 1, 131-138.

319. Hunn, J. V.; U.S. Patent 3,353,979, **1967**.

320. Kirkpatrick, T.; Nilles, J. J.; U.S. Patent 3,677,783, **1972**.

321. Moore, F. W.; Robitaille, D. R.; Barry, H. F.; U.S. Patent 3,726,694, **1973**.

322. Robitaille, D. R.; Vukasovich, M. S.; Barry, H. F.; U.S. Patent 3,874,883, **1975**.

323. Robitaille, D. R.; Vukasovich, M. S.; Barry, H. F.; U.S. Patent 3,969,127, **1976**.

324. Vukasovich, M. S.; Sullivan, F. J.; U.S. Patent 4,017,315, **1977**.

325. Shibasaki, H.; Tsuchiya, H.; Michikawa, T.; Japanese Patent 75119833, **1975**.

326. Kerfoot, D. G. E.; U.S. Patent 4,132,667, **1979**.

327. Kansai Paint Co. Lts., British Patent 1,415,488, **1975**.

328. Nakajo, K.; Kanezewa, K.; Sato, S.; Japanese Patent 7509596, **1975**.

329. Dai Nippon Tokyo Co. Ltd., British Patent 1,459,069, **1976**.

330. Roberts, G. L.; Fessler, Jr. R. G.; U.S. Patent 3,346,604, **1967**.

331. Rozenfeld, I. L.; Verdiev, S. Ch.; Kyazimov, A. M.; Bairamov, A. Kh.; *Zashch. Met.* , **1982**, 18, 866.

332. Vukasovich, M. S.; *Lubr. Eng.*, **1980**, 36, 708.

333. Vukasovich, M. S.; Robitaille, D. R.; U.S. Patent 4,313,837, **1982**.

334. Vukasovich, M.S. in *Proceedings of the 3rd Inter. Colloqium on Lubrication in Metal Working, Machining and Metal Forming Processes*, Technishe Akademie Esslingen, Nellingen, **1982**.

335. Vukasovich, M. S.; *Lubr. Eng.*, **1984**, 40, 456.

336. Buchelt, R. G.; Mmidipally, S. P.; Schmutz, P.; Guan, H.; *Corrosion*, **2002**, 58, 3.

337. Bethancourt, M.; Botana, F.; Calvino, J.; Marcos, M.; Rodriguez-Chacon, M.; *Corros. Sci.*, **1998**, 11, 1803.

338. Baes, C. F.; Mesmer, R. E.; *Hydrolysis of Cations*, Robert E. Kreiger Publishing Co., Malabar, FL, **1986**, 138.

339. Arnott, D. R.; Hinton, B. W. R.; Ryan, N. E.; Cationic-Film-Forming Inhibitors for the Protection of the AA 7075 Aluminum Alloy Against Corrosion in Aqueous Chloride Solution, *Corrosion*, **1989**, 45, 12.

340. Buchheit, R. G.; Drewien, C. A.; Martinez, M. A.; Chromate-Free Corrosion Resistant Conversion Coatings for Aluminum Alloys, *Advances in Coatings Technologies for Corrosion and Wear Resistant Coatings*, The Minerals, Metals&Materials Society, **1995**, 173-182.

341. Mor, E. D.; Bonino, G.; *Proceed. 3rd Eur. Symp. Corros. Inhibitors*, Ferrara, Italy, **1970**, 659.

342. Kadek, V. M.; Lepin, L. K.; *Proc. 3rd Europ. Symp. Corr. Inhibitors*, Ferrara, Italy, **1970,** 643.

343. Lahodny-Sarc, O.; *Proc. 8th Europ. Symp. Corr. Inhibitors*, Ferrara, Italy, 1995, 421.

344. Wruble, C.; Mor, E. D.; Montini, U.; *Proc. 6th Europ. Symp. Corr. Inhibitors*, Ferrara, Italy, **1985**, 557.

345. Lahodny-Sarc, O.; Orlovic-Leke, P.; *Proc. 11th Internat. Corr. Congress*, Florence, Italy, **1990**, 3, 17.

346. Roti, J. S.; Thomas, P. A.; *Proceed. Internat. Corros. Forum*, New Orleans, LA, US, **1984**, 318.

347. Lahodny-Sarc, O.; Popov, S.; *Surface and Coatings Technology*, **1998**, 34, 537.

348. Krasts, E.; Kadek, V.; Klavina, S.; *Proc. 7th Europ. Symp. Corr. Inhibitors*, Ferrara, Italy, **1990**, 569.

349. Lahodny-Sarc, O.; Orlovic-Leke, P.; *RAD Crotian Acad. Sc.&Arts*, **1991**, 9, 11.

350. Krasts, H. B.; Kadek, V. M.; Lepin, L. K.; *Proc. 4th Europ. Symp. Corr. Inhibitors*, Ferrara, Italy, **1975**, 204.

351. Mor, E.D.; Wruble, C.; *Br. Corrsoion J.*, **1976**, 11, 199.

352. Lahodny-Sarc, O.; *Proc. 5th Europ. Symp. Corr. Inhibitors*, Ferrara, Italy, **1980**, 609.

353. Lahodny-Sarc, O.; *RAD Yug. Acad. Sc. &Arts*, **1982**, 394, 18.

354. Kadek, V. M.; Krasts, H. B.; *Corrosion Inhibitors on the Basis of Polyhydroxy-complexes of Boric Acid*, 2273-R 1000 JT 05129, **1983**.

355. Lahodny-Sarc, O.; Orlovic-Leke, P.; *Proceed. 9th Eur. Congress on Corrosion*, Utrecht, The Netherlands, FU-133, **1989**.

356. Li, H. M.; *Proceed. Ibid.*, **1990**, 3, 3147

357. Lahodny-Sarc, O.; Orlovic-Leke, P.; *Proceed. 7th Eur. Symp. Corros. Inhibitors*, Ferrara, Italy, **1990**, 1025.

358. Lahodny-Sarc, O.; Orlovic-Leke, P.; *Proceed. UK Corrosion and Eurocorr'94*, Bournemouth, UK, **1994**, 1, 120.

359. Mor, E.D.; Wrubl, C.; *Br. Corrosion J.*, **1983**, 18, 142.

360. Lahodny-Sarc, O.; Orlovic-Leke, P.; Skanst, V.; *Proceed. U.K. Corrosion 88 and Eurocorr.*, Brighton, U.K., **1988**, 1, 97.

361. Lahodny-Sarc, O.; Popov, S.; *Surface and Coatings Technology*, **1988**, 34, 537.

362. Rajendran, S.; Apparao, B. V.; Palaniswamy, N.; *Br. Corrosion J.*, **1998**, 33, 315.

363. Rajendran, S.; Apparao, B. V.; Palaniswamy, N.; *Symposium on Corrosion Control by Coatings, Cathodic Protection and Inhibitors in Seawater*, 23rd Event of the European Federation of Corrosion, Dubrovnik, Crotia, **1998**.

364. Talalina, A. S.; Kochanova, L. G.; Ananeva, A. I.; Romanova; A. A.; Corrosion Inhibitors in the Sterilization and Disinfecting of Medical Instruments, *Meditsinskaya Tekhnika*, **1984**, 4, 30-33,.

365. Opresko, D. M.; Chemical Hazard Evaluation Group, Biomedical and Environmental Information Analysis Section, Health and Safety Research Division, by Martin Marietta Energy Systems, Inc., for the U.S. Department of Energy under Contract No. DE-AC05-84OR21400, Oak Ridge, Tennessee, **1991**.

366. Davenport, J.; Aldykiewicz Jr. A. J.; Isaacs, H. S.; Kendig, M. W.; Mundy, A. M.; *Proc. Symp. On X-ray Methods in Corrosion and Interfacial Electrochemistry*, Eds. Davenport, A. J.; Gordon II, J. G.; The Electrochem Soc., Pennington. NJ, USA, **1992**, 92, 1, 306-314.

367. Lake, D. L.; *Industrial Corrosion*, **1989**, 7, 4, 12.

368. Opresko, D. M.; Chemical Hazard Evaluation Group, Biomedical and Environmental Information Analysis Section, Health and Safety Research Division, by Martin Marietta Energy Systems, Inc., for the U.S. Department of Energy under Contract No. DE-AC05-84OR21400, Oak Ridge, Tennessee, **1992**.

369. Colturi, T. F.; Kozelski, K. J.; *Mater. Perform.*, **1984**, 23, 8, 43.

370. Jones, C. A.; *J. Cooling Tower Inst.*, **1985**, 6, 1, 9.

371. Franco, R. J.; Dinielli, N.; Nowicki, R. J.; *Corrosion*, National Assoc. of Corros. Engineers, Houston, TX, **1985**, 85, 133.

372. Weber, T. R.; Stranick, M. A.; Vukasovich, M. S.; National Assoc. of Corros. Engineers, Houston, TX, *Corrosion*, **1985**, 85, 122.

373. Osborne, J. H.; Observations on Chromate Conversion Coatings from a Sol-Gel Perspective, *Progress in Organic Coatings*, **2001**, 41, 280-286.

374. Brinker, C. J.; Scherer, G. W.; *Sol-Gel Science*, Academic Press, New York, **1989**.

375. Plueddemann, E.; *Silane Coupling Agents*, Plenum Press, New York, **1982**.

376. *Better Ceramics through Chemistry Series,* Materials Research Society.

377. van Ooij, W. J.; *Symposium: A Systems Approach to Service Life Prediction of Organic Coatings*, Breckrenridge, Colorado, **1997**.

378. van Ooij, W. J.; Song, J.; Subramanian, V.; *Proceedings International Symposium on Aluminum Surfaces Science and Technology*, Antwerp, Belgium, ATB Metallurgie, **1997**, XXXVII, 137.

379. Kasten, L. S.; Grant, J. T.; Grebasch, N.; Voevodin, N.; Arnold, F. E.; Donley, M. S.; An XPS Study of Cerium Dopants in Sol-Gel Coatings for Aluminum 2024-T3, *Surface and Coatings Technol.,* **2001**, 140, 11.

380. Voevodin, N. N.; Grebasch, N. T.; Soto, W. S.; Arnold, F. E.; Donley, M. S.; Potentiodynamic Evaluation of Sol-Gel Coatings with Inorganic Inhibitors, *Surface and Coatings Technol.*, **2001**, 140, 24.

381. Nylund, A.; Chromium-Free Conversion Coatings for Aluminum Surfaces, *Aluminum Transactions*, **2000**, 2, 121.

382. Smith, C. J. E.; Baldwin, K. R.; Garrett, S. A.; Gibson, M. C.; Hewins, M. A. H.; Lane, P. L.; The Development of Chromate-Free Treatments for the Protection of Aerospace Aluminum Alloys, *ATB Metallurgie*, **1997**, 37, 266.

383. Twite, R.L.; Bierwagen, G.P.; Review of Alternatives to Chromate for Corrosion Protection of Aluminum Aerospace Alloys, *Prog. Org. Coat.*, **1998**, 33, 91.

384. Kasten, L. S.; Grant, J. T.; Grebasch, N.; Voevodin, N.; Arnold, F. E.; Donley, M. S.; XPS Study of Cerium Dopants in Sol-Gel Coatings for Aluminum 2024-T3, *Surface and Coatings Technology*, **2001**, 140, 11-15.

385. Wilkes, G.L.; Orter, B.; Huang, H.; *Polymer Prep*, **1985**, 26, 300.

386. Schmidt, H.; *J. Non-Crystal. Solids*, **1985**, 73, 681.

387. Schmidt, H. K.; Aspects of Chemistry and Chemical Processing of Organically Modified Ceramics, *Mater. Res. Soc. Symp. Proc.*, **1990**, 180, 961.

388. Mackenzie, J. D.; Structures and Properties of Ormosils, *J. Sol-Gel Sci. Technol.*, **1994**, 2, 81.

389. Mackenzie, J. D.; Structures and Properties of Ormosils, *Journal of Sol-Gel Sci. and Technol.*, **1994**, 2, 81-86.

390. Brinker, C. J.; Scherer, G. W.; *Sol Gel Science*, Academic Press, San Diego, CA 1190.

391. Jackson, C. L.; Bauer, B. J.; Nakatani, S. I.; Barnes, J. D.; *Chem. Mater.*, **1996**, 8, 727.

392. Wen, J.; Wilkes, G. L.; Organic/Inorganic Hybrid Network Materials by the Sol-Gel Approach, *Chem. Mater.*, **1996**, 8, 1667-1681

393. Wen, J.; Wilkes, G. L.; *J. Sol-Gel Sci. Technol.*, **1995**, 5, 115.

394. Schmidt, H.; *Mater. Res. Soc. Symp. Proc.*, **1990**, 171, 3.

395. Kasemann, R.; Schmidt, H.; *New J. Chem.*, **1994**, 18, 1117.

396. Schmidt, H.; Kasemann, R.; Burkhart, T.; Wagner, G.; Arpac, E.; Geiter, E. in *Hybrid Organic-Inorganic Composites*; Mark, J. E., Ed.; ACS Series 585; American Chemical Society, Washington, DC, **1995**, 331.

397. Tamami, B.; Betrabet, C.; Wilkes, G. L.; *Polym. Bull.*, **1993**, 30, 393.

398. Wang, B.; Wilkes, G. L.; *J. Macromol. Sci., Pure Appl. Chem.*, **1994**, A31, 249.

399. Betrabet, C.; Wilkes G. L.; *Polym. Prepr.*, **1992**, 33, 2, 286.

400. Wen, J.; Wilkes, G. L.; *J. Inorg. Organomet. Polym.*, **1995**, 5, 343.

401. Wen, J.; Wilkes, G. L.; *PMSE Prepr.*, **1995**, 73, 429.

402. Lebeau, B.; Guermeur, S. C.; *Mater. Res. Soc. Symp. Proc.*, **1994**, 346, 315.

403. Sugama, T.; Du Vall, J.E.; *Thin Solid Films*, **1996**, 289, 39.

404. Montemor, M. F.; Simoes, A. M.; Ferreria, M. G. S.; Williams, B.; Edwards, H.; The Corrosion Performance of Organosilane Based Pretreatments for Coatings on Galvanized Steel, *Prog. Org.Coat.*, **2000**, 38, 17.

405. Metroke, T. L.; Parkhill, R. L.; Knobbe, E.T.; Passivation of Metal Alloys Using Sol-Gel Derived Materials-A Review, *Prog. Org. Coat.*, **2001**, 41, 233.

406. Mackenzie, J. D.; Bescher, E. P.; Structures, Properties and Potential Applications of Ormosils, *J.Sol.-Gel. Sci. Tecnol.*, **1998**, 13, 371.

407. Guglielmi, M.; Sol-Gel Coatings on Metals, *J. Sol-Gel Sci. Technol.*, **1997**, 8, 443.

408. Ooij, W. J.; *Symposium: A Systems Approach to Service Life Prediction of Organic Coatings*, Breckrenridge, Colorado, **1997**.

409. Nylund, A.; Chromium-Free Conversion Coatings for Aluminum Surfaces, *Alum. Trans.*, **2000**, 2, 1, 121–137.

410. Ooij, W. J.; Corrosion Protection of Aluminum Alloys by Conversion Systems and Organic Coatings, *Chemtech*, **1998**.

411. Cleveland Society for Coatings Tecnhology Technical Committee, *Jour. Coat. Tech.*, **1979**, 51, 653, 53-57.

412. Walker, P.; *Jour. Coat. Tech.*, **1980**, 52, 670, 49-61.

413. Bierwagen, G. P.; Reflections on Corrosion Control by Organic Coatings, *Progress in Organic Coatings*, **1996**, 28, 43-48.

414. Kasten, L. S.; Grant, J. T.; Grebasch, N.; Voevodin, N.; Arnold, F. E.; Donley, M. S.; An XPS Study of Cerium Dopants in Sol-Gel Coatings for Aluminum 2024-T3, *Surface and Coatings Technol.*, **2001**, 140, 12-13.

415. Metroke, T. L.; Apblett, A.; Corrosion resistance properties of Ormosil coatings on 2024 - T3 aluminum, *Proceedings of the 22nd Heat Treating Society Conference and the 2nd International Surface Engineering Congress*, Indianapolis, IN, pp. 327-331, **2003**.

416. Pleuddeman, E. P.; Adhesion Aspects of Polymeric Coatings, Ed. K. Mittal, Plenum Press, New York, USA, **1983**, 363-377.

417. Metroke, T. L.; Parkhill, R. I.; Knobbe, E. T.; Synthesis of Hybrid Organic-Inorganic Sol-Gel Coatings for Corrosion Resistance, *Mater. Res. Soc. Symp. Proc.*, **1999**, 576, 293.

418. Schmidt, H. H.; Philipp, G.; *J. Non-Cryst. Solids*, **1984**, 63, 283.

419. Schmidt, H.; Scholze, H.; Kaiser, H.; *J. Non-Cryst. Solids*, **1984**, 63, 1.

420. Schmidt, H.; *Mater. Res. Soc. Symp. Proc.*, **1984**, 32, 327.

421. Mackenzie, J. D.; Bescher, E.P., Structures, Properties, and Potential Applications of Ormosils, *Journal of Sol-Gel Sci. Technol.*, , **1998**, 13, 371-377.

422. Avnir, D.; Levy, D.; Reisfeld, R.; *J. Phys. Chem.*, **1984**, 88, 5956.

423. Pope, J. A.; Asami, A.; Mackenzie, J. D.; *J. Mater. Res.*, **1989**, 4, 1018.

424. Wilkes, G. L.; Otter, B.; Huang, H.; *Polymer Prep.*, **1985**, 26, 300.

425. Schmidt, H.; J. Non-Cryt. Solids, **1985,** 73, 681.

426. Mittal, K. L.; Silanes and Other Coupling Agents, *VSP*, **1992**.

427. Stratmann, M.; *Adv. Mater.*, **1990**, 2, 191.

428. Vetter, K. J.; Schultze, J. W.; *J. Electroanal. Chem.*, **1974**, 53, 67.

429. Schultze, J. W.; Koppitz, K. D.; *Electrochim. Acta*, **1976**, 21, 327.

430. Hackermann, N.; Hard, R. M.; *1. Int. Congr. Met. Corros.*, Butterworths, London, **1962**.

431. Pearson, R. G.; *Science*, **1966**, 151, 172.

432. Horner, L.; *Chem. Ztg.*, **1976**, 100, 247.

433. Ulman, H.; *Ultrathin Organic Films*, Academic Press, New York, **1993**.

434. Wilkes, G. L.; Orler, B.; Huang, H.; *Polym. Prepr.*, **1985**, 26, 300.

435. Dislich, H.; *Angew. Chem.*, **1971**, 83, 428.

436. Sakka, S.; Kamiya, K.; *J. Non-Crystl. Solids*, **1980**, 42, 403.

437. Sakka, S.; *J. Non-Crystl. Solids*, **1985**, 73, 651.

438. Klein, L. C.; *Sol-Gel Technology for Thin Films, Fibers, Preforms, Electronics, and Especially Shapes*; Noyes Publications: Park Ridge, NJ, **1988**.

439. Yoldas, B. E.; *J. Non-Crystl. Solids*, **1984**, 63, 145.

440. Ulrich, D. R.; *Chemtech*, **1988**, 18, 242.

441. Brinker, C. J.; Scherrer, G. W.; *Sol-Gel Science, the Physics and Chemistry of Sol-Gel Processing*; Academic Press: San Diego, CA, **1990**.

442. Mackenzie, J. D.; Ulrich, D. R.; Eds.; *Itrastructure processing of Advanced Ceramics*; Wiley-Interscience: New York, **1988**.

443. Yoldas, B. E.; *J. Mater. Sci.*, **1986**, 21, 1086.

444. Sugama, T.; Taylor, C.; Pyrolysis-induced polymetallosiloxane coatings for aluminum substrates, *J. Mater. Sci.*, **1992**, 27, 1723.

445. Koehler, E. L.; Corrosion Under Organic Coatings, *Proc. U.R. Evans International Conference on Localized Corrosion*, NACE, Houston, **1971**, 117.

446. Guruviah, S.; *J. of the Oil and Colour Chemists' Assoc.*, **1970**, 53, 669.

447. Mayne, J. E. O.; *J. of the Oil and Colour Chemists' Assoc.*, **1949**, 32, 481.

448. Thomas, A. M.; Gent, W. L.; *Proc. Phys. Soc.*, **1945**, 57,324.

449. Anderson, A. P.; Wright, K. A.; *Industr. Engng. Chem.*, **1941**, 33, 991.

450. Edwards, J. D.; Wray, R. I.; *Industr. Engng. Chem.*, **1936**, 28, 549.

451. Maitland, C. C.; Mayne, J. E. O.; *Off. Dig.*, **1962**, 34, 972.

452. McSweeney, E. E.; *Off. Dig.*, **1965**, 37, 626.

453. Wheat, N.; *Prot. Coat. Eur.*, **1998**, 3, 24.

454. Hare, C. H.; *Mod. Paint Coat.*, **1986**, 76, 38.

455. Boxall, J., *Polym. Paint Colour J.*, **1989**, 179, 127.

456. Bieganska, B.; Zubielewicz, M.; Smieszek, E.; *Prog. Org. Coat.*, **1988**, 16, 219.

457. Piens, M.; *Evaluations of Protection by Zinc Primers*, Coat. Res. Inst., Limelette, **1990**.

458. Boxall, J.; *Polym. Paint Colour J.*, **1991**, 181, 443.

459. Zimmerman, K.; *Eur. Cot. J.*, **1991**, 1, 14.

460. De Lame, C.; Piens, M.; Reactivite de la Poussiere de zinc avec l'oxygene dissous, *Proc. XXIII Fatipec Congress*, Paris, A29-A36, **1996.**

461. Forsgren, A.; *Corrosion Control Through Organic Coatings*, CRC Press, Boca Raton, FL, **2006**, 115-121.

462. Antropov, L. I.; *Corros. Sci.*, **1967**, 7, 607.

463. Iofa, Z. A.; Batrakov, V. V.; Ba, ChoNgok; *Electrochim. Acta*, **1964**, 9, 1645.

464. Scully, J. C.; *Corros. Sci.*, **1968**, 8, 513.

465. McBee, C. L.; Kruger, J.; *Proceedings, U. R. Evans, International Conference on Localized Corrosion*, 1971, National Association of Corrosion Engineers, Houston, **1974**, 252.

466. Lin, L. F.; Chao, C. Y.; MacDonald, D. D.; *J. Electrochem. Soc*., **1981**, 128, 1194.

467. Abd El Kader, J. M.; El Warraky, A. A.; Abd El Aziz, A. M.; Corrosion Inhibition of Mild Steel by Sodium Tungstate in Neutral Solution, *British Corrosion Journal*, **1998**, 33, 2, 152-157.

CHAPTER II

SYNTHESIS AND CHARACTERIZATION OF OXYANION ESTERS OF α-HYDROXY ACIDS AND THEIR SALTS

2.1 Introduction

In this investigation, environmentally friendly metallo-organic corrosion inhibitors for protection of mild steel and certain aluminum alloys are being sought to replace hexavalent chromium based corrosion inhibitors. For this reason, several corrosion inhibiting species such as hydroxyacids and metal oxyanions were combined in a single compound with the general formula, $(M)_x(\text{hydroxyacid})_y(M'_aO_b)_z$. These were tested alongside the individual components in order to determine whether there were any synergistic interactions. It is important to note that most of the chosen individual components are corrosion inhibitors that were previously commercialized.

Some of these species such as gluconates were commercially available resulting in their direct use with no synthesis required. The common commercial use for these readily available gluconates is in the field of medicinal health as nutritional supplements. Such gluconates of zinc, calcium, magnesium and sodium were used and tested throughout this study as corrosion inhibitors, precursors, or constituents of synergistic corrosion inhibitor formulations.

2.1.1 D-gluconic acid

D-Gluconic acid or 2,3,4,5,6-pentahydroxyhexanoic acid is an organic compound with the formula of $HOCH_2(CHOH)_4CO_2H$. Reported pKa values of D-gluconic acid are in the range of 3.44[1]-3.86[2] with 3.60[3] the most common. Thus in aqueous solutions at neutral pH, gluconic acid produces the gluconate ion, which forms gluconate salts with corresponding metal ions, known as gluconates.

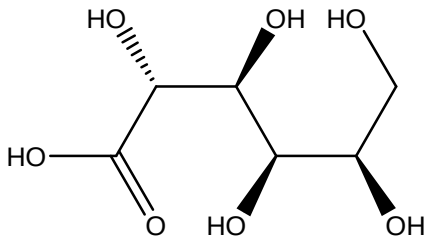

Figure 2-1 Structure of D- gluconic Acid

Gluconic acid and gluconates occur widely in nature due to oxidation of glucose, while in chemistry D-gluconic acid is widely used as an efficient masking reagent for cations.[4] For the purposes of this study, a 50% weight solution of D-gluconic acid was used as a precursor to synthesize gluconate salts that are not readily available such as borogluconate, aluminum gluconate and chromium gluconate. In addition to its use as a precursor, D-gluconic acid has been tested for corrosion inhibition efficiency via the weight-loss method.

2.1.2 Zn(gluconate)$_2$

Zinc gluconate or zinc (2R,3S,4R,5R)-2,3,4,5,6-pentahydroxyhexanoate is a popular form for the delivery of zinc as a dietary supplement. It is found naturally, while

industrially it is manufactured via fermentation of glucose. In its pure form, it is a white to off-white powder. It can also be manufactured by electrolytic oxidation, which yields a lower microbiological profile with longer shelf life, although it is a more expensive process.[5]

Zinc(II) aqua complex reacts with gluconate ion to form monovalent zinc gluconate complex, which leads to the formation of divalent zinc gluconate complex;

$$[Zn(OH_2)_6]^{2+} + HO\text{-}CH_2\text{-}(CH\text{-}OH)_4\text{-}COO^- \longleftrightarrow \{Zn[HO\text{-}CH_2\text{-}(CH\text{-}OH)_4\text{-}COO^-]\}^{+1}$$

(Eq. 2.1)

$$\{Zn[HO\text{-}CH_2\text{-}(CH\text{-}OH)_4\text{-}COO^-]\}^{+1} + HO\text{-}CH_2\text{-}(CH\text{-}OH)_4\text{-}COO^- \longleftrightarrow$$

$$Zn[HO\text{-}CH_2\text{-}(CH\text{-}OH)_4\text{-}COO^-]_2 \qquad \text{(Eq. 2.2)}$$

Formation constant of divalent zinc gluconate is 1.70 indicating a relatively low-strength complex. [6]

Zinc cation mostly forms octahedral complexes, however its tetrahedral complexes are also known. A tetrahedral structure might be favored in aqueous solutions due to charge neutrality and the size difference between the zinc cation with that of gluconate anion as pointed out in the literature. [7]

In this investigation zinc gluconate has been used both as a precursor and as an individual corrosion inhibitor. It is favored due to the additional corrosion inhibition property provided by zinc cations.

2.1.3 Ca(gluconate)$_2$

Calcium gluconate is commonly used as a mineral supplement. It is the form of calcium most widely used in the treatment of hypocalcemia. Calcium gluconate has also been used extensively in this study for the same reasons as zinc gluconate. Calcium gluconate is also a coordination compound with a low stability constant of 1.21[6].

2.1.4 Mg(gluconate)$_2$

Magnesium gluconate is used as a supplement to maintain adequate magnesium in the body and is used to treat low blood magnesium. The latter condition is caused by gastrointestinal disorders, prolonged vomiting or diarrhea, kidney disease, or certain other conditions. Certain drugs lower magnesium levels as well. Magnesium gluconate was tested for its corrosion inhibition efficiency in this investigation for comparison to other gluconates with different cationic constituents. It has not been used as a precursor. Similar to the aforementioned gluconate salts magnesium gluconate is a coordinaton complex compound with a low stability constant of 0.70[6].

2.1.5 Na(gluconate)

Sodium Gluconate is a high quality crystalline sodium salt of gluconic acid. It appears as white crystals that exhibit high solubility. This non-corrosive, non-toxic and highly pure gluconate is an excellent choice when dry material is preferred. Like

magnesium gluconate, sodium gluconate also has not been used as a precursor and has only been tested for its corrosion inhibition efficiency in this investigation.

2.2 Other Readily Available Compounds

Readily available compounds could be further categorized based on their use as corrosion inhibitors, precursor, or both.

2.2.1 Readily available compounds solely tested as corrosion inhibitors

These compouns included L-lactic acid, aluminum acetate hydroxide stabilized with boric acid, aluminum lactate, chromium acetate hydroxide, commercial chromium oxyhydroxide, chromium acetate molybdate, and MEEA {[(methoxyethoxy)ethoxy]acetic acid} that is tested for aluminum corrosion inhibition. MEEA is used in synthesis of carboxylate-alumoxanes, that serve as precursors for developing aluminum-based ceramic membranes and filters[8] and the coating procedure based on carboxylate-alumoxanes is economical and environmentally benign.[8,9]

2.2.2 Readily available compounds solely used as precursor

Among these compounds were benzilic acid, octanoic acid, caproic acid, butyric acid, propionic acid, acetic acid, methoxy acetic acid, gallic acid, mandelic acid, tartaric acid, aluminum acetate hydroxide, chromium nitrate, chromium chloride, molybdenum trioxide, vanadium oxide, potassium carbonate, sodium hydroxide, ammonium hydroxide, potassium hydroxide, sodium tetraborate, iron nitrate, and zinc nitrate.

2.2.3 Readily available compounds used both as precursor and corrosion inhibitors

Examples to this category of compounds are boric acid, D-glucose, chromium acetate in addition to the gluconates explained individually in the first section.

2.3 Synthesis

Salts of α-hydroxy acids, that were not commercially available, were synthesized by reacting the corresponding α-hydroxy acid with metal cation hydroxide, carbonate, or acetate. All reagents were ACS reagent grade or higher and used without further purification. Small amounts of reactants, such as 20 mmols equaling to one equivalance, were refluxed in 100 ml up to several hundred ml of distilled water for a few hours up to a period of overnight, followed by the isolation of product mostly via rotary evaporation or by precipatition in methanol given the product is not soluble in methanol. Examples of hydroxy acid salts synthesized via described method were $Al(gluconate)_2OH$, $B(gluconate)_2OH$ and $Cr(gluconate)_3$. Please refer to Table 2-1 for further details.

Table 2-1 Designated Reagent/Solvent Amounts for Synthesis Reactions

Product	Reagents	Amount (mmols)	Water/Soln. (ml)	Additional Information
Calcium Gluconate	Calcium Gluconate	20	100	
	Molybdenum Trioxide	20		
Zinc Gluconate Molybdate	Zinc Gluconate	20	100	
	Molybdenum Trioxide	20		
Calcium Gluconate	Calcium Gluconate	20	100	
	Vanadium Penta Oxide	10		
Zinc Gluconate Vanadate	Zinc Gluconate	20	100	
	Vanadium Penta Oxide	10		
Potassium Benzilate	Potassium Carbonate	10	200	Room Temp.
	Benzilic Acid	20		
Potassium Benzilate	Potassium Benzilate	20	200	
	Molybdenum Trioxide	10		
Potassium Benzilate	Potassium Benzilate	20	200	
	Vanadium Pentaoxide	10		
Calcium Gluconate Borate	Calcium Gluconate	20	200	
	Boric Acid	20		
Zinc Gluconate Borate	Zinc Gluconate	20	200	
	Boric Acid	20		
Potassium Benzilate Borate	Potassium Benzilate	20	200	
	Boric Acid	20		
Borogluconate	D-Gluconic Acid Soln.	10	96 or 98 ml water,	
	Boric Acid	10 or 20	100 ml soln.	
Boroglucose	D-Glucose	20	100	
	Boric Acid	20 or 40		
Aluminum Gluconate	D-Gluconic Acid Soln.	400	75 ml water,	18%*
	Aluminum $(Acetate)_2$	200	150 ml soln.	
Zinc Benzilate Molybdate	Zinc Chloride	20	100.	room temp.
	Potassium Benzilate	20		

Table 2-1 (Continued)

Product	Reagents	Amount (mmols)	Water/Soln. (ml)	Additional Information
Chromium Gluconate	D-Gluconic Acid	30	88 or 94 ml water, 100 ml soln.	
	Chromium Acetate	10		
Chromium Methoxyacetic	Methoxyacetic Acid	30	100	
	Chromium Acetate	10		
Chromium Gluconate Borate	Chromium Gluconate	30	150	
	Boric Acid	30 or 60		
Chromium Borate	Chromium Gluconate-1borate	1 g	fired at 350 ˚C	66.86%**
	Chromium Gluconate-2borate	1 g	fired at 380 ˚C	73.71%***
Chromium Oxyhydroxide	Chromium Borate	20	100	room temp.[1] 137%[2]
	0.1 M NaOH Soln.	20		
Chromium Gluconate	Chromium Gluconate	20	100	
	Molybdenum Trioxide	20		
Chromium Gluconate	Chromium Gluconate	20	100	
	Vanadium Pentaoxide	10		
Sodium Octanoate	Octanoic Acid	500	500	
	Sodium Hydroxide	500		
Chromium Octanoate	Sodium Octanoate	500	250	
	Aqua Chromium Nitrate	167		
Sodium Caproate	Caproic Acid	500	500	
	Sodium Hydroxide	500		
Chromium Caproate	Sodium Caproate	500	500	[3]
	Nona Aqua Chromium Nitrate	167		
Chromium Hydroxide	Hexaaqua Chromiumtrichloride	45	23 ml of 30% NH_4OH diluted to 100 ml + 500 ml water = 600 ml soln.	62.4%*
	2N Ammonium Hydroxide	200		

Table 2-1 (Continued)

Product	Reagents	Amount (mmols)	Water/Soln. (ml)	Additional Information
Chromium Hydroxide	0.05M Nona Aqua Chromium Nitrate	10	200 ml of first + 600 ml of second, 800 ml total soln.	58.3%* , [4]
	0.05M Potassium Hydroxide	30		
Chromium Tetraborate	Sodium Tetraborate	20	fused using a torch	
	Nona Aqua Chromium Nitrate or Chromium Acetate	1 of first, 3.5 of second		
Chromium Tetraborate	Sodium Tetraborate	15	50 ml of the first added to 400 ml of the second = 450 ml	75%[5]
	Nona Aqua Chromium Nitrate	10		
Iron Chromium Tetraborate	Iron Nitrate	10	250	90%[6]
	Nona Aqua Chromium Nitrate	20		
	Sodium Tetraborate	45		
Sodium Butyrate	Butyric Acid	500	500	
	Sodium Hydroxide	500		
Chromium Butyrate	Sodium Butyrate	300	250	[7]
	Nona Aqua Chromium Nitrate	100		
Sodium Propionate	Propionic Acid	500	500	
	Sodium Hydroxide	500		
Chromium Propionate	Hexa Aqua Chromium Chloride	100	250	[8]
	Sodium Propionate	300		
Sodium Methoxy Acetate	Methoxy Acetic Acid	300	23 ml of first + 227 ml water = 250 ml soln.	
	Sodium Hydroxide	300		

Table 2-1 (Continued)

Product	Reagents	Amount (mmols)	Water/Soln. (ml)	Additional Information
Chromium Methoxy Acetate	Hexa Aqua Chromium Chloride	100	100	[9]
	Sodium Methoxy Acetate	300		
Ammonium Mandelate	Ammonium Hydroxide	20	100	
	Mandelic Acid	20		
Zinc Mandelate	Zinc Nitrate	15	150	75%[10]
	Ammonium Mandelate	15		
Sodium Tartrate	Sodium Hydroxide	20	100	
	Tartaric Acid	20		
Zinc Tartrate	Zinc Nitrate	40	150	
	Sodium Tartrate	40		
Ammonium Gallate	Ammonium Hydroxide	100	250	
	Gallic Acid	100		
Zinc Gallate	Zinc Nitrate	50	150	
	Ammonium Gallate	50		

*ceramic yield

**ceramic yield for chromium gluconate with one equivalence of borate

*** ceramic yield for chromium gluconate with two equivalences of borate

[1] reflux leads to oxidation of Cr^{3+} to Cr^{6+}

[2] yield calculated w/ respect to product formula of CrOOH, result suggested dihydrate structure

[3] Product is slightly soluble in methanol

[4] using reagents with 0.01 M concentration did not result in precipitation

[5] w/respect to product formula of $Cr_2(B_4O_7)_3$

[6] w/respect to product formula of $FeCr(B_4O_7)_3$

[7] Product is soluble in methanol

[8] Due to oxidation of chromium nitrate, chromium chloride was preferred. Product is slightly soluble in water. Ethanol was used to purify product from NaCl.

[9] Ethanol was used to purify product from NaCl

[10] w/respect to product formula of sodium mandelate

Additional Information

- Unless stated all products were obtained via reflux. Exceptions were reactions at room temperature, at 350 ˚C, and at 380 ˚C.
- D-gluconic acid was available as a water solution, thus water from the reagent solution in included in total water amount as well.
- In addition to the mentioned amounts of reagents, very high amounts of reagents were also used in the same proportions to synthesize products in bulk amounts when needed in weight-loss and salt fog chamber tests.
- Yield was not measured for many products, in particular for gluconate salts and their esters due to their very high hygroscopic nature leading to errors.

2.3.1 Synthesis of Gluconate Salts

$Al(gluconate)_2OH$

$Al(gluconate)_2OH$ was synthesized by reacting $Al(acetate)_2OH$ and D-gluconic acid via reflux for overnight. Thermogravimetric analysis of the product conducted using a Seiko EXSTAR 6000 TG/DTA 6200 instrument with temperature ramped from 25 °C to 1000°C at a rate of 5 °C/min under a 50 ml/min flow of dry air, revealed a single decomposition step above 400 ˚C corresponding to oxidation of the gluconate. The ceramic yield was recorded as 18 %.

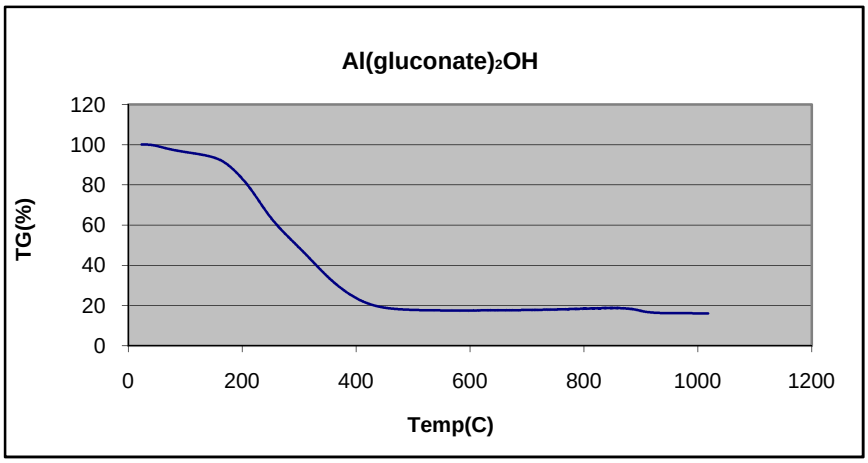

Figure 2-2 Thermogravimetric Analysis of Aluminum Gluconate Hydroxide

B(gluconate)$_2$OH and B(glucose)

Boron gluconate, or with its more common name borogluconate is used to treat hypocalcemia, also called parturient paresis and commonly called milk fever, in the form of calcium borogluconate.[10,11]

Calcium Borogluconate is one of the most widely used calcium salts for the treatment of hypocalcaemia, since it is more soluble, more rapidly absorbed, and less irritating than calcium gluconate.[12]

B(gluconate)$_2$OH was synthesized via reaction of D-gluconic acid with boric acid, while boron glucose was synthesized via reaction of D-glucose with boric acid. Both products were soluble in methanol, thus they were isolated via rotary evaporation. Different from the other tested metal oxyanion salts, structure of borogluconate is likely a monovalent complex in which gluconate is a bidentate ligand.

Cr(gluconate)$_3$

Chromium gluconate in the form of violet crystal powder is used as the additive of medicine or food. It is easily absorbed by human body and serves to promote childhood growth and cure diabetes, arteriosclerosis, coronary heart disease and myopia of young boys and girls. It is a marvelous nutritional supplement to take when on a weight-loss diet and is sold in vitamin stores. Thus, chromium gluconate was synthesized due to trivalent chromium compounds are much more acceptable environmentally than hexavalent chromium compounds as corrosion inhibitors. One equivalence of Cr(acetate)$_3$ is refluxed with three equivalences of gluconic acid in a sufficient amount of distilled water. Gluconate replaces acetate in time to form the desired product of chromium gluconate. The reaction proceeds slowly due to the low solubility of acetate. Only after several hours gluconate starts to replace the acetate extensively, thus this particular reflux process took more time than the other gluconate syntheses. After the reflux, the solution was cooled down and evaporated via rotary evaporation. The final precipitate was dried in vacuum to yield a dark violet-black solid. Chromium gluconate complex is also reported in the literature.[13-15]

2.3.2 Synthesis of Gluconate Esters of Selected Oxyanions

Synergistic combinations of corrosion inhibitors have been the most promising candidates for the replacement of hexavalent chromium compounds. For this reason, benzilate and gluconate salts were reacted with molybdenum, and vanadium oxides and boric acid to produce the corresponding esters. Most often 20 mmols of gluconate salt was reacted with sufficient amount of metal oxyanion in 100 ml to 200 ml distilled water.

Three metal oxyanions used as reactants with gluconates; thus the following reactions were performed;

$$M(\text{gluconate})_2 + MoO_3 \xrightarrow[2)\ \text{precipitation/methanol}]{1)\ \text{reflux}/H_2O} M(\text{gluconate})_2\text{molybdate} \quad \text{(Eq. 2.3)}$$

$$2M(\text{gluconate})_2 + V_2O_5 \xrightarrow[2)\ \text{precipitation/methanol}]{1)\ \text{reflux}/H_2O} 2M(\text{gluconate})_2\text{vanadate} \quad \text{(Eq. 2.4)}$$

$$M(\text{gluconate})_2 + H_3BO_3 \xrightarrow[2)\ \text{precipitation/methanol}]{1)\ \text{reflux}/H_2O} M(\text{gluconate})_2\text{borate} \quad \text{(Eq. 2.5)}$$

where M = Zn^{2+} or Ca^{2+}.

Various complexes of molybdenum and vanadium with gluconic acid have been reported in the literature.[16,17]

In addition to calcium and zinc gluconates, trivalent chromium gluconates were used as reactants with proper stoichiometry. After completion of reflux, resulting solution was partially evaporated until a concentrate solution is obtained via rotary evaporation. The saturated solution was then added dropwise to 100 ml to 200 ml of methanol under constant stirring for precipitation of the product. The product was then filtered followed by rinsing with acetone to remove excess water. Finally, the product was isolated after drying in vacuum. Products with various colors such as dark blue-purple $Ca(\text{gluconate})_2$molybdate, navy-black $Cr(\text{gluconate})_3$molybdate or dark green-black $Cr(\text{gluconate})_3$vanadate were synthesized.

Although the same method has been used for the synthesis of all gluconate metal oxyanion esters, not all the products could be isolated due to their highly hygroscopic

nature. Such products were kept in solution form as in the cases of zinc gluconate molybdate and calcium gluconate vanadate. Other products, that were less hygroscopic enough to isolate, were still too hygroscopic to perform gravimetric calculations.

- M = Zn++ or Ca++

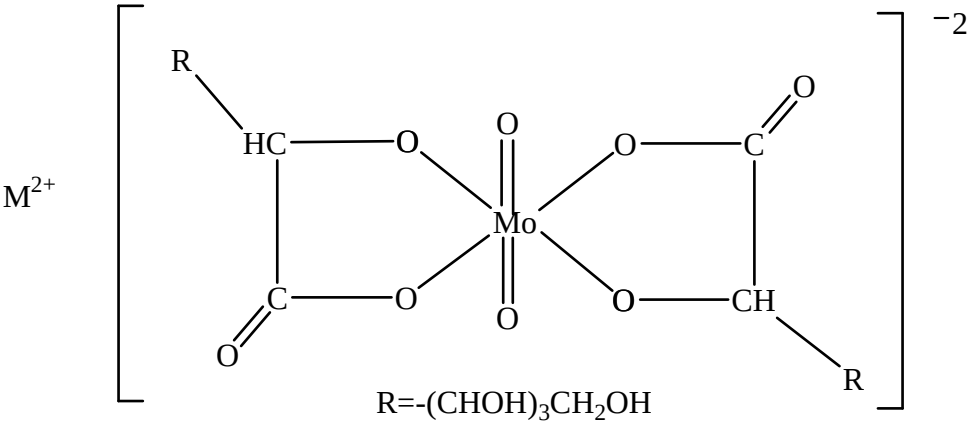

Figure 2-3 Structure of Zinc or Calcium Gluconate Molybdate

Synthesis of Cr(gluconate)$_3$.xborate

Chromium gluconate borate was synthesized with both one and two equivalences of boric acid per equivalence of Cr(gluconate)$_3$. Both mixtures were refluxed for two days in sufficient amount of water and after isolating the products, they were obtained as black and hygroscopic solids. Attempts to obtain a less hygroscopic product by either decreasing the amount of water in the solution or purification of the chromium gluconate beforehand, or changing the reaction time were not effective.

Thermogravimetric analyses of both chromium gluconate borates revealed that increasing the proportion of the boron constituent within chromium gluconate borate ester resulted in an increase in both the decomposition temperature from 350 $^{\circ}$C up to 380 $^{\circ}$C and the ceramic yield from 21% to %28.

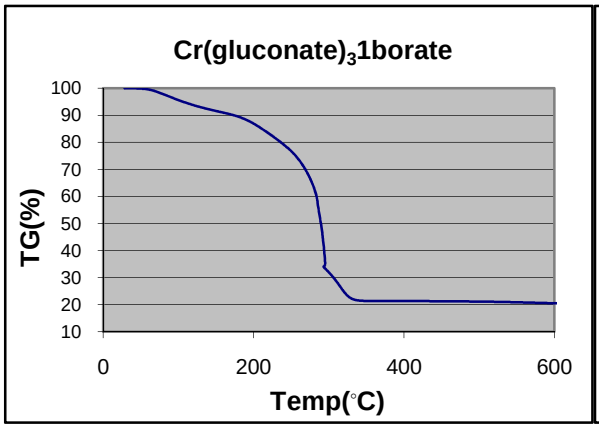

Figure 2-4 Thermogravimetric Analysis of Chromium Gluconate Borate with One Equivalence

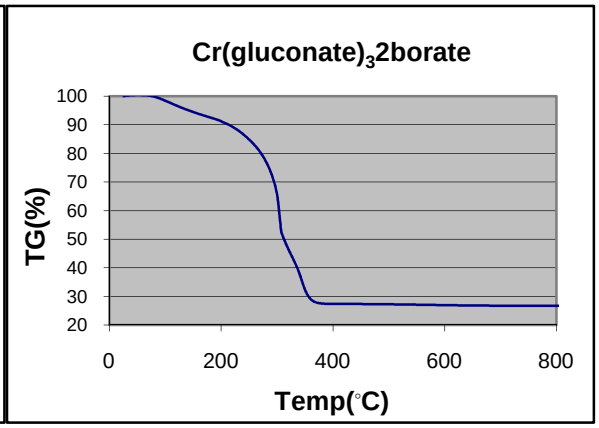

Figure 2-5 Thermogravimetric Analysis of Chromium Gluconate Borate with Two Equivalences

Similar to the other metal oxyanion esters of gluconates, chromium gluconate borates were also very soluble in water.

2.3.3 Syntheses of Benzilate Salts and Their Metal Oxyanion Esters

Benzilates were expected to be promising complexing agents primarily for use in synergistic corrosion inhibitor formulations. The primary reason for this consideration was the relatively lower solubility of benzilates compared to gluconates, which could lead to optimum corrosion protection since most of the inhibitor formulations inhibit corrosion eventually by precipitating on anodic and cathodic sites, where further corrosion reactions are blocked.

For the syntheses of metal oxyanion benzilates, first potassium benzilate was synthesized by dissolving 20 mmols of benzilic acid in about 200 ml distilled water.

Later 10 mmols of K_2CO_3 was added to the stirred benzilic acid solution at a rate that avoided foaming of the solution by the released carbon dioxide.

Next the potassium benzilate solution obtained from the first step was refluxed with the corresponding metal oxide in water until a clear solution was obtained. The products were relatively easier to isolate than the corresponding gluconate esters due to their less hygroscopic nature. An exception was dark gray-black K(benzilate)vanadate that was kept in solution due to its highly hygroscopic nature compared to other benzilate esters. After several months the initially soluble K(benzilate)vanadate particles were observed to precipitate out of the solution forming a brown precipitate compared to the initial dark grayish color. Filtering this solution and attempting to redissolve it in water easily led to the formation of a suspension that is stable for several days.

$$\text{K(benzilate)} + MoO_3 \xrightarrow[\text{2) precipitation/methanol}]{\text{1) reflux/}H_2O} \text{K(benzilate)molybdate} \qquad \text{(Eq. 2.6)}$$

$$2\text{K(benzilate)} + V_2O_5 \xrightarrow[\text{2) precipitation/methanol}]{\text{1) reflux/}H_2O} 2\text{K(benzilate)vanadate} \qquad \text{(Eq. 2.7)}$$

$$\text{K(benzilate)} + H_3BO_3 \xrightarrow[\text{2) precipitation/methanol}]{\text{1) reflux/}H_2O} \text{K(benzilate)borate} \qquad \text{(Eq. 2.8)}$$

It is reported in the literature that molybdenum(VI)-benzilic acid system forms stable complexes.[18,19] One of these complexes is in dimeric structure similar to the structure of gluconate molybdate complex as shown in Figure 2-3, while the other complex consists of two benzilate ligands along with two molybdenum cores connected via oxygen bridges with formation constants of $\beta = 17.35$ for the former and $\beta = 29.07$ for the latter.[18]

Complexes of vanadium(V)-benzilic acid are also mentioned in the literature, however these complexes usually seem to involve another ligand as well such as pyridine, thiol, or salen.[20-26]

In addition to the salts and esters of benzilic acid and gluconic acid; salts of lactic acid, methoxyacetic acid, D-glucose and a few others were also synthesized via similar methods.

2.3.4 Synthesis of $CrBO_3$

TGA analyses of the previously synthesized Cr(gluconate)$_3$.xborate samples revealed decomposition temperatures of 350 ˚C and 380 ˚C, for Cr(gluconate)$_3$.1borate, and Cr(gluconate)$_3$.2borate, respectively. The samples were fired overnight at corresponding decomposition temperatures under ambient conditions. Weight losses due to firing the samples were recorded in the range of 68.89 % to 78.37 % indicating the loss of bulky gluconate groups. Preliminary XRD of the fired Cr(gluconate)$_3$.xborate samples revealed mixed phases due to possible byproducts and excess reactants. One of the phases was found to be boric acid. Therefore, fired Cr(gluconate)$_3$.xborate samples were washed and stirred with sufficient water overnight and then filtered following by drying in vacuum yielding a black colored product. The washing solution had a yellow color, suggesting that some chromium oxidized to hexavalent chromium during firing. Presence of hexavalent chromium was also confirmed by weight-loss tests using the nonpurified batch of chromium borate, which had inhibited corrosion of mild steel successfully unlike the purified batch. The additional weight-loss, after thorough washing, filtering and drying processes, was recorded as 10.4 %. XRD of the purified product after firing

revealed the product was amorphous. The absence of crystalline impurities indicated successful purification. Weight-losses due to firing of chromium gluconate borate suggested the product formula to be $CrBO_3$.

Thermogravimetric analysis of this purified $CrBO_3$ sample revealed a decomposition temperature of 670 ˚C. Overnight firing of the sample at 670 ˚C resulted in a product that had a one-to-one match with XRD pattern of chromium oxide.

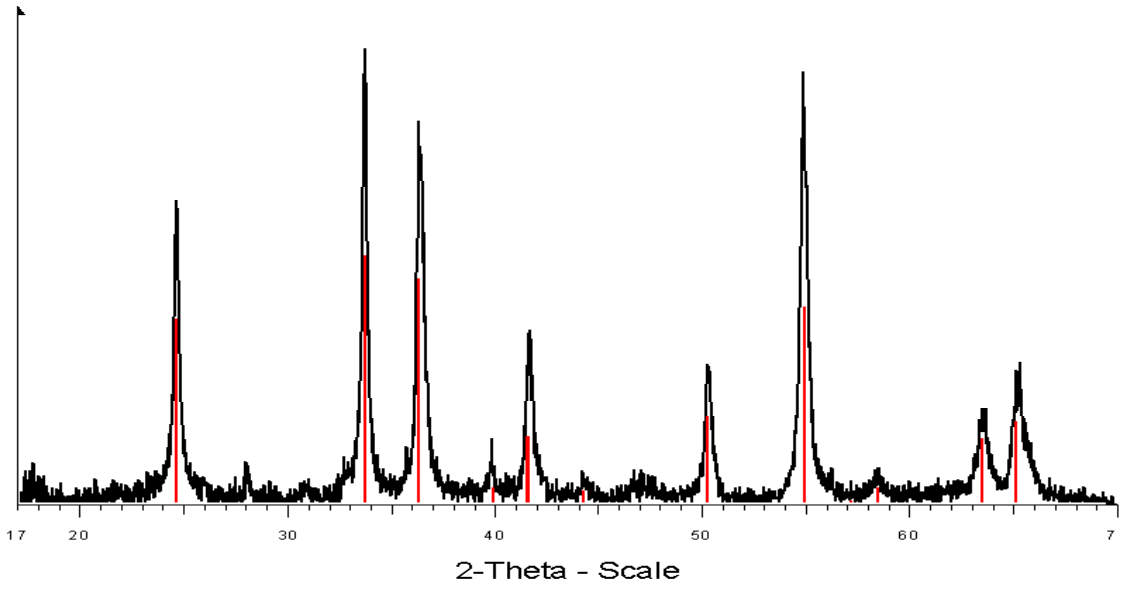

Figure 2-6 X-ray Diffraction Pattern of Sintered $CrBO_3$

The same result was also reported in the literature that firing of chromium borate results in the formation of Cr_2O_3.[27-29]

2.3.5 Synthesis of CrO(OH)

A few milimoles of purified $CrBO_3$ was added to 100 ml of NaOH and stirred for 12 hours. The solution was filtered and a green product was obtained after drying in

vacuum. A high yield of 96.8% was recorded. In the literature, green pigments based on CrO(OH) with low hardness and low particle sizes along with high coloring ability are manufactured for use in cosmetics by calcination of a 1:4 alkali metal dichromate-H_3BO_3 mixture at 600 ˚C to 800 ˚C. Also known with its common name in cosmetics, chromium hydroxide green is approved by the FDA (U.S. Food and Drug Administration) for use in cosmetics to be applied to the skin and eye area.[30]

The CrOOH produced in this investigation had a small particle size and dispersed well in water and sol-gel coating. Dynamic light scattering of a sample dispersed in water by 15 minutes of sonication gave an average particle size of 318 nm (with a polydispersity of 0.388) indicating the CrOOH pigment is nanoparticulate. In addition, the method used for synthesis is a straightforward, one step reaction, which is performed at ambient conditions rather than syntheses via calcinations, which require high temperatures.[30]

Suspensions of synthesized chromium oxyhydroxide remained stable over a period of one week, but eventually precipitated out due to agglomeration of the particles thereafter, parallel to the results obtained in other studies in the literature.[31] UV visible spectroscopy of the suspended sample of commercial grade CrO(OH), which was conducted using an HP 8453 UV-visible spectrometer via quartz cell with a 10 mm path length, revealed a maximum peak at λ = 267 nm, while UV spectra of suspended sample of synthesized CrO(OH) also revealed a maximum peak at 269 nm with A = 1.381 matching the value for commercial grade CrO(OH). However, the UV spectra of synthesized CrO(OH) resulted in an additional peak at λ = 372 nm with an absorption value of 1.353.

X-ray measurements did not reveal a crystalline pattern suggesting an amorphous structure. X-ray diffraction studies of nanoparticulate chromium hydroxide prepared via different methods also yielded amorphous structures as reported in the literature.[32]

Notably, commercial grade CrO(OH) required sieving with a sieve of 25 µ opening to obtain fine particles in contrast to the synthesized CrO(OH), which had sufficiently fine particles after synthesis with no requirement of sieving.

Heating chromium borate and sodium hydroxide to obtain chromium oxyhydroxide was also attempted, however the resulting solution obtained was dark yellow in color indicating the presence of hexavalent chromium via oxidation of trivalent chromium.

2.3.6 Synthesis of Zinc Carboxylates

Due to well-known cathodic inhibitive property of zinc cations, synergistic combinations of zinc cations with hydroxy acids were attempted. For this purpose, hydroxy acids with varying solubilities were chosen as reactants such as mandelic, tartaric, and gallic acids. The first step of the synthesis was the formation of the sodium or ammonium salt of the hydroxy-acid by reacting it with ammonium or sodium hydroxide. The byproducts NH_4NO_3 and $NaNO_3$ were washed away during filtration. In the second step, these hydroxy acid salts were reacted with zinc nitrate to form the desired product.

Zinc tartrate

Zinc tartrate was synthesized from sodium tartrate and zinc nitrate. Zinc tartrate's XRD pattern was isostructured to that of manganese tartrate as shown in Figure 2-8.

Zinc mandelate

Zinc mandelate was synthesized via reaction of ammonium salt of mandelic acid with zinc nitrate.

Zinc gallate

Like zinc mandelate, zinc gallate was synthesized from ammonium salt of gallic acid and zinc nitrate. Gallic acid has been chosen as a reactant since its structure mimics the chemicals that mussels use to adhere to both inorganic and organic surfaces. Among this group of chemicals of substituted phenols that mussels use is 3,4-dihydroxy-L-phenylalanine.

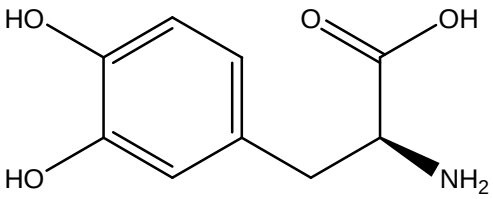

Figure 2-7 Structure of 3,4-dihydroxy-L-phenylalanine

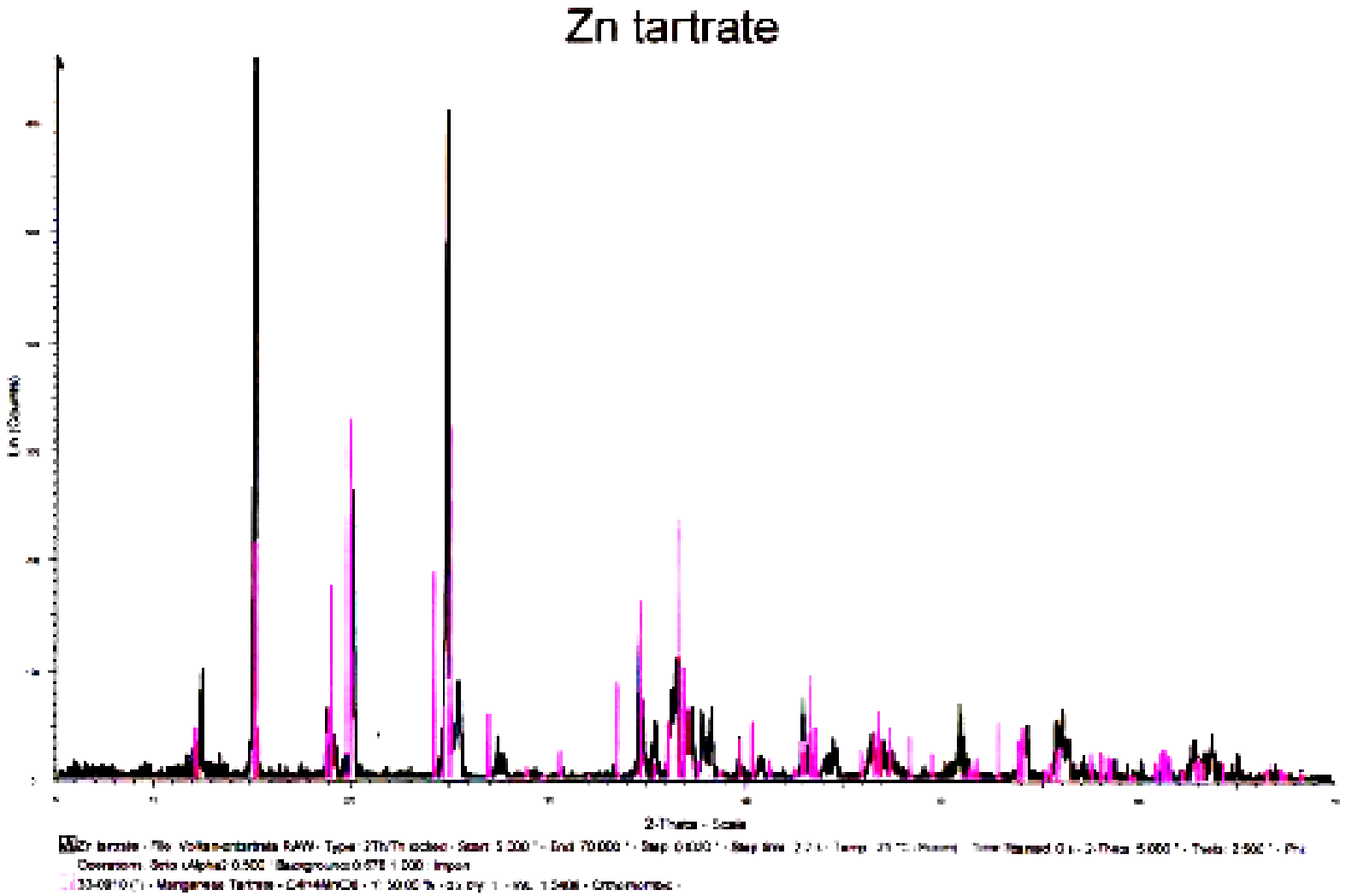

Figure 2-8 X-ray Diffraction Pattern of Zinc Tartrate

2.3.7 Synthesis of Chromium(III) Carboxylates

Various chromium carboxylates were synthesized in the search for one that was optimally soluble to incorporate into sol-gel coatings. Among these carboxylic acid precursors were octanoic acid, caproic acid, butyric acid, propionic acid, and acetic acid in the order of decreasing number of carbon atoms in the alkyl chains.

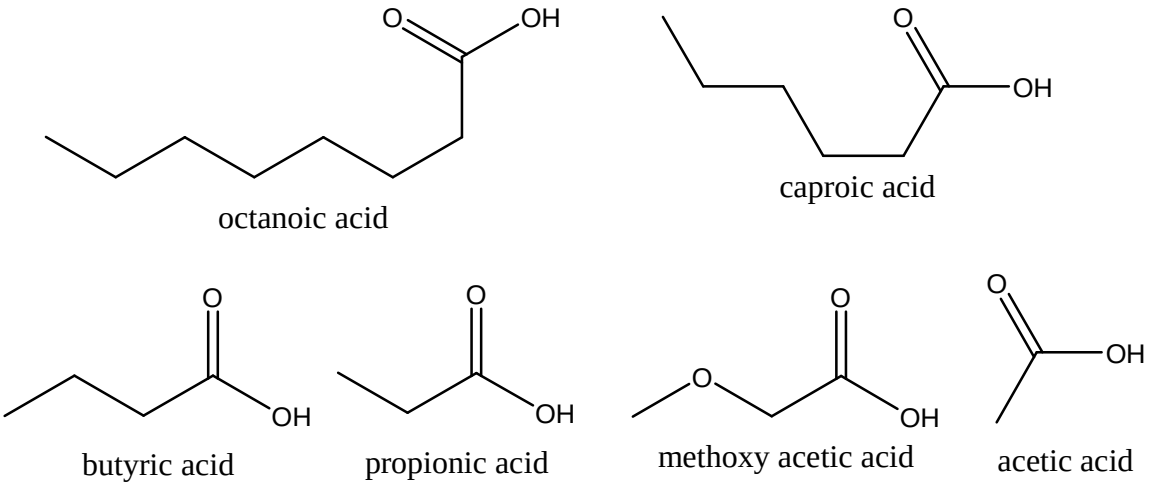

Figure 2-9 Structures of Carboxylic Acids That were Used for Trivalent Chromium Carboxylate Syntheses

The first step of the syntheses was preparation of the sodium salts by reacting them with sodium hydroxide. The sodium carboxylates were then isolated as yellow to clear yellow color jelly-like substances.

Secondly, sodium salts produced from the first step were reacted with chromium(III) nitrate in 3:1 proportions to obtain the corresponding chromium carboxylate. In general, chromium(III) nitrate was preferred over chromium(III) chloride as precursor to avoid corrosion accelerating chloride ions with the exception of synthesis

of chromium butyrate, in which byproduct sodium nitrate was observed to decompose into nitrogen dioxide during filtration.

Chromium Octanoate and Chromium Caproate

Both chromium octanoate and chromium caproate were precipitated out of the solution during reflux due to insolubility in water. Excess water, which contains the byproduct sodium nitrate, was decanted. Chromium octanoate was dried in oven at 55 ˚C, while chromium caproate was first dissolved in methanol due to its sufficient solubility unlike chromium octanoate followed by its drying at 55 ˚C after evaporation of methanol. Cleaning of glassware containing both chromium caproate and chromium octanoate was proven to be difficult. Both chromium octanoate and chromium caproate were very viscous products such that nitric acid has been used to clean the glassware containing both products.

Chromium Butyrate

Chromium butyrate formed a suspension in water, so there was no phase separation after the reflux unlike chromium carboxylates with longer alkyl chains. The product was thoroughly washed with water and filtered afterwards to remove the byproduct sodium nitrate. Subsequent vacuum drying yielded a green colored product. Chromium butyrate forms suspensions in water and methanol as implied by dynamic light scattering measurements in Figure 2-11 and Figure 2-12.

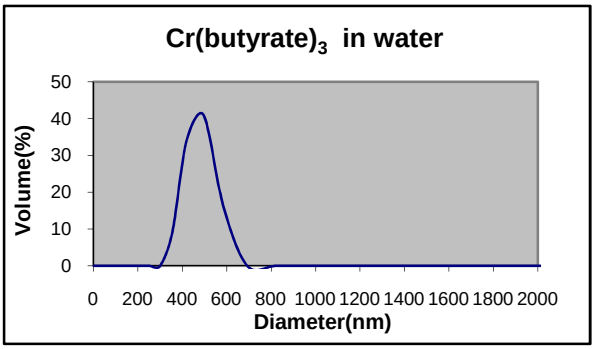

Figure 2-10 Dynamic Light Scattering Result for Chromium Butyrate in Water

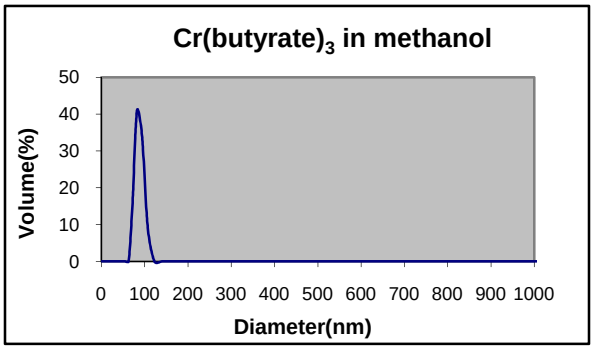

Figure 2-11 Dynamic Light Scattering Result for Chromium Butyrate in Methanol

Attempts to crystallize chromium butyrate for X-ray diffraction measurements were unsuccessful. Among these attempts were dissolving the product in ethanol, in which chromium butyrate was considerably soluble, followed by its slow evaporation in narrow vials under refrigeration or trying various other solvent compositions besides ethanol such as pure isopropanol or 90% isopropanol-10% water mixture. Initially used sodium nitrate was discontinued to be used due to problems occurred during reflux. It was likely that the batch of sodium nitrate contained oxides or possibly even acids since a redox process occurred during the synthesis. NO_2 was observed to evolve from the refluxing solution by its characteristic orange fumes. The solution pH also decreased. Therefore, chromium chloride was used as a reagent. To remove sodium chloride the product was washed first with water and secondly with ethanol since the product is soluble in ethanol while sodium chloride is not. Finally, the product was tested for presence of chloride with silver nitrate and no precipitation was observed indicating absence of chloride.

Chromium Propionate

Chromium propionate was synthesized in the same manner chromium butyrate was synthesized. Given that its alkyl chain is one carbon atom shorter than chromium butyrate, chromium propionate was slightly soluble in water and did not form suspensions.

Chromium Acetate and Chromium Methoxyacetate

Commercially available chromium acetate was directly used without synthesis, while the dark green chromium methoxyacetate was synthesized from methoxyacetic acid and chromium chloride. It was found to be highly soluble in water and methanol and most soluble in the former. However, the byproduct HCl could not be rid completely during rotary evaporation indicated by a low pH and precipitation of silver chloride. Thus a second batch of chromium methoxyacetate was synthesized using sodium methoxyacetate. This produced sodium chloride as a byproduct that could be filtered out after dissolving the product in ethanol in which the chromium methoxyacetate is soluble. The resulting product was checked for chloride presence with silver nitrate and no chloride was found.

2.3.8 Synthesis of Selected Chromium(III) Compounds

Due to the success that was achieved with chromium oxyhydroxides inhibiting corrosion; other inorganic trivalent chromium compounds were synthesized. Among these chemicals were chromium tetraborate, iron chromium tetraborate, and chromium

hydroxide. In addition commercially available chromium acetate hydroxide was also tested.

Chromium tetraborate

For the synthesis of chromium tetraborate, chromium nitrate was first fused with borax (sodium tetraborate) with a 1:10 proportion. However despite a homogenous bead shaped product phase being obtained, Cr^{6+} was also formed during the process due to the high temperatures provided by the torch.

Considering the potential ability of nitrate to oxidize Cr^{3+} to Cr^{6+}; chromium acetate was used as a replacement for chromium nitrate. As a result no yellow or orange colored by-products and, thus, no hexavalent chromium were formed. A single product with a green color was obtained instead. However, isolating the product by its removal from the crucible has proven to be difficult despite trying many solvents.

Finally, a solution chemistry approach was developed, in which stoichiometric amounts of highly soluble reactants were reacted in a small amount of water to produce chromium tetraborate with %70 efficiency after thorough washing to remove sodium nitrate.

$$3Na_2B_4O_7(s) + 2Cr(NO_3)_3.9H_2O\,(s) \xrightarrow[2)\text{vacuum drying}]{1)\,H_2O/\text{filtration}} Cr_2(B_4O_7)_3(s) + 6NaNO_3(s)$$

(Eq. 2.9)

Thermogravimetric analysis of the product indicated a one-phase chromium tetraborate.

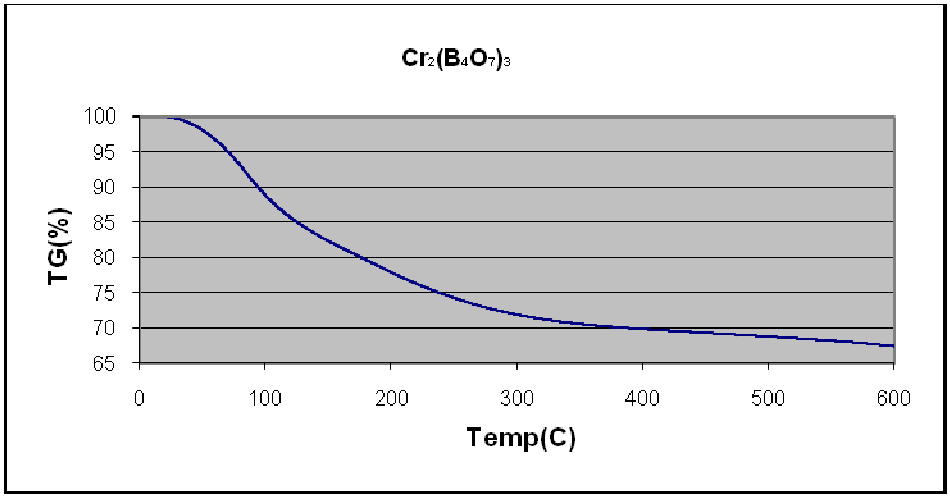

Figure 2-12 Thermogravimetric Analysis of Chromium Tetraborate

Iron Chromium Tetraborate

Sodium tetraborate, chromium nitrate and iron nitrate were precipitated in proportions of 4.5, 2 and 1, respectively yielding a mixed metal borate in a 65% efficiency based on the product formula in eq. 2.10.

$$4Na_2B_4O_7(s) + 2Cr(NO_3)_3.9H_2O\,(s) + Fe(NO_3)_3\,(s) \xrightarrow[2)\text{vacuum drying}]{1)\ H_2O/\text{filtration}} FeCr_2(B_4O_7)_4(s) + 8NaNO_3(s) \qquad \text{(Eq. 2.10)}$$

Chromium Hydroxides

Chromium hydroxide was initially synthesized using very dilute solutions of chromium nitrate and ammonium hydroxide. When mixed resulted in precipitation of fine particles that redissolved due to formation of chromium amine complexes. Attempts to saturate the mixture with KOH to reprecipitate $Cr(OH)_3$ were not successful.

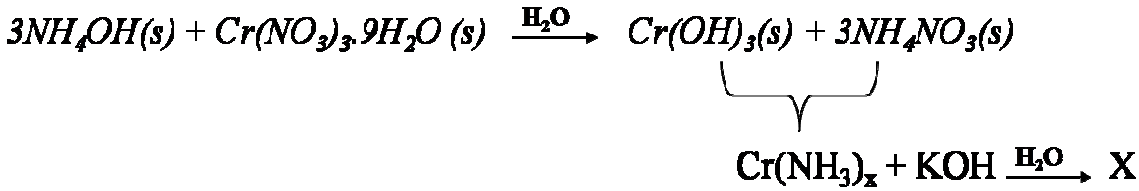

(Eq. 2.11)

Using KOH instead of NH_4OH, and $CrCl_3$ instead of $Cr(NO_3)_3.9H_2O$ prevented formation of soluble products such as chromium ammonia complexes but the product was formed in large particles as demonstrated by dynamic light scattering measurements. Replacing KOH with NH_4OH but keeping $Cr(NO_3)_3.9H_2O$ in the reaction mixture did not produce precipitates at first but increasing the concentrations of the reactants from 0.1 M to 0.3M-0.4M resulted in precipitation of lumpy particles that were hygroscopic in nature.

Finally, using chromium chloride instead of chromium nitrate and ammonium hydroxide instead of potassium hydroxide resulted in stable fine precipitates. The amounts of reactants used were 100 ml 2N ammonium hydroxide and 12 g of chromium chloride, $[Cr(H_2O)_6]Cl_3$, in 500 ml water as described in the literature[33-36] as a method for the synthesis of chromium hydroxide nanoparticles. The product was filtered after decanting and thoroughly washed thereafter until free of NH_4Cl and was then air dried.

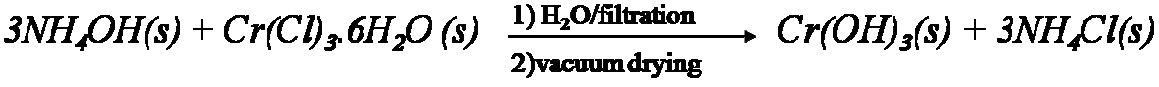

(Eq. 2.12)

Comparison of the thermogravimetric analyses of the chromium hydroxide batches synthesized from chromium chloride and ammonia with that synthesized from chromium nitrate and potassium hydroxide revealed similar results. Chromium oxide was obtained after a loss of water at temperatures of 441 ˚C with 62.4% ceramic yield for the former and at 452 ˚C with 58.3% ceramic yield for the latter.

2.4 Characterization Studies of the Synthesized Compounds

2.4.1 FT-IR Spectroscopic Studies

FT-IR spectroscopy has been used extensively for the characterization of the synthesized chemicals and substrate coupon surfaces immersed in inhibitor solutions. Infrared spectroscopy measurements were performed using a Nicolet Magna-IR 75 spectrometer. Spectra were collected in the 400–4000 cm^{-1} range using 128 scans and a resolution of 4 cm^{-1}. The background was eliminated using spectra of degreased blank alloy coupon as a reference. For the infrared spectra of the synthesized compounds, KBr pellets are prepared carefully. The compositions of the KBr pellets were determined based on the predicted strength of the absorptions of functional groups present in the sample.

Gluconate Salts and Other Hydroxy Salts

Interpretation of IR spectra of the gluconate salts and their esters was based on comparison with spectra of compounds such as calcium gluconate[32] and sodium gluconate[33] that are available at public databases.

Chromium gluconate

FT-IR spectrum of chromium gluconate revealed bands at 3301 cm^{-1}, 1581 cm^{-1}, 1451 cm^{-1}, and 1363 cm^{-1}. Broad band at 3301 cm^{-1} was attributed to symmetric and asymmetric hydroxyl stretchings. It is reported in the literature that bands observed at ca. 1600 and 1385 cm^{-1} in the spectra of metal hydroxyacid salts are due to asymmetric and symmetric OCO^- stretching vibrations[39]. Thus the bands at 1581 cm^{-1} and at 1363 cm^{-1} in the spectra of chromium gluconate were assigned to the asymmetric and symmetric OCO^- stretching vibrations, respectively.

A separation of more than 200 cm^{-1} between the observed OCO^- components in the spectra of the chromium gluconate (also observed for other gluconate salts in this study) can be attributed to monodentate carboxylate coordination as stated in the literature.[40] When compared to the reference compounds, interactions between the hydroxyl groups of the gluconate and the metal ions produces broadening of OH stretching vibrations while interactions between the metal ion and the hydroxy acid in general produces both broadening and shifting of CH_2, COH and CHO bending vibrations, which appear in the region 1400–1100 cm^{-1} in agreement with the literature data.[41] Relatively weaker bands at 1100–940 cm^{-1} could be assigned to the hydroxy acid C–O stretching vibrations in general for gluconates.[39] These absorptions were common to all synthesized gluconate salts with few cm^{-1} frequency differences. In the specific case of chromium gluconate however, additional absorptions at 960 cm^{-1} and in the range of 550-560 cm^{-1} were present due to Cr-O stretching vibrations.[42-46]

Metal Oxyanion Esters of Hydroxy Acid Salts

Calcium gluconate molybdate

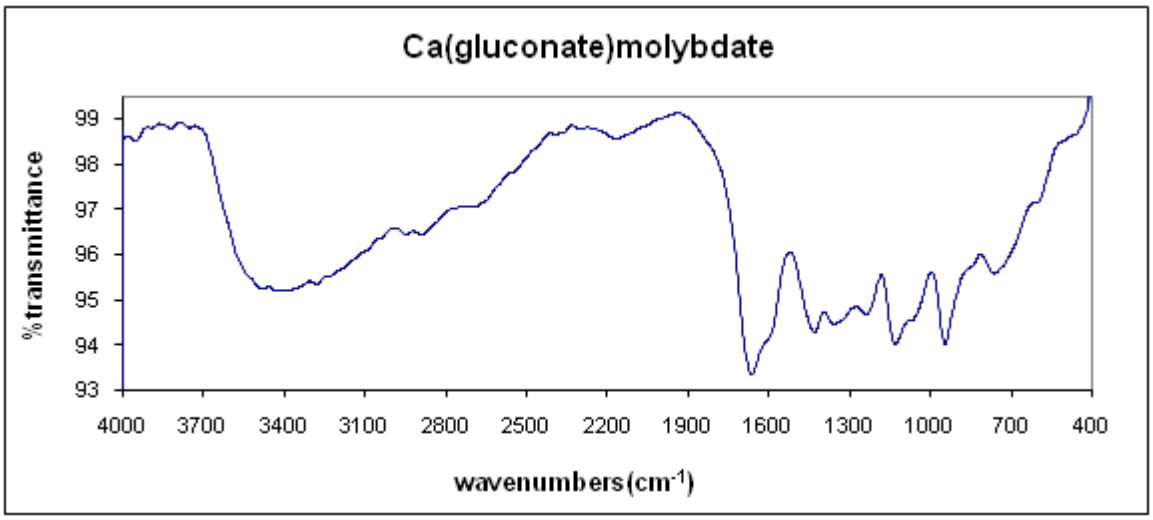

Figure 2-13 Infrared Spectrum of Calcium Gluconate Molybdate

In addition to asymmetric and symmetric stretching of hydroxy group at 3500 cm^{-1}, the asymmetric and symmetric OCO^{-} stretching vibrations at 1620 cm^{-1} and at 1400 cm^{-1}, and CH_2, COH and CHO bending vibrations at 1400–1100 cm^{-1} were present. Absorption at 975 cm^{-1} is assigned to Mo-O vibrational mode since for similar compounds molybdenum oxygen vibrational modes were reported in the literature at 972 cm^{-1} [47], 994 cm^{-1} [48], and 996 cm^{-1} [49].

Chromium gluconate molybdate

As a difference between the FT-IR spectra of calcium and chromium gluconate molybdates, the band for chromium gluconate molybdate that is due to asymmetric stretching vibration of OCO^{-} absorbed at 1594 cm^{-1} corresponding to a shift of around 25 cm^{-1}. [42-45]

Chromium gluconate vanadate

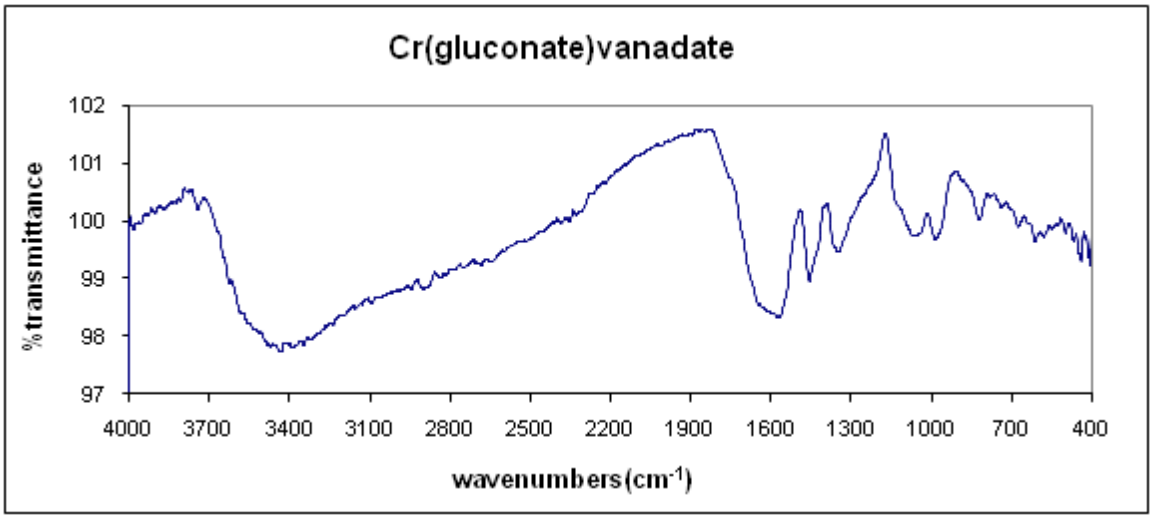

Figure 2-14 Infrared Spectrum of Chromium Gluconate Vanadate

Compared to the infrared spectrum of crystalline V_2O_5[50], absorption bands between 400 cm^{-1} and 1000 cm^{-1} are indexed to various group vibrations of V-O type in general[51,52], which includes bands at 1019 cm^{-1}, 850 cm^{-1}, and between 400 cm^{-1} to 650 cm^{-1} [53]. Thus, in the case of chromium gluconate vanadate band at 1030 cm^{-1} is assigned to stretching vibrations of V=O and band at 850 cm^{-1} is assigned to stretching vibrations of V-O among others. The band at 960 cm^{-1} next to the band of V=O stretching vibration, and bands in the range of 550-560 cm^{-1} are assigned to Cr-O stretching vibrations.[42-46]

Zinc gluconate borate

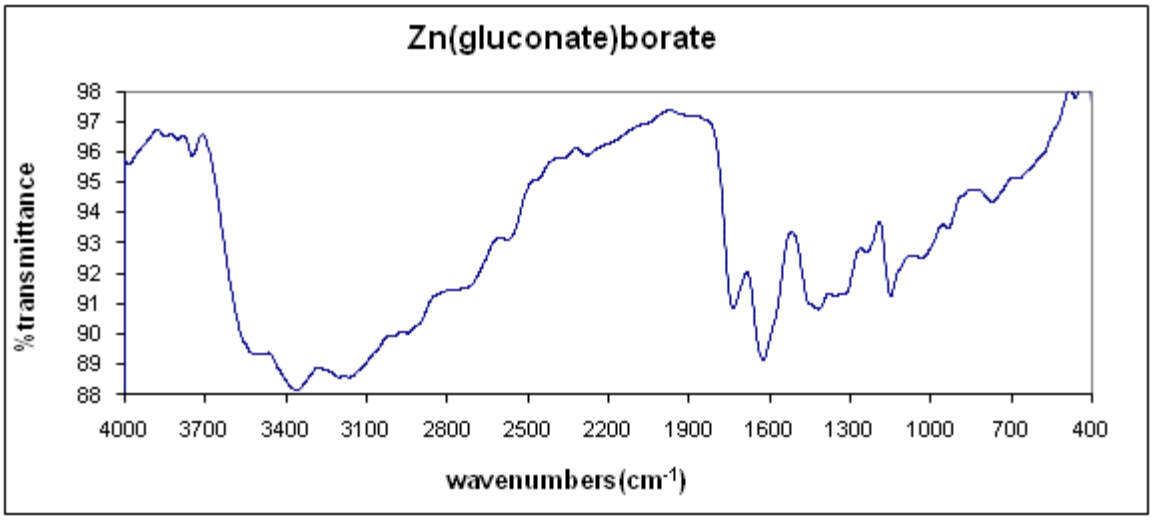

Figure 2-15 Infrared Spectrum of Zinc Gluconate Borate

In addition to the bands due to gluconate, bands between 1300 cm^{-1} and 1450 cm^{-1} were due to trigonal B-O asymmetric stretching, while the band at 1200 cm^{-1} was attributed to bending of B-O-H plane. Relatively weaker bands due to boron constituent between 400 cm^{-1} and 1000 cm^{-1} region are attributed to tetrahedral B-O asymmetric stretching, trigonal B-O symmetric stretching, tetrahedral B-O symmetric stretching, out of plane B-O-H bending, O-B-O ring bending in the order of decreasing frequencies.[54-59] The absence of absorption at 840 cm^{-1} and around 420 cm^{-1} suggests the absence of tetrahedral coordination of Zn[60] and absence of Zn-O[61,62] bond, respectively.

Chromium gluconate borate compounds

As a difference from the FT-IR spectrum of zinc gluconate borate, bands at 960 cm^{-1} were present for both chromium gluconate borates due to Cr-O stretching vibrations, while it was sharper for the one with two equivalences of boron. Another difference between the spectra of chromium gluconate borates was that at 1200 cm^{-1} no band was

present for chromium gluconate borate with one equivalence of boron opposed to the one with two equivalences of boron. Thus, it is assigned to either the bending of the B-O-H plane of the product or to excess boric acid.

Zinc carboxylates

Zinc tartrate

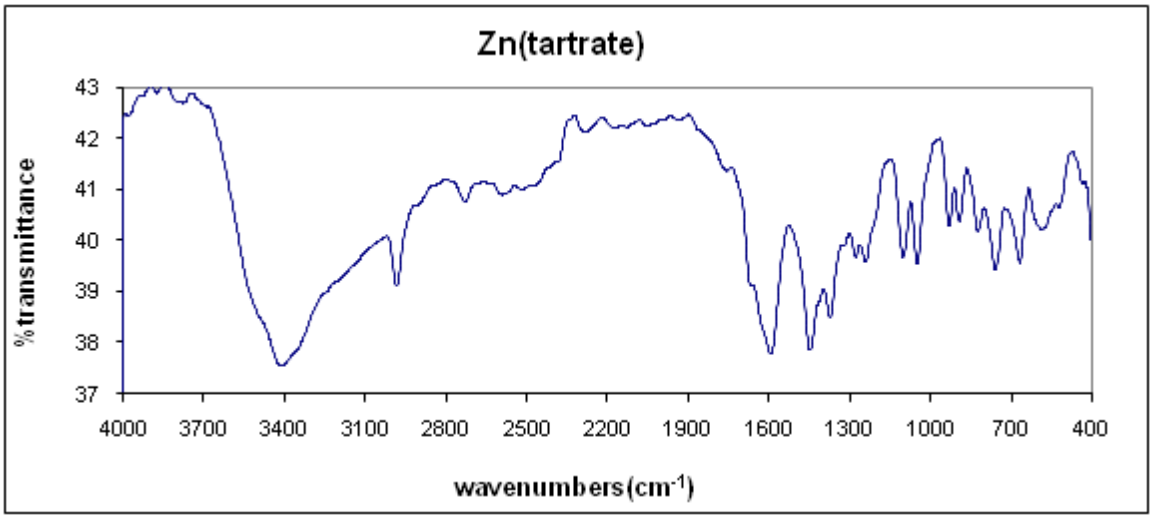

Figure 2-16 Infrared Spectrum of Zinc Tartrate

The IR spectra of zinc tartrate and other zinc carboxylates were similar to the spectra of other hydroxy-acid salts in general with the distinction of broadening of CH_2, COH and CHO bending vibrations and OH stretching vibrations due to metal hydroxy-acid interactions. All bands due to the tartrate constituent had one to one match with that of potassium tartrate measured by a Nicolet 20SX FT-IR as reported in the literature.[63] The absorption at 840 cm^{-1} suggests the presence of tetrahedral coordination of Zn.[60] Absence of any bands at 420 cm^{-1} indicates the absence of Zn-O bond.[61,62]

Other Trivalent Chromium Compounds

Commercial Grade CrO(OH)

Comparison of infrared spectra of synthesized and commercial grade CrO(OH) batches assisted in assessment of the purity of the samples as well as their characterization.

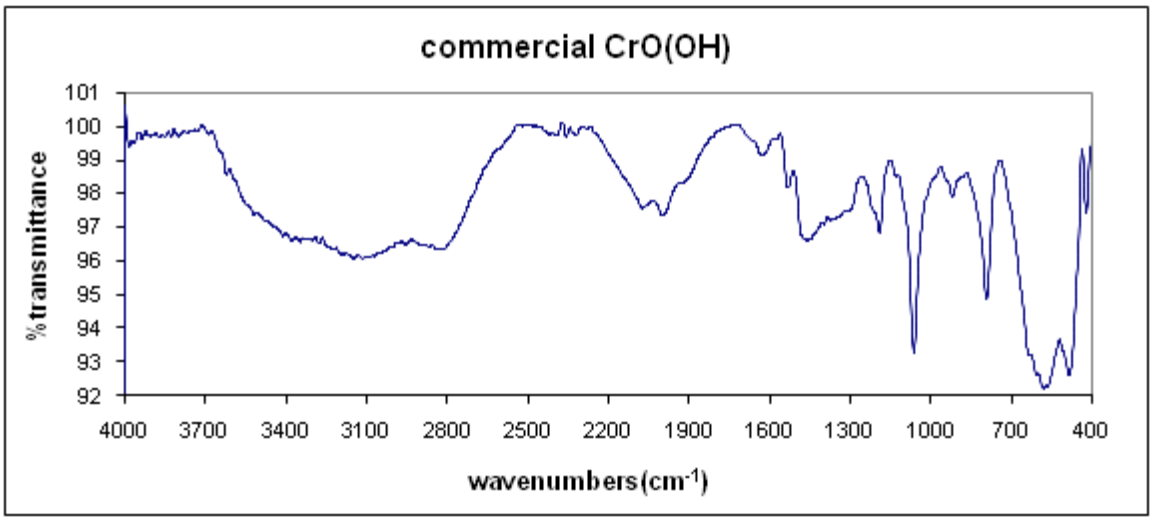

Figure 2-17 Infrared Spectrum of Commercial Grade Chromium Oxyhydroxide

Bands between 2125 cm^{-1} and 1986 cm^{-1}, with one of them being at 1994 cm^{-1}, were attributed to Cr-O bond and CO_2 interactions, while a relatively weak band at 950 cm^{-1} was attributed to vibration of Cr-O corresponding to its literature value of 960 cm^{-1}.[64] A sharp band at 1061 cm^{-1} is assigned to Cr-O stretching vibration corresponding to its literature value of 1050 cm^{-1} and the band at 550-560 cm^{-1} region at 563 cm^{-1} is also assigned to Cr-O stretching vibrations, corresponding to the literature value of 560 cm^{-1}.[42-45]

Synthesized CrO(OH)

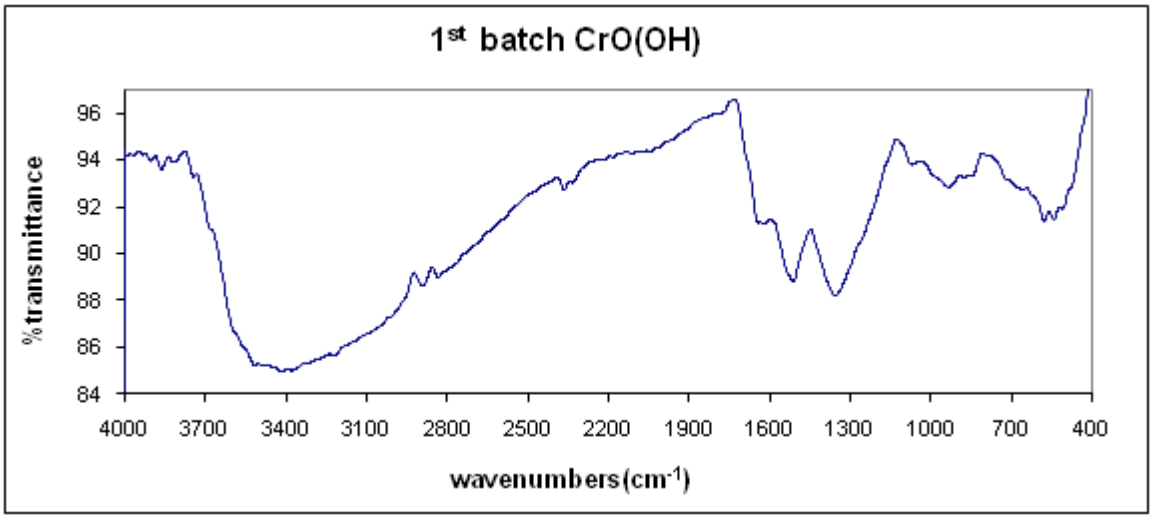

Figure 2-18 Infrared Spectrum of Synthesized Chromium Oxyhydroxide-1st Batch

The bands at 1050 cm^{-1} and 560 cm^{-1} or 550 cm^{-1} [65] are due to stretching vibrations of Cr–O. Broadening and weakening of these Cr-O bands were observed due to interactions of chromium with hydroxyl group.[42-46] Two bands between 1300 cm^{-1} and 1450 cm^{-1} were attributed to the B-O trigonal asymmetric stretching vibrations, thus implying the presence of boric acid impurity in the sample, which was confirmed via X-ray diffraction studies as well.[54] Therefore, additional batches of the product were synthesized with more thorough washing. As a result, bands due to free boric acid disappeared.

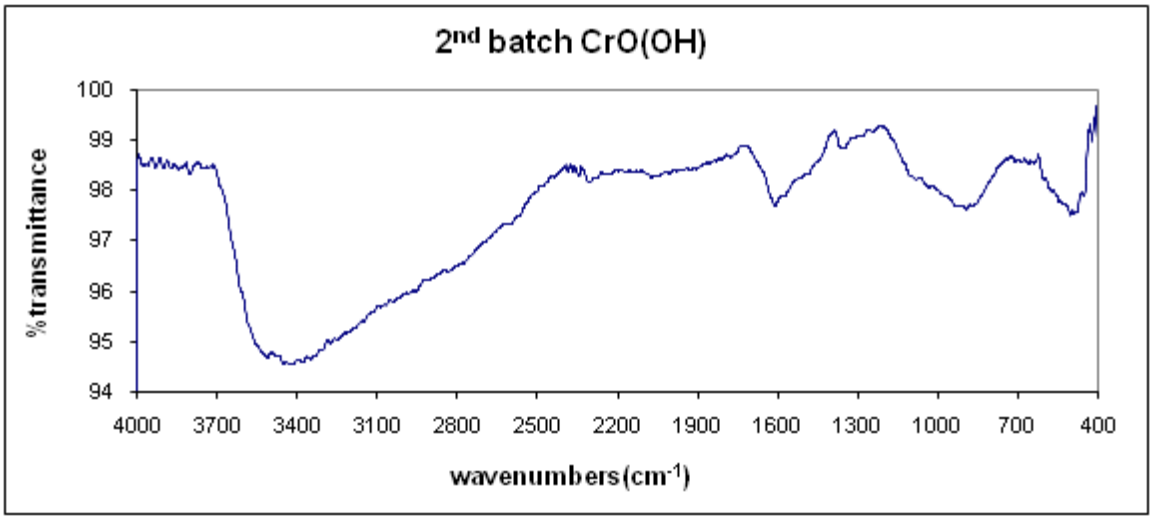

Figure 2-19 Infrared Spectrum of Synthesized Chromium Oxyhydroxide-2nd Batch

Chromium Tetraborate

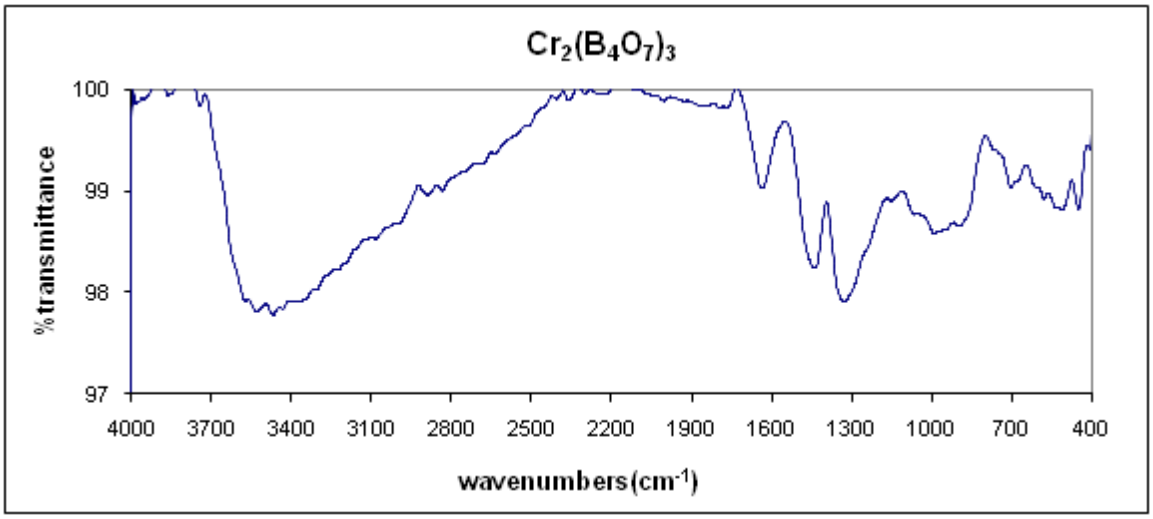

Figure 2-20 Infrared Spectrum of Chromium Tetraborate

In the literature, three main bands of 708 cm^{-1}, 1019 cm^{-1}, and 1347 cm^{-1} are assigned to symmetric stretchings compared to the reference spectra of pure sodium tetraborate powder with KBr pellets annealed at 400 ˚C [66]. Corresponding bands exist in the spectra of synthesized chromium tetraborate with the band at 1347 cm^{-1} being stronger

than the other two. Other bands include Cr-O stretching vibrations at 560 cm^{-1} and 960 cm^{-1}, H-O-H bending at 1600 cm^{-1},[42-46] symmetric and asymmetric stretchings due to hydroxyl groups of water at 3500 cm^{-1}.[67,68]

The presence of bands due to water may imply that a hydrate of chromium tetraborate has been synthesized; unfortunately X-ray diffraction pattern indicated an amorphous structure for the product. Relatively weaker bands due to the boron constituent between 400 cm^{-1} and 1000 cm^{-1} region are assigned to tetrahedral B-O asymmetric stretching, trigonal B-O symmetric stretching, tetrahedral B-O symmetric stretching, out of plane B-O-H bending, O-B-O ring bending in the order of decreasing frequencies.[54-57]

2.5 Solubility Measurements

Depending on different types of applications, the range of solubility had a major impact on the efficiency of the corrosion inhibitors. Both in aqueous solutions and in sol-gel coatings, inhibitors must possess an optimum solubility sufficient to migrate to the sites of corrosion and react with corrosive agents. Solubility also has to be low enough not to cause leaching of the inhibitor, or blistering and delamination which may lead to the degradation of the coating as well as loss of its hydrophobicity. On the other hand, too high solubility values increase the conductivity of the solution among other things, which accelerates corrosion.

Based on many tests, an inhibitor concentration of 200 ppm or less for a system of 100 ml of distilled water solution has been determined as an optimum concentration. The concentration unit has been chosen as ppm (part per million) for reasons of convenience

considering performing several thousands of tests with using very small amounts of inhibitors. In most cases however, molecular weights of the tested inhibitors were 200 g/mol and higher due to high weights of hydroxy-acid constituents such as gluconates and benzilates, which corresponds to a concentration range of 0.01M for a molecular weight of 200 g/mol and 0.005M for a molecular weight of 400 g/mol, thus leading to comparable inhibition efficiency values with little error caused by concentration discrepancies. These seemingly low concentrations were often sufficient since the corrosion process itself is not a very fast process. Thus, the supply provided by a low-solubility inhibitor was sufficient unless the environment is too warm or contains very high concentrations of aggressive anions especially in the case of mild steel, which is prone to heavy corrosion. In addition to direct inhibition of corrosion, formation of conversion coatings is another desired outcome for longer term corrosion protection. This often requires precipitation of inhibitor products on the metal surface. Thus, optimum solubilities are essential for the formation of protective conversion coatings on substrate surfaces. Gluconate salts, given their very high solubility, were not predicted to form a conversion coating and results supported that prediction with the exception of $Al(gluconate)_2OH$, which formed a protective layer composed of aluminum oxides and aluminum hydroxides on the substrate surface. Metal oxyanion esters of gluconate salts were also tested for conversion coating formation; however no positive result has been obtained.

Solubilities of inhibitors, especially those intended to be used in sol-gel coatings, were measured by means of different methods such as colorimeter, flame atomic absorption spectrometer and particle size analyzer.

2.5.1 Colorimeter

The maximum solubility that could be measured by colorimeter is 0.70 ppm, thus it has been primarily used to measure the solubilities of the poorly soluble chromium(III) compounds. Solubilities of some chemicals that were more soluble than the upper limit of the colorimeter were measured by diluting the samples before testing. Solubilities in pure water as well as solubilities in 0.5 M salt water have been measured to observe the common or foreign ion effect, by placing 0.5 g of sample into 50 ml of distilled water, which was then filtered by a 0.2 μm syringe filter.

2.5.2 Flame Atomic Absorption Spectrometer

Flame atomic absorption measurements were conducted using a Varian flame atomic absorption spectrometer with the working conditions of 7 mA lamp current, acetylene fuel, air support, and reducing flame stoichiometry. Interference is reported in the literature for metals such as barium, aluminum, magnesium, and calcium in air-acetylene flame.[68-70] Thus, primarily trivalent chromium compounds have been measured using the technique. Based on the Varian Flame Atomic Absorption Spectrometer handbook, standards have been prepared using A.R. grade potassium dichromate. Samples for flame atomic absorption measurements have been prepared from saturated solutions of inhibitors in distilled water filtered with 0.2 μm syringe filter.

Measurements have been performed at varying wavelengths as the following;

λ = 520.8 nm is appropriate for concentrations ranging from 20 ppm to 2600 ppm with standards of 100 ppm, 250 ppm, 500 ppm, and 1000 ppm needed for calibration purposes.

λ = 428.9 nm is appropriate for concentrations ranging from 1 ppm to 100 ppm with standards of 100 ppm, 250 ppm, and 500 ppm needed for calibration purposes.

λ = 425.4 nm is appropriate for concentrations ranging from 0.4 ppm to 40 ppm with standards of 50 ppm, 100 ppm, and 250 ppm needed for calibration purposes.

Table 2-2 Solubility Values in ppm obtained via colorimeter and flame atomic absorption spectrometer

Solubility Values	**Colorimeter (ppm)**		**AAS in DI water (ppm)**		
	In DI water	in 0.5 M salt water	λ=520.8 nm	λ=428.9 nm	λ=425.4 nm
CrO(OH)	0.07	0.06			
Commercial CrO(OH)					0.72
$Cr(octanoate)_3$	0.07	0.11			
$Cr(caproate)_3$	0.04	0.05			
$Cr(butyrate)_3$	0.22	0.35			0.83
$Cr(propionate)_3$			1190		
$Cr(acetate)_3$			4035		
$Cr(acetate)_2OH$			3317		
$Cr(methoxyacetate)_3$			2572		
$Cr_2(tetraborate)_3$	0.14				1.03
$FeCr(tetraborate)_3$	0.48			0.03	
$CrBO_3$	0.27				
$Cr(OH)_3$	0.21				0.97
$Cr(OH)_3$*			55.1	63.6	
$Cr(OH)_3$**				1.6	

Table 2-2 (Continued)

Solubility Values	**Colorimeter (ppm)**		**AAS in DI water (ppm)**		
	In DI water	in 0.5 M salt water	λ=520.8 nm	λ=428.9 nm	λ=425.4 nm
$Cr(gluconate)_3$			1308		
Cr(gluconate)molybdate			428.2		
Cr(gluconate)vanadate			304		
Cr(gluconate)1borate				18.7	

$Cr(OH)_3$ = synthesized from $CrCl_3.6H_2O$ + 2N NH_4OH,

*$Cr(OH)_3$ = synthesized from $CrCl_3.6H_2O$ + 30% NH_4OH,

**$Cr(OH)_3$ = synthesized from $Cr(NO_3)_3.9H_2O$ + KOH

Despite that exact matches could not be obtained using two methods; solubilities of the same compounds were found to be within a narrow range. Since better results in sol-gel coating were obtained with synthesized CrO(OH), $CrBO_3$, and $Cr(octanoate)_3$, it was concluded that even very low solubilities could be sufficient and may even be desirable for use in sol-gel coatings. On the other hand for aqueous solutions, the minimum solubility limit appears to be around 20 ppm due to positive results obtained using Cr(gluconate)1borate in such concentrations, while other compounds such as $Cr(butyrate)_3$, which has a solubility less than 1 ppm yielded negative results in weight-loss tests.

2.6 Particle Size Measurements

Particle size measurements have been conducted using a dynamic light scattering particle size analyzer. Other than complimenting colorimeter and flame atomic absorption spectrometer for solubility measurements, average particle size information is also important in engineering of the sol-gel coatings which are designed to incorporate such inhibitors.

Particle sizes of very soluble inhibitors were found to be very small. Size distribution by volume graph indicated the Z-average size values to be between 0 and 2 nanometers for the highly water soluble compounds shown below.

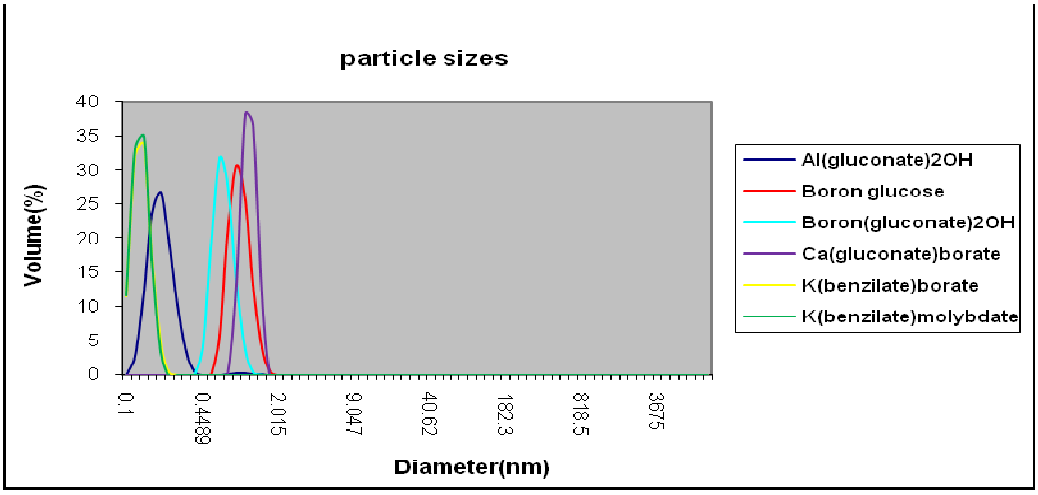

Figure 2-21 Dynamic Light Scattering of Selected Tested Compounds

Large particle size values have been found for insoluble chemicals such as zinc carboxylates, and most of the trivalent chromium compounds. For instance, chromium carboxylates with longer alkyl chains were predicted to suspend as micellar particles and the large particle sizes were obtained for these chromium carboxylates.

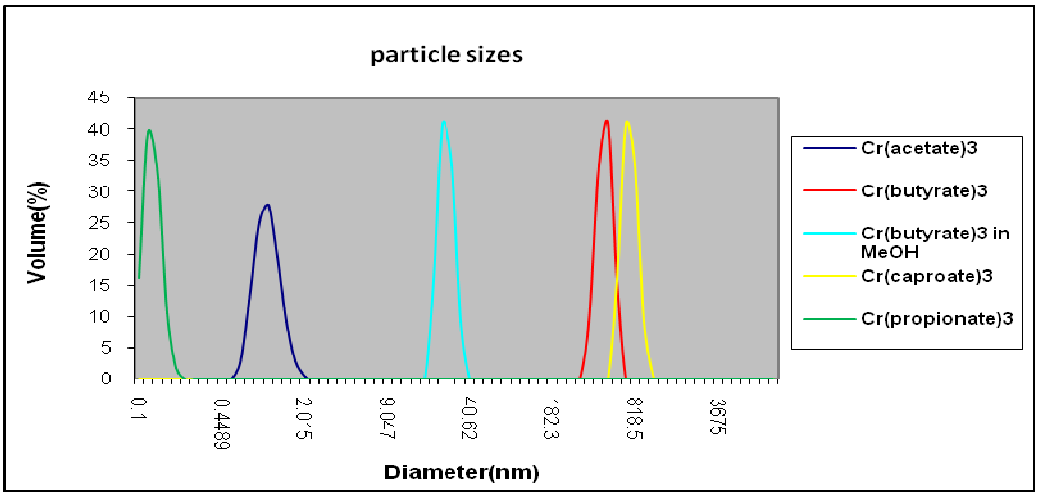

Figure 2-22 Dynamic Light Scattering of Chromium Carboxylates

The effect of solvent type was also evident in the particle sizes. Particle size of chromium butyrate in methanol was found to be significantly lower than in water as expected due to aggregation of hydrophobic particles.

2.7 Surface Area Measurements

The surface area measurements were conducted using a Quantachrom Nova 1200 surface area analyzer, via a nitrogen adsorption isotherm, using the Brunauer-Emmett-Teller (BET) method, and six points in the range of 0.05 to 0.30 P/P_o. A high surface area for an inhibitor is a positive contribution to its inhibition efficiency that correlates with higher reactivity, and more rapid dissolution kinetics. High surface areas may rightfully imply effective barrier properties. Inhibitors, those were found to have siginifant specific surface areas in decreasing order are as follows;

- CrO(OH), synthesized by reacting synthesized $CrBO_3$ with NaOH, 344 m^2/g,

- $CrBO_3$, synthesized by firing chromium gluconate borates, 246 m^2/g, opposed to commercially available CrO(OH), 87 m^2/g,
- $Cr(OH)_3$, synthesized by reacting $CrCl_3.6H_2O$ with 2N NH_4OH, 148 m^2/g,
- Chromium gluconate molybdate ester, synthesized by reacting chromium gluconate with molybdenum(VI) oxide, 68 m^2/g,
- Chromium gluconate vanadate, synthesized by reacting chromium gluconate with vanadium(VI) oxide, 68 m^2/g

The surface areas of chromium carboxylates; of chromium gluconate, chromium butyrate, chromium propionate, and chromium acetate hydroxide, were measured as less than 1 m^2/g. The significant difference between the specific surface areas of commercially available CrO(OH) and the synthesized CrO(OH) is noteworthy. Accordingly, commercially available CrO(OH) had low inhibition efficiency opposed to very high inhibition efficiency of synthesized CrO(OH) measured by weight-loss tests.

2.8 Powder X-Ray Diffraction Studies

X-ray powder diffraction patterns were recorded on a Bruker AXS D-8 Advance X-ray powder diffractometer using copper K_α radiation. X-Ray diffractometer studies did not reveal many results since the synthesized compounds were all amorphous with a few exceptions such as zinc tartrate, and zinc mandelate. At times, it was also used as a complimentary tool to other characterization methods as in the case of detection of crystalline boric acid impurity in a batch of chromium borate that was obtained by firing of chromium gluconate.

2.9 Discussions and Conclusions

Compounds, which were tested for their corrosion inhibition properties, were synthesized via a single-source precursor method, which is a relatively easier synthesis method. The problems arose particularly due to the nature of the products, which were too hygroscopic preventing them to be handled for characterization. Such products were kept in solution form even after isolating them. Overall, the syntheses reactions were reproducible regardless of the amounts of the reagents reacted.

Characterization studies on the other hand were proven to be difficult first due to amorphous structure of the products, which in turn resulted in no structural information through X-ray analysis. Secondly, difficulty in handling most of these products resulted in very little gravimetric measurements to be performed. Such examples were chromium octanoate and chromium caproate, which were very viscous and most gluconate esters, which were too hygroscopic. However, this disadvantage was tried to be overcome using various techniques resulting in some characterization information for each and every inhibitor that were tested. Among these techniques were flame atomic absorption spectrometry, dynamic light scattering, colorimetry, infrared analysis, X-ray analysis, UV visible spectrometry, thermogravimetric analysis, and surface area measurement.

2.10 References

1. Motekaitis, R. J.; Martell, A. E.; Complexes of Aluminum(III) with Hydroxy Carboxylic Acids, *Inorganic Chemistry*, **1984**, 23, 1, 18.
2. Fasman, G. D. Ed.; *Handbook of Biochemistry and Molecular Biology*, 3^{ed}, CRC Press, Boca Raton, FL, **1976**, 1, 310.

3. Boudreaux, E.; Desai, P. M.; Elder, V. A.; Fulcher, J. G.; Leung, H. K; Li, W.; Topor, M. G.; Method for Reducing Acrylamide Formation, U.S. Pat. Appl. Publ., **2007**, 40.
4. Blomqvist, K.; Still, E. R.; Solution Studies of Systems with Polynuclear Complex Formation: Copper(II) and Cadmium(II**)** D-Gluconate Systems, *Anal. Chem.*, **1985**, 57, 749-752.
5. de Wilt, H. G. J.; Part I: The oxidation of Glucose to Gluconic Acid, *Ind. Eng. Chem. Prod. Res. Develop.*, **2006**, 11, 4, 370.
6. Furia, T. E.; Sequestrants in Foods, *Handbook of Food Additives*, CRC Press, 2nd ed., 1972, revised **2006**, 271.
7. Graves, C. R.; Campbell, E. J.; Nguyen, S. T.; Aluminum-based catalysts for the asymmetric Meerwein–Schmidt–Ponndorf–Verley–Oppenauer (MSPVO) reaction manifold, *Tetrahedron: Asymmetry*, **2005**, 16, 21, 3465.
8. Jones, C. D.; Wiesner, M. R.; Barron, A. R.; Carboxylate-alumoxanes: Environmentally Benign Precursors for Developing Aluminum-Based Ceramic Membranes And Filters, *Abstracts of Papers of the American Chemical Society*, **1999**, 218, U877.
9. Fey, G. T.; Chen, J. G.; Kumar, T. P.; Carboxylate-Alumoxanes as Precursors for Alumina Coatings To Enhance The Cyclability of $LiCoO_2$, *Journal of Power Sources*, **2005**, 146, 1-2, 250-253.
10. NOSB TAP Materials Database Compiled by OMRI, **2000**.
11. Allen, D.G.; Pringle, J. R.; Smith, D.; Conlon, P.; Burgmann, P.; *Handbook of Veterinary Drugs*. Philadelphia, J.B., Lippincott Co., **1993**.

12. *Summary of Product Characteristics, Product: Calcibor CBG20*, Arnold Veterinary Products Ltd., **2004**.
13. Schullerus, P. G.; Patron, L.; Plostinaru, S.; Contescu, A.; Segal, E., Thermal Stability and Non-Isothermal Decomposition Kinetics of Some Compounds of Lanthanoids with Chromium and Gluconic Acid, *Thermochimica Acta*, **1989**, 153, 263-267.
14. Beneitez, P.; Ayllon, S.; Studies of Chromium (III)-Gluconate Complexes in Acidic Solutions by Liquid-Liquid Extraction, *Zeitschrift fuer Physikalische Chemie*, **1989**, 270, 2, 377-383.
15. Signorella, S. R.; Santoro, M. I.; Mulero, M. N.; Sala, L. F.; Oxidation of D-Gluconic Acid by Chromium(VI) in Perchloric Acid, *Can. J. Chem.*, **1994**, 72, 398-402.
16. Ramos, M. L.; Caldeira, M. M.; Gil, V. M. S.; NMR Spectroscopy Study of The Complexation of D-Gluconic Acid with Tungsten(VI) and Molybdenum(VI), *Carbohydrate Research*, **1997**, 304, 2, 97-109.
17. Guiotoku, M.; Silva, F. R. M. B.; Azzolini, J. C.; Merce, A. L. R.; Mangrich, A. S.; Sala, L. F.; Szpoganicz, B.; Monosaccharides and The VO(IV) Metal Ion: Equilibrium, Thermal Studies and Hypoglycemic Effect, *Polyhedron*, **2007**, 26, 1269–1276.
18. Cervilla, A.; Llopis, E.; Ribera, A.; Domenech, A.; White, A. J. P.; Williams, D. J.; Potentiometric Study of the Molybdenum(VI)-Benzilic Acid System. Structural Characterisation and Electrochemical Properties of

$[NH_4]_2[MoO_2\{O_2CC(O)Ph_2\}_2].2H_2O$, *J . Chem. Soc. Dalton Trans.*, **1995**, 3891-3895.

19. Cui, L.; Dong-Mei L.; Wu, J.; Cui, X.; Wang, T.; Xu, J.; Synthesis, Structural Determination And Photochromism Characterization Of Two Complexes With $[MO_2(O_2CCOPh_2)_2]^{2-}$ Cores [M = Mo or W], *Journal of Molecular Structure*, **2006**, 797, 1-3, 34-39.
20. Kiparisov, S. S.; Meerson, G. A.; Morozov, V. N.; Fistul, A. D.; Formation of chromium borates, *Neorg. Mater.*, **1973**, 9, 3, 512-513.
21. Money, J. K.; Huffman, J. C.; Christou, G.; Vanadium(IV) Thiolate Chemistry: Preparation, Structure, and Properties of $[VE(SCH_2CH_2S)_2]^{2-}$ (E= O,S), *Inorg. Chem.*, **1985**, 24, 3297-3302.
22. Vergopoulos, V.; Jantzen, S.; Rodewald, D.; Rehder, D.; [Vanadium (Salen)Benzilate]-A Novel Non-Oxo Vanadium (IV) Complex, *Journal of the Chemical Society, Chemical Communications*, **1995**, 3, 377-378.
23. Charykov, A. K.; Ivanenko, N. B.; Dmitrieva, I. A., Extraction of Vanadium (V) and (IV) By Solutions of Benzyilic Acid In Heptanol, *Vestnik Leningradskogo Universiteta, Seriya 4: Fizika, Khimiya*, **1991**, 1, 122-124.
24. Fan, Y.; Du, Y.; Ding, Y.; Wang, X.; Xiu, Z., Study on The Complex of Vanadium (V) with Benzilic Acid and Pyridine, (II) Preparation of Single Crystal and Determination of Crystal Structure, *Gaodeng Xuexiao Huaxue Xuebao*, **1988**, 9, 1, 17-22.
25. Du, Y.; Xiu, Z., Synthesis, Characterization and Properties of A Vanadium (V) Complex of Benzilic Acid, *Jilin Daxue Ziran Kexue Xuebao*, **1984**, 2, 109-114.

26. Belford, R. L.; Chasteen, N. D.; So, H.; Tapscott, R. E., Triplet State of Vanadyl Tartrate Binuclear Complexes and Electron Paramagnetic Resonance Spectra of The Vanadyl α-Hydroxycarboxylates, *Journal of the American Chemical Society*, **1969**, 91, 17, 4675-4680.
27. Schmidt, H.; X-ray evidence for $CrCO_3$, VBO_3 and $TiBO_2$ with Calcite Structure, *Acta Cryst.*, **1964**, 17, 1080-1081.
28. Tombs, N. C.; Croft, W. J.; Mattraw, H. C.; Preparation and Properties of Chromium Borate, *Inorganic Chemistry*, **1963**, 2, 4, 872.
29. Paun, C.; Parvulescu, V.; Anger, I. E.; Seicaru, O. L.; Simion, G.; Dinca, I.; *Manufacture of Green Pigment Based on Chromium Hydroxide Oxide for Cosmetics*, Rom. Patent application # 1988-132809, **1990**.
30. Stengl, V.; Subrt, J.; Bezdicka, P.; Marikova, M.; Bakardjieva, S.; Homogeneous Precipitation with Urea - An Easy Process for Making Spherical Hydrous Metal Oxides**,** Diffusion and Defect Data--Solid State Data, Pt. B: *Solid State Phenomena*, **2003**, 90-91, 121-126.
31. Morales, J. G.; Carmona, J. G.; Clemente, R. R.; Muraviev, D.; Preparation of Chromium Hydroxide Sub-micro and Nanoparticles by Microwave Dielectric Heating, *Langmuir*, **2003,** 19, 9110-9113.
32. Hantzsch, A.; Torke, E.; *Anorg. Allg. Chem.*, **1932**, 209, 72-73.
33. Ruthruff, R. F. in W. C. Fernelius, *Inorg. Syntheses*, New York-London, **1946**, 2, 190.
34. Werner, A. A.; Gubser. Ber.; *Dtsch. Chem.. Ges.* **1901**, 34, 1591.
35. Higley, G. O.; *J. Amer. Chem. Soc.*, **1904**, 26, 620.

36. Sigma-Aldrich product database, http://www.sigmaaldrich.com/spectra/ftir/FTIR003241.PDF
37. Sigma-Aldrich product database, http://www.sigmaaldrich.com/spectra/ftir/FTIR002189.PDF
38. Nakamoto, K.; Infrared and Raman Spectra of Inorganic and Coordination Compounds-I and II, Wiley, **1986**, I, 231–233; **1986**, II, 228–229.
39. Deacon, G. B.; Phillips, R. J.; *Coord. Chem. Rev.*, **1980**, 33, 227.
40. Nyquist, R. A.; Kagel, R. O.; *Infrared Spectra of Inorganic Compounds* (3800-45 cm^{-1}), Academic Press, New York, **1971**.
41. Yao, Z. M.; Li Z. H.; Zhang, Y.; *J. Colloid Interface Sci.*, **2003**, 266, 382–387.
42. Shigeharu, K.; Tohru, M.; Kohji, K.; Tetsuo M.; *J. Solid State Chem.*, **1985**, 58 187–193.
43. Schraml-Marth, M.; Wokaun, A.; Curry-Hyde, H. E.; Baiker, A.; *J. Catal.*, **1992**, 133, 415–430.
44. Sousa, P. M.; Silvestre, A. J.; Popovici, N.; Parames, M. L.; Conde, O.; *Mater. Sci. Forum*, **2004**, 20**,** 455–456.
45. Guimin, A; Yang, Z; Zhimin, L; Zhenjiang, M; Buxing, H; Shiding M, Jianping L.; Preparation of Porous Chromium Oxide Nanotubes Using Carbon Nanotubes as Templates and Their Application as An Ethanol Sensor, Iop Publishing, *Nanotechnology*, **2008**, 19, 3.
46. Irons, T.V.; Stafford, F. E.; *J. Am. Chem. Soc.*, **1966**, 88, 4819.
47. Ward, B.G.; Stafford, F. E.; *Inorg. Chem.*, **1968**, 7, 2569.
48. Barraclough, C. G.; Kew, D. J.; *Aust. J. Chem.*, **1966**, 19, 741.

49. Bouhaouss, P. A.; *Mater. Res. Bull.*, **1983**, 18, 1247.

50. Chen, W.; Peng, J.; Mai, L.; Zhu, Q.; Xu, Q.; Synthesis of Vanadium Oxide Nanotubes from V_2O_5 Sols, *Materials Letters*, **2004**, 58, 2277–2278.

51. Wilhartitz, P.; Dreer, S.; Ramminger, P.; Can Oxygen Stabilize Chromium Nitride?—Characterization of High Temperature Cycled Chromium Oxynitride, *Thin Solid Films*, **2004**, 293, 447 –448.

52. Ewissa, M. A. Z.; Ansoor, S. A. A.; Electrical, IR Spectroscopy, and DTA Studies of Some Sodium Tetraborate Glasses Containing Vanadium Oxide, *Physica Status Solidi (a)*, 156, 2, 428.

53. Peak, D.; Luther, G. W.; Sparks, D. L.; ATR-FTIR Spectroscopic Studies of Boric Acid Adsorption on Hydrous Ferric Oxide, *Geochimica et Cosmochimica Acta*, **2003**, 67, 14, 2552.

54. Burkholder, T. R.; Andrews, L.; Reactions of Boron Atoms with Molecular Oxygen, Infrared spectra of BO, BO_2, B_2O_2, B_2O_3, and BO^{-2} in solid argon, *J. Chem. Phys.*, **1991**, 95, 8705.

55. Kawaguchi, K.; Hirota, E.; Yamada, C.; *Mol. Phys.*, **1981**, 44, 509.

56. Maki, J. B.; Burkholder, A. S.; Howard, C. J.; *I. Mol. Spectrosc.*, **1988**, 130, 238.

57. Indian Academy of Sciences, *Bull. Mater. Sci.*, **2002**, 25, 1, 75–78.

58. Motke, S. G.; Yawale, S. P.; Yawale, S. S.; Infrared Spectra of Zinc Doped Lead Borate Glasses, *Bull. Mater. Sci.*, **2002**, 25, 1, 75–78.

59. Yawale, S. P.; Pakade, S. V.; Adgaonkar, C. S.; *Indian J. Pure Appl. Phys.*, **1995**, 33, 35.

60. Yawale, S. S.; Yawale, S. P.; Adgaonkar, C. S.; *Indian J. Engg. Mater. Sci.*, **2000**, 7, 150.

61. Sigoli, F. A.; Davolos, M. R.; Jafelicci, M. Jr.; Morphological Evolution of Zinc Oxide Originating from Zinc Hydroxide Carbonate, *J. of Alloys and Compounds*, **1997**, 262-263, 293.

62. Sigma-Aldrich product database,

http://www.sigmaaldrich.com/spectra/ftir/FTIR004652.PDF

63. Almond, M. J.; Hahne, M.; Formation Of Molecular Chromium(IV) Oxide (CrO_2) By Photolysis Of $Cr(CO)_6$ in O_2-Doped Argon Matrices, *J. Chem. Soc. Dalton Trans.*, **1988**, 2256.

64. Wilhartitz, P.; Dreer, S.; Ramminger, P.; Can Oxygen Stabilize Chromium Nitride?—Characterization of High Temperature Cycled Chromium Oxynitride, *Thin Solid Films*, **2004**, 293, 447–448.

65. Kutub, A. A.; Al-Ghorabiea, F. H.; Natto, S.; *J. Mater. Sci.*, **1991**, 26, 4421.

66. Lemus, R.; Vibrational Excitations in H_2O in the Framework of a Local Model, *J. Mol. Spectrosc.*, **2004**, 225, 73-92.

67. Tereszchuk, J. K.; Bernath, P. F.; Zobov, N. F.; Shirin, S. V.; Polyansky, O. L.; Tennyson, J.; Emission Spectrum of Hot HDO Below 4000 cm^{-1}, *J. Mol. Spectrosc,*. **2003**, 219, 132-135.

68. Yanagisawa, M.; Suzuhri, M.; Takreuchi, T.; *Anal. Chim. Acta*, **1970**, 52, 386-389,.

69. Wilson, L.; *Anal. Chim. Acta*, **1968**, 40, 503-512.

70. Taylor, R. W.; *American Laboratory*, **1970**, 11, 33-35.

CHAPTER III

AQUEOUS CORROSION INHIBITION FOR MILD STEEL

Corrosion inhibition of mild steel in aqueous solutions has been studied using various techniques that can be categorized under three groups;

First, *synthesized corrosion inhibitors* were tested for both direct corrosion inhibition efficiencies and for conversion coating formation using *weight-loss tests*. Effects of inhibitor concentrations, immersion periods, and cationic constituents have been discussed individually. Inhibition efficiency data were recorded using statistics.

Secondly, *surfaces of substrates* immersed in inhibitor solutions have been characterized by means of different surface techniques such as *FT-IR, X-Ray, SEM, XPS, digital imaging*.

Third, *immersion solutions* have been characterized by means of *oxidation–reduction potential, pH meter, and conductivity probes*.

3.1 Weight-loss Test Method

The weight-loss method was used extensively throughout this study to assess inhibition efficiencies of corrosion inhibitors. Using metal coupons to assess inhibition

efficiencies is the oldest and simplest method in monitoring of corrosion.[1] Coupons are described as small pieces of metal, usually of rectangular shape, which are inserted in the process stream and removed after a period of time that is greater than 24 hours.[2,3] The most common and basic use of coupons is to determine average corrosion rate over the period of exposure.[4] This is accomplished by weighing the degreased coupon before and after immersions followed by its exposure to various acidic solutions to remove corrosion deposits on the substrate surface. The difference between the initial and final weights of the coupon, that is the weight loss, is compared to the control. The control coupon is the substrate of the same metal alloy exposed to the same environment with no inhibitor present. At least two, and preferably more specimens should be exposed for each condition.[5] The reasons why the weight-loss method has been chosen to assess inhibition efficiencies were first, tested inhibitors are all water soluble and second it is easy to obtain accelerated corrosion conditions, and third small amounts of inhibitors are sufficient for testing.

3.1.1 Preparation of Coupons/Weight-loss Apparatus

For the preparation of coupons, mild steel and aluminum alloy metal sheets were cut in dimensions of 1x1 inch. A hole is drilled at the corner of the coupon so that the coupon could be hanged in solution via a durable polymeric material such as a fishing-line that does not corrode.

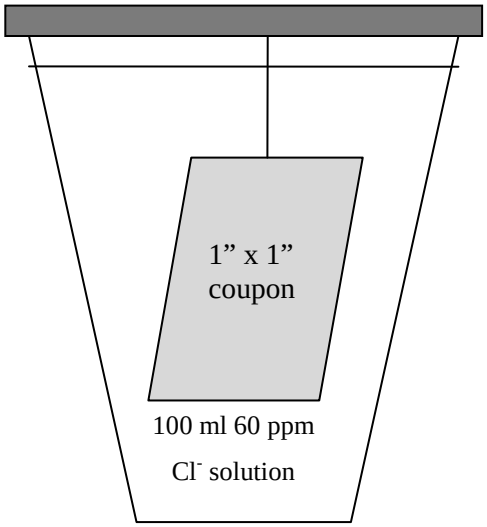

Figure 3-1 Weight-loss Apparatus

Standards determined for Preparing Specimens for Weight-Loss Tests by ASTM (American Society for Testing and Materials)[6,7] were followed with no alteration. For both aluminum alloy and mild steel specimens, the first step is described as degreasing in an organic solvent or hot alkaline cleaner or both. Mild steel specimens used in this study were cut out of large rolls of mild steel sheets that were previously heavily greased to prevent them from corroding. This grease was removed from the mild steel coupons by dipping them in hexane and rubbing them with paper towels soaked with hexane when necessary. Secondly, coupons were placed in Oakite Products Inc. brand Oakite-164 alkaline cleaner solution at 150 $^{\circ}$F for 10 minutes to complete degreasing of the coupons. Oakite solution was prepared by dissolving 60 g of Oakite detergent in 1000 ml of water at 180 $^{\circ}$F. An additional step before performing immersion tests that is instructed by ASTM is pickling of specimen in an appropriate solution if oxides or tarnish are present in the case of aluminum specimens. After degreasing and cleaning, the coupons were weighed and fully immersed in 100 ml solutions of 60 ppm Cl^- and various

concentrations of inhibitors for various periods of time (3 days, 7 days or for 14 days). As a controlled variable, 100 ml has been chosen as the volume of the solution due to the low amount of inhibitors that was required. Another controlled variable was the salt content of the solution, which was chosen as 60 ppm Cl^- since it is a situation commonly encountered in cooling water systems based on mild steel construction.[3]

Immersion periods of 3, 7 and 14 day periods were chosen since periods less than 24 hours are not enough for the system to come into an equilibrium[8], while a period of more than 14 days was too long to test many samples, that are needed for comparison purposes. Given the condition of accelerated corrosion, a period of 7 days has been determined to be the optimum period of immersion. After completion of immersion tests, coupons were exposed to an acidic solution described by ASTM to remove corrosion products for accurate weight-loss results. This solution has been prepared by dissolving 3.5 g hexamethylene tetramine in 500 ml of distilled water followed by adding 500 ml HCl. Specimens were exposed to this reagent for 10 min at 20°C to 25°C. It is indicated by ASTM that longer times may be required in certain instances; however such instances did not occur in this study meaning all specimens were cleaned of corrosion deposits thoroughly after 10 minutes of exposure. In case of specimens of aluminum and aluminum alloys, direct use of concentrated HNO_3 is inscribed by ASTM to remove corrosion deposits for periods of 1 to 5 min at 20°C to 25°C.

3.1.2 Inhibition Efficiency Calculations

Inhibition efficiencies were calculated based on the comparison of weight loss values of inhibitor treated coupons and those of controls with the following formula;

$$IE = 100[1-(W_2/W_1)]\% \quad \text{(Eq. 3.1)}$$

where

- W_1 = corrosion rate in the absence of inhibitor
- W_2 = corrosion rate in the presence of inhibitor
- W_1 & W_2 = $(W_{final} - W_{initial}) / W_{initial}$

The concentration of the inhibitors and the immersion periods were varied to obtain any possible trends of inhibition efficiencies, however inhibitor concentration of 200 ppm in 100 ml distilled water and a period of 7 days were chosen as the standard conditions after many trials as explained earlier.

Inhibition efficiency values calculated by means of the above formula were inserted into a t-distribution function formula to obtain statistically significant results. T-distribution is used rather than Z-distribution due to the low number of samples according to following formula;[9]

$$IE = \mu \pm t \frac{\sigma}{\sqrt{n}} \quad \text{(Eq. 3.2)}$$

where t is equal to the critical t-distribution value for 90% confidence limit with usually two degrees of freedom based on n, which is the number of samples. Often, only one sample has been put into test at the beginning to determine the presence of any kind of inhibition. When corrosion inhibition was observed, three more samples of the same inhibitor have been put into test, thus resulting in n = 3 and degrees of freedom, that is (n-

1), equaling to 2. Critical t-distribution value for 90% confidence limit with two degrees of freedom is reported as 2.920[10].

Formulas for the mean (μ) value and standard deviation (σ) are as follows;

$$\mu = \frac{1}{n}\sum_{i=1}^{n} x_i = \frac{1}{n}\left(x_1 + \cdots . + x_n\right) \quad \text{(Eq. 3.2)}$$

$$\sigma = \sqrt{\frac{1}{n}\sum_{i=1}^{n}(x_i - \bar{x})^2} \quad \text{(Eq. 3.3)}$$

The results found with inhibition efficiency formula were calculated to be statistically significant by hypothesis testing. For the inhibition efficiency values to be significant, the difference between the mean inhibition efficiency value and that of control must be bigger than the following;[11]

$$\mu - \mu_{standard} > t\left(\sigma/\sqrt{n}\right) \quad \text{(Eq. 3.4)}$$

Since there is no inhibition efficiency for control solutions, $\mu_{standard} = 0$, thus the equation is simplified to the following;

$$\mu > t\left(\sigma/\sqrt{n}\right) \quad \text{(Eq. 3.5)}$$

Insertion of critical value for t-distribution, standard deviation, and number of sample values into the above equation lead to the conclusion that mean inhibition efficiency values even for inhibitors with slight inhibition properties were statistically significant.

3.2 Categorization of Weight Loss Test Results

The weight-loss results were categorized based on the type of inhibitor, inhibitor amount in the immersion solution in ppm (part per million), chloride ion concentration in immersion solution in ppm, and the immersion period in number of days. Three immersion periods were shown in the inhibition efficiency graphs, 3 days, 7 days, and 14

days. 200 ppm is used as the standard concentration, with 25, 50, 100, and 500 ppm were other tested concentrations in addition to little used higher concentrations in molarity.

3.2.1 Gluconate Salts

All gluconate salts with the formula of $M^{+n}(X^{-1})_n$ yielded very high inhibition efficiencies both for 3 days and 7 days immersion periods with the exception $Cr(gluconate)_3$.

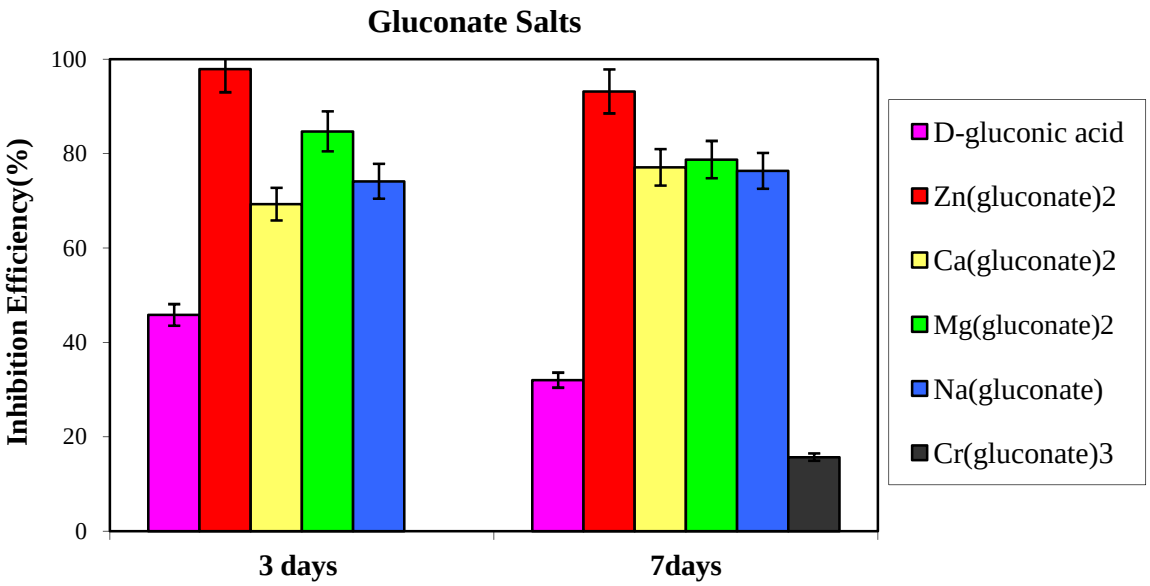

Figure 3-2 Inhibition Efficiency vs. Immersion Time Graph for $M^{+n}(X^{-1})_n$ Type Gluconates

$Zn(gluconate)_2$ performed better than others, which was due to cathodic inhibitive activity of Zn^{+2} cations in addition to the inhibitive activity of gluconate anions. Zn^{+2} cations are known to form insoluble $Zn(OH)_2$ precipitates on cathodic sites by reacting with hydroxide ions provided by corrosion reactions of iron and thus diminish further corrosion activity. On average, only slight decreases in the corrosion inhibition

efficiencies have been observed when the immersion period was increased to 3 days from 7 days in contrast to the results of a similar study indicating an inhibition efficiency of 99% for one day immersion and 65% for immersion of 5 days in 200 ppm $Ca(gluconate)_2$ solution.[3] The exception of low inhibition efficiency of chromium gluconate can be explained with strong complexation of chromium with gluconates; which as a result prevented complexation of iron cations with gluconates, thus leading to no positive effect. Notably, D-gluconic acid also inhibited corrosion with an average inhibition efficiency of 40% despite being an acid with a pKa of 3.86.[12]

3.2.2 Group III Gluconates and D-Glucose

The inhibition effciciency of $Al(gluconate)_2OH$ was high comparable to the $M^{+n}(X^{-1})_n$ type gluconate salts, while $B(gluconate)_2OH$ showed only slight inhibitive activity.

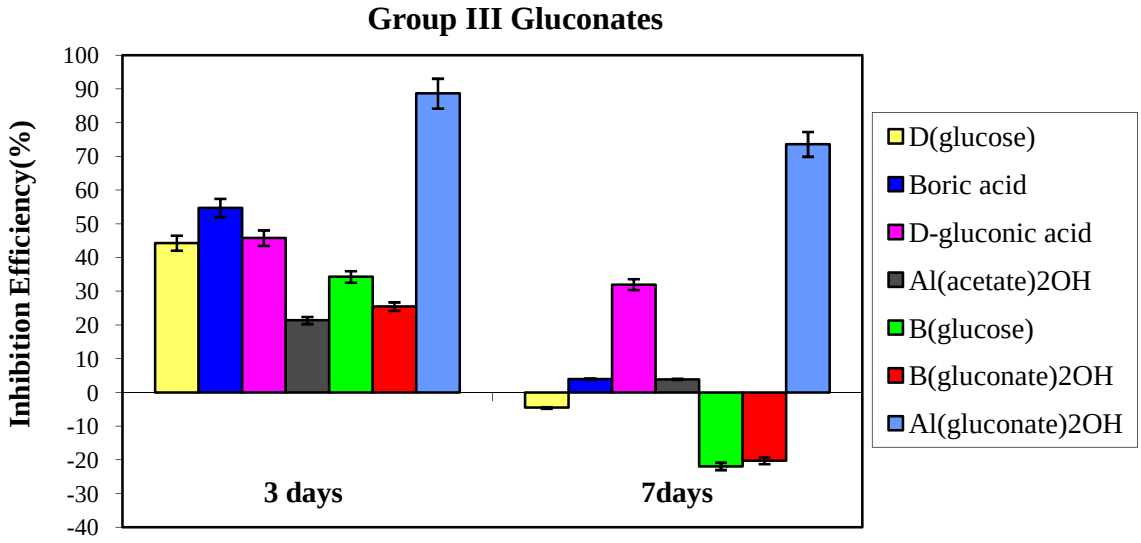

Figure 3-3 Inhibition Efficiency vs. Immersion Time Graph for $M^{+n}(X^{-1})_{n-1}OH$ Type Gluconates

Gluconate's and D-glucose's corrosion inhibiting abilities were lowered by coupling with the Boron constituent. Also boric acid performed better than borogluconate and boroglucose. Thus, it was concluded that boroglucose and borogluconates were in fact not synergistic formulations. Similarly negative results were predicted for Al(gluconate)$_2$OH, opposite to what was observed. This difference was due to the exceptionally strong bonding between gluconate and borate as opposed to aluminum or it may be due to the influence of the aluminum ions themselves[13].

3.2.3 Application of Other $M^{+n}(X^{-1})_{n-1}OH$ and $M^{+n}(X^{-1})_n$ Type Compounds

Being similar in structure to gluconates, lactate and acetate salts have also been tested. All of the salts under this category were already commercially available. Among them, lactic acid or 2-hydroxypropanoic acid, also known as milk acid, is a chemical compound that plays important roles in several biochemical processes and is produced naturally, while chromium (III) acetate is used to fix certain textile dyes, to harden photographic emulsions and as a catalyst.

Among tested salts, Al(lactate) has shown good inhibitive activity with values slightly lower to that of Al(gluconate)$_2$OH. Notably the difference was the similar to the difference between the inhibition efficiencies of D-gluconic acid and lactic acid. Al(acetate)$_2$OH was the only other compound with slight inhibitive activity.

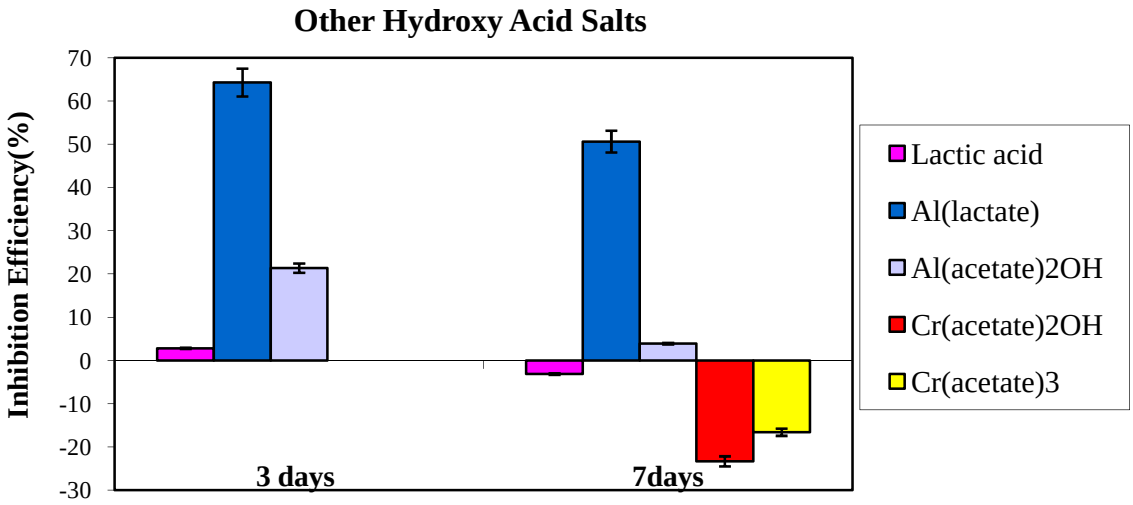

Figure 3-4 Inhibition Efficiency vs. Immersion Time Graph for $M^{+n}(X^{-1})_{n-1}OH$ and $M^{+n}(X^{-1})_n$ Type Hydroxy Acid Salts Other Than Gluconates

3.2.4 Molybdenum Esters of Gluconate Salts

Opposite to what had been anticipated, inhibition efficiencies of molybdenum oxyanion esters of gluconate salts were substantially lower than those of gluconate salts. Thus, metal oxyanions esters of gluconate salts were not synergistic combinations similar to borogluconates and boroglucose. Apparently, both constituents lose their inhibitive properties by forming a third product with very different chemical properties rather than a product of combined inhibitive activities of both constituents.

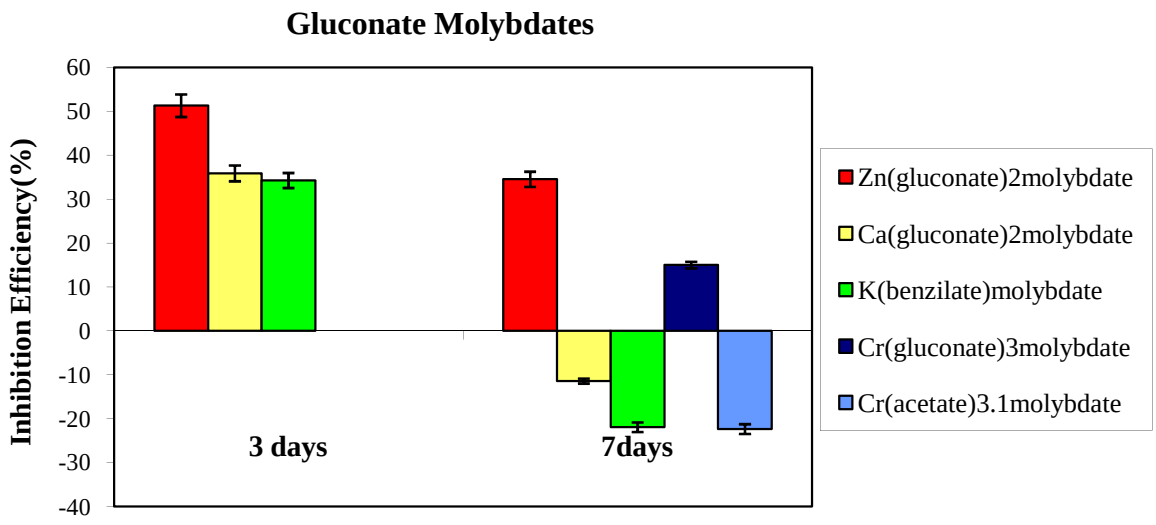

Figure 3-5 Inhibition Efficiency vs. Immersion Time Graph for Molybdenum Esters of Gluconate Salts

Zinc gluconate molybdate among others has shown inhibitive activity for both immersion periods due to cathodic inhibitive activity of zinc cations included in the formulation. Both calcium gluconate molybdate and potassium benzilate molybdate have shown similar inhibitive activity during the first immersion period and none in the second, probably due to molybdate's anodic inhibitive activity which disappeared when the immersion period has been prolonged.

3.2.5 Vanadium Esters of Gluconate Salts

Inhibition efficiencies of vanadium esters of gluconate salts were also substantially lower than those of gluconate salts. Instead of being reduced to form insoluble oxides and hydroxides like chromates, vanadium constituent formed a complex

compound with gluconate and benzilate which as a result diminished inhibitive properties of both constituents.

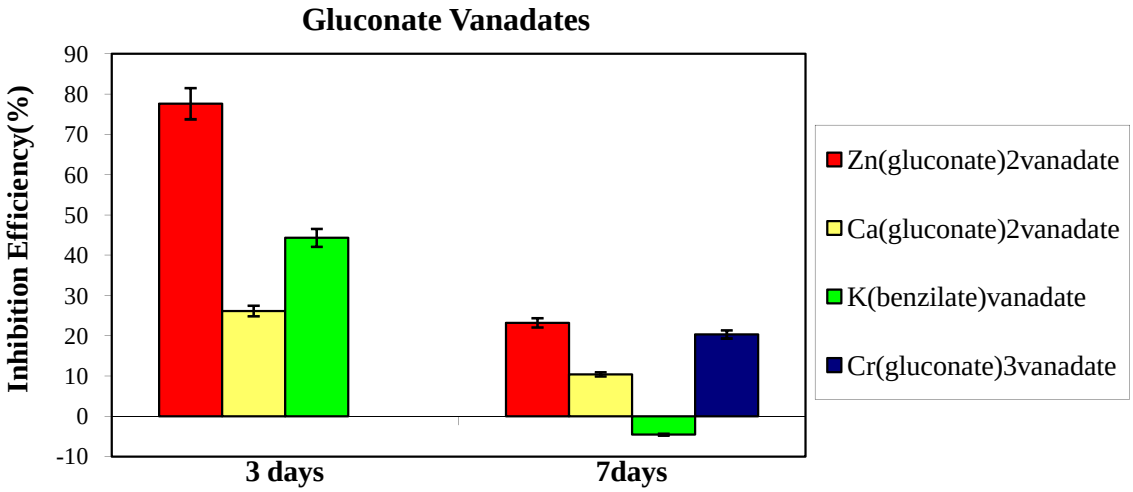

Figure 3-6 Inhibition Efficiency vs. Immersion Time Graph for Vanadium Esters of Gluconate Salts

3.2.6 Boron Esters of Gluconate Salts and Derivatives

Unlike molybdenum and vanadium esters of gluconate salts, boron esters performed very well in terms of corrosion inhibition of mild steel with the exception of the borate ester of chromium gluconate.This is opposite to what had happened with the molybdenum and vanadium esters. Since the boron constituent did not diminish the inhibitive activity of the gluconate constituent. In fact, when the inhibition efficiencies for the 3 day immersion period are taken into account, the borate esters of gluconate salts performed better than gluconate salts alone indicating that combination of gluconate salts and borate constituents was a synergistic combination, where both constituents preserved their inhibitive activity.

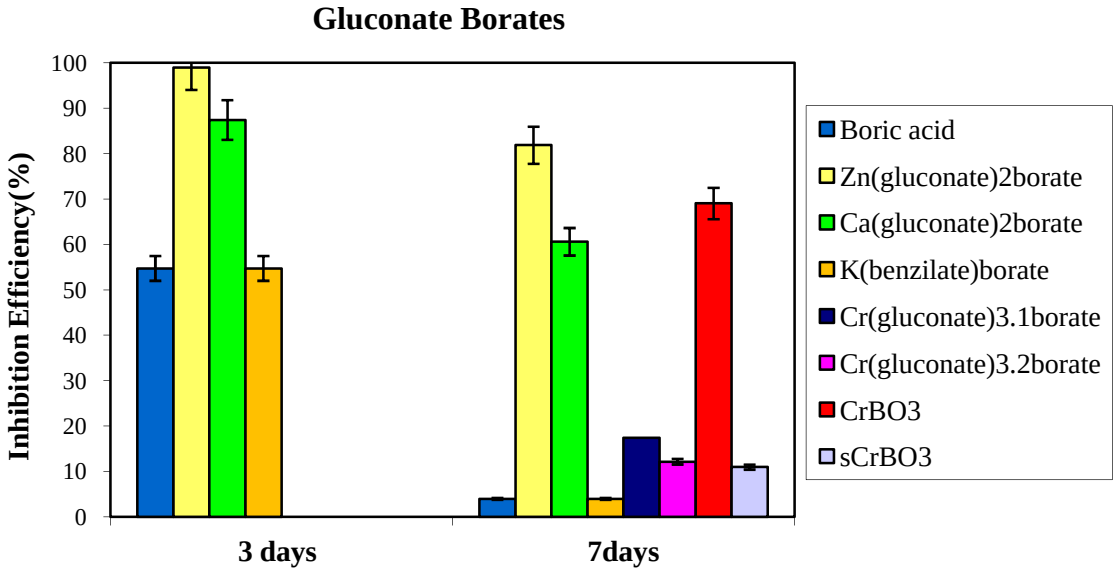

Figure 3-7 Inhibition Efficiency vs. Immersion Time Graph for Boron Esters of Gluconate Salts and Their Derivatives

The facts that zinc gluconate borate had higher inhibition efficiency than calcium gluconate borate, which had higher inhibition efficiency than potassium benzilate borate implied the positive effect of the cationic constituent on the inhibition efficiency results. In fact, potassium benzilate borate had inhibition efficiencies almost same as boric acid, indicating that potassium and benzilate constituents in potassium benzilate borate were not effective on the inhibition efficiency results. These observations also revealed that cationic constituent, anionic hydroxy-acid constituent and the borate constituent synergisticly inhibited corrosion with cationic constituent having the most pronounced positive effect on the inhibition efficiency results.

3.2.7 Zinc Carboxylates

Except for Zn(tartrate) all the other compounds had negligible inhibitive activity. And that of Zn(tartrate) was likely high due to cathodic inhibitive activity of Zn cations. Surprisingly Zinc cations did not show any inhibitive activity when combined with other α-hydroxy acids. At this time, it is difficult to explain why the other α-hydroxy acids promote corrosion or are poor inhibitors.

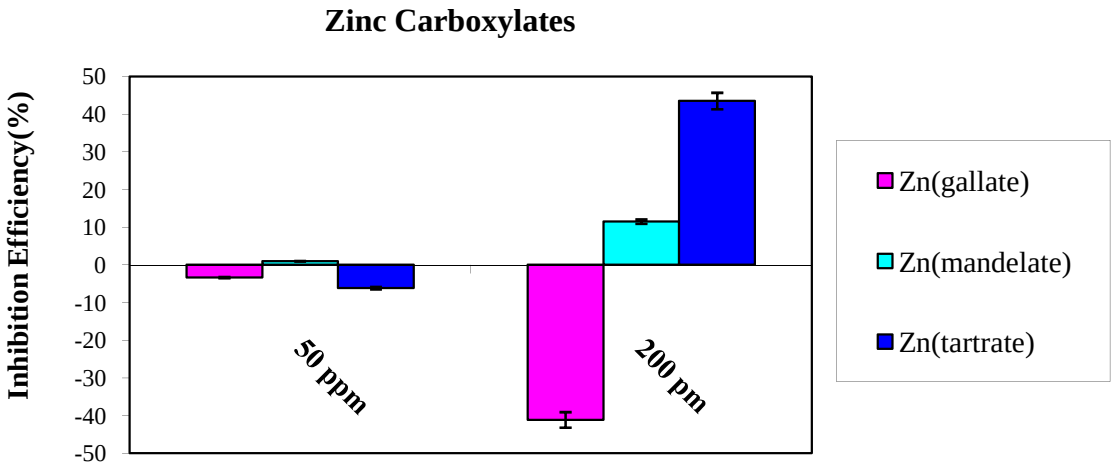

Figure 3-8 Inhibition Efficiency vs. Concentration Graph for Zinc Carboxylates

3.2.8 Chromium Carboxylates

It was found that Cr(III) carboxylates do not successfully inhibit corrosion. Chromium propionate slightly inhibited mild steel corrosion, while chromium methoxy acetate inhibited more when concentrations of 25 ppm were used. However, increasing the concentration chromium methoxyacetate to 200 ppm from 25 ppm yielded negative inhibition efficiencies. The results suggest that at elevated concentrations corrosion is accelerated, possibly due to increased solution conductivity.

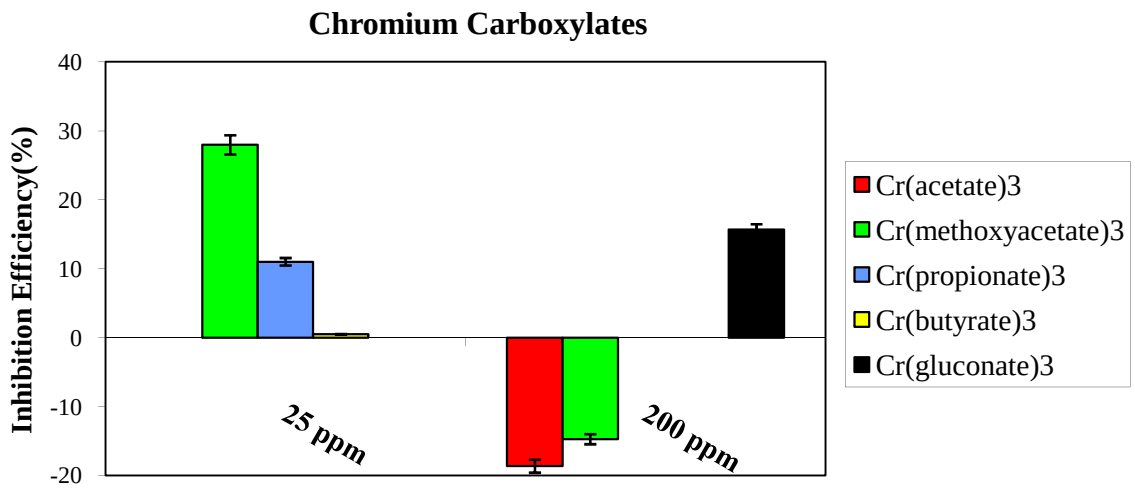

Figure 3-9 Inhibition Efficiency vs. Concentration Graph for Chromium Carboxylates

3.2.9 Various Cr(III) compounds

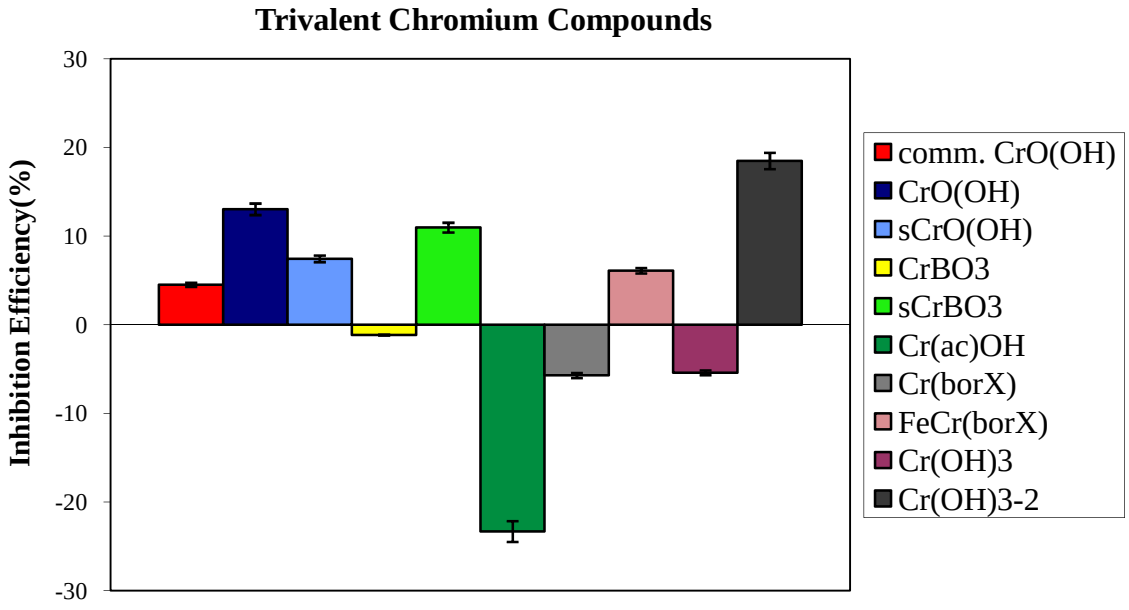

Figure 3-10 Inhibition Efficiency Graph for Various Trivalent Chromium Compounds

Similar to chromium carboxylates, selected trivalent chromium compounds did not inhibit corrosion of mild steel. Notably, nanoparticulate chromium hydroxide slightly inhibited corrosion while the material with larger particle size actually promoted corrosion.

3.3 Effects of Independent-Controlled Variables on Corrosion Inhibition Efficiency

The effect of independent variables that are inhibitor concentration and cationic constituents on inhibition efficiency has been examined. These variables were varied to yield higher values of dependent variables that are the final weights of the coupons (thus are the weight-losses and the inhibition efficiencies).

On the other hand, the effect of various immersion periods has also been examined. Since the controls were immersed for the same periods as the tested coupons, the immersion periods were controlled variables rather than independent variables.

3.3.1 Effect of Concentration&Immersion Periods on Inhibition Efficiency

Concentration is one of the major factors determining the inhibition efficiency. Inhibitors prevent corrosion by reacting with aggressive chemicals, preventing them to react with the metal substrates. Thus, inhibitor concentration decreases with time unless provided. Various concentrations of inhibitors were used from 25 ppm up to 500 ppm and also from 0.05 M up to 1 M for immersion tests. However, as stated earlier, among the various concentrations, the optimum concentration for an immersion test of a 1x1 mild

steel coupon in a 100 ml solution of 60 ppm Cl^- was determined to be 200 ppm after many tests. Tests revealed that inhibition efficiencies generally increased with increasing concentrations up to 200 ppm and decreased thereafter. Similar observations have been reported in the literature, in which 100 ppm, 150 ppm, and 200 ppm concentrations were recorded as sufficient concentrations for corrosion inhibition in similar systems.[3]

200 ppm corresponds to a weight percentage of about 0.2%, which is in between literature values of 1%, that is claimed to be the optimum concentration of calcium gluconate tested in seawater,[14] and 0.1%, that is claimed to be the optimum concentration since higher concentrations could produce a soluble iron-gluconate complex resulting in pronounced corrosion.[15]

It has been pointed out in a previous study that zinc gluconate's inhibition efficiency decreases with increasing concentration from 200 ppm to 500 ppm due to the competition between Zn^{+2} and Fe^{+2} cations for the counter ions.[3]

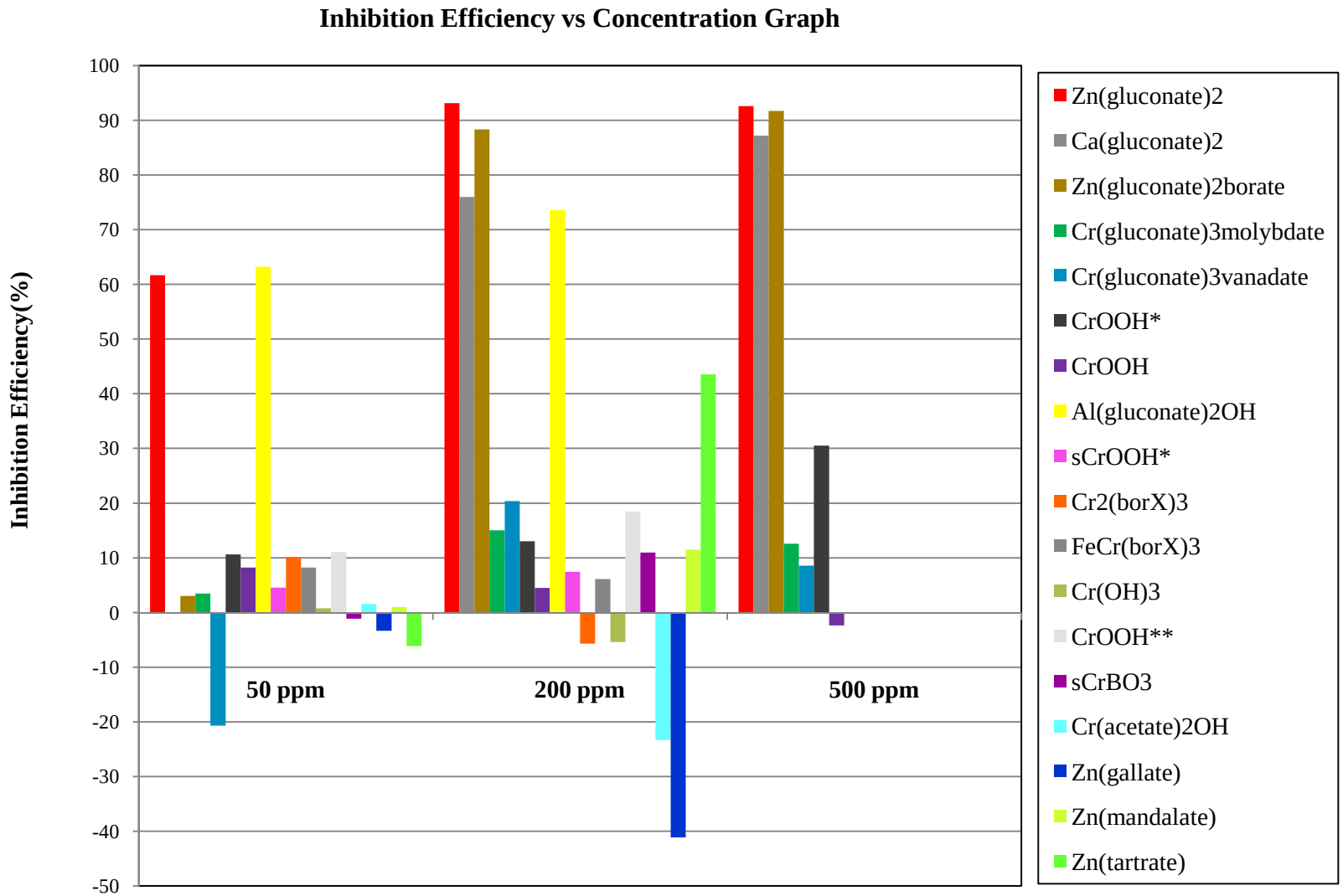

Figure 3-11 General Inhibition Efficiency vs. Concentration Graph

3.3.2 Effect of Cationic Constituent on Inhibition Efficiency

Cationic constituents had considerable influence when compounds with similar anionic constituents were compared in terms of inhibition efficiencies. Zinc cations are known for their cathodic inhibitive activity in the literature. Zn^{+2} cations form insoluble $Zn(OH)_2$ precipitates on cathodic sites at high pH values due to the production of OH^{-1} by corrosion of iron substrate with dissolved oxygen. Zinc hydroxide gradually changes to zinc oxide resulting in a passive film of zinc oxides and hydroxides.[16]

$$Zn(OH)_2 \longrightarrow ZnO + H_2O \qquad \text{(Eq. 3.6)}$$

However, when chloride anions are present in the media, they react with zinc hydroxide to form soluble Zn^{2+}-Cl^--OH^- complexes[17], thus leading to breakdown of the localized passive film resulting in pitting corrosion.

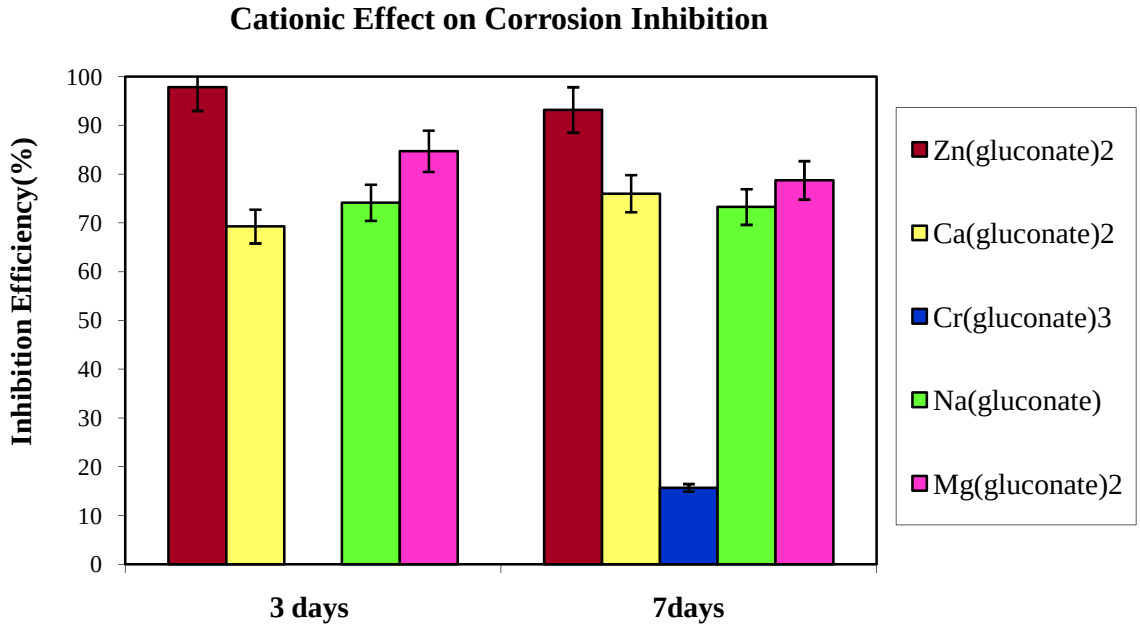

Figure 3-12 Inhibition Efficiency vs. Immersion Time Graph for Formulations with Different Cationic Constituents

Other than zinc cations, calcium and magnesium ions, which constitute the hardness of water, are also known to have slight cathodic inhibitive activity due to their little soluble hydroxides especially in near neutral-basic conditions such as seawater. However, no major differences were observed in terms of inhibition efficiencies between sodium, magnesium, and calcium gluconates. The sodium cation, all of its salts being soluble, and also inert towards redox reactions is primarily considered ineffective for corrosion inhibition of any metal. It is only effective in determination of secondary solution properties such as solubility and conductivity. Therefore, this indifference between sodium, magnesium, and calcium gluconates indicate that the inhibition by gluconate was the primary mechanism of corrosion inhibition. Trivalent chromium did not seem to inhibit mild steel corrosion even when combined with metal oxyanions. If anything, Cr^{3+} either prevented the gluconate's inhibition mechanism or promoted corrosion.

3.4 Conversion Coating Formation Studies

Corrosion inhibitors prevent corrosion either by continuously reacting with the aggressive chemicals, which requires a continuous supply of the corrosion inhibitor or by forming conversion coatings on the metal surface, which protects the metal substrate for longer periods of times. Thus, in addition to direct inhibition of corrosion, the inhibitors were tested for conversion coating formations and if present, the nature of this film was studied and characterized. Notably, chromates prevent corrosion both directly and indirectly leading to the formation of conversion coatings that have self-healing abilities.

3.4.1 Using the Weight-Loss Method

To examine the coupons for conversion coating formation, coupons that previously immersed in the solutions of inhibitors were immersed in salt water with no inhibitor present for a second period of time. The presence of corrosion inhibition during this second immersion period would imply the presence of a protective conversion coating on the substrate surface.

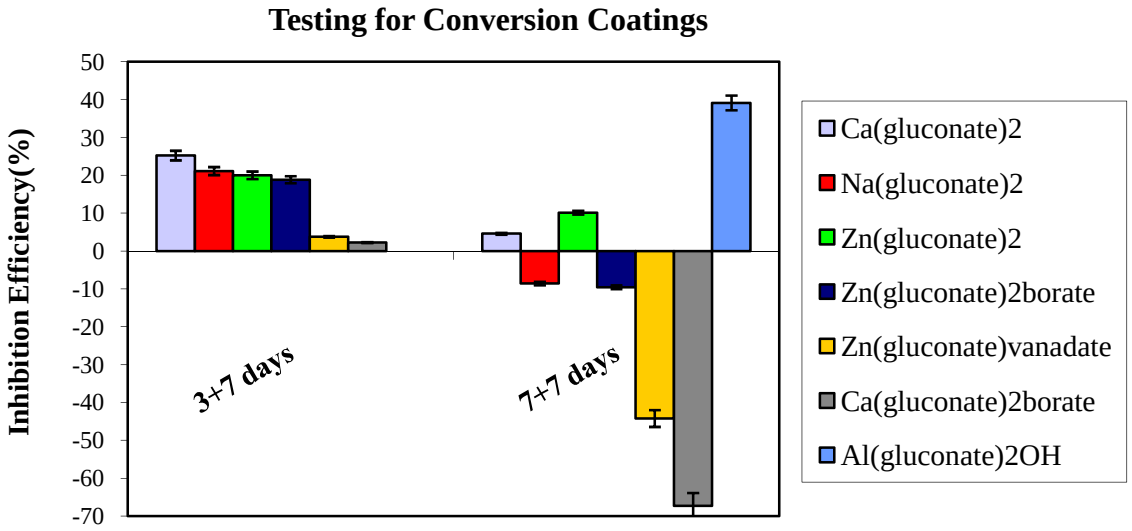

Figure 3-13 Inhibition Efficiency vs. Immersion Time Graph for Testing Conversion Coating Formations

The results revealed that for all of the gluconate-containing inhibitors there was corrosion protection present during the first 3 days of the second immersion period but the inhibition efficiency was significantly less than that found when the corrosion inhibitor was present in the solution. This suggests that the inhibition was due to inhibitors leached from deposits of corrosion products on the substrate surfaces. This was confirmed by further substantial decreases in inhibition efficiencies during the next 4 days of the second immersion periods. Upon completion of second immersion periods of

7 days, only a few inhibitors yielded positive inhibition efficiencies; among them were zinc and calcium gluconate, and aluminum gluconate hydroxide.

The weight changes of mild steel coupons after immersions into solution of $Al(gluconate)_2OH$ with or without 60 ppm Cl^- has also been measured. Less weight-loss was recorded for the coupon immersed in solution of $Al(gluconate)_2OH$ without Cl^- compared to the control coupon under the same conditions indicating that conditions with no Cl^- were favored for the formation of aluminum gluconate conversion coatings.

The slight inhibition by calcium and zinc gluconates during second immersion periods could be attributed to the same reasons explained for their inhibition efficiencies during first immersion periods. However, this reasoning cannot explain the high inhibition efficiency of $Al(gluconate)_2OH$ since for one, aluminum is not known with its cathodic activity and since, unlike calcium and zinc hydroxides, at highly basic local conditions, aluminum hydroxide dissolves due to complexation. Thus, further examination was needed using other methods such as surface characterization techniques.

3.4.2 Weight Difference Measurements

Weight changes of the coupons during immersions were determined prior to cleansing of corrosion deposits, since the presence of any type of deposition on the surface would have increased the weight of the coupon. To determine whether the increase in weight was caused by corrosion deposits or a protective coating, weights prior to the removal of corrosion deposits were compared to the weights after removal of corrosion deposits. Almost no weight-loss values were recorded for $Al(gluconate)_2OH$ and $Ca(gluconate)_2$borate treated coupons prior to the removal of corrosion products. In

the case of Zn(gluconate)$_2$vanadate treated coupon's weight had increased. After the application of the cleaning solution, both Al(gluconate)$_2$OH and Ca(gluconate)$_2$borate treated coupons still had negligible weight-losses. These results correlated with the inhibition efficiency results. Also the formation of a protective coating due to Al(gluconate)$_2$OH was visually apparent. In the case of Ca(gluconate)$_2$borate treated coupons a possibly formed protective coating was certainly not stable since a highly negative inhibition efficiency was observed during second immersion periods. On the other hand, the Zn(gluconate)$_2$vanadate treated coupon had a significant weight-loss correlating with its lower inhibition efficiency values than those of Al(gluconate)$_2$OH, and Ca(gluconate)$_2$borate.

In conclusion boron esters and Al(gluconate)$_2$OH had the least weight-losses during first immersions followed by vanadium, and molybdenum esters; respectively. Trivalent chromium compounds had the highest weight-loss values among all.

3.4.3 Qualitative Analysis of the Coupons after Immersions

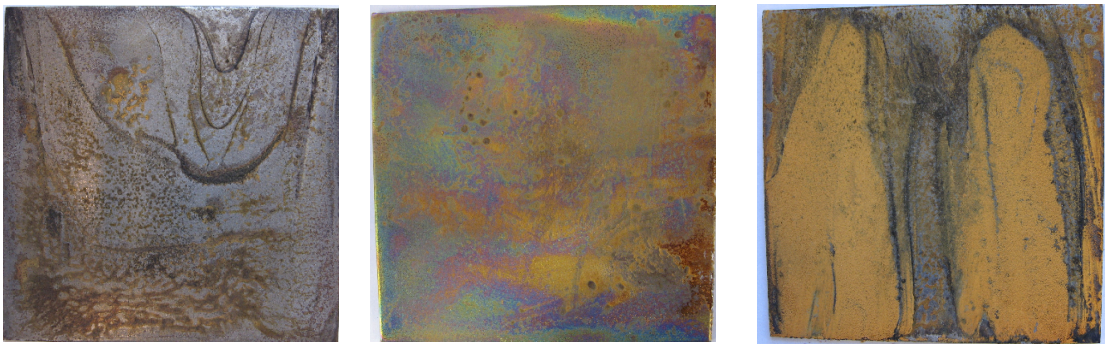

mild steel control in 60 ppm Cl^- soln. for 1 week

200 ppm Al(gluconate)$_2$OH in 60 ppm Cl^- soln. for 1 week

200 ppm CrO(OH) in 60 ppm Cl^- soln. for 1 week

Figure 3-14 Images of control, uncorroded, and corroded coupons; respectively.

Comparison of the images of coupons treated with synthesized CrOOH, and $Al(gluconate)_2OH$ revealed that the CrOOH treated coupon and control coupon seemed to be extensively corroded while there was a greenish-blue colored layer on the surface of the coupon that was treated with $Al(gluconate)_2OH$.

mild steel control in 60 ppm Cl^- soln. for 1 week

200 ppm $Cr(butyrate)_3$ in 60 ppm Cl^- soln. for 1 week

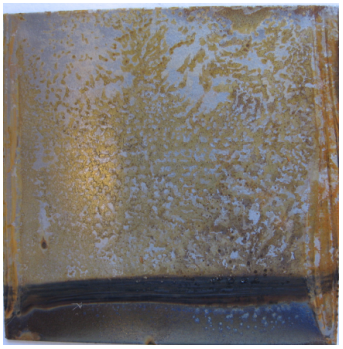

200 ppm $Cr(propionate)_3$ in 60 ppm Cl^- soln. for 1 week

Figure 3-15 Images of control coupon and coupons immersed in solutions of chromium carboxylates; respectively.

Coupons treated with other Cr(III) compounds, such as $Cr(butyrate)_3$ and $Cr(propionate)_3$ also revealed extensive corrosion taking place on the substrate surface. These observations were in agreement with the weight loss test results.

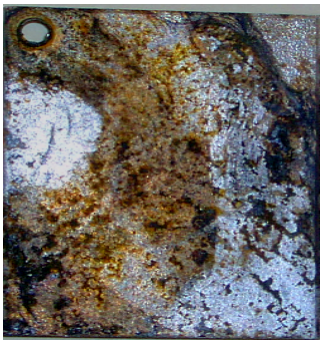

mild steel control in 60 ppm Cl^- soln. for 1 week

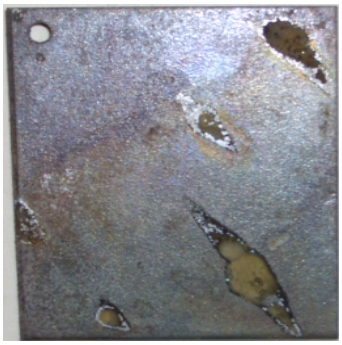

200 ppm K(benzilate)vanadate 60 ppm Cl^- for 1 week

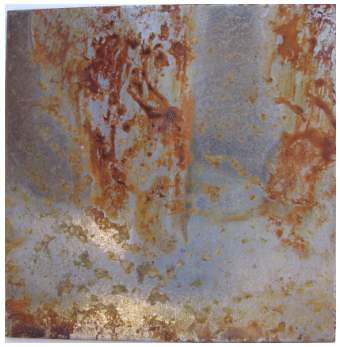

200 ppm Ca(gluconate)borate 60 ppm Cl^- for 1 week

Figure 3-16 Images of control coupon and coupons immersed in solutions of metal oxyanion esters; respectively.

The image of the Ca(gluconate)borate treated coupon revealed less corrosion products than that of the control confirming the weight-loss test results. On the contrary, the weight-loss test results contradicted the visual observation of K(benzilate)vanadate treated coupon, which seemed clear despite a few large pits. The clear surface indicates that K(benzilate)vanadate inhibits uniform corrosion but not pitting corrosion.

3.4.4 X-Ray Powder Diffractometer Studies

As a complimentary technique, X-ray powder diffraction patterns of the inhibitor treated substrate surfaces revealed phase composition in agreement with those of weight-loss test results and visual observations.

Correlated with their positive inhibition efficiencies, X-ray diffraction patterns of relatively uncorroded steel coupons, such as the ones treated with 60 ppm Cl^- solutions of 200 ppm Al(gluconate)$_2$OH, Ca(gluconate)$_2$borate, Zn(gluconate)vanadate, and Cr(propionate)$_3$ revealed only iron without corrosion products. In contrast, the X-ray pattern of a steel coupon dipped into 60 ppm Cl^- solution of CrOOH revealed peaks due to corrosion products of iron such as rust FeO(OH) both in the form of lepidocrocite and goethite along with magnetite $FeFe_2O_4$. Two examples are shown in Figure 3-17 and 3.18.

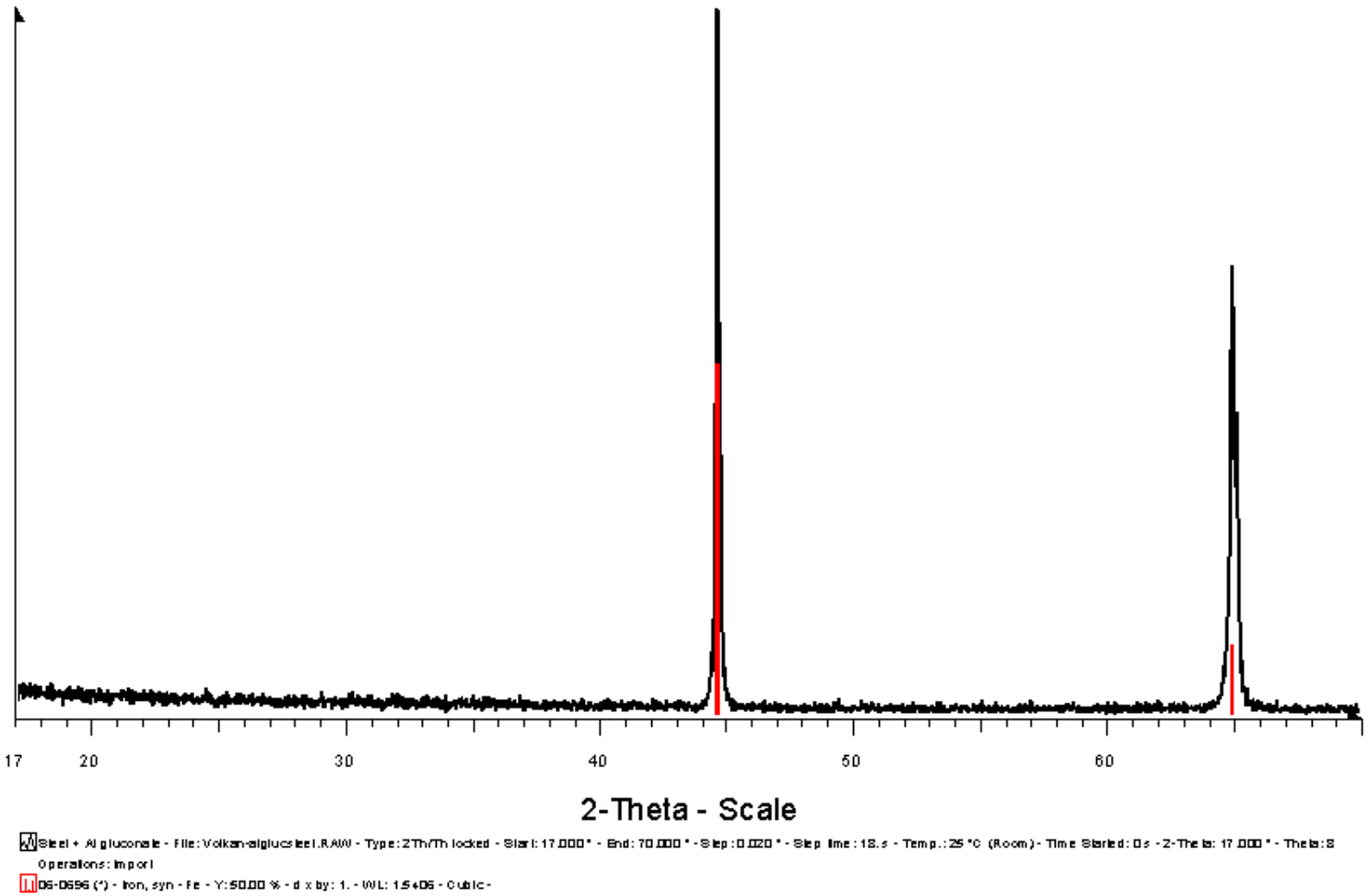

Figure 3-17 X-ray Diffraction Pattern of a Mild Steel Coupon Immersed in Al(gluconate)$_2$OH-salt solution for 7 days

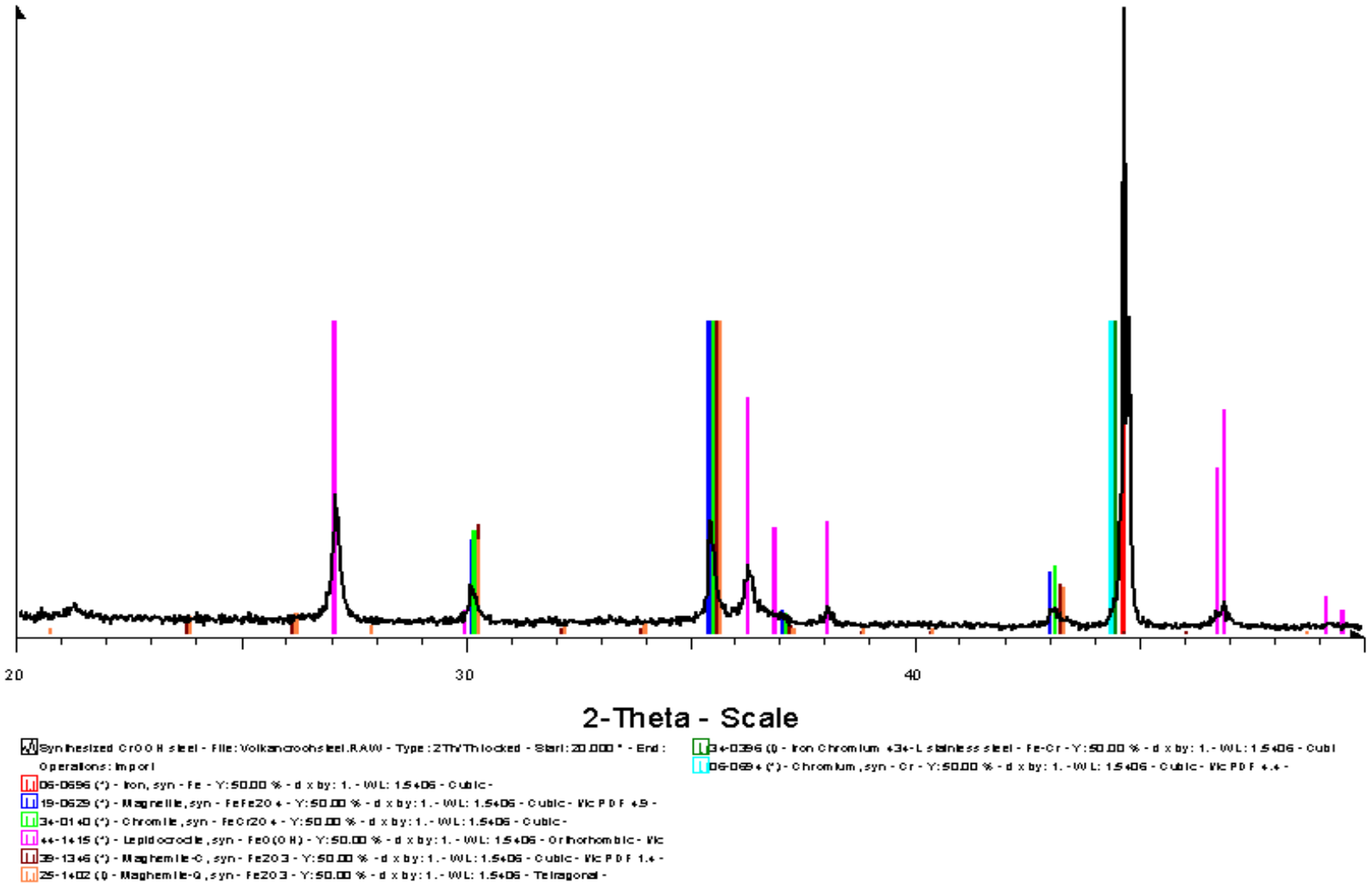

Figure 3-18 X-ray Diffraction Pattern of a Mild Steel Coupon Immersed in CrOOH-salt solution for 7 days

The X-ray diffraction pattern of steel coupon treated with 60 ppm Cl^- solution of 200 ppm potassium benzilate molybdate for 3 days did not reveal any corrosion products confirming the positive inhibition efficiency. Immersion of the same coupon into the same potassium benzilate molybdate-salt solution for 7 days was just enough for the peaks due to corrosion products such as goethite FeO(OH), and magnetite $FeFe_2O_4$ to appear in agreement with inhibition efficiency data.

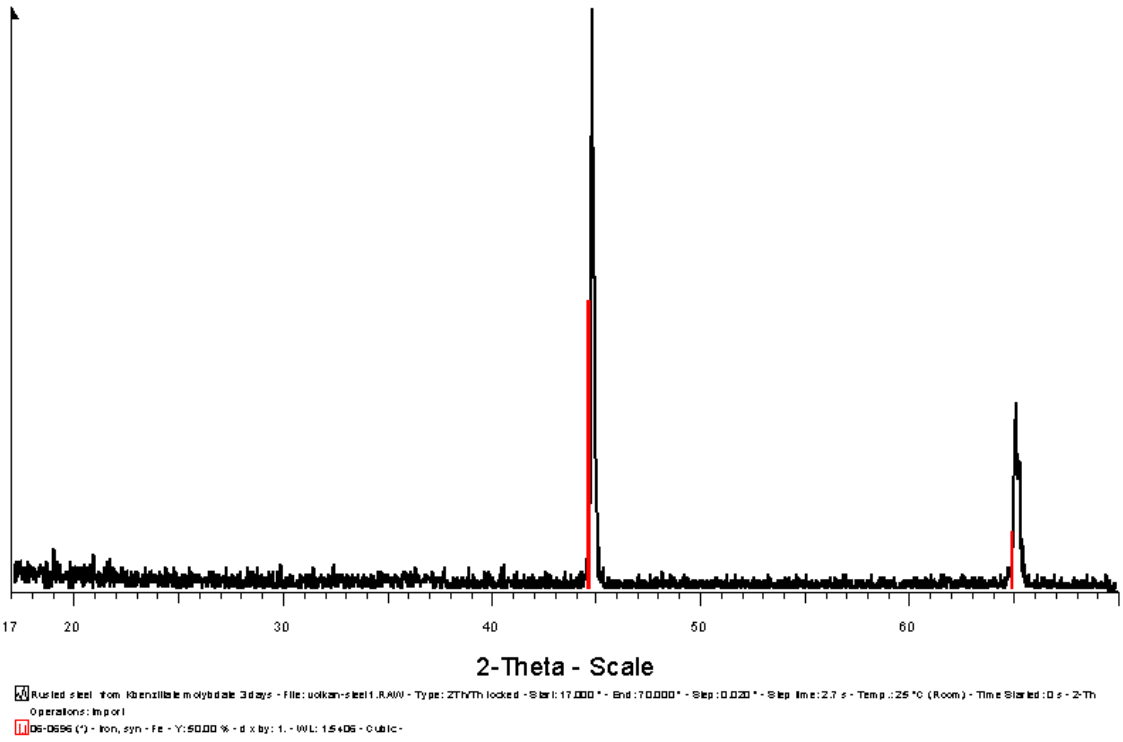

Figure 3-19 X-ray Diffraction Pattern of a Mild Steel Coupon Immersed in K(benzilate)molybdate-salt solution for 3 days

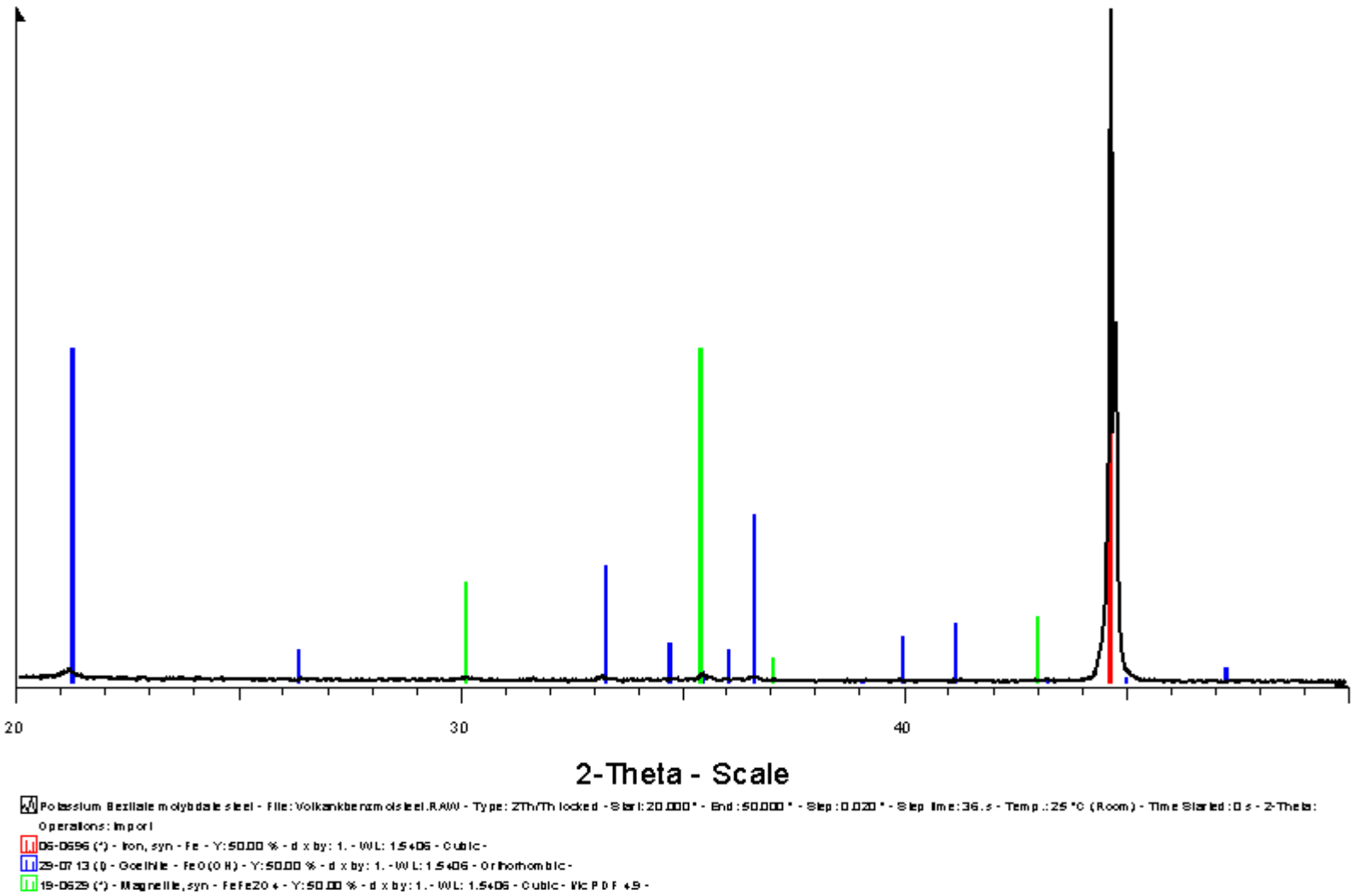

Figure 3-20 X-ray Diffraction Pattern of a Mild Steel Coupon Immersed in K(benzilate)molybdate-salt solution for 7 days

3.4.5 Scanning Electron Microscope Studies

Scanning electron microscopy (SEM) is a morphological surface analysis technique that uses electrons, rather than light to form an image. There are many advantages for using the SEM instead of a light microscope. The SEM has a large depth of field, which allows a large amount of the sample to be in focus at one time. The SEM also produces images of high resolution, which means that closely spaced features can be examined at a high magnification. Preparation of the samples is relatively easy since most SEMs only require the sample to be conductive. If the sample is not conductive, then it should be coated with a conductive material. The combination of higher magnification, larger depth of focus, greater resolution, and ease of sample observation makes the SEM one of the most heavily used techniques in research areas today. In this study a JEOL JXM 6400 SEM was used for surface imaging of substrates both before and after immersions. As an example, SEM micrographs revealed substantially less corrosion products on the surface of the coupon that was immersed into the solution of 200 ppm $Al(gluconate)_2OH$ for a period of 1 week. The micrograph of the 3 day $Al(gluconate)_2OH$ treated coupon immersed into salt water for a subsequent period of 7 days revealed the presence of an intense deposition layer; which was possibly a mixed coating composed of protective aluminum oxides and hydroxides and corrosion products.

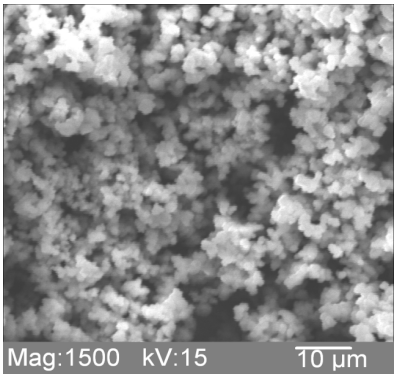

Steel in 60 ppm Cl^- water for 7 days

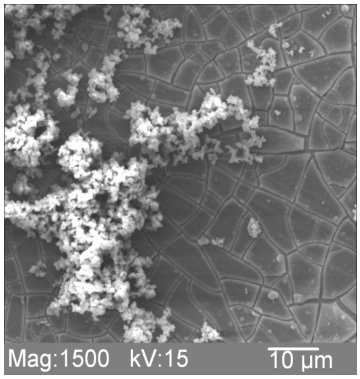

200ppm $Al(gluconate)_2OH$, 60 ppm Cl^- for 7 days

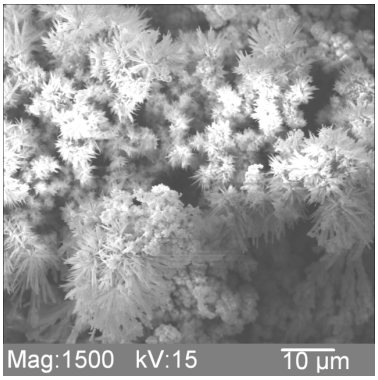

200ppm $Al(gluconate)_2OH$, 60 ppm Cl^- 3 days + 60 ppm Cl^- 7 days

Figure 3-21 1500 Times Magnified Scanning Electron Micrographs of Control Coupons and of Coupons Immersed in Solutions of Aluminum Gluconate Hydroxide for 7 days and 10 days.

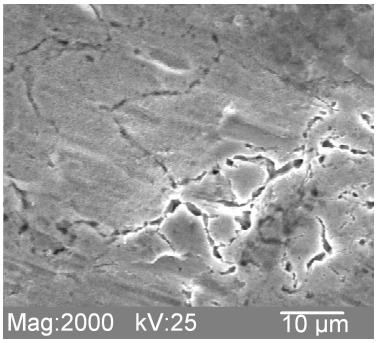

Blank steel

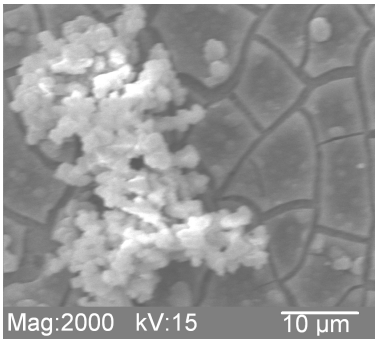

200ppm $Al(gluconate)_2OH$, 60 ppm Cl^- 7days

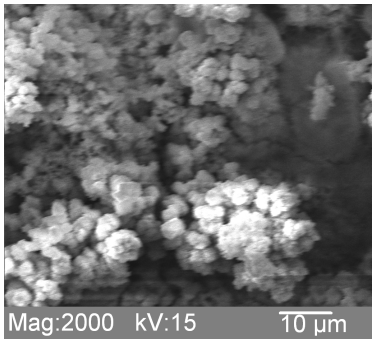

0.01M $Al(gluconate)_2OH$, 60 ppm Cl^- 3 days + 60 ppm Cl^- 7 days

Figure 3-22 2000 Times Magnified Scanning Electron Micrographs of Control Coupons and of Coupons Immersed in Solutions of Aluminum Gluconate Hydroxide for 7 days and 10 days.

There was no difference between the control coupon and the coupon that was immersed into salt water for a second period of time after treating it with 0.01 M of Al(gluconate)2OH in agreement with the poor corrosion inhibition results. This most likely was due to the increased conductivity of the solution caused by high ion

concentrations.

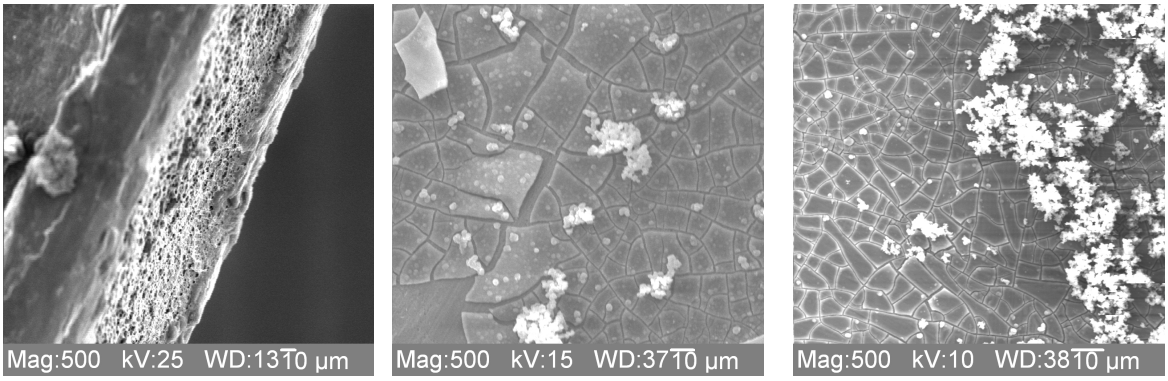

Blank Steel | 200ppm Al(gluconate)$_2$OH, 60 ppm Cl^- 7days | 200 ppm Al(gluconate)$_2$OH, no Cl^- 7days

Figure 3-23 Scanning Electron Micrographs of Control Coupon and of Coupons Immersed in Solutions of Aluminum Gluconate Hydroxide with or without 60 ppm Chloride, respectively.

No significant difference was observed between SEM micrographs of coupons treated with 200 ppm solution of Al(gluconate)$_2$OH with or without 60 ppm Cl^-.

3.4.6 Infrared Spectra Studies

Infrared spectra studies of inhibitor treated coupons and control coupons have been performed both before and after immersions. Since the substrate surfaces were examined, three types of absorptions were possible; absorptions purely due to structure of the substrate, absorptions purely originated from adsorption of inhibitor compound on the substrate surface, and absoptions due to deposition of compounds such as corrosion products formed by the reactions between the mild steel substrate, the inhibitor compound, and the corrosive chemicals.

The immersion in water is expected to lead to broad bands due to symmetric and asymmetric stretchings of hydroxyl of water centered around 3500 cm^{-1} and due to bending of hydroxyl of water around 1600 cm^{-1} were expected.[18-25] However, the substrates were air dried for several days before taking their spectra to minimize absorptions caused by physically adsorbed water. The difference in absorptions in the 1600 cm^{-1} region of the spectra of control substrates and substrates treated with gluconates, benzilates and other hydroxyl acid salts led to the conclusion that air drying was successful in minimizing the effects of water. Thus, the absorptions around 1600 cm^{-1} region were assigned to carbonyl stretchings in general and specifically to OCO^{-} stretchings. Other bands in the 1600 cm^{-1} region were assigned to hydroxyl groups of organic compounds rather than hydroxyl of water. IR spectra of different compounds differed depending on the IR active functional groups leading to a categorization based on the IR active constituent.

Gluconate Salts

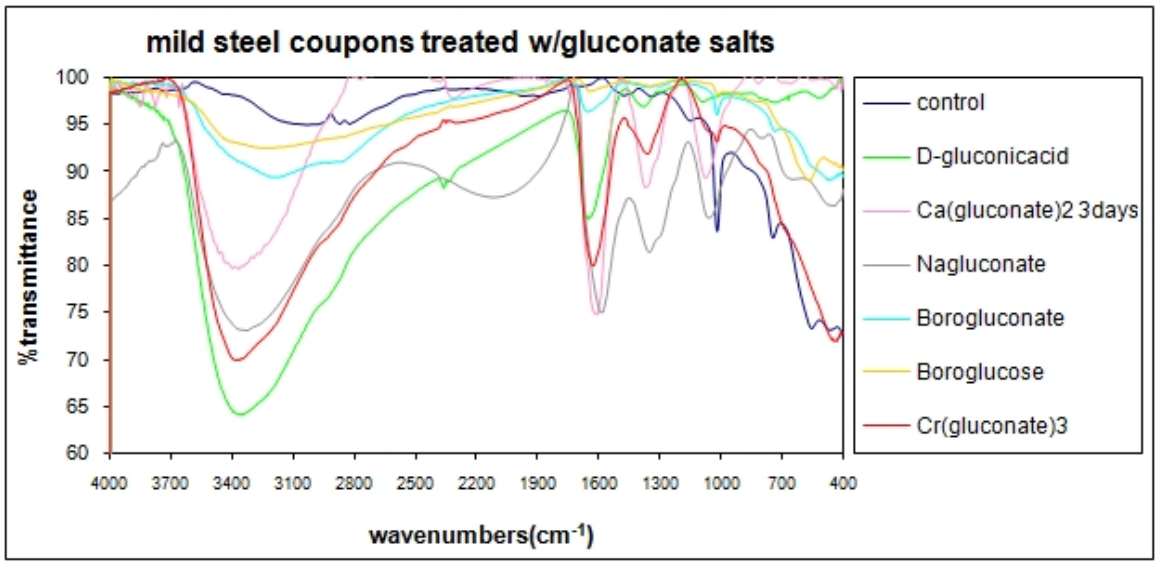

Figure 3-24 Combined Infrared Spectra of Coupons Immersed in Solutions of Gluconates for 7 days with 60 ppm Chloride

In accordance with literature values of ca. 1600 and 1385 cm^{-1}, [26] the bands centered at 1600 cm^{-1} and at 1380 cm^{-1} in the spectra of gluconate salts were assigned to the asymmetric and symmetric OCO^- stretching vibrations. The strength of the absorptions seemed to be somewhat proportional to the inhibition efficiency values with boroglucose, borogluconate, gluconic acid having weaker absorptions in that order indicating little adsorption of gluconates on the substrate surface in agreement with their low inhibition efficiency results. The only exception to this trend was chromium gluconate which had a strong absorption despite its low but still positive inhibition efficiency. In addition, the separation of more than 200 cm^{-1} between the observed OCO^- components in the spectra of the gluconate salts was assigned to monodentate carboxylate coordination as stated in the literature[27].

Based on literature data, broadening of the OH stretching vibrations due to interactions between the hydroxyl groups of the gluconate with the metal ions was observed. However broadening and shifting of CH_2, COH and CHO bending vibrations,

which appear in the region 1400–1100 cm^{-1} due to interactions between the metal ion and the hydroxy acid were not observed.[28] Relatively weaker bands at 1100–940 cm^{-1} were assigned to the hydroxy acid C–O stretching vibrations in general for gluconates.[26]

Al(gluconate)$_2$OH

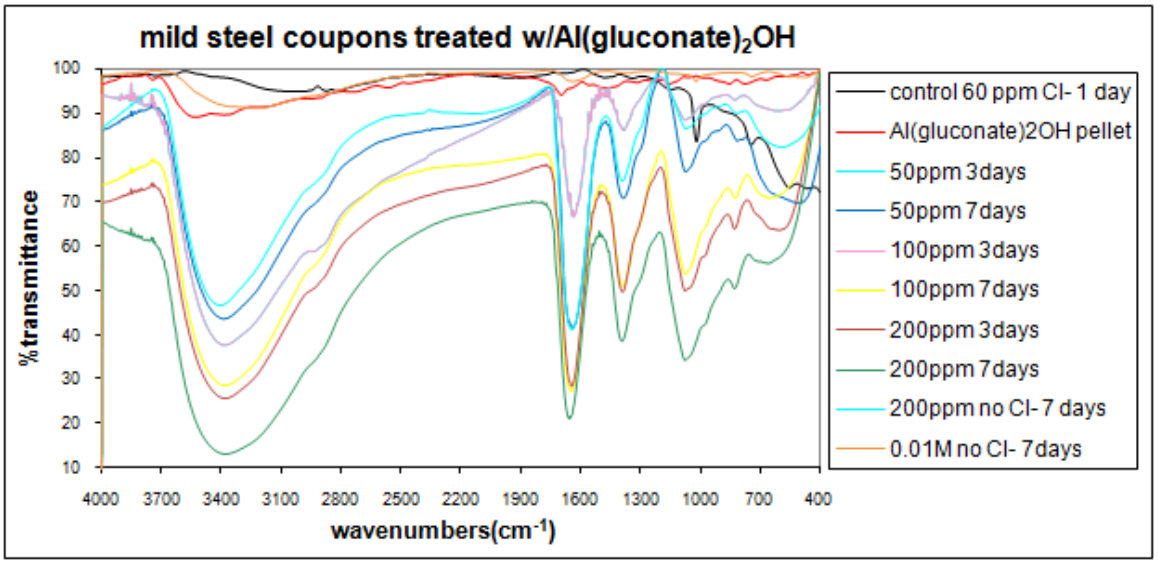

Figure 3-25 Combined Infrared Spectra of Coupons Immersed in Solutions of Aluminum Gluconate Hydroxide with Varying Immersion Times, Chloride Concentrations, and Inhibitor Concentrations

Infrared Spectra of the coupons treated with Al(gluconate)$_2$OH, revealed absorptions similar to the gluconates for frequencies higher than 1200 cm^{-1} with symmetric and asymmetric stretching vibrations of hydroxyl groups centered at 3500 cm^{-1}, OCO^- stretching vibrations centered at 1600 cm^{-1} and 1370 cm^{-1}. Notably a shift to lower frequency region was observed with increasing inhibitor concentration. In the low frequency region, the OH bending vibrations at 1050 cm^{-1} were assigned to AlOOH, and Al-O stretching vibrations at 770 cm^{-1} were assigned to AlOOH (as opposed to the

absorptions of Fe-O stretching vibration due to γ-FeOOH at 750 cm^{-1} and the OH bending vibration at 1000 cm^{-1} due to γ-FeOOH in the spectra of the control coupons).[29-34]

The presence of OCO^- stretching vibration bands at 1600 cm^{-1} and 1370 cm^{-1} on the other hand suggested the adsorption of the gluconate constituent on the substrate surface as well as bound to the protective aluminum oxide/hydroxide layer. More evidence for the formation of a conversion coating of aluminum oxides/hydroxides was provided by XPS results, which revealed the presence of aluminum on the surface of the coupons treated with $Al(gluconate)_2OH$ and also by weight-loss test results, which revealed positive inhibition efficiencies during second immersion periods for $Al(gluconate)_2OH$ treated coupons opposed to coupons treated with other gluconates salts.

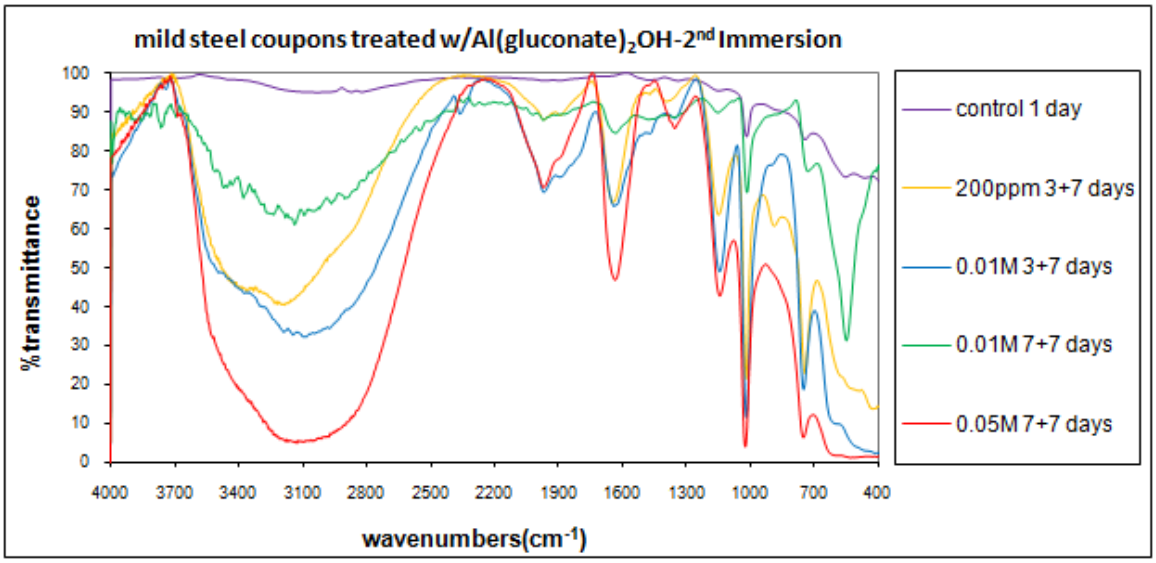

Figure 3-26 Combined Infrared Spectra of Coupons Immersed in Solutions of Aluminum Gluconate Hydroxide for 14 days for Testing Conversion Coating Formation

In the spectra of coupons immersed for a second period of time, bands matching with FeOOH bands of the control coupons were also present along with bands due to AlOOH confirming the previous assignment of bands due to AlOOH suggesting that they were not just shifted bands due to FeOOH. Despite the presence of bands due to corrosion products of FeOOH; bands due to AlOOH were still strong as opposed to the other gluconate salts where either no or very weak bands were present. However, it is also important to note that a lot of weaker similar bands were also present in the spectra of some coupons of other gluconate salts in the regions of 1050 cm^{-1} and 750 cm^{-1} matching bands of $Al(gluconate)_2OH$ treated coupons, which may imply that an eventually soluble iron gluconate layer was formed on the substrate surface of coupons treated with other gluconate salts, while for coupons treated with $Al(gluconate)_2OH$ both iron gluconate and aluminum oxides and hydroxide layers were present. Lastly, shifting of the bands due to hydroxyl stretchings with increasing inhibitor concentration was observed similar to the spectra of coupons of 1^{st} immersions.

Other carboxylic acids and their salts

Infrared spectra of the other tested carboxylic salts such as aluminum acetate, aluminum lactate and chromium acetate revealed mostly similar absorptions to those of gluconate salts with weaker absorptions in general along with several differences.

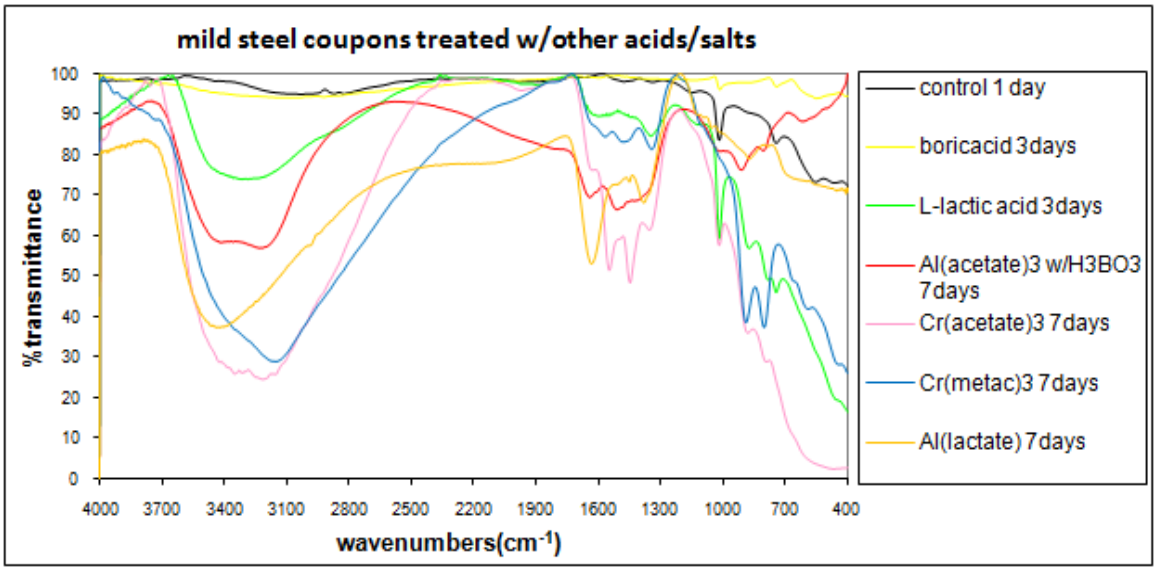

Figure 3-27 Combined Infrared Spectra of Coupons Immersed in Solutions of Other Carboxylic Acid Salts with 60 ppm Chloride for either 3 or 7 days

One difference was in the OCO^- stretching vibrations, where the separations were less than 200 cm^{-1} for acetate salts indicating the chelating or bridging structures of acetates. Another difference was the absence of bands in the 1050 cm^{-1}.

Molybdenum Esters of Hydroxy Acid Salts

Calcium&Zinc Gluconate Molybdates

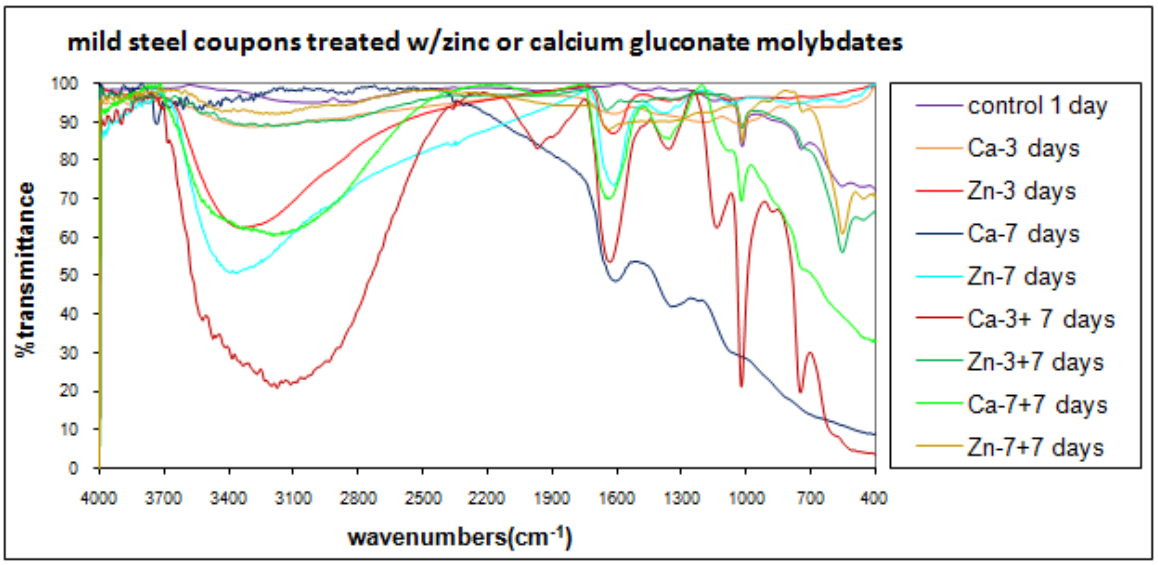

Figure 3-28 Combined Infrared Spectra of Coupons Immersed in Solutions of Molybdenum Esters of Calcium and Zinc Gluconates with 60 ppm Chloride for Various Immersion Periods

Absorptions due to carbonyl groups of carboxylates were present in two bands with 200 cm^{-1} separation as in gluconate salts, however no absorptions were observed due to the Mo-O bending vibrational modes at 972 cm^{-1} [35], 994 cm^{-1} [36], and 996 cm^{-1} [37] as stated in the literature. Additional bands due to corrosion products at 1020 cm^{-1} and at 750 cm^{-1} were assigned to γ-FeOOH and band at 580 cm^{-1} was assigned to magnetite (Fe_3O_4).[33,34]

A possible absorption at 1398 cm^{-1} [3] due to $Zn(OH)_2$ was not observed. This could still be present but overwhelmed by OCO^- stretchings common to other gluconate salts in the same region.

Potassium Benzilate Molybdates

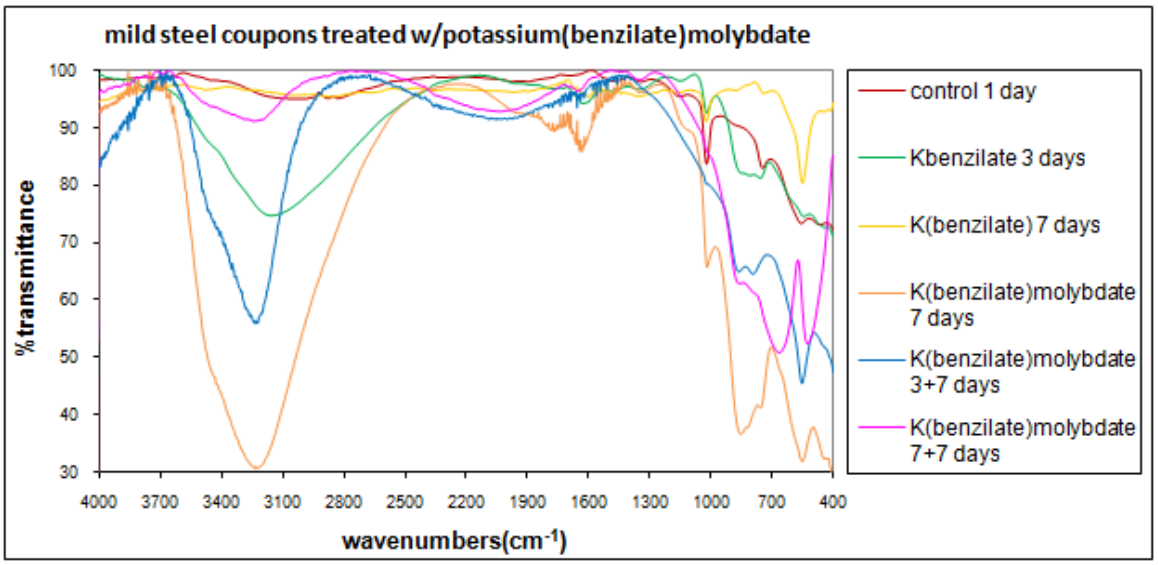

Figure 3-29 Combined Infrared Spectra of Coupons Immersed in Solutions of Molybdenum Esters of Potassium Benzilate with 60 ppm Chloride for Various Immersion Periods

In contrast to the gluconate salts and their esters, only one weak band at 1600 cm^{-1} was assigned to the carbonyl of benzilate, which was present only in the spectra of coupons immersed in potassium benzilate solutions for one week. Other bands in the spectra of coupons immersed in potassium benzilate molybdate solutions were due to corrosion products of iron at 1020 cm^{-1} and at 750 cm^{-1} assigned to γ-FeOOH, at 890 cm^{-1} assigned to α-FeOOH, at 580 cm^{-1} assigned to magnetite (Fe_3O_4), at 470 cm^{-1} also assigned to δ-FeOOH. The difference compared to the spectra of coupons immersed in solutions of potassium benzilate and calcium and zinc gluconate molybdates was the weak γ-FeOOH bands and emergence of α-FeOOH bands.[33,34]

Vanadium Esters of Hydroxy Acids

Calcium&Zinc Gluconate Vanadates

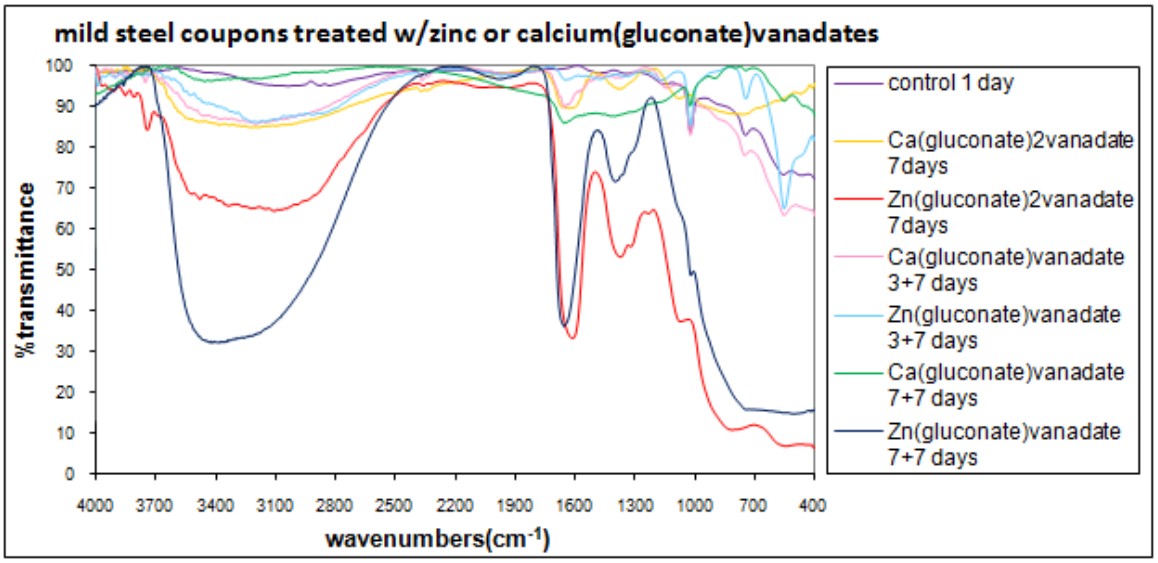

Figure 3-30 Combined Infrared Spectra of Coupons Immersed in Solutions of Vanadium Esters of Calcium and Zinc Gluconates with 60 ppm Chloride for Various Immersion Periods

Spectra of coupons immersed in solutions of calcium and zinc gluconate vanadates revealed more pronounced carbonyl bands and weaker bands due to corrosion products, otherwise all bands were the same as spectra of coupons immersed in calcium and zinc gluconate molybdate solutions. However, the spectra of coupons immersed in zinc(gluconate)vanadate solutions for 1st and 2nd immersion periods revealed shifted bands at 1020 cm^{-1} and at 850 cm^{-1} which could imply presence of vanadium on the substrate surface since absorption bands between 400 cm^{-1} and 1000 cm^{-1} are indexed to various group vibrations of V-O type in general[38-39] including bands at 1019 cm^{-1}, 850 cm^{-1}, and between 400 cm^{-1} to 650 cm^{-1} [40]. The slight inhibition efficiency of zinc

gluconate vanadate during 3 days of second immersion period, the increase in weight of the coupon after immersion for one week, and visual observation of the coupon after completion of immersion may all be explained by the presence of a vanadium conversion coating on the substrate surface although other results clearly indicate a low corrosion resistance of this coating even if it exists.

Potassium Benzilate Vanadates

Spectra of coupons immersed in potassium benzilate vanadate solutions were one to one match to the spectra of coupons immersed in potassium benzilate molybdate solutions with no indication of vanadium on the substrate surface but only corrosion products.

Boron Esters of Hydroxy Acids

Spectra of coupons immersed in solutions of boron esters of hydroxy acids revealed weak absorptions, which were mostly assigned to corrosion products with no indication of boron.

3.5 Characterization of Immersion Solutions

Immersion solutions were also indicators of the extent of corrosion. For instance, salt solutions of gluconate salts remained clear throughout the immersion of mild steel coupons, while the salt solution in which the control coupon was immersed, changed its color from clear to dark brown indicating the presence of iron corrosion products. On the

other hand, the color of salt solutions of molybdenum esters of gluconate salts changed from clear to yellow and the salt solution of vanadium ester of potassium benzilate changed color from clear to light yellow indicating some corrosion was taking place. In addition to visual color observations revealing the extent of corrosion qualitatively, the pH, conductivity and oxidation-reduction potential of the immersion solutions were measured prior to and after the immersions.

3.5.1 ORP Measurements

ORP is proportional to the concentration of oxidizers or reducers in a solution, and their activity or strength. It provides an indication of the solution's ability to oxidize or reduce another material. The addition of an oxidizer will raise the ORP value, while the addition of a reducer will lower the ORP value.

The ORP values of immersion solutions were measured to determine whether the redox capable inhibitor compounds had gone thorugh redox reactions or not. Dissolved oxygen may be reduced by the metal substrate and leading to lowering of the ORP value but comparison to the control solution should negate this effect.

Overall, the ORP values were decreased in average by half during immersions for both the control and inhibitor containing solutions. The exceptions were the gluconate salts of zinc and calcium, and their vanadate esters, where only a slight decrease in ORP occurred. As expected, inclusions of salt ions into the immersion solutions and increasing the immersion period led to further decrease in ORP.

In contrast to the molybdenum esters of gluconate salts, the ORP values for immersion solutions of vanadium esters of gluconates did not decrease. The amount of

slight decrease or even increase was approximately the same for all vanadium esters regardless of whether the hydroxy-acid constituent was gluconate or benzilate with the exception of zinc salts of vanadium esters, in which slight increases in ORP have been observed compared to almost no decrease to very little decreases when calcium and potassium cations were in the formulation, respectively. These results were unusual considering the decrease in ORP values of the control solutions and the immersion solutions of other tested inhibitor compounds that had similar inhibition efficiencies. Qualitative analyses of the vanadium ester treated coupons revealed clear surfaces with no uniform corrosion except a few pits. In the IR spectra of coupons treated with vanadate esters, contained absorptions that might have been due to vanadium oxides in the low frequency region of 400 cm^{-1} to 1000 cm^{-1}, but these were not resolved sufficiently to deduce such a conclusion. Overall, the vanadates seemed to work similarly to chromates; however any conversion coating that might be formed is either not adherent to the substrate surface or not resistant to the cleaning solution of 50% hydrochloric acid.

In agreement with the results for the vanadium esters, the ORP values of the immersion solutions of calcium and zinc gluconate salts did not decrease as opposed to magnesium and sodium gluconate salts, which showed significant decrease. The zinc salt had the lowest decrease of all of the gluconates. Since all gluconate salts had similar high inhibition efficiency values, the difference in ORP values is likely due to the cathodic inhibitive properties of zinc and calcium cations resulting in precipitation of zinc and calcium hydroxides at cathodic sites.

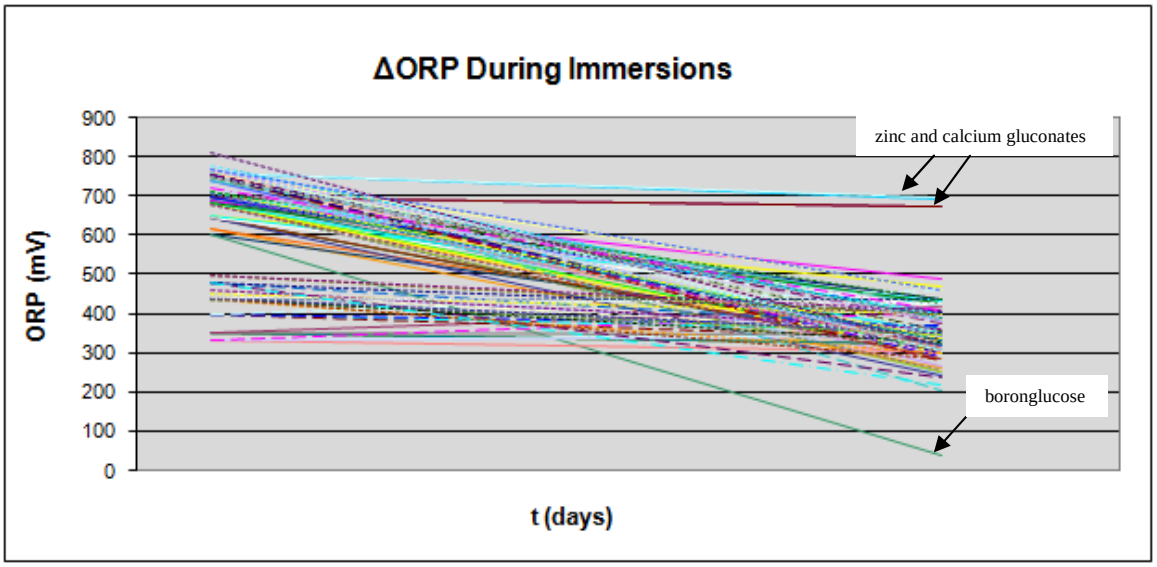

Figure 3-31 ORP (Oxidation-Reduction Potential) vs. Time Graph of Immersion Solutions of Various Inhibitors During Immersions of Coupons

Below ΔORP graph indicates the majority of corrosion inhibiting compounds' ORP values lowered by an average of roughly 350 mV.

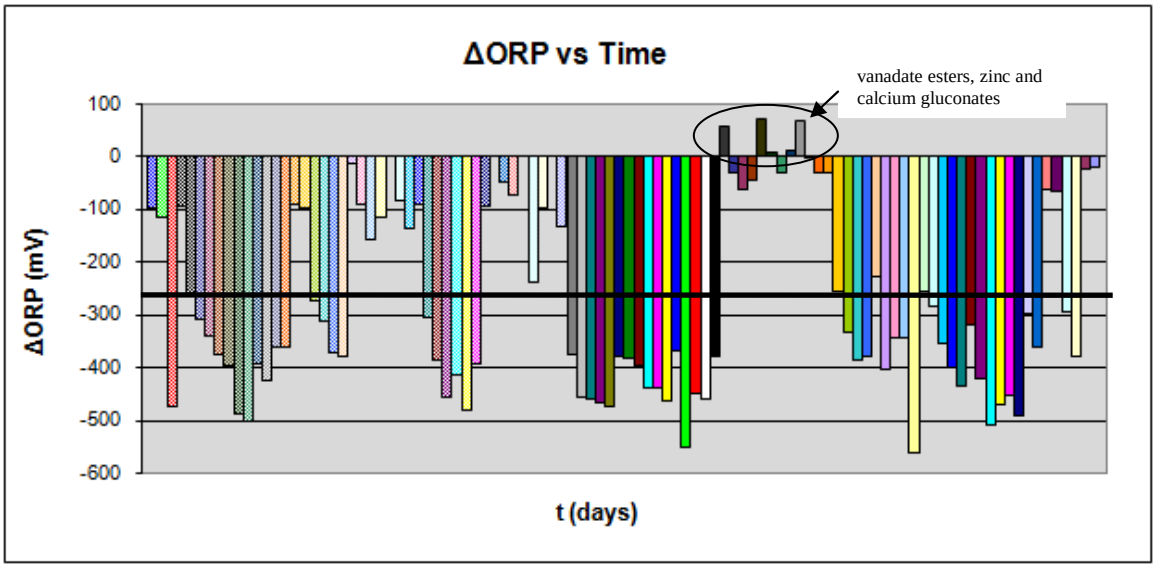

Figure 3-32 ΔORP vs. Time Graph of Immersion Solutions of Various Inhibitors During Immersions of Coupons

The ΔORP vs IE graph shown below indicates that the majority of the compounds that had ORP values decreased by an average of ~350 mV had positive inhibition efficiencies in the range of 50% to 100%.

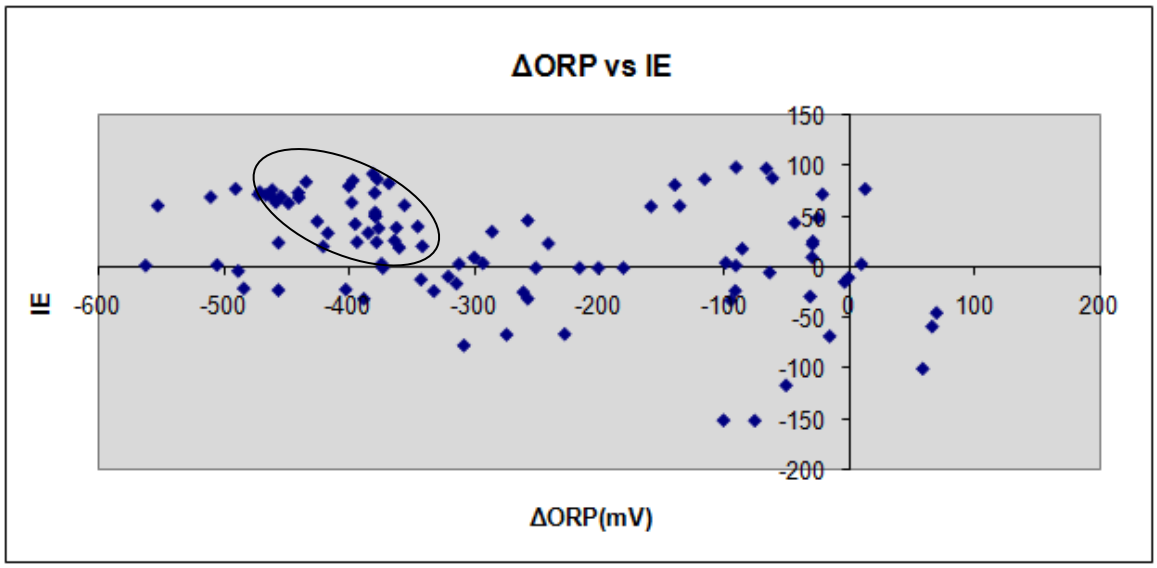

Figure 3-33 ΔORP vs. Inhibition Efficiency Graph of Immersion Solutions of Various Inhibitors

The $\Delta ORP/ORP_{initial}$ vs IE graph below indicates that the average ORP values were roughly halved for over 100 tested compounds with the exception of zinc and calcium gluconates and the vanadate esters.

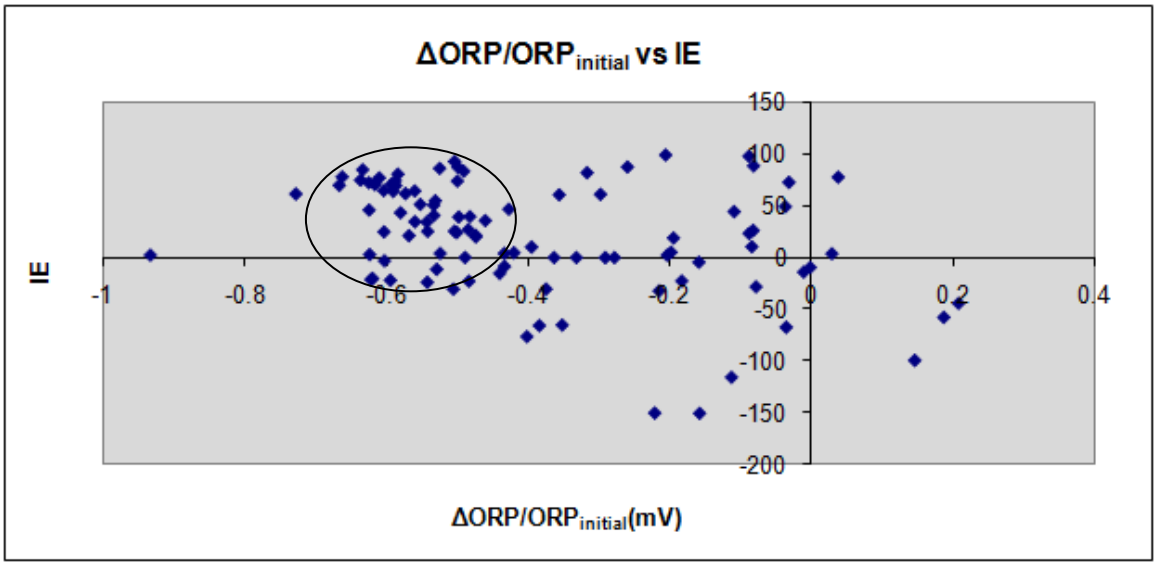

Figure 3-34 $\Delta ORP/ORP_{initial}$ Ratios vs. Inhibition Efficiency Graph of Immersion Solutions of Various Inhibitors

The vast majority of the ORP values were found to be within the range of 200 mV and 500 mV with the exceptions of the immersion solutions with various concentrations of calcium or zinc gluconate salts and the boroglucose solution which had an ORP value down from 600 mV to almost 0 mV.

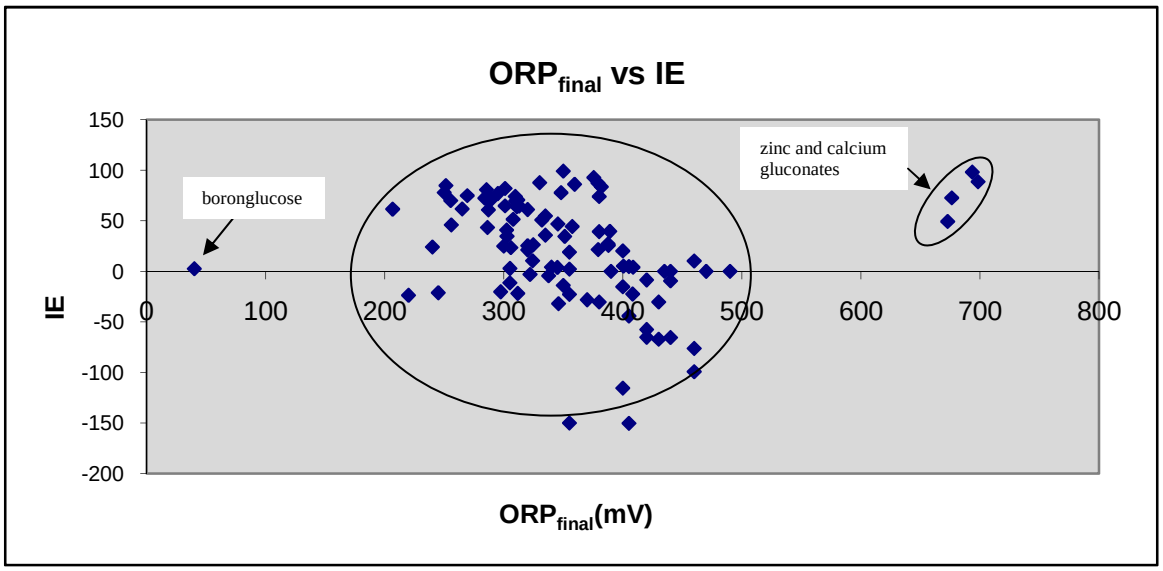

Figure 3-35 Final ORP Values vs. Inhibition Efficiency Graph of Immersion Solutions of Various Inhibitors

3.5.2 pH Graphs

In acidic solutions an increase in pH occurs due to hydrogen evolution caused by the reduction of hydronium ions. In near neutral to basic solutions, the system chosen for this study, the pH also increases due to the anodic reaction of corrosion process, that is

$$O_2 + 2H_2O + 4e^- \longrightarrow 4OH^-, \qquad \text{(Eq. 3.7)}$$

Accordingly, pH of the immersion solutions of good inhibitors increased only slightly, while a large increase was observed for compounds with poor corrosion inhibition ability. One week immersion solutions containing boroglucose, borogluconate, and the molybdenum esters of gluconate salts had higher ΔpH and final pH values than the other tested compounds. This is also correlated with the trends observed by ORP measurements.

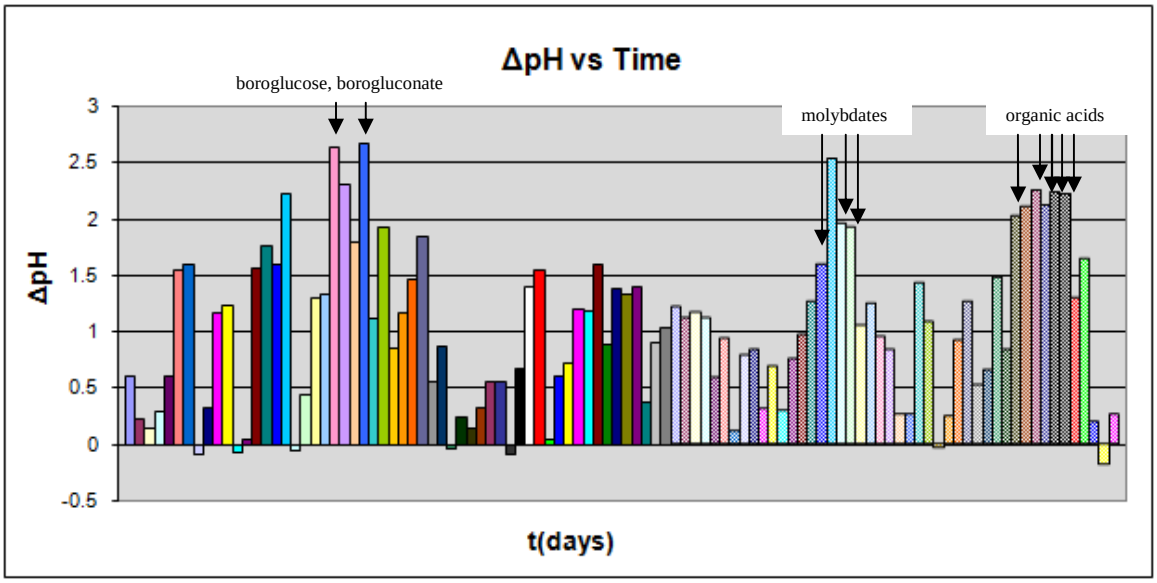

Figure 3-36 ΔpH vs. Time Graph of Immersion Solutions of Various Inhibitors During Immersions of Coupons

On the other hand, the gluconate salts and vanadium esters of gluconate salts had either very little increase or very little decrease in their pH values, again agreeing with the ORP measurements and inhibition efficiency results. Overall, the ΔpH values were within ~ -0.2 and 2.6. The final pH values vs IE and $\Delta pH/pH_{initial}$ values vs IE graphs did not reveal any other trends other than the aforementioned ones.

3.5.3 Conductivity Graphs

The conductivities of the immersion solutions initially originated mainly from the initially present inhibitor concentration of 200 ppm and the 60 ppm chloride. However, as the corrosion and corrosion inhibition processes took place many other products contributed to the final conductivity values.

Most decreases in conductivity occurred for immersions of 10 and 14 day periods with no inhibitor present during the second immersion period. These results are in harmony with the inhibition efficiency results suggesting the total consumption of the inhibitors and precipitation of ions originated from corrosion reactions leading to a lower final conductivity. The exception to this trend was the immersion solution of the $Al(gluconate)_2OH$ treated coupon, which revealed a slight increase in conductivity in harmony with the inhibition efficiency results.

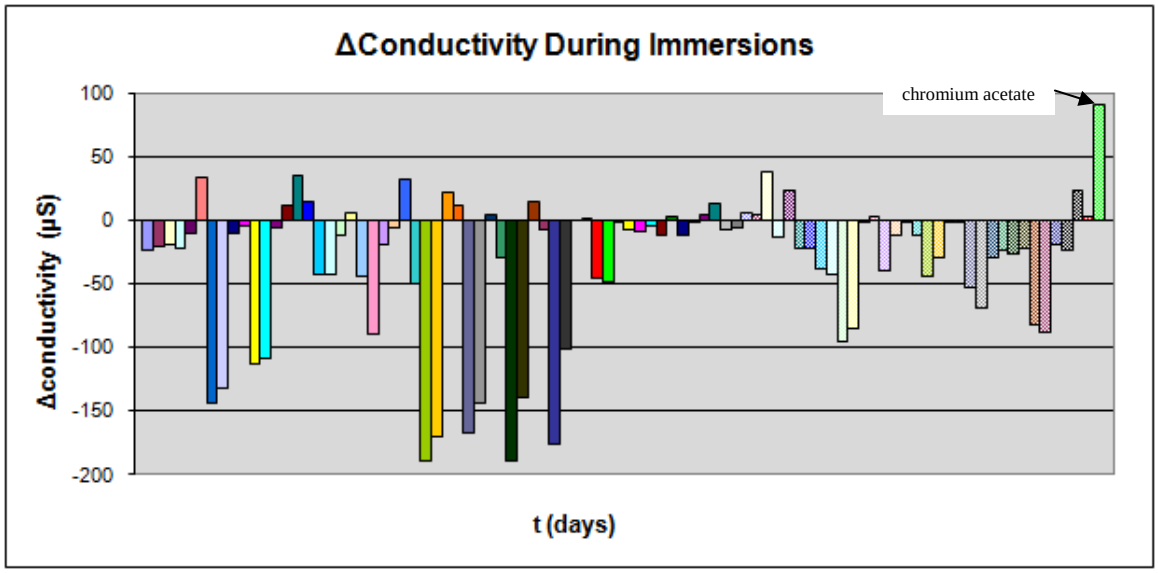

Figure 3-37 Δσ (Conductivity) vs. Time Graph of Immersion Solutions of Various Inhibitors during Immersions of Coupons

The immersion solutions with high inhibition efficiencies revealed no or slight positive increases in their conductivities. This included one week immersion solutions of gluonate salts and their esters in general. The immersion solution of chromium acetate revealed the only out of trend result with the highest increase in conductivity. Notably, the inhibition efficiency of chromium acetate treated mild steel coupon was also highly negative.

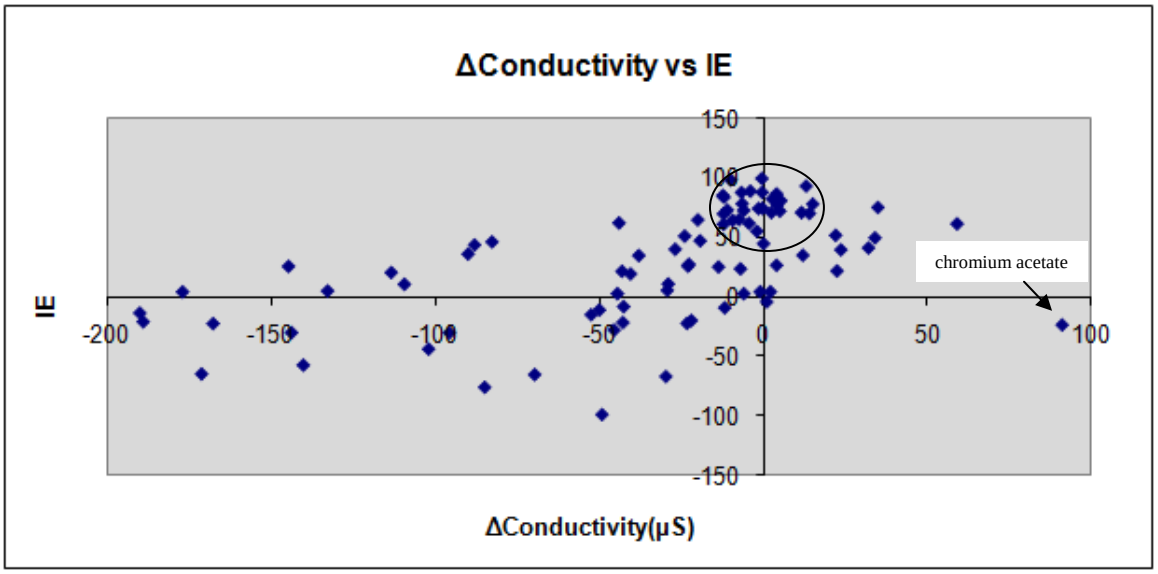

Figure 3-38 Δσ (Conductivity) vs. Inhibition Efficiency Graph of Immersion Solutions of Various Inhibitors

Most of the final conductivity values were within the range of 100 μS to 200 μS, close to the initial conductivity values. Plotting final conductivity values vs IE and Δconductivity/initial conductivity values vs IE did not reveal other trends but the aforementioned ones.

3.6 Discussion and Conclusions

3.6.1 Discussion of the Inhibition Mechanisms of Gluconate Salts in Literature

The inhibition effect of gluconates has been discussed by several authors in the literature.[42-57] Most of the authors agree that gluconates inhibit the corrosion by influencing the anodic reaction of metal dissolution, but there is no general agreement on the mechanism of that action.[46,47,54,58,59] On the other hand, there seems to be an agreement on the contribution of the cationic constituent to the corrosion inhibition. The

most commonly used gluconate salts are zinc gluconate and calcium gluconate, which form zinc and calcium hydroxides at the cathodic sites inhibiting the cathodic corrosion reaction. Initially, the cathodic corrosion reaction, that is the oxygen reduction reaction, provides the OH^- leading to increases in local pH values enough to precipitate zinc and calcium hydroxides. Thus, the process is a repassivation process. Among zinc and calcium gluconates, the effect of zinc gluconate is described as more pronounced in the literature due to the higher insolubility of zinc hydroxide.[15,48,54,58,59] The following mechanisms have been proposed for corrosion inhibition action of gluconates on iron and mild steel in near neutral solutions;[48,54,58-61]

1. Repair of the oxide film by adsorbing on the weak spots of an inhomogeneous, porous oxide film,
2. Incorporation into the oxide film during its formation,
3. Reaction with iron ions forming complexes that precipitate on the metal surface,
4. Forming complexes with iron cations while they are still bound up in the metal lattice rather than forming precipitates.

The third action mechanism among others seemed to be favored in several recent studies,[3,62] while it is being questioned by some others[49,51-54] There are other studies that favor simultaneous occurrence of both the third and fourth mechanisms, in which gluconate forms insoluble complexes weith Fe(II) cations, while at the same time forming soluble complexes with the Fe(III) cations. In these studies, it is claimed that complexation of both Fe^{2+} and Fe^{3+} with oxalate or gluconate inhibits mild steel corrosion by keeping Fe^{3+} ions in solution but forming insoluble complexes with Fe^{2+}. In one of these studies, insoluble β-$Fe(C_6H_{11}O_7)_2$ precipitate was claimed to be observed through

X-ray analyses of the surfaces. However, our X-ray analyses of mild steel substrate surfaces treated with gluconates revealed peaks due only to the substrate metal and corrosion products. Also a frequency shift of the C=O peak of calcium gluconate from 1606 cm^{-1} to 1622 cm^{-1} after completion of immersion was claimed to be an evidence of precipitation of iron gluconates on the surface as well.[63-65] A similar shift in the spectra of coupons immersed in calcium gluconate solutions was observed in this study.

It is well-known that gluconic acid and gluconate salts form water-soluble complexes with most metal cations. Stability constant measurements also indicate that stabilities, thus the solubilities of these complexes increase with pH.[59]

Therefore, the differences between proposed action mechanisms is reduced to a problem of determination of the micro conditions such as whether the pH is suitable for gluconate complexes to precipitate on the metal substrate. Testing of the alloy substrates treated with inhibitor solutions for conversion coating formation revealed substantially low inhibiton efficiencies with the exception of $Al(gluconate)_2OH$. This indicates that an insoluble protective iron-gluconate film does not exist on the metal surface or it is only present when gluconate ions are provided in the solution. In practical terms, a non-stable film of iron gluconates that dissolves in very short time when no gluconate is present in the solution is equal to having no film at all since, in both cases, gluconates have to be supplied steadily. In agreement with this statement, practical applications such as the use of gluconates to eliminate iron oxide corrosion deposits in cooling water equipments[66] or as sequestering agents that prevent deposition of calcium carbonate from hard waters also requires steady supply of gluconates.[54,58,59] This fact has been implied in one of the studies of the authors who favor iron-gluconate precipitation on the substrate surface. It

has been stated that the decrease in inhibition efficiency with increasing period of immersion time, from 1 to 3 days to 5 days, was due to the dissolution of the Fe^{2+}-gluconate complex formed on the metal surface.[62] In another study, it has been mentioned that concentrations by weight over 0.1% would result in soluble iron gluconate complexes.[15] This concentration corresponds to the 100 ppm of inhibitor used in weight-loss experiments in this research. Considering 200 ppm was determined to be an optimal concentration in this research, it is likely that soluble iron gluconate complexes were adsorbed on the substrate surface, thus repairing the protective oxide film rather than forming a protective coating on the substrate surface. A similar behavior of gluconates has been pointed out in a study of sodium borogluconate adsorption on an iron surface that revealed it was adsorbed on the protective oxide film and not directly on the iron.[47]

3.6.2 Suggested Inhibition Mechanism of Salts of Gluconic Acid and Other Hydroxy-Acids

Prior to the discussion of the inhibition mechanism of gluconates a few points should be considered:

Gluconate is known as a complexing agent widely used as an efficient masking reagent for cations[67]. When comparing the complexing ability of the hydroxycarboxylic acids however, a larger negative charge corresponds to stronger complexing ability, which also translates to having more carboxyl groups. Another point is that gluconic acid has a pKa of 3.86[12] therefore, it is fully ionized at near neutral conditions to gluconate, thus pH does not play any role and conjugate acid-base equilibrium of gluconate does not have to be considered. When mild steel coupon is immersed in a solution containing 60

ppm Cl^- and 200 ppm gluconate salt, the gluconate salt diffuses from the bulk of the solution to the metal surface, where initially an iron(II) gluconate complex is formed on the anodic regions and the cationic constituent of the gluconate salt is released to the solution or to the cathodic sites in the case of zinc, calcium or magnesium cations. Thus, first iron(II) cations form, driven by the negative standard reduction potential of the following reaction at ambient conditions;

$$Fe \longrightarrow Fe^{2+} + 2e^- \qquad \text{(Eq. 3.8)}$$

Normally, driven by thermodynamics, iron (II) cations oxidize quickly to iron (III) cations in water[68], leading to the corrosion products as follows;

$$Fe^{3+} + 3H_2O \longrightarrow Fe(OH)_3 + 3H^+ \qquad \text{(Eq. 3.9)}$$

$$Fe(OH)_3 \longrightarrow FeOOH + H_2O \qquad \text{(Eq. 3.10)}$$

However gluconates form complex compounds with the iron (II) cation preventing its oxidation to iron (III) cation and preventing further corrosion reactions from taking place by stopping mass transport of ions resulting in an incomplete electrochemical cell.[67] Iron(II) cations can form monodentate or bidentate complexes with gluconates.

$$Fe^{2+} + M(gluconate)_n \longleftrightarrow Fe(gluconate)^+ + M^{n+} \qquad \text{(Eq. 3.11)}$$

$$Fe(gluconate)^+ + M(gluconate)_n \longleftrightarrow Fe(gluconate)_2 + M^{n+} \qquad \text{(Eq. 3.12)}$$

Other studied carboxylic acid salt and its esters, that is benzilate, also form stable complexes with iron(II) and iron(III)cations[68-70], thus same arguments that is being made for gluconates herein may as well be considered for benzilate compounds to some extent.

It is also mentioned in the literature that ligands which form complex compounds with iron cations with comparable low formation constants will cause precipitation of $Fe(OH)_2$ and $Fe(OH)_3$ in highly alkaline conditions.[72]

$K_{sp}(Fe(OH)_2 = 8.0 \times 10^{-16}$, $K_{sp}(Fe(OH)_3 = 4.0 \times 10^{-38}$ [73]

Conversion of iron gluconates to more stable iron hydroxides with increasing pH may explain the presence of weak bands due to corrosion products of iron in the IR spectra of coupons immersed in gluconate salts.

Gluconates are also reducing agents, similar to ascorbic acid although less strong, preventing oxidation of iron(II) to iron(III).[74] In addition, the formation of a more stable complex when the metal has the lower oxidation number favors reduction and as a result the reduction potential becomes more positive.[75] In this case, the comparison is with the Fe(II)hexahydrate vs Fe(II)gluconate. The gluconate complex is more stable and therefore favors remaining in the reduced state. Meanwhile, the cationic constituents such as zinc and calcium cations form insoluble hydroxides at the cathodic sites, thus lead to the blocking of the galvanic corrosion cell.

$$M^{n+} + nOH^- \longrightarrow M(OH)_n \qquad \text{(Eq. 3.13)}$$

when M = Zn, Ca, or Mg

Thus, trivalent iron gluconate formation is ruled out unless breakdown of the gluconate inhibitor occurs due to extreme conditions or if it is consumed totally. However, if present, due to conditions favoring corrosion reactions, iron (III) cations can also form stable complex compounds with gluconates preventing further corrosion reactions that involve trivalent iron.

$$Fe^{3+} + M(\text{gluconate})_m \longrightarrow Fe(\text{gluconate})^{2+} + M^{m+} \qquad \text{(Eq. 3.13)}$$

$$Fe^{3+} + M(gluconate)_m \longrightarrow Fe(gluconate)_2^{+} + M^{m+} \quad \text{(Eq. 3.14)}$$

$\log(\beta_1) = 22.23$, $\log(\beta_2) = 10.51$ [76]

Iron (III) gluconates can further form complex compounds with calcium cations to form very stable water soluble products.[76]

$$Fe(gluconate)^{2+} + Ca^{2+} \longrightarrow CaFe(gluconate)^{+3} \quad \text{(Eq. 3.15)}$$

$$Fe(gluconate)_2^{+} + Ca^{2+} \longrightarrow CaFe(gluconate)_2^{+2} \quad \text{(Eq. 3.16)}$$

In the specific case of $Al(gluconate)_2OH$, the low stability constant of aluminum gluconate may facilitate forming of iron(II)gluconates and a protective coating of aluminum oxides/hydroxides as implied by the IR results. In addition, the greenish color that was visible on substrate surface might be due to iron(II)gluconate since iron(II) products are known to be greenish in color.

3.6.3 Metal Oxyanion Esters of Gluconate Salts

The combined use of metal oxyanions with gluconates have been reported to result in increased inhibition effect such as, for example, the application of sodium gluconate together with tetraborate, nitrite or molybdate.[49,51-54] Other studies reporting synergistic effects of gluconate include literature cite gluconates as scaling inhibitors that improve the action of molybdate and tungstate.[66,77]

The combination of these constituents under one formulation yielded only slightly positive inhibition efficiencies in the case of molybdenum and vanadium esters but high inhibition efficiencies in the case boron esters.

Clearly, complexation of molybdenum and vanadium constituents with gluconate led to a diminished complexing ability of the gluconates with iron cations due to highly

stable complexes. Gluconate and benzilate complexes of molybdenum and vanadium with various oxidation states are reported in the literature.[78-88]

The boron esters of gluconates on the other hand produced high inhibition efficiencies. As a reason, the formation constant of boron gluconate complex is very low compared to transition metal complexes of gluconates. Hence, boron ester may facilitate the formation of iron gluconate complex due to its higher solubility compared to other gluconate salts.

3.7 References

1. Rajendran, S.; Apparao, B. V.; Palaniswamy, N.; Corrosion Inhibition by Calcium Gluconate, *J. Electrochem Soc. India*, **1999**, 48-3, 242-249.
2. Baboian, R. (Ed.); *Corrosion Tests and Standards: Application and Interpretation*, American Society for Testing and Materials, Philadelphia, **1995**.
3. Rajendran, S.; Joany, R. M.; Palaniswamy, N.; An Encounter with Microheterogeneous Systems as Corrosion Inhibitors, *Corrosion Reviews*, **2002**, 20, 3, 231-252.
4. Baboian, R.; Dean, S. W. (Eds.); *Corrosion Testing and Evaluation*, STP 1000, American Society for Testing and Materials, Philadelphia, **1990**.
5. Abdel-Gaber, A. M.; Khalil, N.; El-Fetouh, A. A.; The Dissolution Mechanism of Steel in Inorganic Acids, *Anti-Corrosion Methods and Materials*, **2003**, 50, 6, 442-447.

6. ASTM (American Society for Testing and Materials) *Designation G1–90*, Undergone editorial change, Standard Practice for Preparing, Cleaning, and Evaluating Corrosion Test Specimen, **1999**.
7. ASTM Designation G31-72, Undergone editorial change, Standard Practice Test for Laboratory Immersion Corrosion Testing of Metals, based upon NACE Standard TM-01-69, Test Method-Laboratory Corrosion Testing of Metals for the Process Industries, **1995**.
8. Baboian, R. (Ed.); *Corrosion Tests and Standards*, American Society for Testing and Materials, Philadelphia, **1995**.
9. Sternstein, M.; *Statistics*, Barron's Educational Series, New York, **1994**, 105.
10. Merrington, M.; Table of Percentage Points of the t-distribution, *Biometrika 32*, **1941**, 300.
11. Sternstein, M.; *Statistics*, Barron's Educational Series, New York, **1994**, 110.
12. Fasman, G. D. (Ed.); *Handbook of Biochemistry and Molecular Biology*, 3^{ed}, CRC Press, Boca Raton, FL, **1976**, 1, 310.
13. Dias, A.; Jay, O.; Joseph, A.; *Ion-Exchange Reactions For Polymeric Alkali Metal Carboxylates*, International Application no. PCT/US1990/003124, Exxon Chemical Patents Inc., **1991**.
14. Mor, E.; Bonino, G.; *Proc. 5th Europ. Symp. Corr. Inhibitors*, Ferrara, Italy, **1971**, 659-70.
15. Sarc, O. L.; Kapor, F.; Halle, R.; Corrosion Inhibition of Carbon Steel in Chloride Solutions by Blends of Calcium Gluconate and Sodium Benzoate, *Materials and Corrosion*, **2000**, 51, 147-151.

16. D'Alkaine, C. V.; Boucherit, M. N.; *J. Electrochem. Soc.*, **1997**, 144, 3331.

17. Peulon, S.; Lincot, D.; *J. Electrochem. Soc.*, **1998**, 145, 864.

18. Rochester, C. H.; Topham, S. A.; Infrared Study of Surface Hydroxyl Groups on Haematite, *Chem. Soc., Faraday Trans.*, 1979, 1, 75, 1073–1088.

19. Walrafen, G. E. in Water, A Comprehensive Treatise, Franks, F. (ed.); Plenum, New York, 1972, 1, 151.

20. Draegert, D. A.; Stone, N. W. B.; Curnutte, B.; Williams, D.; *J. Opt. Soc. Am.*, 1966, 56, 64.

21. Hasted, J. B.; Husain, S. K.; Frescura, F. A. M.; Birch, J. R.; *Chem. Phys. Lett.*, 1985, 118, 622.

22. Madden, P. A.; Impey, R. W.; *Chem. Phys. Lett.*, 1986, 123, 502.

23. Bansil, R.; Berger, T.; Toukan, K.; Ricci, M. A.; Chen, S. H.; *Chem. Phys. Lett.*, 1986, 132, 165.

24. Guillot, B.; *J. Chem. Phys.*, 1991, 95, 1543.

25. Corongiu, G.; *Int. J. Quant. Chem.*, 1992, 42, 1209.

26. Nakamoto, K.; Infrared and Raman Spectra of Inorganic and Coordination Compounds I-II, Wiley, **1986**, I, 231–233; **1986**, II, 228–229.

27. Deacon, G. B.; Phillips, R. J.; *Coord. Chem. Rev.*, **1980**, 33, 227.

28. Nyquist, R. A.; Kagel, R. O.; *Infrared Spectra of Inorganic Compounds* (3800-45 cm^{-1}), Academic Press, New York, **1971**.

29. Lewis, D. G.; Farmer, V. C.; Infrared Absorption of Surface Hydroxyl Groups and Lattice Vibrations in Lepidocrocite (γ-FeOOH) and Boehmite (γ-AlOOH), *Clay Minerals*, **1986**, 21, 93-100.

30. Parfitt, R. L.; Russell, J. D.; Farmerr, V. C.; Confirmation of the Surface Structures of Goethite (α-FeOOH) and phosphate goethite by infrared spectroscopy, *J. Chem. Soc., Faraday Trans.*, **1976**, I, 72, 1082-1087.
31. Parfitt, R. L.; Russell, J. D.; Adsorption on Hydrous Oxides IV: Mechanism of Adsorption on Various Ions on Goethite, *J. Soil Sci.*, **1977**, 28, 297-305.
32. Taylor, R.M.; Influence of Chloride On the Formation of Iron Oxides From Fe(II) Chloride: Effect of Chloride on the Formation of Lepidocrocite and Crystallinity, *Clays Clay Miner.*, **1984**, 32, 175-180.
33. Misawa, T.; Kyuno, T.; Suetaka, W.; Shimodaira, S.; The Mechanism of Atmospheric Rusting and the Effect of Cu and P on the Rust Formation of Low Alloy Steels, *Corrosion Science*, 1971, 11, 35-48.
34. Misawa, T.; Asami, K.; Hashimoto, K.; Shimodaira, S.; The Mechanism of Atmospheric Rusting and the Protective Amorphous Rust on Low Alloy Steel, *Corrosion Science*, 1974, 14, 279-289.
35. Irons, T. V.; Stafford, F. E.; *J. Am. Chem. Soc.*, **1966**, 88, 4819.
36. Ward, B. G.; Stafford, F. E.; *Inorg. Chem.*, **1968**, 7, 2569.
37. Barraclough, C. G.; Kew, D. J.; *Aust. J. Chem.*, **1966**, 19, 741.
38. Chen, W.; Peng, J.; Mai, L.; Zhu, Q.; Xu, Q; Synthesis of Vanadium Oxide Nanotubes from V_2O_5 Sols, *Materials Letters*, **2004**, 58, 2277–2278.
39. Wilhartitz, P.; Dreer, S.; Ramminger, P.; Can Oxygen Stabilize Chromium Nitride?—Characterization of High Temperature Cycled Chromium Oxynitride, *Thin Solid Films*, **2004**, 293, 447 –448.

40. Ewissa, M. A. Z.; Ansoor, S. A. A.; Electrical, IR Spectroscopy, and DTA Studies of Some Sodium Tetraborate Glasses Containing Vanadium Oxide, *Physica Status Solidi (a)*, 156, 2, 428.
41. Bouhaouss, P. A.; *Mater. Res. Bull.*, **1983**, 18, 1247.
42. Kadek, V. M.; Lepin, L. K.; *Proc. 3rd Europ. Symp. Corr. Inhibitors*, Ferrara, Italy, **1970**, 643.
43. Mor, E. D.; Bonino, G.; *ibid.*, 659.
44. Krasts, H. B.; Kadek, V. M.; Lepin, L.K.; *Proc. 4th Europ. Symp. Corr. Inhibitors*, Ferrara, Italy, **1975**, 204.
45. Mor, E. D.; Wruble, C.; *Br. Corrsoion J.*, **1976**, 11, 199.
46. Lahodny-Sarc, O.; *Proc. 5th Europ. Symp. Corr. Inhibitors*, Ferrara, Italy, **1980**, 609.
47. Lahodny-Sarc, O.; *Yug. Acad. Sc. &Arts, RAD, Chem.*, **1982**, 394, 18.
48. Wruble, C.; Mor, E. D.; Montini, U.; *Proc. 6th Europ. Symp. Corr. Inhibitors*, Ferrara, Italy, **1985**, 557.
49. Lahodny-Sarc, O.; Popov, S.; *Surface and Coatings Technology*, **1998**, 34, 537.
50. Krasts, E.; Kadek, V.; Klavina, S.; *Proc. 7th Europ. Symp. Corr. Inhibitors*, Ferrara, Italy, **1990**, 569.
51. Lahodny-Sarc, O.; Orlovic-Leko, P.; *ibid.*, **1990**, 1025.
52. Lahodny-Sarc, O.; Orlovic-Leke, P.; *Proc. 11th Internat. Corr. Congress*, Florence, Italy, **1990**, 3, 17.
53. Lahodny-Sarc, O.; Orlovic-Leke, P.; *RAD Crotian Acad. Sc.&Arts, Chem.*, **1991**, 9, 11.

54. Lahodny-Sarc, O.; *Proc. 8th Europ. Symp. Corr. Inhibitors*, Ferrara, Italy, **1995**, 421.

55. Lahodny-Sarc, O.; Kapor, F.; Proc. 6th Internat. Symp. Electrochemical Methods in Corrosion Research (EMCR VI), Trento, Italy, *Materials Science Forum*, **1998**, 289-292, 1205.

56. Lahodny-Sarc, O.; Kapor, F.; Halle, R.; Ext. Abstracts, *Symp. Corrosion Control by Coatings, Cathodic Protection and Inhibitors in Seawater*, 223rd Event of EFC, Dubrovnik, Croatia, **1998**, 72.

57. Rajendran, S.; Apparao, B. V.; Palaniswamy, N.; *Br. Corrosion J.*, **1998**, 33, 315.

58. Sarc, O. L.; Kapor, F.; Corrosion Inhibition of Carbon Steel by Blends of Gluconate/Benzoate at Room Temperature up to 60 C, *Materials Science Forums*, **1998**, 289-292, 1205-1216.

59. Martell, A. E.; Calvin, M.; *Chemistry of the Metal Chelate Compounds*, Prentice Hall, N.Y., **1952**, 90 ff.

60. Hackermann, N.; *Electrochem. Soc. Bull. Indian Section*, **1959**, 87, 9.

61. Leroy, R. L.; *Corrosion*, NACE, **1978**, 34, 98.

62. Rajendran, S.; Apparao, B. V.; Palaniswamy, N.; Calcium Gluconate as Corrosion Inhibitor For Mild Steel in Low Chloride Media, *British Corrosion Journal*, **1998**, 33, 4, 315-317.

63. Subrahmanyam, D. V.; Hoey, G. R.; *Inhibitors for the Prevention of Mild Steel Corrosion in Synthetic Mine Waters*, Mines Branch Research Report R274, Department of Energy, Mines and Resources, Ottawa, **1974**.

64. Subrahmanyam, D. V.; Hoey, G. R.; *Corrosion*, **1977**, 33, 295.

65. Singh, G.; Inhibition of Mild Steel Corrosion in Acid Mine Waters Containing Ferric Ions, *Br. Corros. J.*, **1988**, 23, 4250-4253.

66. Roti, J. S.; Thomas, P. A.; *Proceed. Internat. Corros. Forum*, New Orleans, LA, US, **1984**, 318.

67. Blomqvist, K.; Still, E. R.; Solution Studies of Systems with Polynuclear Complex Formation: Copper(II) and Cadmium(II**)** D-Gluconate Systems, *Anal. Chem.*, **1985**, 57, 749-752.

68. Sen Gupta, K. K.; Moulik, S. P.; Chatterjee, A. K.; Dey, K.; Metallic Benzilates of Iron (II), Cobalt(II), Nickel(II), and Copper(II) Ions, *Journal of Inorganic and Nuclear Chemistry*, **1971**, 33, 12, 4368-4370.

69. Sengupta, Kalyan K.; Moulik, S. P.; Dey, K., Chelation of Benzilate with Iron (III), *Zeitschrift fuer Anorganische und Allgemeine Chemie*, **1970**, 379, 1, 72-78.

70. Sengupta, Kalyan K.; Moulik, S. P.; Dey, K., Physicochemical Studies on Iron(III)- Benzilate Chelate, *Journal of Inorganic and Nuclear Chemistry*, **1970**, 32, 3, 1052-1053.

71. *The Merck Index*, 12^{ed}, CRC Press, Boca Raton, FL, 4087-4089.

72. Kongdee, T. B.; The Complexation of Fe(III)-Ions In Cellulose Fibres: A Fundamental Property, *Carbohydrate Polymers*, **2004**, 56, 47–53.

73. Lide, D. R.(Ed.); *CRC Handbook of Chemistry and Physics*, The Chemical Rubber Co., **1999**.

74. Vitachlor Corporation, *Compositions and Methods for Removing Minerals from Hair*, US Patents, Patent No. 5804172, **1998**.

75. Shriver, D. F.; Atkins, P. W.; Cooper Haroldold Langford, *Inorganic Chemistry*, 2ed, W. H. Freeman & Co, **1994**, 308.

76. Bechtold, T.; Burtscher, E.; Turcanu, A.; Ca^{2+}–Fe^{3+}–D-Gluconate-Complexes in Alkaline Solution, Complex Stabilities and Electrochemical Properties, *J. Chem. Soc., Dalton Trans.*, **2002**, 2685.

77. Lu, Z.; Zheng, S.; *J. East China Inst. Chem. Technol.*, Shanghai, **1985**, 338.

78. Ramos, M. L.; Caldeira, M. M.; Gil, V. M. S.; NMR Spectroscopy Study of The Complexation of D-Gluconic Acid with Tungsten(VI) and Molybdenum(VI), *Carbohydrate Research*, **1997**, 304, 2, 97-109.

79. Guiotoku, M.; Silva, F. R. M. B.; Azzolini, J. C.; Merce, A. L. R.; Mangrich, A. S.; Sala, L. F.; Szpoganicz, B.; Monosaccharides and The VO(IV) Metal Ion: Equilibrium, Thermal Studies and Hypoglycemic Effect, *Polyhedron*, **2007**, 26, 1269–1276.

80. Cervilla, A.; Llopis, E.; Ribera, A.; Domenech, A.; White, A. J. P.; Williams, D. J.; Potentiometric Study of the Molybdenum(VI)-Benzilic Acid System. Structural Characterisation and Electrochemical Properties of $[NH_4]_2[MoO_2\{O_2CC(O)Ph_2\}_2].2H_2O$, *J . Chem. Soc. Dalton Trans.*, **1995**, 3891-3895.

81. Cui, L.; Dong-Mei L.; Wu, J.; Cui, X.; Wang, T.; Xu, J.; Synthesis, Structural Determination And Photochromism Characterization Of Two Complexes With $[MO_2(O_2CCOPh_2)_2]^{2-}$ Cores [M = Mo or W], *Journal of Molecular Structure*, **2006**, 797, 1-3, 34-39.

82. Kiparisov, S. S.; Meerson, G. A.; Morozov, V. N.; Fistul, A. D.; Formation of chromium borates, *Neorg. Mater.*, **1973**, 9, 3, 512-513.

83. Money, J. K.; Huffman, J. C.; Christou, G.; Vanadium(IV) Thiolate Chemistry: Preparation, Structure, and Properties of $[VE(SCH_2CH_2S)_2]^{2-}$ (E= O,S), *Inorg. Chem.*, **1985**, 24, 3297-3302.

84. Vergopoulos, V.; Jantzen, S.; Rodewald, D.; Rehder, D.; [Vanadium (Salen)Benzilate]-A Novel Non-Oxo Vanadium (IV) Complex, *Journal of the Chemical Society, Chemical Communications*, **1995**, 3, 377-378.

85. Charykov, A. K.; Ivanenko, N. B.; Dmitrieva, I. A., Extraction of Vanadium (V) and (IV) By Solutions of Benzyilic Acid In Heptanol, *Vestnik Leningradskogo Universiteta, Seriya 4: Fizika, Khimiya*, **1991**, 1, 122-124.

86. Fan, Y.; Du, Y.; Ding, Y.; Wang, X.; Xiu, Z., Study on The Complex of Vanadium (V) with Benzilic Acid and Pyridine, (II) Preparation of Single Crystal and Determination of Crystal Structure, *Gaodeng Xuexiao Huaxue Xuebao*, **1988**, 9, 1, 17-22.

87. Du, Y.; Xiu, Z., Synthesis, Characterization and Properties of A Vanadium (V) Complex of Benzilic Acid, *Jilin Daxue Ziran Kexue Xuebao*, **1984**, 2, 109-114.

88. Belford, R. L.; Chasteen, N. D.; So, H.; Tapscott, R. E., Triplet State of Vanadyl Tartrate Binuclear Complexes and Electron Paramagnetic Resonance Spectra of The Vanadyl α-Hydroxycarboxylates, *Journal of the American Chemical Society*, **1969**, 91, 17, 4675-4680.

CHAPTER IV

AQUEOUS CORROSION INHIBITION FOR ALUMINUM ALLOYS

4.1 Introduction

Following the testing of inhibitors for mild steel alloy in aqueous solutions, the inhibitors were tested for aluminum alloys as well. As explained in the introduction, three aluminum alloys were chosen for the tests, Al 2024, Al 6061, and Al 7075 alloys due to their common use in industry and, specifically, in aircrafts. Sol-gel coatings on Al 2024 alloy are also the subject of an investigation in Dr. Apblett's laboratories, so the inhibitors that successfully inhibit aluminum 2024 corrosion in aqueous solutions could also be incorporated into the sol-gel coatings to inhibit corrosion of Al 2024 alloy.

4.2 Weight Loss Test Results

The standard methods for "Preparing Specimens for Weight-Loss Tests" developed by the ASTM (American Society for Testing and Materials)[1,2] were followed with no alteration. Before immersion, aluminum coupons were degreased first by dipping in hexane followed by dipping in methanol. Afterwards, the coupons were placed in aerated Oakite-164 alkaline cleaner solution at 150 ˚F for 10 minutes. The Oakite bath

was prepared in the same manner used for degreasing of mild steel coupons by dissolving 60 g of Oakite detergent in 1000 ml of water at 180 °F. Next the coupons were treated with a pickling solution composed of Henkel Surface Technologies brand acid-based Deoxalume 2310 (70% water, and 20% concentrated nitric acid, and 10% Deoxalume). The Deoxalume is composed of 10-30% sulfuric acid, 10-30% ferric sulfate, 1-10% ammonium bifluoride. Coupons were dipped into the pickling solution for 6.5 minutes. After the immersions were completed, coupons were dipped into concentrated nitric acid for 5 minutes followed by drying and weighing.

4.2.1 Inhibition Efficiency Results

Weight-loss tests were performed based on the following parameters; type of the substrate, type of inhibitor, inhibitor amount in the immersion solution in ppm (part per million), chloride ion concentration in immersion solution in M, and immersion period. The type of the substrate is of crucial importance since the alloying elements in the substrate have different corrosion resistivities and might also react differently with the tested inhibitors. For instance, Aluminum 2024 alloy has high amounts of copper and Aluminum 7075 alloy has high amounts of zinc, which is why both alloys have lower corrosion resistivities than Aluminum 6061 alloy. Please refer to Table 1-2 for detailed composition of the alloys. An inhibitor concentration of 200 ppm was determined to be optimal for a system of 100 ml solution. Also, a 7 day immersion period was found to be the best immersion period. Instead of the chloride concentration of 60 ppm used in the weight-loss tests of mild steel coupons, a concentration of 0.5 M was used for the aluminum. The high 0.5 M chloride concentration is closer to seawater values as is

required to achieve measurable weight losses. Seawater chloride concentration is given as 19000 mg/L or ppm[3] by USGS (United States Geological Survey) for Pacific Ocean of California, which is close to 0.325 M in molarity terms or 3.5% by weight. The reason why 0.5 M salt concentration or 5% salt percentage by weight has been chosen as the concentration instead of 0.35 M was to match the traditional 5% salt concentration of salt fog chambers so that the inhibition efficiencies of the same inhibitors in aqueous solutions and in sol-gel coatings could be compared.

Gluconate Salts

Only zinc and chromium gluconates were effective for inhibiting corrosion of aluminum alloys. Therefore, it can be concluded that the metal ions were the main corrosion preventing constituents. This conclusion is supported by the acceleration of corrosion by sodium gluconate.

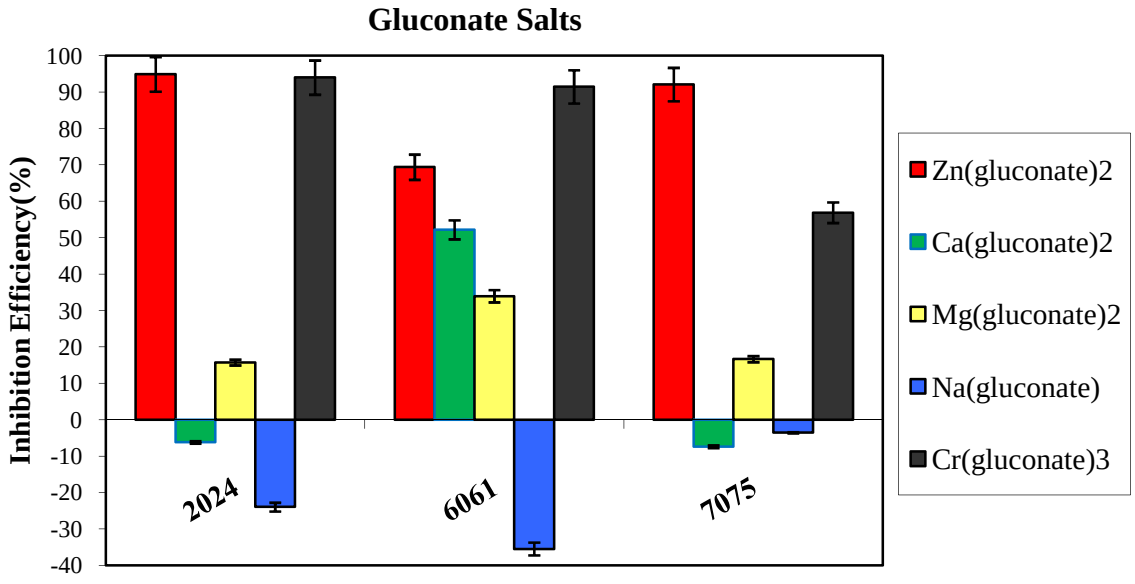

Figure 4-1 Inhibition Efficiency Graph of Gluconate Salts of 200 ppm

Group III Gluconates and D-Glucose

Results for the inhibitors in this category were quite different from those observed with mild steel corrosion. $Al(gluconate)_2OH$, for example, did not have effect on corrosion inhibition except for 7075 alloy. However, $B(gluconate)_2OH$, and B(glucose) and their precursors, boric acid and D-glucose, had better inhibition efficiencies than those of $Al(gluconate)_2OH$ and gluconate salts of Mg, Ca, and Na.

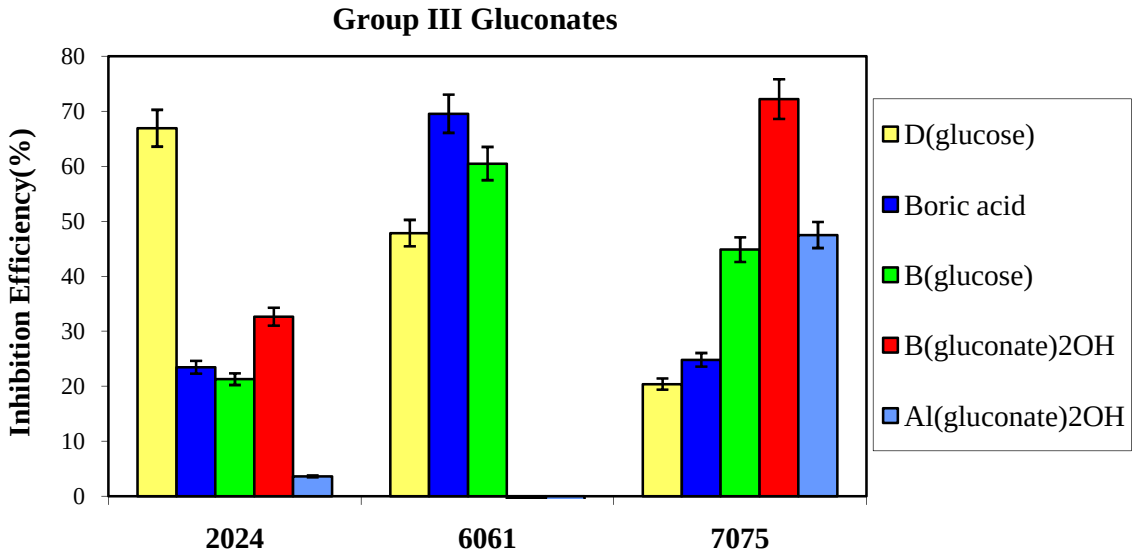

Figure 4-2 Inhibition Efficiency Graph of $M^{+n}(X^{-1})_{n-1}OH$ Type Gluconates

Application of Other $M^{+n}(X^{-1})_{n-1}OH$ and $M^{+n}(X^{-1})_n$ Type Compounds

Compounds similar to gluconate salts were tested and the results are shown in Figure 4-3.

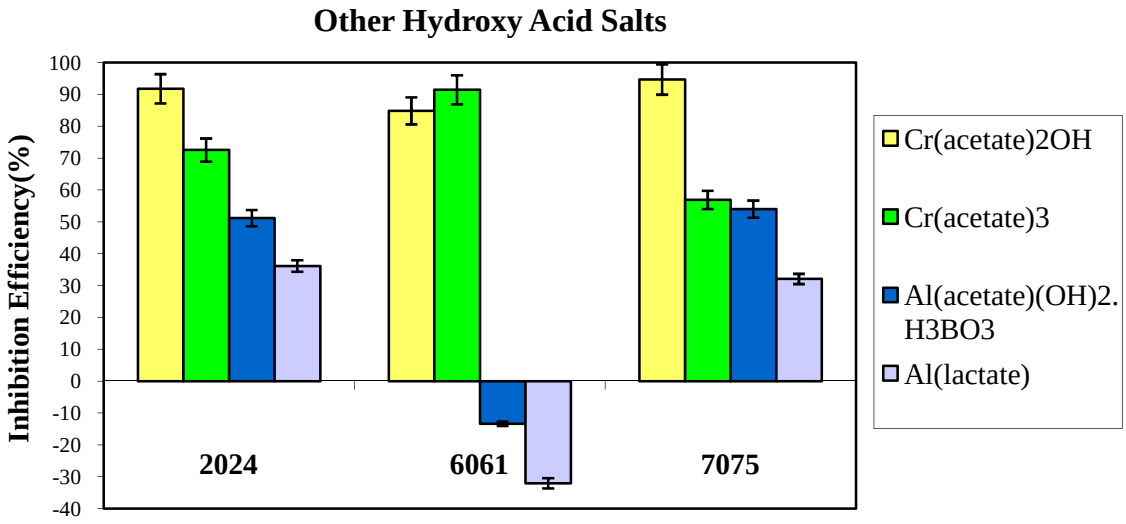

Figure 4-3 Inhibition Efficiency Graph of $M^{+n}(X^{-1})_{n-1}OH$ and $M^{+n}(X^{-1})_n$ Type Salts of Other Carboxylic Acids Other than Gluconates

Among the tested salts, $Cr(acetate)_3$ and $Cr(acetate)_2OH$ performed very well and were similar to $Cr(gluconate)_3$. Aluminum salts inhibited corrosion for 2024 and 7075 alloys, while they accelerated corrosion in the case of 6061 alloy. The reason that $Al(acetate)(OH)_2.H_3BO_3$ performed slightly better than Al(lactate) could be due to presence of boric acid, which also inhibited corrosion when tested seperately. Overall, when gluconate and other carboxylic acid salts of metal cations such as Cr^{+3}, Al^{+3} are compared; acetate and lactate salts seemed to perform better than gluconate.

Molybdenum Esters of Gluconate Salts

In contrast to what was observed with gluconate salts, the inhibition efficiencies of molybdenum esters of gluconates were almost perfect for 2024 alloy and also very high for 6061 and 7075 alloys. This observation indicated that the molybdenum

constituent inhibited corrosion since earlier results already revealed that gluconates had a slightly negative effect on corrosion inhibition.

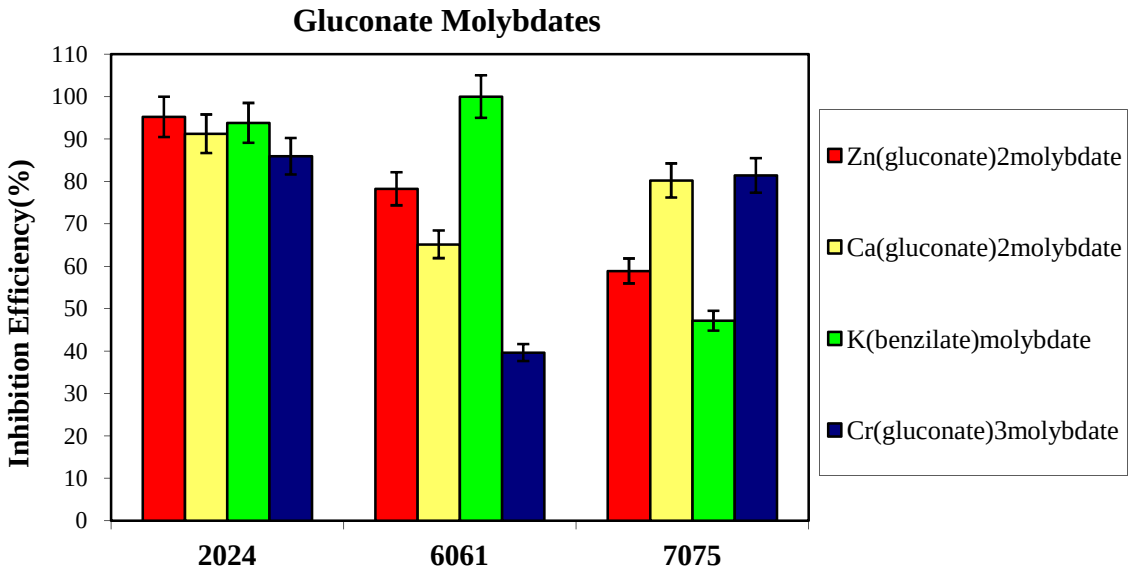

Figure 4-4 Inhibition Efficiency Graph of Molybdenum Esters of Gluconates and Benzilates

Vanadium Esters of Gluconate Salts

The vanadium esters of gluconates inhibited corrosion even better than the molybdenum esters. Surface characterization indicated that vanadium esters and molybdenum esters inhibited corrosion by forming insoluble oxides and hydroxides on the substrate surface, thus assisting repassivation.

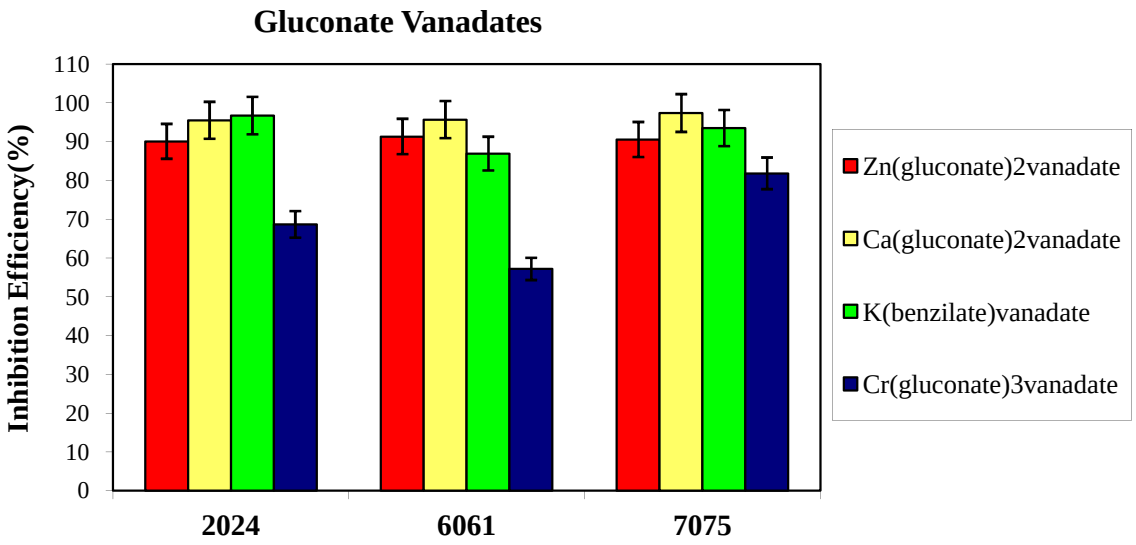

Figure 4-5 Inhibition Efficiency Graph of Vanadium Esters of Gluconates and Benzilates

Boron Esters of Gluconate Salts and Derivatives

Boron esters of gluconate salts inhibited corrosion to varying extent depending on the cationic constituent. When compared to the parent gluconate salts, the boron esters have almost identical inhibition efficiencies. Thus, the boron consitutent did not seem to inhibit corrosion unlike the molybdenum and vanadium esters of gluconates. Neutral to slightly negative effect of borates on corrosion of aluminum is reported in the literature.[4]

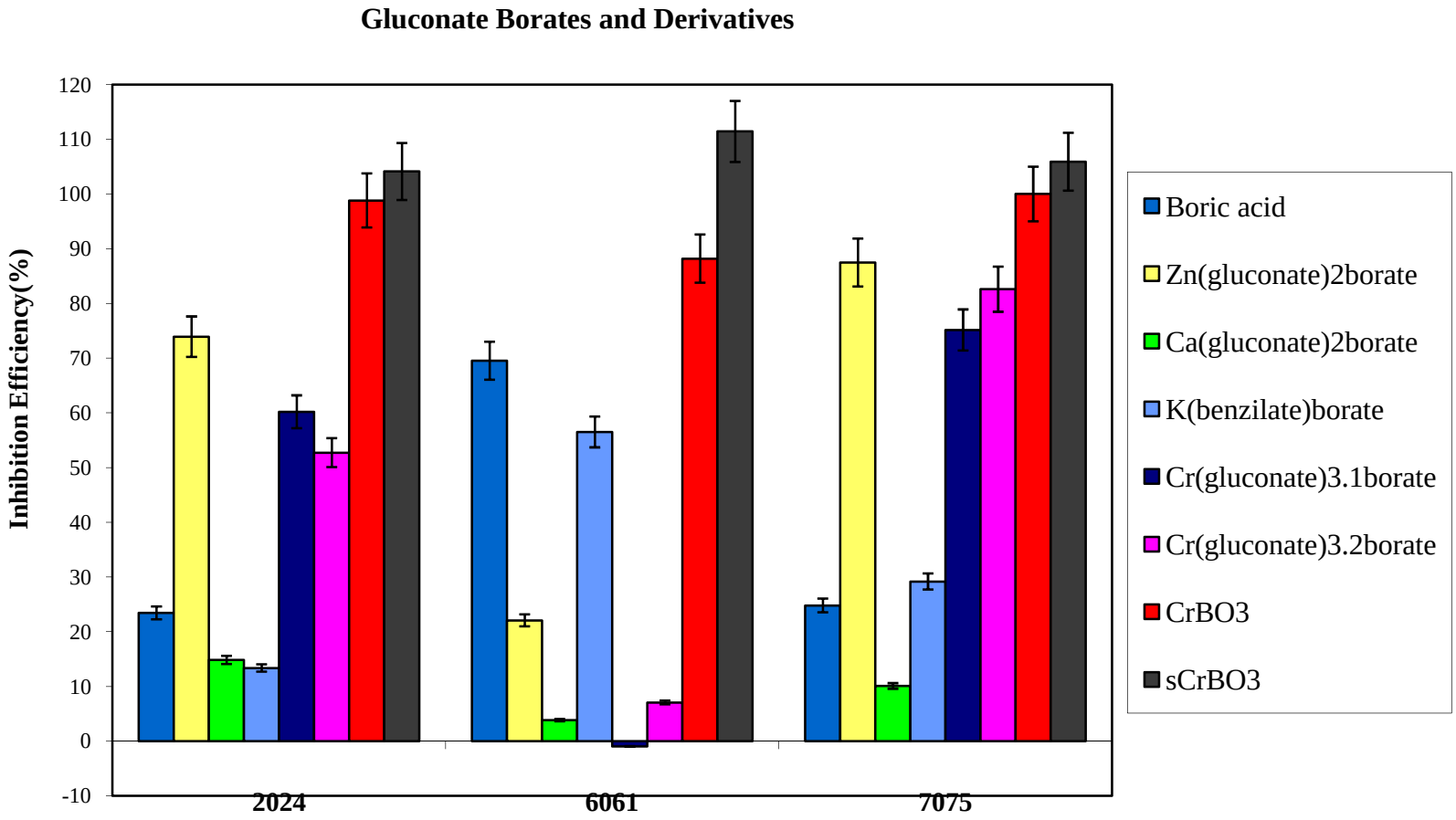

Figure 4-6 Inhibition Efficiency Graph of Boron Esters of Gluconates and Benzilates and Their Derivatives

The perfect inhibition efficiencies of chromium borates are also noteworthy. Separation of a very fine fraction of chromium borate with a sieve of 25 µm resulted in better inhibition efficiencies. This could be due to forming a better suspension in water and higher surface area. Inhibition efficiencies were even higher than 100% in some tests, which indicated deposition on the substrate surface. Amorphous chromium borate could lead to the formation of chromium oxides and hydroxides at sufficiently high local pH values that passivates surface while boron constituent might act as a facilitator in this process or more likely it could be a part of the passive layer as in the case of traditional chromium phosphate conversion coatings[5]. X-ray powder diffraction of the samples however revealed that the synthesized $CrBO_3$ was amorphous (The product was also found to be insoluble when tested both with Atomic Absorption Spectrometer and Colorimeter).

Zinc Carboxylates

Unlike what was observed for mild steel all three tested zinc carboxylates revealed very good results. Zinc tartrate was the best reagent with %100 inhibition efficiency for all three aluminum alloys.

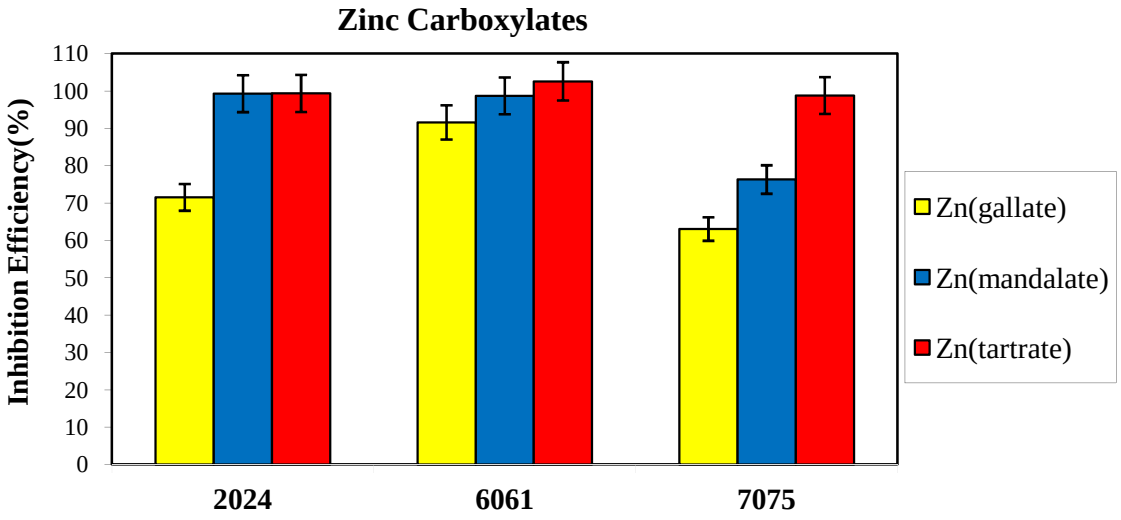

Figure 4-7 Inhibition Efficiency Graph of Zinc Carboxylates

Chromium Carboxylates

Cr(III) carboxylates also inhibited the corrosion of aluminum alloys extremely well even at concentrations as low as 25 ppm for poorly soluble chromium butyrate and chromium propionate salts. Chromium octanoate and chromium caproate salts could not be tested due to their total insolubility in water. The results confirmed the effect of solubility on the inhibition efficiency with the highest soluble Cr(III) carboxylate among tested carboxylates having the highest inhibition efficiency and vice versa.

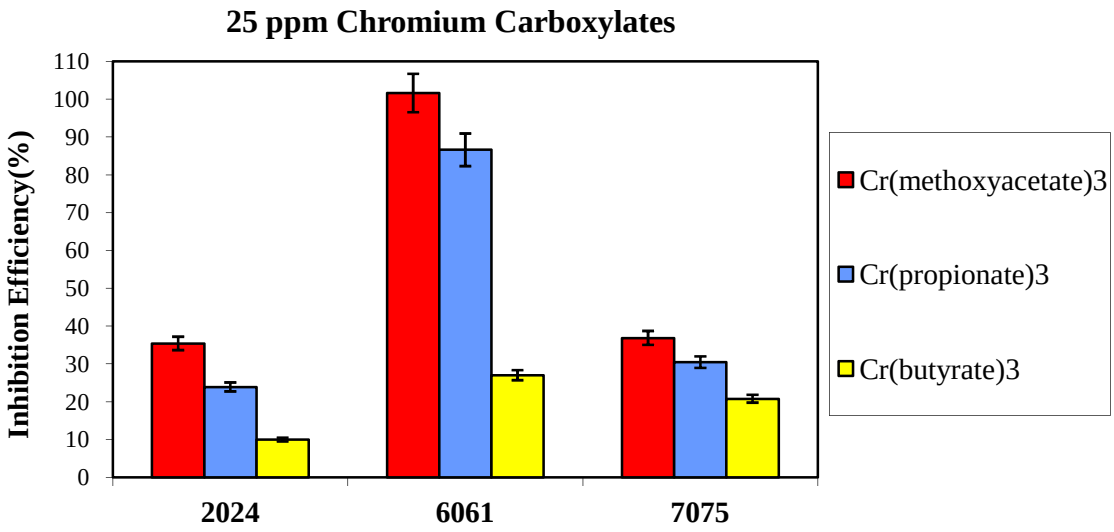

Figure 4-8 Inhibition Efficiency Graph of 25 ppm Chromium Carboxylates

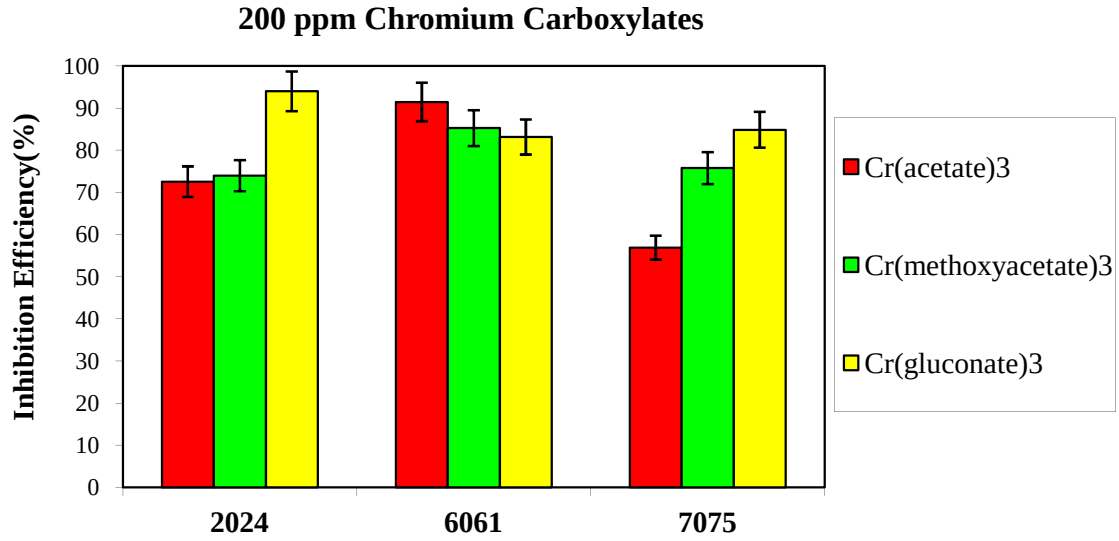

Figure 4-9 Inhibition Efficiency Graph of 200 ppm Chromium Carboxylates

Various Cr(III) Compounds

In addition to the organic acid salts and their oxyanion esters, several Cr(III) and Zn(II) salts were synthesized and tested for corrosion inhibition activity as well. Many chromium(III) salts tested under this category showed considerable inhibitive activity as shown in Figure 4-10. CrOOH synthesized via hydrolysis of chromium borate was the most efficient, while nanoparticulate $Cr(OH)_3$ was the least. In the case of Al 2024 corrosion, commercial grade CrOOH and $Cr(OH)_3$ synthesized using different reagents than the nanoparticulate $Cr(OH)_3$ synthesis had also very little inhibition efficiencies.

4.2.2 Effect of Concentration on Inhibition Efficiency

Varying concentrations from 25 ppm up to 50 ppm resulted in a general trend of increase in inhibition efficiencies with the exception of the molybdenum ester of gluconates. Inhibition efficiencies slightly varied between the 50 ppm and 200 ppm values depending on the type of inhibitor and type of substrate. Inhibitors used to treat 6061 alloy had slightly decreasing inhibition efficiencies when concentrations were increased from 50 ppm to 200 ppm. In contrast, inhibitors that were used to treat 2024 and 7075 substrates had slightly increasing inhibition efficiencies. For concentrations of 200 ppm up to 500 ppm the inhibition efficiencies seemed to decrease in general with the largest decreases observed for the inhibitors used to treat the 6061 alloy. These results suggested that the optimum inhibitor concentration for a 100 ml solution system should be between 50 and 200 ppm; closer to 200 pmm for 2024 and 7075 alloys and closer to 50 ppm for 6061 alloy. As a reason for the discrepancy regarding 6061 alloy, inhibitor

amounts over 50 ppm are more than sufficient in most cases, which only increases the conductivity of the solution leading to lower inhibition efficiencies.

The amount of 25 ppm was also included in the testing, since compounds as chromium borate chromium oxy-hydroxide were only very slightly soluble.

4.2.3 Effect of Cationic Constituent on Inhibition Efficiency

Zinc cations inhibited both mild steel and aluminum corrosion very well. In the case of aluminum corrosion, trivalent chromium cations also inhibited corrosion extremely well.

Effect of Zn Cations

All formulations with zinc cations inhibited aluminum corrosion considerably, with zinc tartrate, zinc mandelate, zinc gluconate vanadate, and zinc gluconate being the best and zinc gluconate borate, zinc gallate, and zinc gluconate molybdate being the worst. Please refer to Figure 4-11 for inhibition efficiencies of the inhibitors with a zinc constituent.

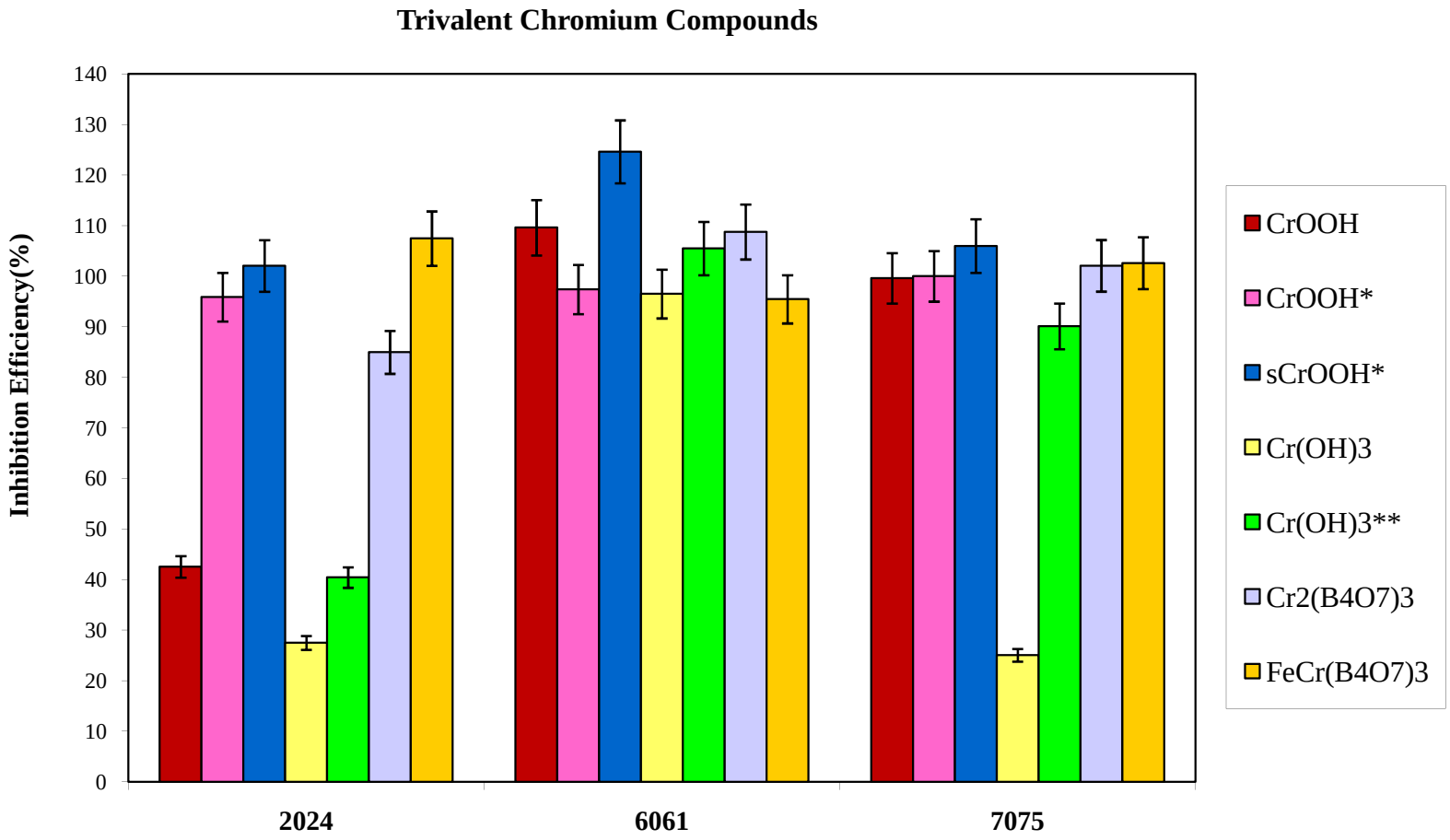

Figure 4-10 Inhibition Efficiency Graph of Various Trivalent Chromium Compounds

*synthesized CrOOH, **nanoparticulate $Cr(OH)_3$

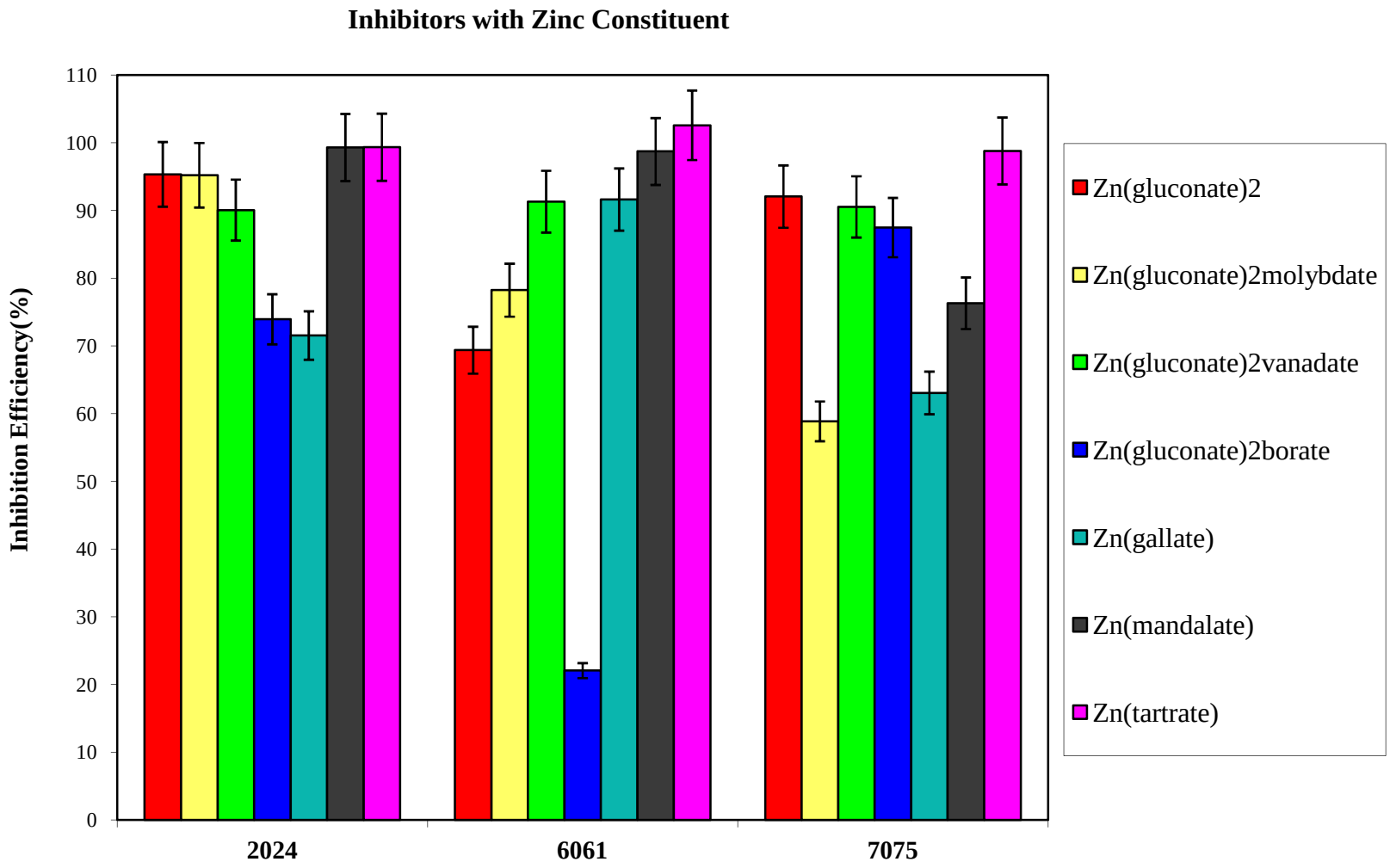

Figure 4-11 Inhibition Efficiency Graph of Various Compounds with Zinc as the Cationic Constituent

Effect of Cr Cations

As shown in Figure 4-12, chromium gluconate vanadate was the most efficient inhibitor among the formulations with trivalent chromium cations. On the other hand, chromium gluconate borate had negligible or negative inhibition efficiencies in the case of aluminum 6061 alloy. These results correspond with the inhibition efficiency results of other boron esters of gluconate and benzilate salts.

The solubilities of chromium(III) carboxylates also seemed to affect the inhibition efficiencies. When inhibition efficiencies of chromium acetate, chromium propionate, chromium butyrate were compared, the least soluble chromium butyrate yielded the least inhibition efficiency and the most soluble chromium acetate resulted in the highest inhibition efficiency as shown in Figure 4-13.

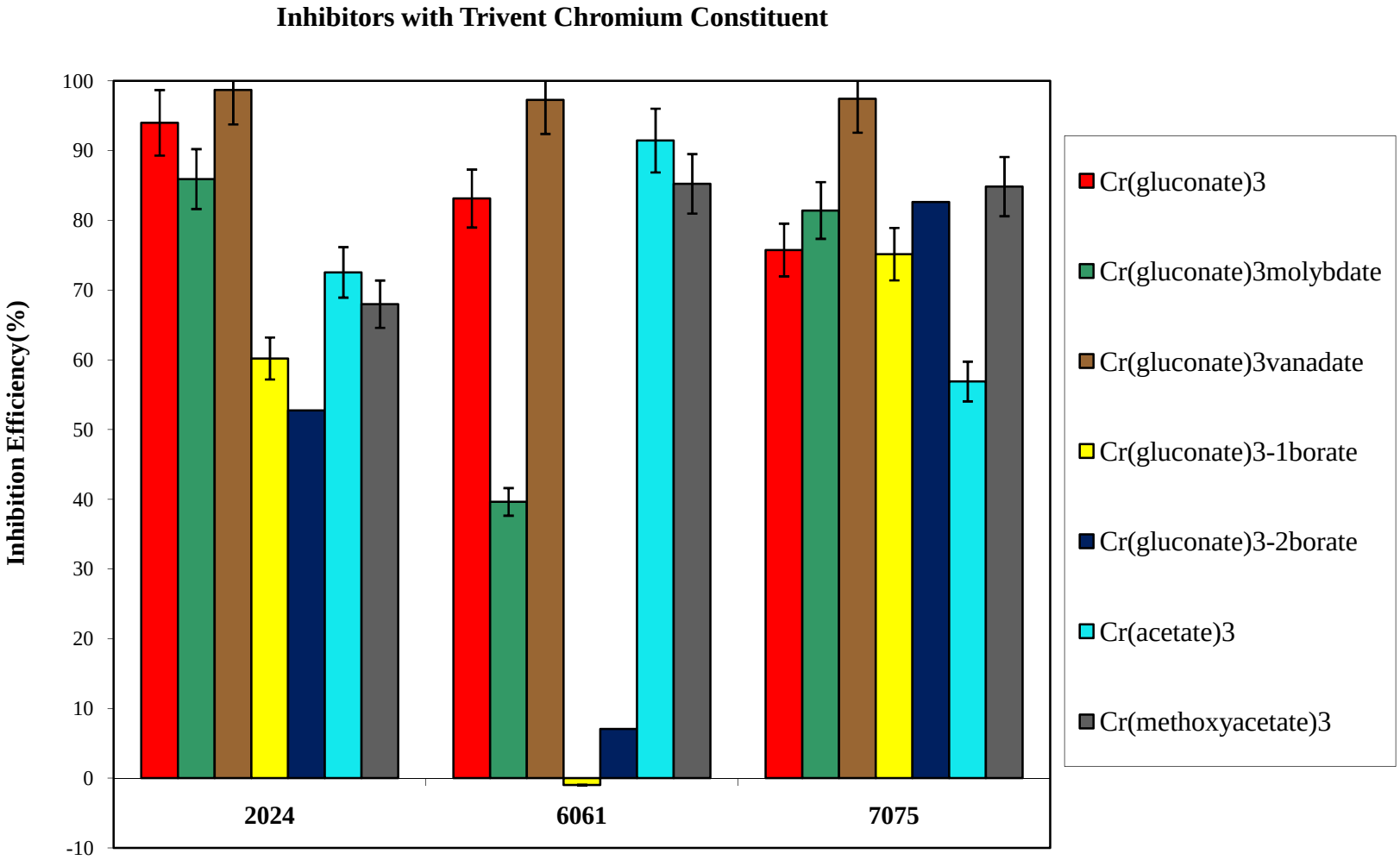

Figure 4-12 Inhibition Efficiency Graph of Various Compounds with Trivalent Chromium as the Cationic Constituent

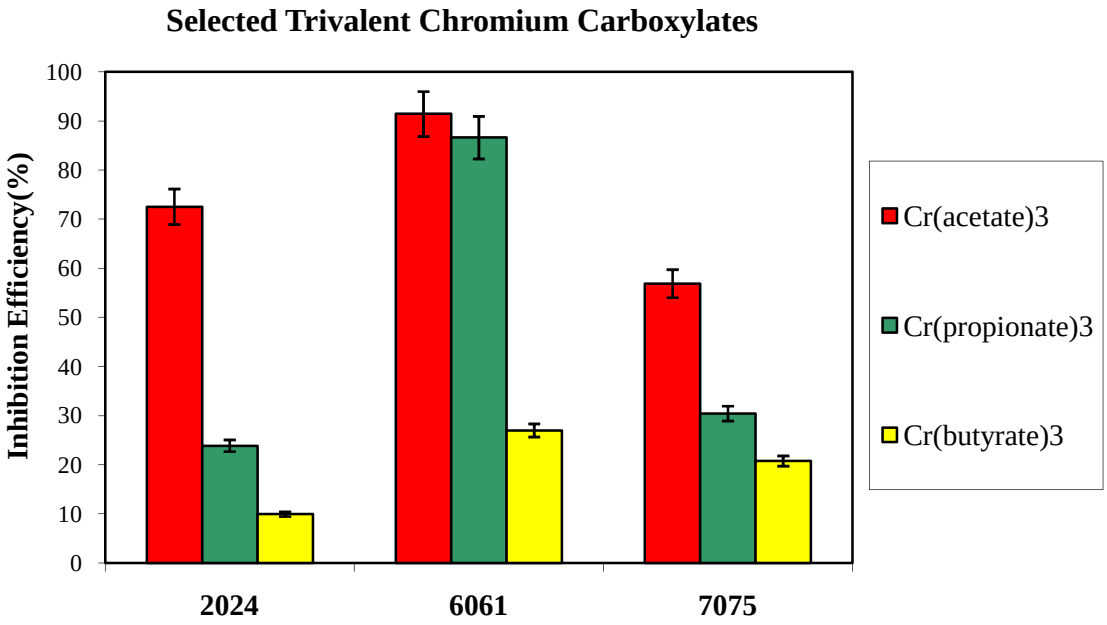

Figure 4-13 Inhibition Efficiency Graph of Trivalent Chromium Carboxylates with Different Water Solubilities

Effect of Ca, K and Other Cations

Magnesium and calcium cations had positive effects on Al 6061 corrosion due to their cathodic inhibitive activity. This was deduced from the comparison of inhibition efficiencies of calcium and magnesium gluconates with that of sodium gluconate.

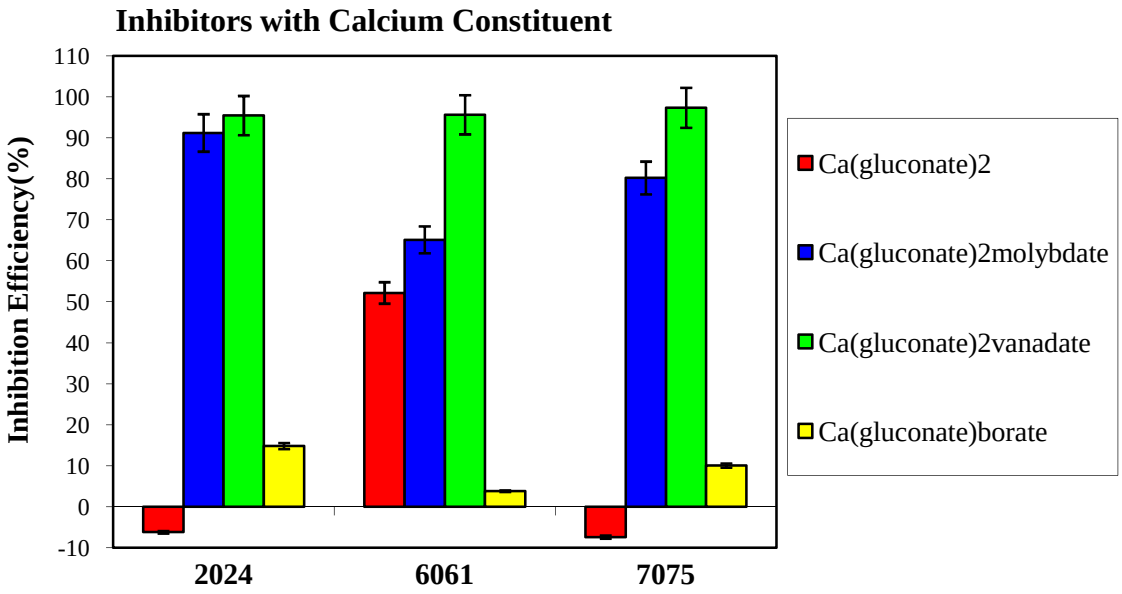

Figure 4-14 Inhibition Efficiency Graph of Various Compounds with Calcium as the Cationic Constituent

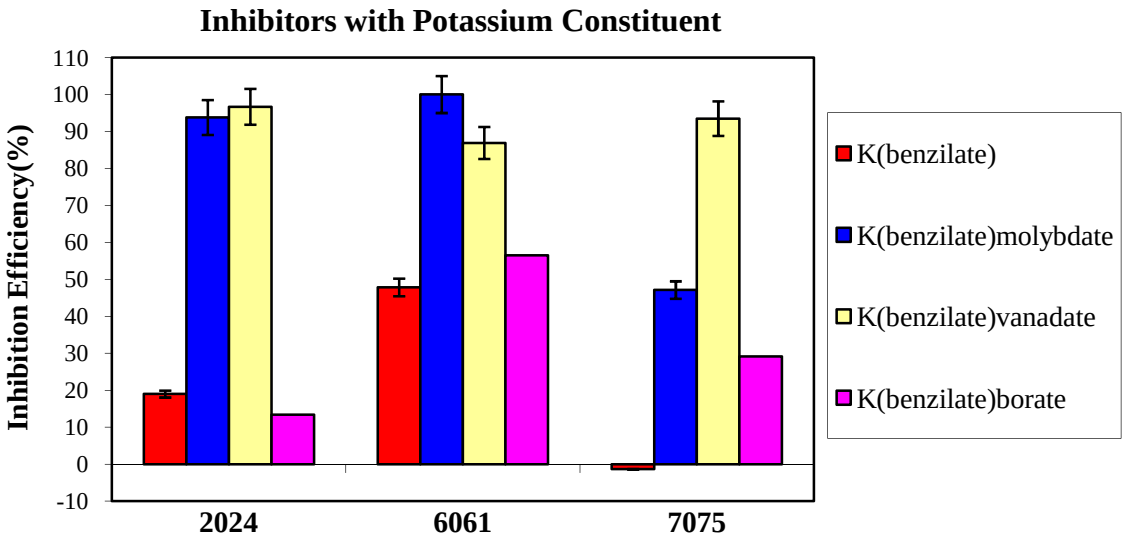

Figure 4-15 Inhibition Efficiency Graph of Various Compounds with Potassium as the Cationic Constituent

From Figures 4-14 and 4-15, it can be deduced that the anionic constituent had the major impact on inhibition efficiency values with vanadates, molybdates, and borates showing pronounced inhibition efficiencies. Other than directly being involved in corrosion reactions, cations also determine the solubilities of reactants due to the common ion or foreign ion effect. For instance, it has been reported that the addition of 1000 ppm of Fe^{2+} had a slight positive effect on the corrosion rate for Al 7075 alloy in the presence of 0.1 M NaCl solution.[6] However due to very small amounts of reactants, the foreign ion effect could not be observed in the weight-loss tests of this study.

4.3 Conversion Coating Formation Studies

In addition to weight-loss tests to measure the direct inhibition efficiencies of inhibitors for aluminum corrosion in aqueous solutions, inhibitors were also tested for conversion coating formations on substrate surfaces and if present these conversion layers were examined and characterized by means of a variety of techniques.

4.3.1 Weight-Loss Method

Coupons those already immersed in the solutions of inhibitors were immersed in salt water for a second period of time to observe any corrosion inhibition due to a possibly formed conversion coating.

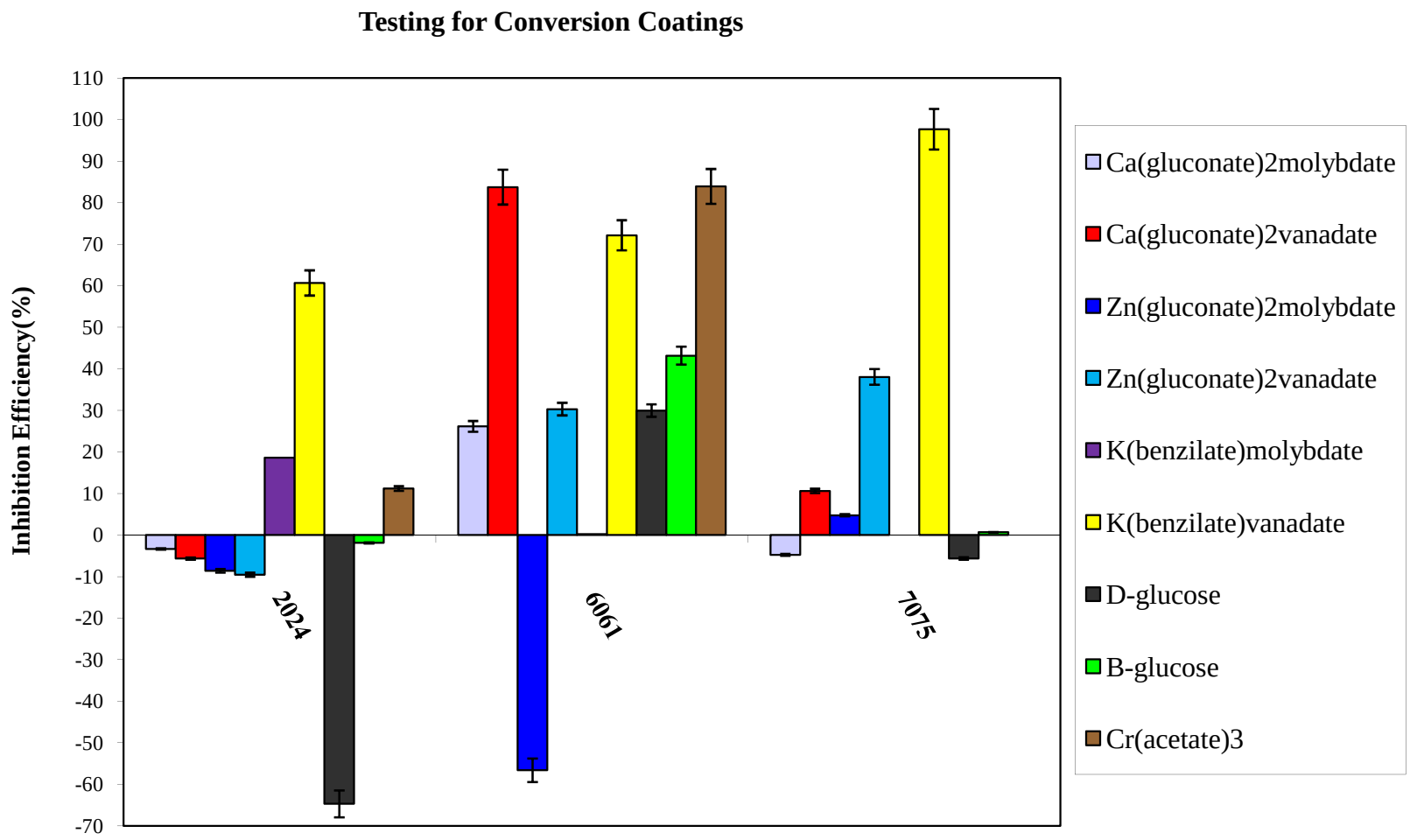

Figure 4-16 Inhibition Efficiency Graph of Various Compounds for an Additional 7 days for Testing Conversion Coating Formation

The results revealed a few successful candidates for conversion coating formation on aluminum substrates such as potassium benzilate vanadate, chromium acetate, zinc gluconate vanadate, calcium gluconate vanadate (These are listed in the order of decreasing inhibition efficiencies). The fact that potassium benzilate vanadate performed better than zinc gluconate vanadate suggested that the cathodic inhibitive activity of zinc cations was no longer effective during second immersion period. Alternatively, the benzilates may have been incorporated into a protective layer on substrate surface during first immersion period resulting in a stable protective layer. The lower benzilate solubility could lead to sufficient stability for prevention of corrosion during second immersion period. Regardless, the vanadate constituent seemed to be the major contributor to the passivation of the substrate surface. Chromium acetate also held up well during second immersion period suggesting the formation of a passive chromium oxide-hydroxide layer on the substrate surface. Other inhibitors with positive inhibition efficiencies during second immersion period were calcium gluconate molybdate, D-glucose, and B-glucose in the case of Al 6061 alloy.

4.3.2 Weight Increase Measurements

In addition to inhibition efficiency calculations based on weight-loss values, changes in weights of the coupons after the immersions but before cleaning with acid solution were measured to provide evidence of a deposition on the surface. A weight increase after completion of the immersions but before cleaning with concentrated nitric acid solution may be due to two types of depositions; first a conversion coating formation due to inhibitor compounds, second a deposition layer of corrosion products.

Comparing weights of coupons before and after the cleaning with concentrated nitric acid solution revealed whether a stable protective coating was present on the substrate surface or not, assuming that a stable protective coating is not dissolved when treated with concentrated nitric acid for 5 minutes. Results are shown in Table 4-1, in which the inhibitors that formed protective depositions on the substrate surface are underlined, while the ones that had depositions of corrosion products or a mixed deposition of both corrosion products and inhibitor originated compounds are written in italic letters.

Table 4-1 Weight Increases of Metal Substrates Due to Immersions in Inhibitor Solutions

Substrate	**Inhibitor**	**Wbefore (g)**	**Wafter (g)**	**W_2-W_1 (g)**	**%Wt Increase***	**IE****
2024 Al	K(benzilate)molybdate	5.0867	5.1041	0.0174	0.34207	93.08
2024 Al	Zn(gluconate)$_2$vanadate	5.0907	5.0905	-0.0002	-0.003929	90.06
2024 Al	*Cr(prop)$_3$*	5.0375	5.0375	0	0	23.87
2024 Al	*Cr(butyrate)$_3$*	5.1161	5.1430	0.0269	0.52579	9.95
2024 Al	Syn. CrO(OH)	5.0701	5.0748	0.0047	0.0927	95.87
2024 Al	Al(gluconate)$_2$OH	5.0918	5.0980	0.0062	0.12176	3.59
2024 Al	Ca(gluconate)$_2$borate	5.0791	5.0936	0.0145	0.28548	14.82
6061 Al	K(benzilate)molybdate	4.6652	4.6688	0.0036	0.07717	100
6061 Al	Zn(gluconate)$_2$vanadate	4.6522	4.6521	-0.0001	-0.00215	91.03
6061 Al	Cr(propionate)$_3$	4.6917	4.6928	0.0011	0.02345	86.62
6061 Al	*Cr(butyrate)$_3$*	4.6539	4.6613	0.0074	0.15901	26.99
6061 Al	Syn. CrO(OH)	4.6893	4.6948	0.0055	0.11729	97.38

Table 4-1 continued

Substrate	Inhibitor	Wbefore (g)	Wafter (g)	W_2-W_1 (g)	%Wt Increase*	IE**
6061 Al	Al(gluconate)$_2$OH	4.6833	4.6899	0.0066	0.14093	-4.67
6061 Al	Ca(gluconate)$_2$borate	4.6501	4.6634	0.0133	0.28602	3.83
7075 Al	*K(benzilate)molybdate*	6.3211	6.3386	0.0175	0.27685	47.14
7075 Al	Zn(gluconate)vanadate	6.2970	6.2979	0.0009	0.01429	90.53
7075 Al	*Cr(prop)$_3$*	6.3318	6.3386	0.0068	0.10739	30.43
7075 Al	*Cr(butyrate)$_3$*	6.3093	6.3225	0.0132	0.20921	20.76
7075 Al	Syn. CrO(OH)	6.2987	6.3086	0.0099	0.15718	100
7075 Al	*Al(gluconate)$_2$OH*	6.2635	6.2685	0.005	0.07983	47.49
7075 Al	Ca(gluconate)$_2$borate	6.2649	6.2664	0.0015	0.02394	10.07

* (before cleaning), ** (after cleaning)

4.3.3 Qualitative Analysis of the Coupons after Immersions

Visual inspection of the coupons compared to the control coupons after completion of immersions but before removal of corrosion products has been a useful qualitative method. When the images of coupons treated with molybdenum esters of hydroxy-acids and those of controls are compared, it is found that coupons treated with molybdate esters had a nonuniform black colored deposition along with depositions of corrosion products around a few pits. The black color is indicative of the presence of molybdenum oxide and hydroxides in a mixed Mo(V)/Mo(VI) oxidation state.

2024 Alloy

Al 2024 alloy control in 0.5M Cl^- soln. for 1 week

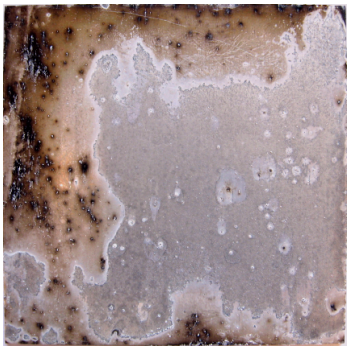

200 ppm K(benzilate)molybdate in 0.5 M Cl^- soln. for 1 week

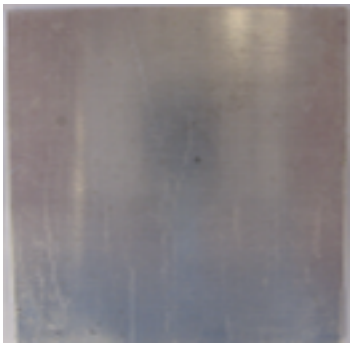

200 ppm Zn(gluconate)vanadate in 0.5M Cl^- soln. for 1 week

Figure 4-17 Images of control coupon and coupons immersed in solutions of metal oxyanion esters; respectively

Thin colored films of molybdenum oxides produced by molybdate salts on Al 7075-T6 alloy that provide slight corrosion resistance have been reported in the literature.[7]

Many other studies have also reported black-colored molybdate coatings on various metal surfaces.[8-12] On the other hand; coupons treated with inhibitors that resulted in high inhibition efficiencies had visually clear surfaces. Among these are zinc gluconate vanadate, potassium benzilate vanadate, and chromium oxyhydroxide. Other coupons had varying amounts of deposited corrosion products that corresponded with the inhibition efficiency results. Examples are chromium butyrate treated coupon that had a deposition of uniform corrosion products, and calcium gluconate borate treated that had a non-uniform deposition of pitting corrosion products.

200 ppm Al(gluconate)OH
in 0.5M Cl^- soln. for 1 week

200 ppm Ca(gluconate)borate
in 0.5M Cl^- soln. for 1 week

200 ppm $Cr(butyrate)_3$
in 0.5M Cl^- soln. for 1 week

200 ppm K(benzilate)vanadate
in 0.5M Cl^- soln. for 1 week

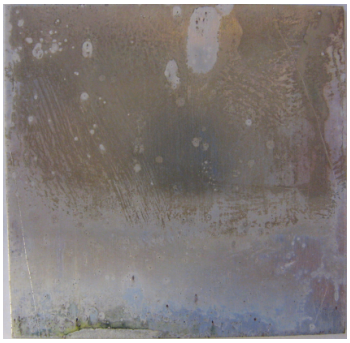

200 ppm $Cr(propionate)_3$
in 0.5M Cl^- soln. for 1 week

200 ppm CrO(OH)
in 0.5M Cl^- soln. for 1 week

Figure 4-18 Images of Aluminum 2024 coupons immersed in solutions of Various Inhibitors

6061 Alloy

Coupons treated with inhibitors with high inhibition efficiencies had images of clear surfaces; while ones with very little inhibition efficiencies had deposition of corrosion products on them mostly around pits indicating pitting corrosion.

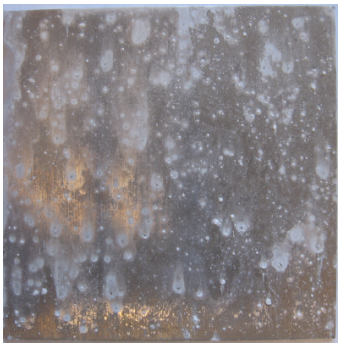

Al 6061 alloy control in 0.5M Cl^- soln. for 1 week

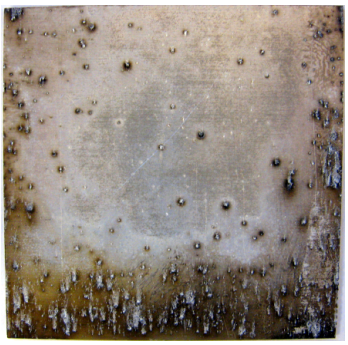

200 ppm K(benzilate)molybdate in 0.5 M Cl^- soln. for 1 week

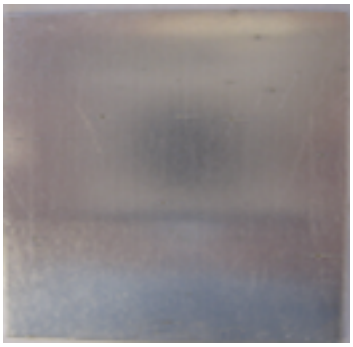

200 ppm Zn(gluconate)vanadate in 0.5M Cl^- soln. for 1 week

Figure 4-19 Images of control coupon and coupons immersed in solutions of metal oxyanion esters; respectively.

The only exception to the direct relation between inhibition efficiencies and images of clear substrate surfaces was the molybdenum ester treated coupons, which had nonuniform deposition of molybdenum oxides on the surface along with corrosion products around a few pits despite the fact that inhibition efficiencies were close to 100%.

200 ppm Al(gluconate)OH in 0.5M Cl^- soln. for 1 week

200 ppm Ca(gluconate)borate in 0.5M Cl^- soln. for 1 week

200 ppm K(benzilate)vanadate in 0.5M Cl^- soln. for 1 week

Figure 4-20 Images of Aluminum 6061 coupons immersed in solutions of Various Inhibitors

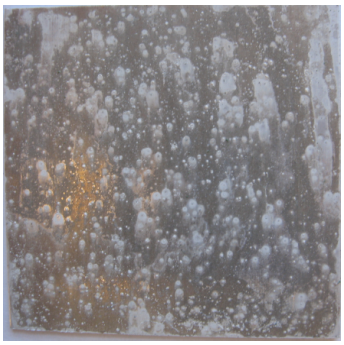

200 ppm Cr(butyrate)$_3$
in 0.5M Cl^- soln. for 1 week

200 ppm Cr(propionate)$_3$
in 0.5M Cl^- soln. for 1 week

200 ppm CrO(OH)
in 0.5M Cl^- soln. for 1 week

Figure 4-21 Images of Aluminum 6061 coupons immersed in solutions of Various Inhibitors

7075 Alloy

Among the tested chromium(III) carboxylates for Al 7075 corrosion, chromium butyrate failed to inhibit corrosion, while chromium propionate was more efficient and chromium acetate was the best among the three. This observation is in agreement with the fact that chromium butyrate is the least and chromium acetate is the most soluble among the three tested chromium(III) carboxylates. Despite being insoluble, the synthesized CrO(OH) inhibited Al 7075 corrosion very efficiently similar to the results with other Al alloys.

200 ppm Cr(butyrate)$_3$
in 0.5M Cl^- soln. for 1 week

200 ppm Cr(propionate)$_3$
in 0.5M Cl^- soln. for 1 week

200 ppm CrO(OH)
in 0.5M Cl^- soln. for 1 week

Figure 4-22 Images of coupons immersed in
Various solutions of trivalent chromium compounds

Potassium benzilate molybdate treated Al 7075 coupon resulted in molybdic oxide deposition starting from the edges similar to the other Al alloys of 2024 and 6061. It may be speculated that a film of molybdic oxides is more adherent on the edges rather than to the surfaces; since a thinner layer of corrosion products or aluminum oxide is expected on edges than the substrate surface resulting in a higher percentage of pure Aluminum on the edges, which molybdic oxides seemed to better adhere on.

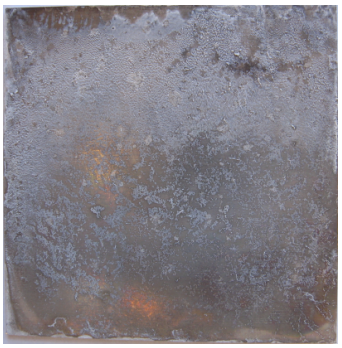

Al 7075 alloy control in
0.5M Cl^- soln. for 1 week

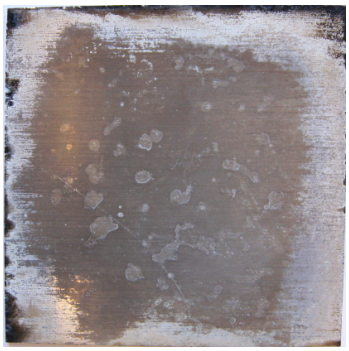

200 ppm K(benzilate)molybdate
in 0.5 M Cl^- soln. for 1 week

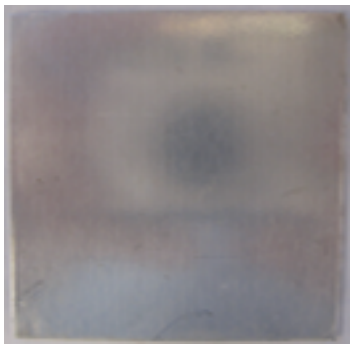

200 ppm Zn(gluconate)vanadate
in 0.5M Cl^- soln. for 1 week

Figure 4-23 Images of control coupon and coupons immersed in
solutions of metal oxyanion esters; respectively.

Coupons treated with calcium gluconate borate revealed virtually no pits, which is in agreement with the inhibition efficiency results of boron esters of hydroxy-acid salts in general. Boron esters of hydroxy-acid salts inhibited corrosion of Al 7075 alloy considerably higher than the other two alloys. This might have something to do with the composition of Al 7075, which is richer in zinc and magnesium. Borate might react with the magnesium and zinc cations to form insoluble borates and contributing to the passivation layer.

200 ppm Al(gluconate)OH in 0.5M Cl^- soln. for 1 week

200 ppm Ca(gluconate)borate in 0.5M Cl^- soln. for 1 week

200 ppm K(benzilate)vanadate in 0.5M Cl^- soln. for 1 week

Figure 4-24 Aluminum 6061 coupons immersed in solutions of various inhibitors

4.3.4 X-Ray Powder Diffractometer Studies

The X-ray powder diffraction patterns of a blank, untreated Aluminum 2024 alloy and the one treated with K(benzilate)vanadate were identical as shown in Figure 4-25. This correlates with the inhibition efficiency of K(benzilate)vanadate, which was almost perfect even during second immersion period.

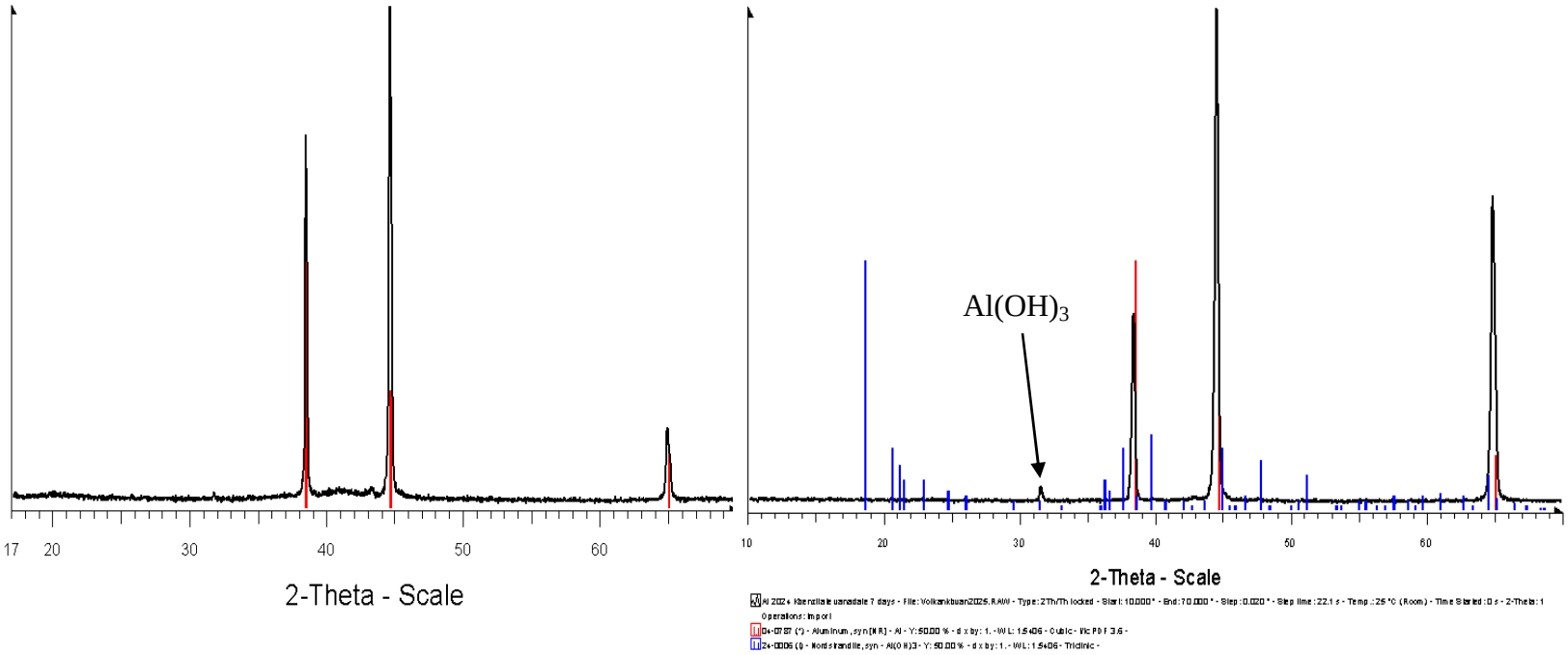

Blank 2024 Aluminum alloy

Aluminum 2024 dipped into 200 ppm K(benzilate)vanadate and 0.5M Cl^- solution

Figure 4-25 X-ray Diffraction Patterns of a blank Aluminum 2024 coupon and one immersed in solution of potassium benzilate vanadate; respectively.

The only slight difference between the X-ray diffraction patterns of the two coupons was the very slight strengthening in the peaks due to $Al(OH)_3$ in the X-ray diffraction of the coupon immersed in the salt solution of potassium benzilate vanadate for 7 days.

4.3.5 X-Ray Flourescence Studies

X-ray fluorescence (XRF) is a powerful tool to detect tiny amounts of elements on the substrate surfaces. Vanadate esters of hydroxy-acid salts had high inhibition efficiencies with no visually observable conversion coating formation. XRD detected only amorphous phases on the substrate surface but XRF spectroscopy detected vanadium on the substrate surfaces of aluminum alloys. Vanadium was detected no matter what other constituents were present in the formulation (e.g. zinc gluconate vanadate or potassium benzilate vanadate). The only possible overlap with the ~4 keV vanadium peak could be due to the L-lines of barium or cesium but even then multiple peaks around the 4 keV range should be present, which was not the case.

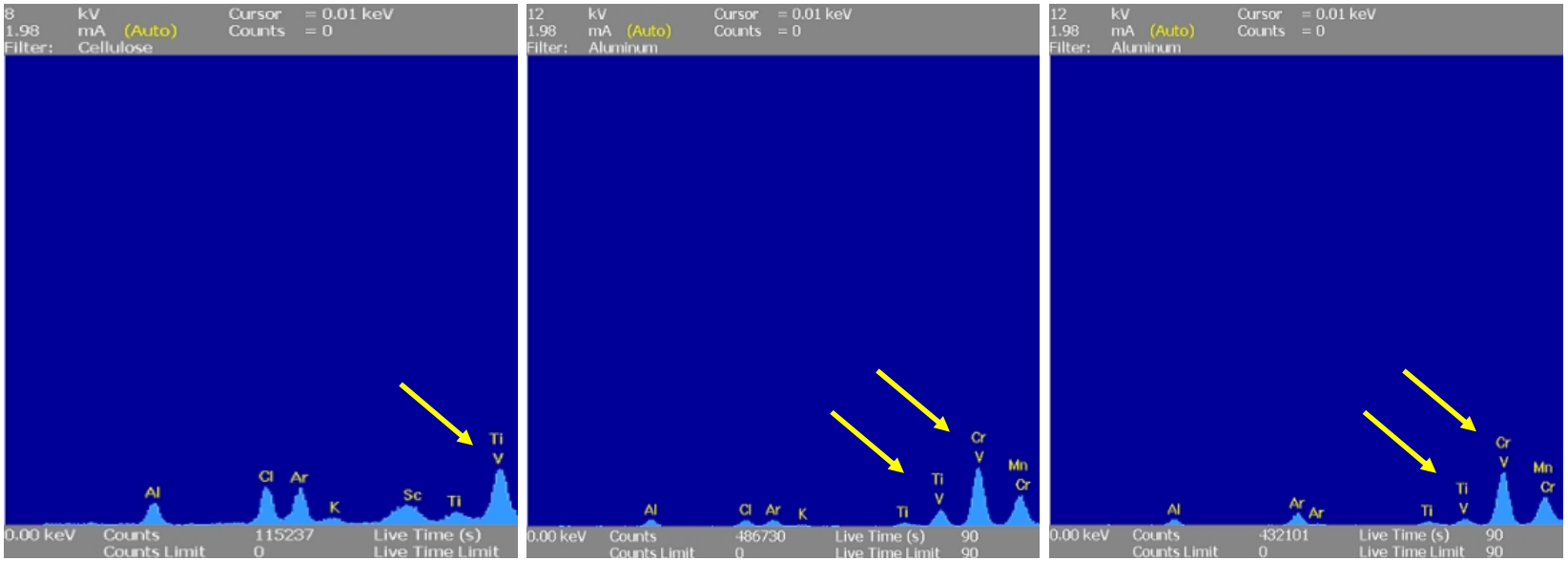

Aluminum 2024 dipped into 200 ppm K(benzilate)vanadate solution

Aluminum 6061 dipped into 200 ppm K(benzilate)vanadate solution

Aluminum 6061 dipped into 200 ppm Zn(gluconate)vanadate solution

Figure 4-26 X-ray Flourescence Diagrams of various Aluminum alloy coupons immersed in solutions of vanadium esters of benzilates and gluconates; respectively.

4.3.6 Scanning Electron Microscope Studies

Scanning Electron Micrographs of aluminum alloys immersed in high concentration salt water for one week revealed extensive corrosion taking place on the substrate surfaces.

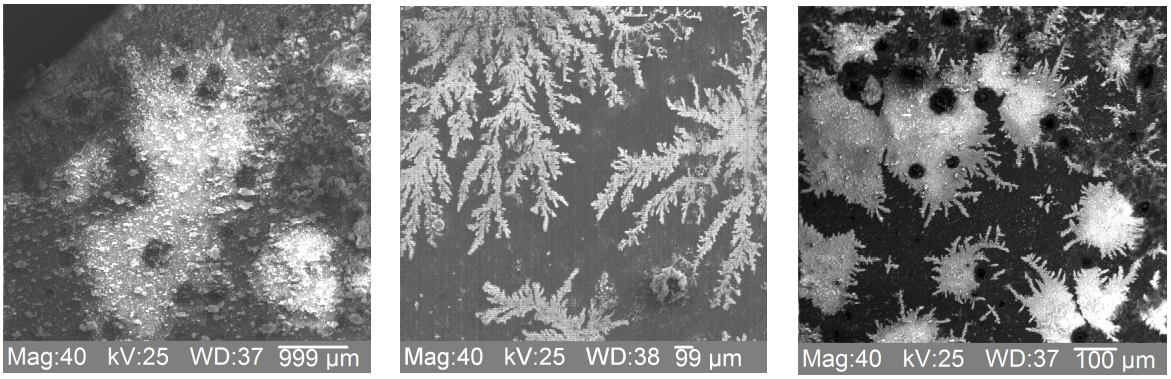

2024 rusted in 0.5 M Cl^- water for 7days

6061 in 0.5 M Cl^- water for 7days

Figure 4-27 Scanning Electron Micrographs of control coupons of various Aluminum alloys immersed for 7 days in 0.5 M Chloride solution

Blank and corroded Al substrate samples were examined at lower magnifications for further investigation. Images indicated Al 7075 alloy as more porous than other alloys; while Al 6061 alloy surface was more homogenous than 2024 alloy as shown in Figure 4-28.

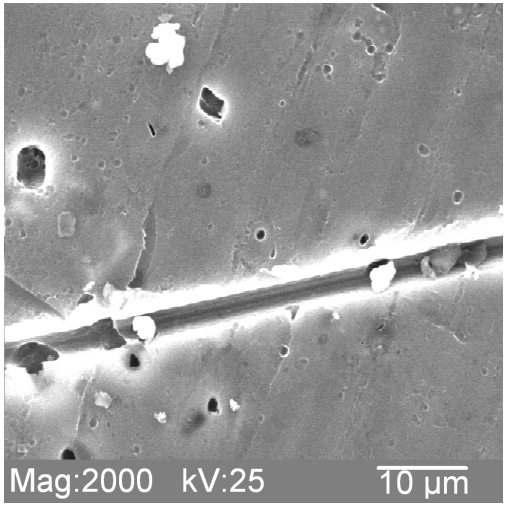

Blank Al 2024

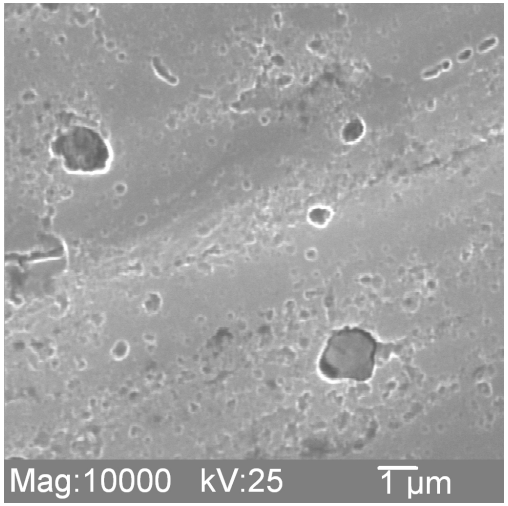

Blank Al 6061

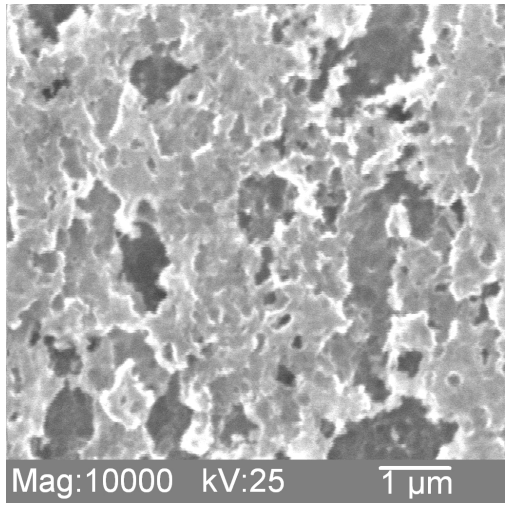

Blank 7075

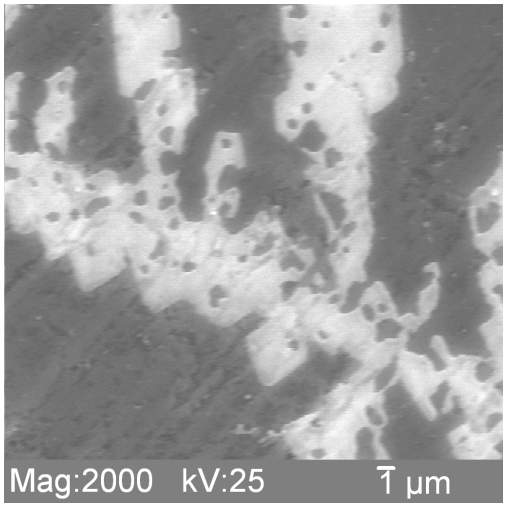

Al 2024 in 0.5M Cl^- water for 7days

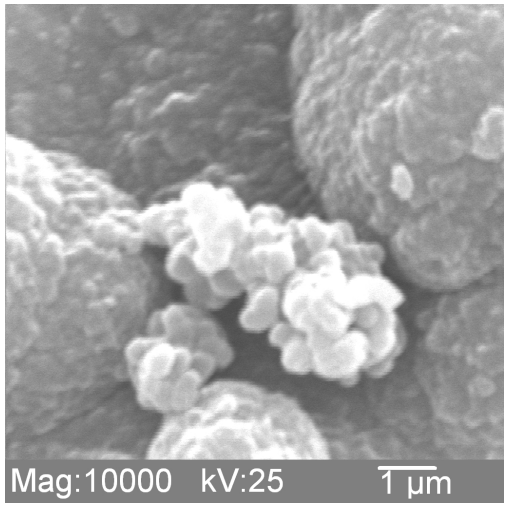

Al 6061 $Al(gluconate)_2OH$ 0.5 M Cl^-, 7days

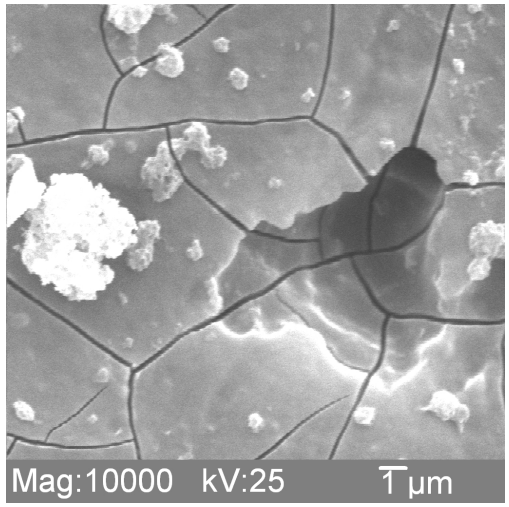

Al 7075 $Zn(gluconate)_2$ 0.5M Cl^-, 7+7days

Figure 4-28 Scanning Electron Micrographs of various Aluminum alloys coupons

Comparison of the blank substrates with gluconate treated substrates revealed the extent of deposition taking place for the latter. However, unlike the case for mild steel, no corrosion protection was observed based on inhibition efficiency results except for the gluconate salts of cations with cathodic inhibitive activity.

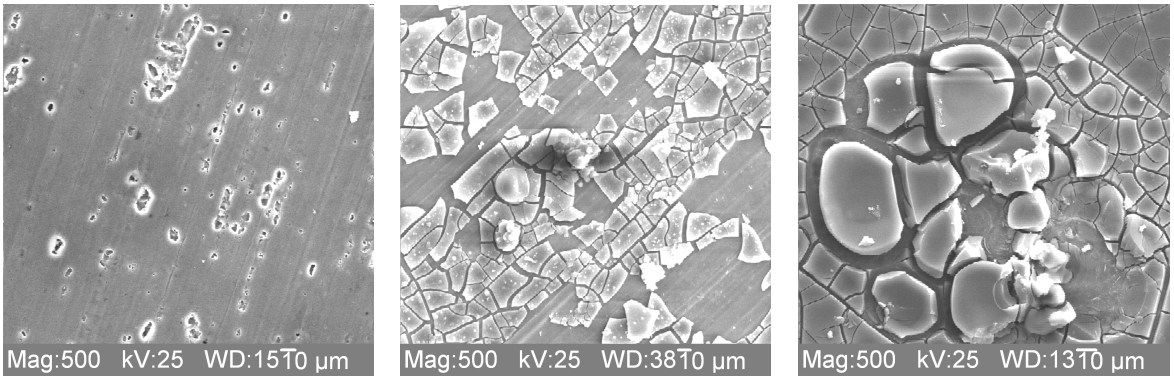

Blank Al 2024

6061 $Al(gluconate)_2OH$
0.5M Cl^-, 7days

7075 $Zn(gluconate)_2$
0.5MCl^-, 7+7days

Figure 4-29 500 Times Magnified Scanning Electron Micrographs of various Aluminum allovs

Consecutive immersions seemed to be destroying the protective coating originated from application of zinc gluconates.

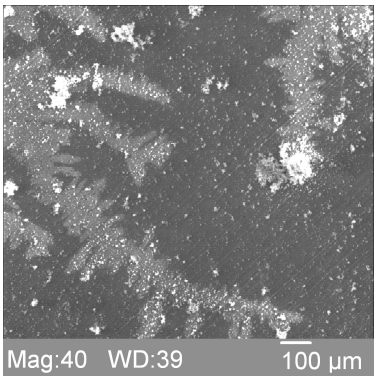

7075 rusted in 0.5 M Cl^- water for 7days

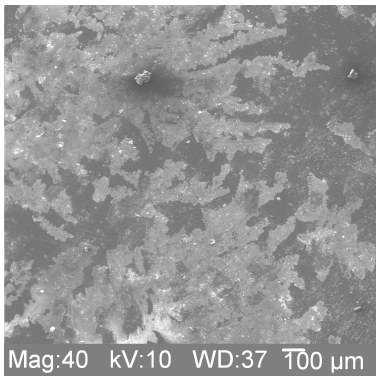

7075 $Ca(gluconate)_2$ 0.5M Cl^-, 7+7days

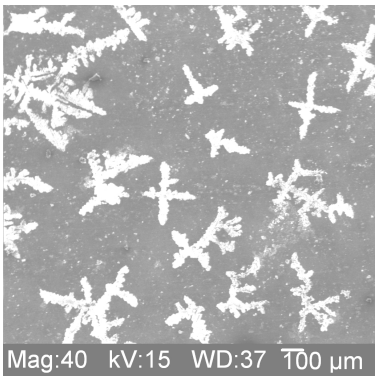

7075 $Cr(acetate)_3$ 0.5M Cl^-, 7+7days

Figure 4-30 40 Times Magnified Scanning Electron Micrographs of Aluminum 7075 Coupons

Scanning electron micrographs of substrates treated with different inhibitors revealed the extent of corrosion during second immersion periods with no inhibitor present in the solution.

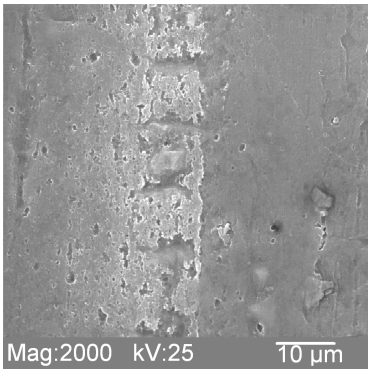

Blank 7075

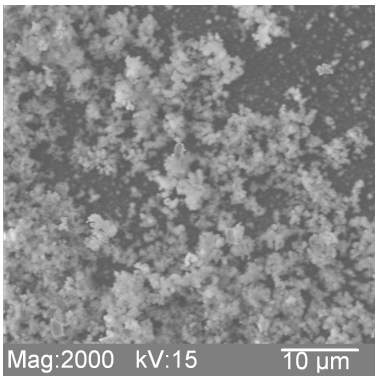

7075 Cr(acetate) 0.5M Cl^-, 7+7days

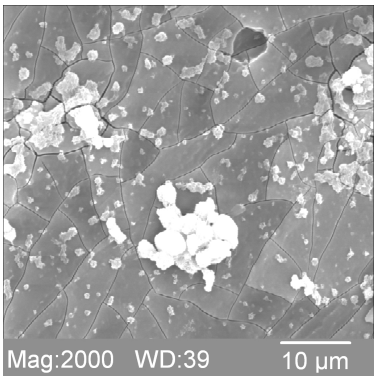

7075 $Zn(gluconate)_2$ 0.5M Cl^-, 7+7days

Figure 4-31 2000 Times Magnified Scanning Electron Micrographs of Aluminum 7075 Coupons

Immersion of chromium acetate treated Al 7075 coupon for a second period of time revealed abundant corrosion deposits on the substrate surface in agreement with its zero inhibition efficiency during the second immersion period. $Al(gluconate)_2OH$ treated Al 6061 substrates were examined at different magnitudes to investigate the nature of the deposition on the substrate surface.

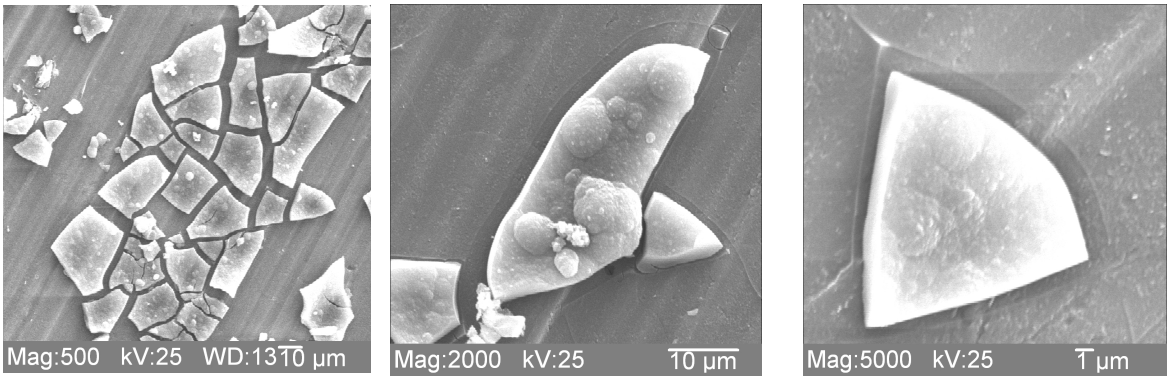

$6061Al(gluconate)_2OH$ 0.5M Cl^- 7days

$6061Al(gluconate)_2OH$ 0.5M Cl^- 7days

$6061Al(gluconate)_2OH$ 0.5M Cl^- 7days

Figure 4-32 Scanning Electron Micrographs of Aluminum 6061 Coupons Immersed in Solutions of Aluminum Gluconate Hydroxide

4.3.7 Infrared Spectra Studies

Gluconate Salts

IR spectra of aluminum alloy coupons treated with gluconate salts revealed significant differences than those of IR spectra of mild steel coupons treated with the same gluconate salts. Firstly, three bands were present in the 1400 cm^{-1} – 1600 cm^{-1} range rather than the two bands in the same region for mild steel coupons treated with gluconate salts. Most importantly, these three bands were exact matches of the three bands present in the IR spectra of untreated control coupons.

Therefore, the presence of gluconate moieties on the substrate surfaces of aluminum alloys can be ruled out and the three bands in the 1400 cm^{-1} – 1600 cm^{-1} region can be assigned to the bending of hydroxyl of water of hydrated aluminum oxide, which is a corrosion product, at 1600s cm^{-1} and Al=O bonds at 1400s cm^{-1}. [13,14] Also, the broad band centered at 3450 cm^{-1} is due to symmetric and asymmetric stretchings of hydroxyl of water. [15-22] Loss of the middle band out of these three bands is observed with increasing inhibition efficiency, and the loss of the band in the lower frequency region occurs with even higher inhibition efficiency. The higher frequency band is present at all times suggesting that it is due to the bending vibration of water. Assignment of these three bands to hydroxyl groups and not to carbonyl/carboxyl groups of hydroxy-acids were in agreement with weight-loss test results, which all gluconate salts and other hydroxy-acid salts revealed very low inhibition efficiencies with the exception of zinc gluconates.

Comparison of the IR spectra of the aluminum alloy substrates treated with different amounts of the same inhibitor supported the assignments of the three bands in 1400 cm^{-1} – 1600 cm^{-1} region. One example is comparison of IR spectra of aluminum gluconate hydroxide treated aluminum 2024 alloy coupons. Comparison of the IR spectra of aluminum gluconate hydroxide powder with those of aluminum 2024 substrates treated with various amounts of aluminum gluconate hydroxide revealed a difference of 20 cm^{-1} between the band due to OCO^{-} asymmetric stretching and the band due to bending vibration of water hydroxyl, respectively.

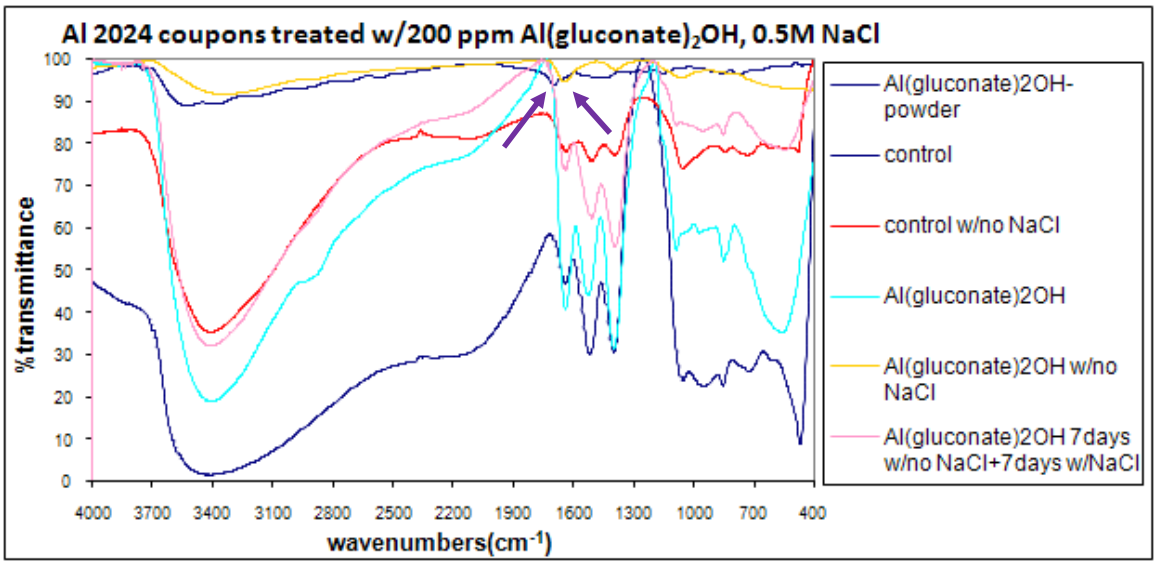

Figure 4-33 Combined Infrared Spectra of Aluminum 2024 Coupons Immersed in Aluminum Gluconate Hydroxide Solutions

Notably, the strength of the three main bands in the 1400 cm^{-1} – 1600 cm^{-1} region varied widely based on the concentrations of chloride ions. When no chloride ions were present in the solution only weak absorptions were observed in the IR spectra of aluminum 2024 control coupon in contrast with the IR spectra of aluminum 2024 control coupon immersed in 0.5 M Cl^- solution. Correspondingly, the control coupon with no chloride present in its solution resulted in significantly less weight-loss than the control coupon immersed in 0.5 M Cl^- solution. Changes in absorptions of these bands with increasing corrosion imply the presence of more aluminum hydroxide corrosion products, thus ruling out the assignment of these bands to carbonyl/carboxyl groups once more. The broadening of OH stretching vibrations centered at 3450 cm^{-1} for all tested aluminum alloys substrates was attributed to interactions between the hydroxyl groups with the surface aluminum metal ions.[15] On the other hand, the corrosion products vary with

different aluminum alloys and with the use of different inhibitors causing shifting of the bands in the 1400 cm^{-1}-1600 cm^{-1} and 3450 cm^{-1} region.

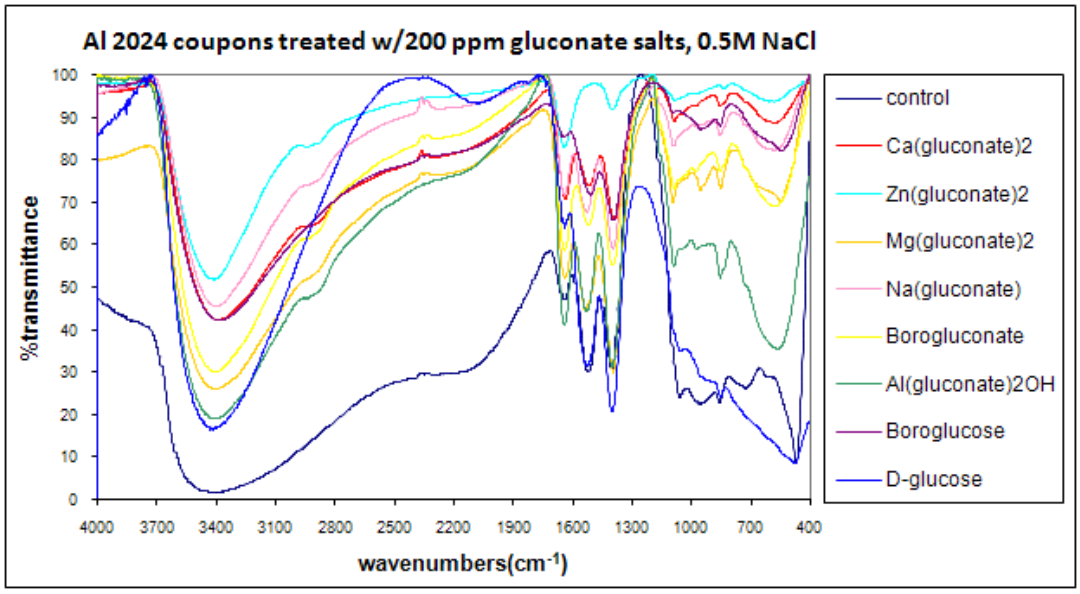

Figure 4-34 Combined Infrared Spectra of Aluminum 2024 Coupons Immersed in Solutions of Various Gluconate and Glucose Salts

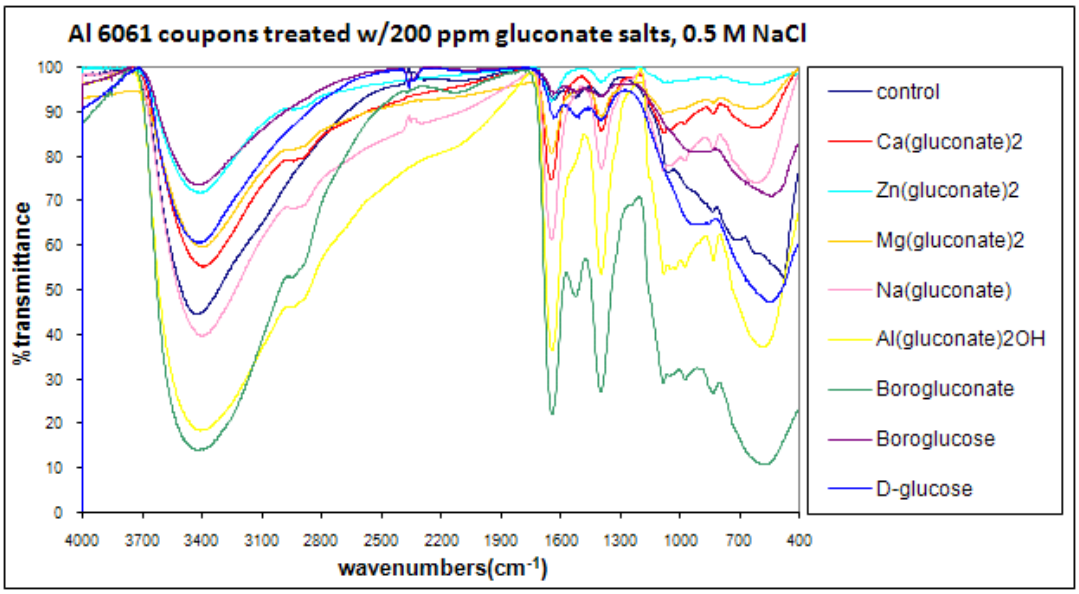

Figure 4-35 Combined Infrared Spectra of Aluminum 6061 Coupons Immersed in Solutions of Various Gluconate and Glucose Salts

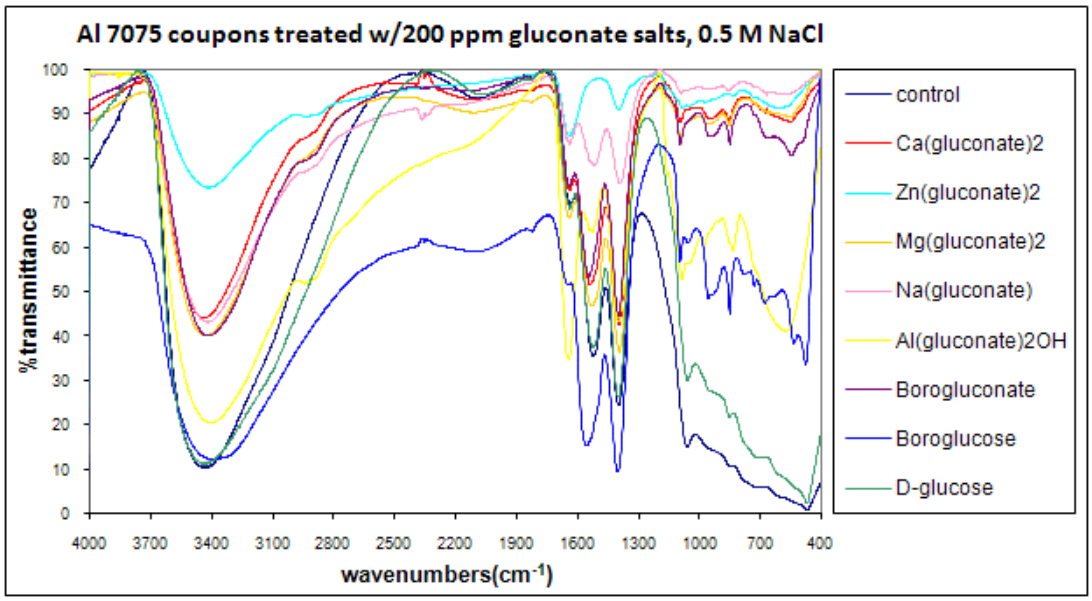

Figure 4-36 Combined Infrared Spectra of Aluminum 7075 Coupons Immersed in Solutions of Various Gluconate and Glucose Salts

In the low frequency region, bands due to aluminum surface were common for all three tested aluminum alloys albeit with slight differences in frequencies and strengths. Major peaks in the order of decreasing frequencies, were at 1155 cm^{-1} and 1067 cm^{-1} assigned to OH in-plane bendings of AlOOH, at 1050 cm^{-1} assigned to OH bending vibrations of AlOOH, at 770 cm^{-1} assigned to Al-O stretching vibrations of AlOOH, at 765 cm^{-1} assigned to O^{2-} displacements, at 736 cm^{-1} assigned to OH out of plane bending of AlOOH and at 411 cm^{-1} assigned to displacements of OH^{-}.[23-28]

Notably, the IR spectra of the zinc gluconate treated coupon revealed only two bands in the 1400 cm^{-1} – 1600 cm^{-1} with the middle band missing. Examination of the IR spectra of other coupons treated with inhibitors consisting of zinc cations revealed the same result, indicating that the cause of this effect was due to the zinc ions. Although not confirmed by any spectroscopic technique, the formation of a protective zinc hydroxide

film might have hindered the bidentate adsorption of hydroxyl group on the substrate surface. However, the absorption at 1397 cm^{-1} [29] characteristic of the presence of $Zn(OH)_2$ protective film was not observed. Thus, an alternative explanation, in agreement with middle band missing in the spectra of coupons treated with other highly efficient inhibitors, might be that middle band is due to bending vibration of hydroxyl of aluminum hydroxide that is a corrosion product of Aluminum, which disappears when the corrosion is efficiently inhibited.

Other carboxylic acids and their salts

The infrared spectra of the other tested acids and their salts such as boric acid, aluminum acetate, and aluminum lactate revealed almost entirely the same absorptions as those of the gluconate salts. Even the strengths of the bands due to use of different aluminum alloys matched when both IR spectra of coupons treated with gluconate salts and other hydroxy-acid salts were compared once more leading to the confirmation of the assignments of the bands in the 1400 cm^{-1} – 1600 cm^{-1} region to the bending vibrations of hydroxyl groups.

Molybdenum Esters of Hydroxy Acid Salts

The presence of molybdic oxides on aluminum substrate surfaces was apparent from the visual observations. Absorptions due to Mo-O bending vibrational modes normally are observed at 972 cm^{-1} [30], 994 cm^{-1} [31], and 996 cm^{-1} [32] as stated in the literature, however OH bending vibrations of AlOOH also do absorb in the same region. Regardless, a band due to Mo-O bending vibrations present in most of the IR spectra of

aluminum coupons exposed to molybdenum esters of hydroxy-acid salts was observed around 990 cm^{-1}. Notably, bands due to OH bending vibrations above 1000 cm^{-1} were not present in the IR of potassium benzilate molybdate treated coupons suggesting the presence of a barrier film in between water and substrate surface. Bands due to Mo-O bending vibrations also appear in the IR spectra of the coupon immersed for a second period of time, but this time the OH bending vibrations of AlOOH also appear matching the same bands of controls indicating the extent of corrosion taking place despite the layer of molybic oxides.

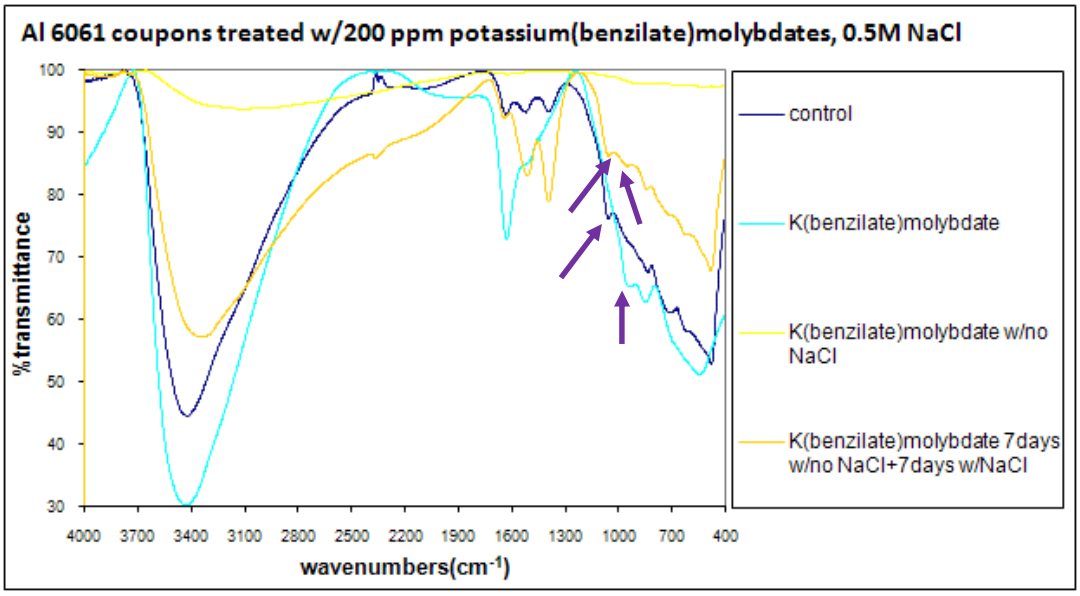

Figure 4-37 Combined Infrared Spectra of Aluminum 6061 Coupons Immersed in Potassium Benzilate Molybdate Solutions

Out of the three bands due to bending vibrations of hydroxyl groups, the middle band was found to be missing in the spectra of coupons treated with calcium gluconate molybdates and zinc gluconate molybdates. The highest frequency band among the three bands was also absent in the spectra of coupons treated with potassium benzilate

molybdates. Together with weight-loss test results, the absence of bands due to bending vibrations of hydroxyl of water of corrosion product, that is hydrated aluminum oxide, seemed to be an indication for better inhibition efficiency.

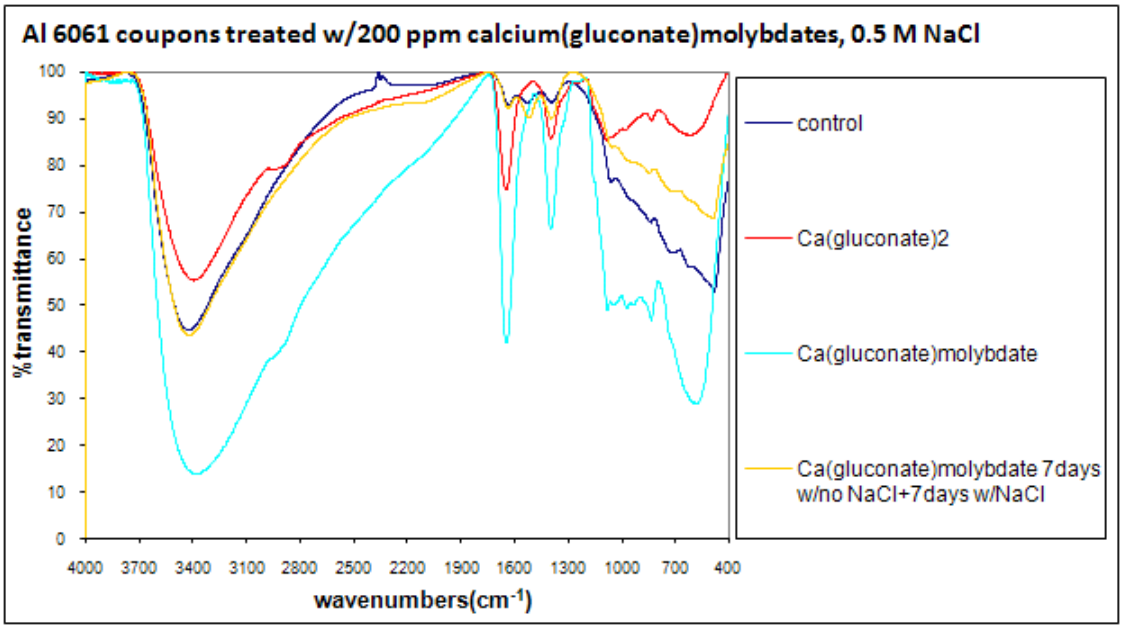

Figure 4-38 Combined Infrared Spectra of Aluminum 6061 Coupons Immersed in Calcium Gluconate Molybdate Solutions

Vanadium Esters of Hydroxy Acids

Calcium&Zinc Gluconate Vanadates

Absorption bands due to presence of vanadium are given in the literature to be between 400 cm^{-1} and 1000 cm^{-1} indexed to various group vibrations of V-O. [33,34] This includes bands at 1019 cm^{-1}, 850 cm^{-1}, and between 400 cm^{-1} to 650 cm^{-1}. [35,36] However, the weak infrared absorptions of the coupons treated with vanadium esters and the presence of many bands due to OH vibrations and stretching of AlOOH in the same region made it impossible to detect the presence of vanadium on the surface. However, along with absence of bands due to vanadium, bands due to corrosion products of

aluminum were also absent. IR spectra of coupons treated with vanadium esters for a second period of 7 days seemed similar to the control coupons with missing bands such as the band at 700 cm^{-1} due to stretching vibrations of AlOOH which might be considered as a complimentary evidence for the positive inhibitive efficiencies of vanadium esters during second immersion periods.

Boron Esters of Hydroxy Acids

Spectra of coupons immersed in solutions of boron esters of hydroxy acids almost entirely matched the spectra of the same alloy coupons treated with gluconate and benzilate salts. Thus, almost all IR spectra had three bands due to bending vibrations of hydroxyl of water due to hydrated aluminum oxide in 1600 cm^{-1} region. Coupons treated with zinc salts of borate esters were missing the middle band as in the case of other inhibitors containing zinc cations.

4.4 Characterization of Immersion Solutions

Characterization of the immersion solutions was conducted using oxidation-reduction potential and pH probes. Two readings were taken per sample, one before immersion and another after completion of immersion.

4.4.1 ORP Measurements

Immersion solutions of gluconate salts and their molybdenum esters revealed decreasing ORP values; while immersion solutions of vanadium esters and boron esters

in general had increasing ORP values with the initial ORP values ranging between 300 mV to 750 mV and the final ORP values ranging from 350 mV to 650 mV.

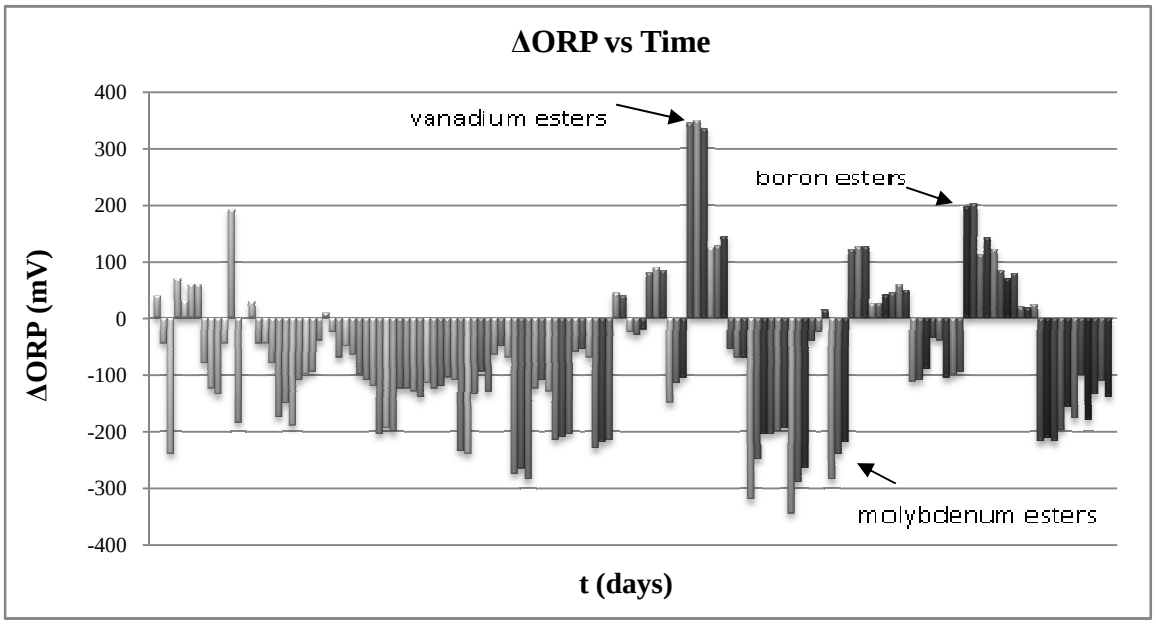

Figure 4-39 ΔORP vs. Time Graph of Immersion Solutions of Various Inhibitors During Immersions

ΔORP graphs indicated that ORP values lowered by an average of roughly 100 mV with molybdenum esters, potassium benzilate, and aluminum lactate having the highest decreases. Potassium benzilate vanadate and calcium gluconate borate esters had the highest increase in ORP values. Vanadate esters had the lowest initial ORP values as well.

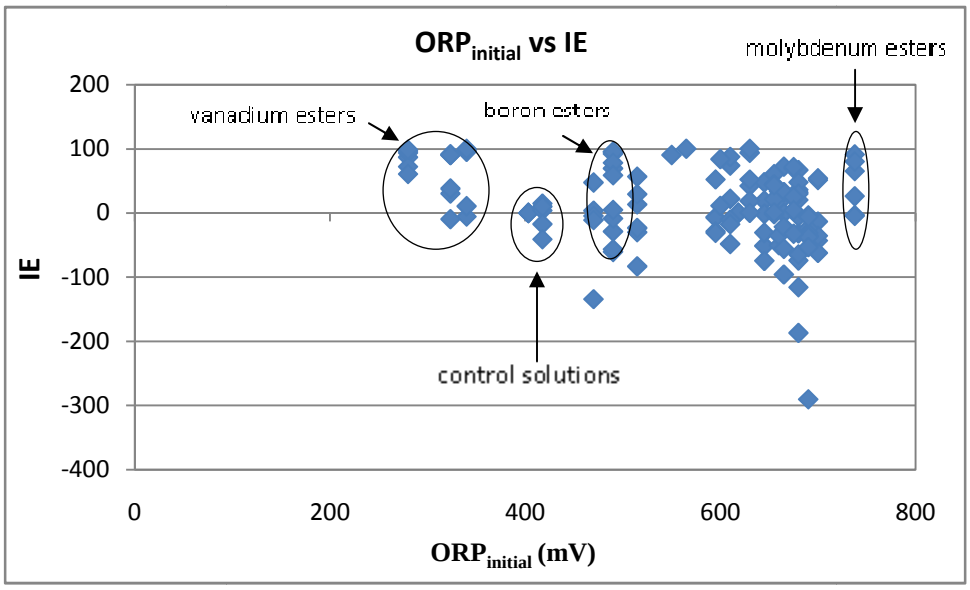

Figure 4-40 Initial ORP values vs. Inhibition Efficiency Graph of Immersion Solutions of Various Inhibitors

ORP is proportional to the concentration of oxidizers or reducers in a solution. It increases with the addition of an oxidizer and the decreases with the the addition of a reducer. Initial and final ORP values of immersion solutions of vanadium esters in particular were opposite to what was predicted. Only the ORP values of immersion solutions of vanadium esters were lower than the controls. Boron esters had slightly higher ORP values than control solutions, while all the other immersion solutions had significantly higher initial ORP values than control solutions. Molybdenum esters had the highest ORP values. Very high initial ORP values implied the preservation of +6 oxidation state of molybdenum in the hydroxy-acid formulation (+6 oxidation state as in the reactant MoO_3 and as in molybdates) corresponding to a strong oxidizing ability, which led to high initial ORP values. Reduction potential of hexavalent molybdenum to

molybdenum oxides such as MoO_2 in near neutral basic solutions is reported as -0.780 V[37-43], thus resulting in the preservation of +6 oxidation state of molybdenum against a mild reducing agent such as gluconate. However, against a very strong reducing agent as aluminum metal, hexavalent molybdenum is likely to reduce to pentavalent state in molybdenum oxide explaining the black depositions on the substrate surfaces. The half-reaction potential of Al to $Al(OH)_3$ is reported to be -2.300 V in basic solutions and as -1.676 V in acidic conditions.[37-43]

As for the boron esters, the fact that the initial ORP values were almost equal to the ORP values of control solutions indicated the inertness of boron esters in terms of redox potentials. In other words boron was already complexed in its +3 oxidation state and was inert towards any oxidation and reduction reaction. The highly negative reduction potentials of trivalent boron to elemental boron support this conclusion.[37-43]

In the case of vanadium esters significantly lower initial ORP values implied the addition of a reducer rather than an oxidizer. The oxidation state of vanadium in V_2O_5, which was used as a precursor to gluconate vanadate esters, is +5. However reacting with gluconate salts, which are known to be mild reducing agents, vanadium seemed to be reduced to its lower oxidation states, which is likely considering the reduction potentials of vanadium. In neutral to basic conditions reduction potential of VO_4^{3-} to V_2O_3 is reported to be 1.366 V. [37-43]

In conclusion, vanadium atoms already were in lower oxidation states initially in the form of vanadium esters, which were then transformed into insoluble vanadium oxides on the substrate surfaces with increasing local pH values without involvement of any oxidation-reduction process, which explains the small changes in ORP values for

vanadate esters. That small changes that are positive and 100 mV in average between the ORP_{final} and $ORP_{initial}$ values of vanadium esters was likely due to the migration of reducing agents that are lower oxidation state vanadiums, from the solution phase to the substrate surface in the form of deposition of vanadium oxides.

ΔORP/ORPinitial vs IE graph below indicates that in average ORP values were roughly decreased about a quarter for the tested compounds.

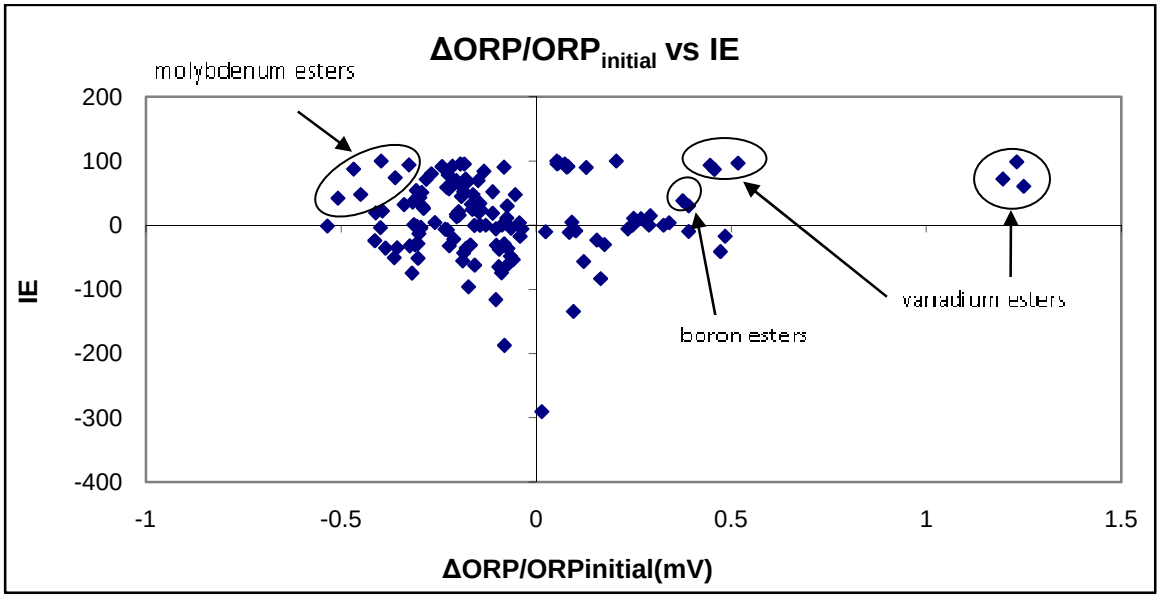

Figure 4-41 $\Delta ORP/ORP_{initial}$ Ratios vs. Inhibition Efficiency Graph of Immersion Solutions of Various Inhibitors

4.4.2 pH Measurements

Due to the anodic reaction of corrosion process, that is,

$$O_2 + 2H_2O + 4e^- \longrightarrow 4OH^-, \qquad \text{(Eq. 4.1)}$$

an increase in pH is expected in corroding systems. Accordingly the pH of the immersion solutions of good inhibitors increased only slightly, while large increases were

observed for compounds with no positive effect to corrosion inhibition. Some inhibitors were organic acids initially, thus resulting in low initial pH values around 2.

ΔpH values of immersion solutions were within ~ -0.1 and 2.9, with ineffective inhibitors such as gluconate salts and their borate esters having ΔpH values around 2 along with control solutions and solutions of second immersions. Highly efficient inhibitors such as chromium(III) acetate, zinc gluconate, and vanadate esters of calcium gluconate, zinc gluconate and potassium benzilate had decreased pH values after immersions. Thus, changes in pH were in agreement with inhibition efficiency and ORP measurements.

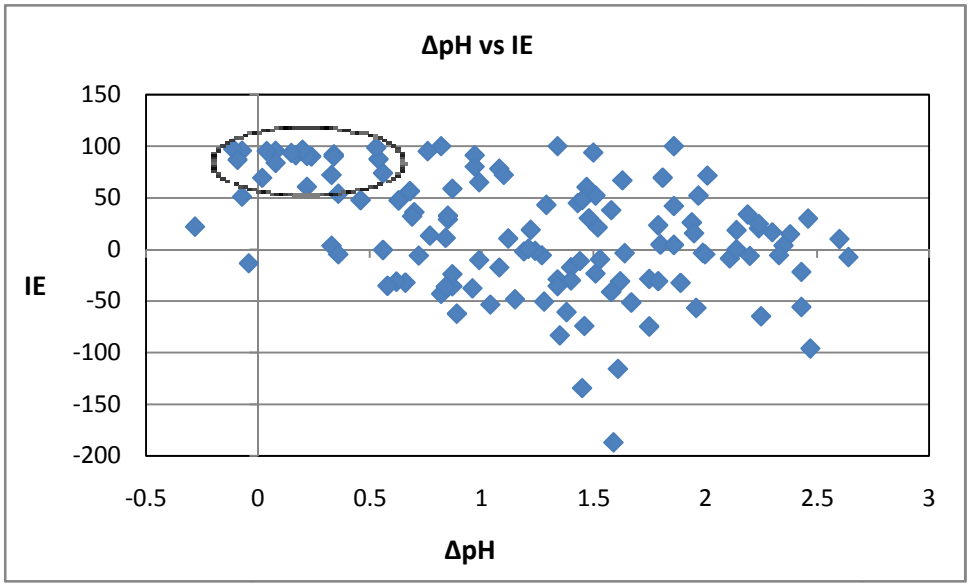

Figure 4-42 ΔpH vs. Inhibition Efficiency Graph of Immersion Solutions of Various Inhibitors

When ΔpH values were plotted versus inhibition efficiencies, it was observed that inhibitors with high inhibition efficiency values had negligible changes in pH opposed to inhibitors with low inhibition efficiencies.

4.5 Discussion and Conclusions

4.5.1 Effect of cationic constituents

In general the results were opposite to what had been observed in the case of mild steel highlighting the positive effect of metal oxyanions and cationic constituents in the formulation. Gluconate salts and their boron esters were the most efficient inhibitors for mild steel corrosion, while molybdenum and vanadium esters together with formulations consisting of zinc and trivalent chromium cations were most efficient inhibitors for aluminum corrosion. Only zinc cations were found to be an efficient inhibitor for both mild steel and aluminum corrosions.

With sodium gluconate revealing slightly negative inhibition efficiencies, the complexing property of gluconate this time aided the dissolution of protective aluminum oxide coating on the surface. Other gluconate salts such as magnesium gluconate and calcium gluconate inhibited corrosion around 10% unlike sodium gluconate while zinc gluconate effectively inhibited corrosion indicating the sole effect of cationic constituent. Magnesium, calcium, and zinc cations are known for their cathodic inhibitive activity due to forming insoluble hydroxides with zinc cations being the most inhibitive ones. Trivalent chromium was also considered to inhibit corrosion through a similar mechanism in which it forms insoluble chromium hydroxides and oxides.

4.5.2 Molybdenum and Vanadium Esters of Hydroxy-Acid Salts

Both molybdenum and vanadium esters of hydroxy-acid salts effectively inhibited corrosion of aluminum alloys with potassium benzilate vanadate inhibiting the corrosion very effectively even during a second immersion period, without a supply of inhibitor. There was much evidence for the formation of protective coatings originating from the molybdenum and vanadium esters through surface characterization studies. Digital imaging and infrared spectroscopy provided evidence for deposition of molybdenum on the substrate surfaces in the form of molybdic oxides, while X-ray fluorescence revealed presence of vanadium on the substrate surfaces. Immersion solution studies revealed that formation of trivalent vanadium oxide coatings might not have been due to a redox reaction but rather due to an ion-exchange mechanism between Al^{3+} and V^{3+} cations in the protective aluminum oxide layer leading to the repair and repassivation of the substrate surface resulting in a uniform clear protective coating, while coating of molybdic oxides were formed as a result of a redox reaction between the molybdenum esters of hydroxy-acid salts and the aluminum substrate leading to the formation of a non-uniform albeit protective, rough coating.

4.6 References

1. ASTM (American Society for Testing and Materials) Designation, G1–90, Undergone editorial change, Standard Practice for Preparing, Cleaning, and Evaluating Corrosion Test Specimen, **1999**.

2. ASTM Designation, G31-72, Undergone editorial change, Standard Practice Test for Laboratory Immersion Corrosion Testing of Metals, based upon NACE Standard TM-01-69, Test Method-Laboratory Corrosion Testing of Metals for the Process Industries, **1995**.
3. http://ca.water.usgs.gov/archive/fact_sheets/b07/up.html, U.S. Geological Survey, California branch report.
4. Lahodny-Sarc, O.; *Yug. Acad. Sc. &Arts, RAD, Chem.*, **1982**, 394, 18.
5. Cheng, B.; Ramamurthy, S.; McIntyre, N. S.; Characterization of phosphate films on aluminum surfaces, *J. of Materials Engineering and Performance*, **1997**, 6, 4, 405-412.
6. Arnott, D. R.; Hinton, B. R. W.; Ryan, N. E.; *Corr.*, **1989**, 45, 1, 12-18.
7. Bishop et al.; U.S. patent 4,171,231, **1979**.
8. Mansfeld, F.; Wang, V.; Shih, H.; *Jour. Electrochem. Soc.*, **1991**, 138, 12, 174-175.
9. Hughes, A. E.; Gorman, J. D.; Paterson, P. J. K.; *Corr. Sci.*, **1996**, 38, 11, 1957-1976.
10. Gorman, J. D.; Johnson, S. T.; Johnsto, P. N.; Paterson, P. J. K.; Hughes, A. E.; *Corr. Sci.*, **1996**, 38, 11, 1977-1990.
11. Fedrizzi, L.; Deflorian, F.; Canteri, R.; Fedrizzi, M.; Bonora, P. L.; *Proc. Prog. In the Understanding and Prevention of Corrosion*, Barcelona, Spain, **1993**, I, 131-138.
12. Romans, H. B.; U.S. Patent. No. 3272665, **1966**.

13. Miljevic, N. R.; Katanic-Popovic, J. D.; Matic, M. D.; *J. Serb. Chem. Soc.* **1988**, 53, 433–437.
14. Dorsey, G.A.; *J. Electrochem. Soc.*, 1966, 113, 169–172.
15. Rochester, C. H.; Topham, S. A.; Infrared Study of Surface Hydroxyl Groups on Haematite, *Chem. Soc., Faraday Trans.*, 1979, 1, 75, 1073–1088.
16. Walrafen, G. E. in: Water, A Comprehensive Treatise, Franks, F.(ed.); Plenum, New York, 1972, 1, 151.
17. Draegert, D. A.; Stone, N. W. B.; Curnutte, B.; Williams, D.; *J. Opt. Soc. Am.*, 1966, 56, 64.
18. Hasted, J. B.; Husain, S. K.; Frescura, F. A. M.; Birch, J. R.; *Chem. Phys. Lett.*, 1985, 118, 622.
19. Madden, P. A.; Impey, R. W.; *Chem. Phys. Lett.*, 1986, 123, 502.
20. Bansil, R.; Berger, T.; Toukan, K.; Ricci, M. A.; Chen, S. H.; *Chem. Phys. Lett.*, 1986, 132, 165.
21. Guillot, B.; *J. Chem. Phys.*, 1991, 95, 1543.
22. Corongiu, G.; *Int. J. Quant. Chem.*, 1992, 42, 1209.
23. Lewis, D. G.; Farmer, V. C.; Infrared Absorption of Surface Hydroxyl Groups and Lattice Vibrations in Lepidocrocite (γ-FeOOH) and Boehmite (γ-AlOOH), *Clay Minerals*, **1986**, 21, 93-100.
24. Parfitt, R. L.; Russell, J. D.; Farmerr, V. C.; Confirmation of the Surface Structures of Goethite (α-FeOOH) and Phosphate Goethite by Infrared Spectroscopy, *J. Chem. Soc., Faraday Trans.*, **1976**, 1, 72, 1082-1087.

25. Parfitt, R. L.; Russell, J. D.; Adsorption on Hydrous Oxides IV: Mechanism of Adsorption on Various Ions on Goethite, *J. Soil Sci.*, **1977**, 28, 297-305.
26. Taylor, R. M.; Influence of Chloride On the Formation of Iron Oxides From Fe(II) Chloride: Effect of Chloride on the Formation of Lepidocrocite and Crystallinity, *Clays Clay Miner.*, **1984**, 32, 175-180.
27. Misawa, T.; Kyuno, T.; Suetaka, W.; Shimodaira, S.; The Mechanism Of Atmospheric Rusting and The Effect of Cu and P On The Rust Formation of Low Alloy Steels, *Corrosion Science*, 1971, 11, 35-48.
28. Misawa, T.; Asami, K.; Hashimoto, K.; Shimodaira, S.; The Mechanism of Atmospheric Rusting and the Protective Amorphous Rust on Low Alloy Steel, *Corrosion Science*, 1974, 14, 279-289.
29. Rajendran, S.; Joany, R. M.; Palaniswamy, N.; An Encounter with Microheterogeneous Systems as Corrosion Inhibitors, *Corrosion Reviews*, **2002**, 20, 3, 231-252.
30. Irons, T. V.; Stafford, F. E.; *J. Am. Chem. Soc.*, **1966**, 88, 4819.
31. Ward, B. G.; Stafford, F. E.; *Inorg. Chem.*, **1968**, 7, 2569.
32. Barraclough, C. G.; Kew, D. J.; *Aust. J. Chem.*, **1966**, 19, 741.
33. Chen, W.; Peng, J.; Mai, L.; Zhu, Q.; Xu, Q.; Synthesis of Vanadium Oxide Nanotubes from V_2O_5 Sols, *Materials Letters*, **2004**, 58, 2277–2278.
34. Wilhartitz, P.; Dreer, S.; Ramminger, P.; Can Oxygen Stabilize Chromium Nitride? Characterization of High Temperature Cycled Chromium Oxynitride, *Thin Solid Films*, **2004**, 293, 447 –448.

35. Ewissa, M. A. Z.; Ansoor, S. A. A.; Electrical, IR Spectroscopy, and DTA Studies of Some Sodium Tetraborate Glasses Containing Vanadium Oxide, *Physica Status Solidi (a)*, 156, 2, 428.
36. Bouhaouss, P. A.; *Mater. Res. Bull.*, **1983**, 18, 1247.
37. Bard, A. J.; Parsons, R.; Jordan, J.; Standard Potentials in Aqueous Solutions, IUPAC Marcel Dekker, New York, USA, 1985.
38. Greenwood, N. N.; Earnshaw, A.; *Chemistry of the Elements*, 2nd edition, Butterworth-Heinemann, Oxford, UK, 1997.
39. Cotton, F. A.; Wilkinson, G.; *Advanced Inorganic Chemistry*, 5th edition, John Wiley & Sons, New York, USA, 1988.
40. Douglas, B.; McDaniel, D. H.; Alexander, J. J.; *Concepts and models of Inorganic Chemistry*, 2nd edition, John Wiley & Sons, New York, USA, 1983.
41. Shriver, D. F.; Atkins, P. W.; Langford, C. H.; *Inorganic Chemstry*, 3rd edition, Oxford University Press, Oxford, UK, 1999.
42. Huheey, J. E.; Keiter, E. A.; Keiter, R. L. in Inorganic Chemistry : *Principles of Structure and Reactivity*, 4th edition, HarperCollins, New York, USA, 1993.
43. Seaborg, G. T.; Loveland, W. D. in *The Elements Beyond Uranium*, John Wiley & Sons, New York, USA, 1990.

CHAPTER V

CORROSION INHIBITION OF SOL-GEL COATED AL 2024-T3 ALLOY VIA INHIBITOR PIGMENT ENRICHMENT

5.1 Introduction

The corrosion resistance behavior of inhibitor enriched organically-modified silane (Ormosil) thin films on 2024-T3 aluminum alloy substrates were investigated using accelerated salt spray analysis techniques. For sol-gel coatings to be used on Al 2024 alloys on aircrafts, an alkoxide precursor with an epoxide functional group was initially chosen because of its ability to react with the chemistry of the permanent foundation layer or the primer. The downside of epoxy silicate sol-gel coatings when compared to chromate conversion coatings is that the sol-gel films cannot passivate a damaged area.[1] In principle, all functional silanes that are trialkoxy esters can be used on metals. The preferred way of applying silanes to a metal substrate is to hydrolyze a dilute solution of the silane in water first; for example,

$$X\text{-}CH_2\,CH_2\,CH_2\text{-}Si(OCH_3)_3 \longrightarrow X\text{-}CH_2\,CH_2\,CH_2\text{-}Si(OH)_3 + 3CH_3OH \quad \text{(Eq. 5.1)}$$

where X is an organofunctional group. The alkoxy groups are, in principle, quantitatively hydrolyzed to active silanol groups; however, if this hydrolysis is not complete, good-quality films can still be formed. The remaining ester groups will then hydrolyze when

the treated metal is exposed to air. The structure of the silane, its concentration, and the pH of the silane solution has to be optimized for each combination of paint and metal. Once these parameters are determined, the film can then be obtained by dipping, spraying, brushing, or wiping the silane solution onto the metal and rinsing off the excess with water. The surface is then ready for further processing, such as painting or adhesive bonding.[2] The dipping time of the clean metal into the silane solution was reported to have no effect on the film thickness. The temperature of the silane solution was reported to have little effect on the film thickness as well. The effect of pH was also reported to be very low. The pH was expected to affect the way in which the first layer is adsorbed but was reported to have no effect on the subsequent layers or on the film thickness.[2]

5.2 Sol-Gel Preparation

Prior to this research, the corrosion resistant coatings laboratory at Oklahoma State University developed Ormosil solutions based on a 11.2 ml TEOS (tetra-ethyl-ortho-silicate or tetraethoxysilane), 15.4 ml VTMOS (vinyl-tri-methoxy-ortho-silane), 3.8 ml MEMO (3-(tri-methoxy-silyl)-propyl-methacrylate) precursor mixture using 0.05M HNO_3 as the catalyst. After thorough stirring for one hour followed by drying at ambient conditions for 24 hours, the thicknesses of Ormosil films on 3 x 5 inch AA (Aluminum alloy) test coupons were reported to be approximately 10-20 microns.[3] The network structure of this ormosil contains pendant vinyl and methacrylate groups that occupy pore space and surface positions. The presence of these groups is anticipated to make the Ormosil coating hydrophobic, slowing the penetration of water and corrosion initiators.[4] Given that parameters such as pH, temperature, dipping time had very little effect on the

quality of the coating; this sol-gel preparation technique has been implemented for the purposes of this study without alteration. The reagents TEOS, VTMOS, and MTMOS were purchased from Aldrich or Gelest and were used as received. Nitric acid (NF Grade, Fisher) was used to catalyze the sol-gel reaction and sodium chloride (reagent A.C.S., Spectrum) for accelerated salt spray analysis was used without further purification. 0.05 M nitric acid solution was prepared by diluting 2.6 ml concentrated nitric acid in one liter of distilled water. The specified literature composition of the sol-gel mixture was used due to its appropriate inorganic/organic ratio producing a highly adherent film to the underlying AA substrate. It is reported in the literature that highly organic films do not to adhere to the metal surface producing differences in texture at regions where gelation occurs as the sol sheets down the AA surface, presumably due to the low inorganic content and insufficient concentrations of Si-OH groups to produce covalent Si-O-Al bonds with the underlying metal surface to stabilize the sol-gel coating on the AA Panel.[5] On the other hand, Ormosils prepared from high water content did not wet the aluminum surface well due to high surface tension of the mainly aqueous sol, resulting in very thin, unevenly coated films.[5]

5.3 Incorporation of Inhibitor Pigments into Sol-Gel

The sol mixture was stirred for an hour before and another half an hour after the inhibitor pigments were added. The mixtures were than coated onto clean AA substrates by spraying with an airbrush. Pressurized air at 400 kPa was used to spray substrates from a distance of approximately 20 cm. Upright, slightly tilted substrates were sprayed several times, generally twice up and twice down with a moderate speed. Since the

pigments used were all solid, it was possible to add them directly to the sol. If the pigments had to be dissolved, their solution could be prepared either in methanol or ethanol, which are byproducts of the sol-gel reaction and, thus already present in the sol mixture. An excessive concentration of the inhibiting ions in the coating however may lead to degradation of its physical and mechanical properties as well as resulting in the inhibitor being washed away from the coating. The concept of an effective, limited range of solubility for any given inhibiting additive has been called the "*window of solubility*". For the purposes of this study, concentrations of 0.05g, 0.1g, 0.5g, 1g and 2 g per 50 ml of sol solution have been used.

5.4 Substrate Cleaning

In order to achieve good protective action of applied layers, it is important to obtain excellent adhesion of the layer to the base metal. For this reason the substrate surface must be cleaned very well before applying the surface layer. Cleaning is done in two steps; first inorganic impurities such as oil, grease, and paint are removed from surface by using organic solvents, strongly alkaline solutions, emulsion baths, or steam cleaning. Then solid inorganic material such as rust, mill scales and other corrosion products are removed by mechanical treatment including brushing, grinding, polishing, sandblasting or by heat treatment with flames, induction heating followed by cooling to obtain sealing or by chemical pickling with strong acids.[6-8]

For degreasing the substrates, procedures commonly used in aerospace applications have been chosen, which includes removal of impurities such as oil, and grease from substrate surface by optional solvent cleaning and then by using an industrial

alkaline cleaner followed by deoxidization using chemical pickling with strong acids.[9,10] For this reason, the same degreasing method that has been used to clean aluminum substrates for weight-loss tests in the fourth chapter of this study has been employed with the sole difference of using 3 x 5 inch substrates instead of the 1 x 1 inch substrates. Thus, 3 x 5 inch coupons were first wiped off with paper towels soaked with hexane and then were wiped off again with paper towels soaked with methanol. Secondly, the substrates were soaked in an aerated Oakite-164 alkaline cleaner solution[11] (Oakite Products, Inc.) for 10 min at 150 ˚F or 65 ˚C for complete degreasing. Oakite-164 alkaline cleaner solution is one of the universal alkaline cleaners on the market that work well for carbon steel, galvanized steel, and aluminum and its alloys. Acid or neutral cleaners are less desirable because the metal oxide should have as many free hydroxyl groups as possible. These are required for the reaction with the acid silanol groups. Lastly, substrates were soaked in Deoxalume 2310 deoxidizing solution[12] for 6.5 minutes at ambient conditions under rigorous air agitation. Deoxalume solution consists of 20% HNO_3, 10% deoxalume (Henkel Surface Technologies), and 70% H_2O. Each of these treatments was followed by thorough rinsing for two minutes using reverse osmosis water. After spraying is done, coupons were allowed to be cured under ambient conditions for 5 days and were then taped on the edges to prevent the ingress of corrosion from underneath the coating. Cured and taped coupons were scanned for comparison purposes before placing them into the salt fog chamber.

5.5 Accelerated Salt Spray Testing

Major factors that cause degradation of the protective coatings are; UV radiation, water and moisture, temperature, aggressive ions such as chlorides. Thus, to simulate long term real life applications some of these factors are accelerated to test the corrosion protective properties of a coating. A coating can be protected from UV exposure simply by painting over it with a paint that does not transmit light. Therefore UV stress is not included in accelerated salt spray analyses.[13] Chemical stress in accelerated testing such as chloride containing salts however is important because airborne contaminants are believed to play a very minor role in aging of paints and organic coatings in general.[14] Moisture and temperature are other accelerating parameters in salt spray testing. Thus, corrosion protection properties of the sol-gel coated AA substrates were evaluated by exposing the substrates to a salt fog atmosphere generated by spraying 5% aqueous NaCl solution by weight at 35±1.7 ˚C or at 95˚ F for 168 hour in accordance with ASTM B117 specifications.[15] After removal from the salt fog chamber, all samples were rinsed with distilled water to remove any residues. After completion of this first ASTM B117 test, samples were scanned for later evaluation and exposed to a second ASTM B117 test totaling an exposure time of 15 days consisting of 1 week of wet + 1 day dry + 1 week of wet cycle. Comparison of scanned images of control coupons and inhibitor pigment added coupons before salt fog exposure, after completion of 1st ASTM B117 test and after completion of 2nd ASTM B117 test revealed an exclusive evaluation of the corrosion resistive behavior of the inhibitor pigment. Resistance to corrosion for a total of 15 days of wet-dry-wet cycle is a strong indication of successful corrosion inhibition for the inhibitor pigment incorporated into the sol-gel coating.

Along with aluminum coupons, steel coupons of same size were also cleaned and placed in different parts of the salt fog chamber to be tested afterwards via weight-loss tests to make sure that the salt fog chamber conditions do not vary at different times. Graduated cylinders were also placed in the different regions inside the salt fog chambers. The amount of moisture collected by the graduated cylinder, the pH and the density of the condensate were all good indicators of how well salt-fog chamber was running.

5.6 Discussion and Results

5.6.1 Evaluation Techniques

When evaluating the substrates after completion of the salt fog chamber test, direct or implicit signs of corrosion and coating degradation or failures were sought. These signs can be seen by the unaided eye such as rust through and creep from scribe marks.[16] Aluminum alloys with properly formed chromate conversion coatings regularly survive this exposure test without any visible signs of corrosion. Thicker coatings are required to protect alloys with higher copper contents. Coatings can be grown sufficiently thick to protect 7075-T6 (estimated to be 10 μm), but chromate conversion coatings cannot protect 2024-T3 sufficiently to pass salt spray testing.[17]

If a coating is properly applied to a well-prepared surface and allowed to cure, then general corrosion across the intact paint surface usually is not a major concern. Hence, sol-gel coated aluminum samples prepared by the aforementioned technique were already reported to pass the ASTM B117 test with no evidence of generalized corrosion or coating delamination on unscribed control coupons after 168 hour of salt spray exposure.[3]

However when the coating is scratched thus exposing the metal surface, the metal in the center of the scratch becomes a cathode because of its best access to the oxygen. The anode arises at the sides of the scratch. As a result corrosion begins at the scratch and can spread outward under coating. Therefore coatings' ability to resist this corrosion is a major concern. Accordingly, localized pitting was commonly observed on the scribed control coupons after 168 hour of salt spray exposure as the primary film failure mode.

In this study, inhibitor enriched sol-gel coated unscribed substrates were tested for comparison with unscribed control substrates, which were already reported to pass the ASTM B117 test. On the other hand, scribed inhibitor enriched sol-gel coated scribed substrates were tested to determine whether corrosion properties of sol-gel coatings were improved or not with the addition of inhibitor pigments.

Inhibitor pigments were chosen based on several factors. One of the criteria was the performance of the inhibitors in aqueous solutions. Inhibition efficiencies of these inhibitors for aluminum 2024 alloy corrosion determined by weight-loss tests were taken into account. Secondly, the water solubility values of these inhibitors were considered. As a result, zinc carboxylates, chromium carboxylates, chromium borate and chromium oxyhydroxide along with a few inorganic trivalent chromium compounds have been tested first in terms of their compatibility with the sol-gel coating and second in terms of their contribution to corrosion protection properties of the sol-gel coating.

5.6.2 Zinc Carboxylates

The low water solubilities of the zinc carboxylates studied in this investigation were a good fit for sol mixture with a few exceptions. Among the five different

concentrations tried 1.0g/50ml concentration of zinc mandelate resulted in a sol with gritty foam on top that clogged the nozzles of the sprayer, making it very hard to spray. An even higher 2.0g/50ml concentration of zinc mandelate made it impossible to spray, so the sol was brushed onto the substrate.

Zinc mandelate

There was some protection with zinc mandelate for the concentration of 1.0g/50ml, while for 2.0g/50ml concentration the inhibitor precipitated. Lower concentrations of zinc mandelate seemed to result in accelerated corrosion compared to the controls as shown in Figure 5.1.

Zinc tartrate

In the case of zinc tartrate added to the sol-gel coated Al 2024 alloy substrates, accelerated corrosion was observed for all five tried concentrations as shown in Figure 5.2.

Zinc gallate

Compared to the controls, a slight improvement of corrosion inhibition was observed for higher concentrations of zinc gallate as shown in Figure 5.3.

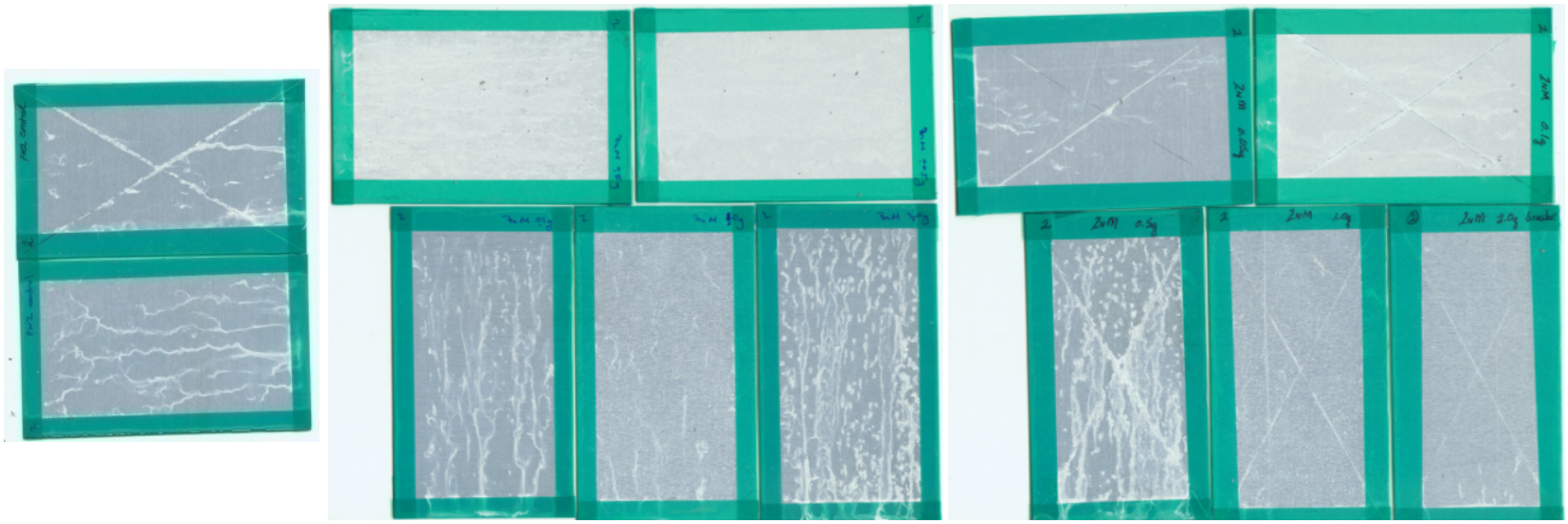

Scribed and unscribed control coupons

On top from left to right: 0.05 g and 0.5 g zinc mandelate added coupons, respectively. At the bottom from left to right: 0.1 g, 1 g, and 2 g zinc mandelate added coupons, respectively.

On top from left to right: 0.05 g and 0.1 g zinc mandelate added coupons, respectively. At the bottom from left to right: 0.5 g, 1 g, and 2 g zinc mandelate added coupons, respectively.

Figure 5-1 Scans of Sol-gel Coated Control Coupons, Unscribed Zinc Mandelate Added Sol-gel Coated Coupons, and Scribed Zinc Mandelate Added Sol-gel Coated Coupons

Immersed in Salt Fog Chamber for 2 weeks; respectively.

Scribed and unscribed control coupons

On top from left to right: 0.05 g and 0.1 g zinc tartrate added coupons, respectively.
At the bottom from left to right: 0.5 g, 1 g, and 2 g zinc tartrate added coupons, respectively.

On top from left to right: 0.05 g and 0.1 g zinc tartrate added coupons, respectively.
At the bottom from left to right: 0.5 g, 1 g, and 2 g zinc tartrate added coupons, respectively.

Figure 5-2 Scans of Sol-gel Coated Control Coupons, Unscribed Zinc Tartrate Added Sol-gel Coated Coupons, and Scribed Zinc Tartrate Added Sol-gel Coated Coupons Immersed in Salt Fog Chamber for 2 weeks; respectively.

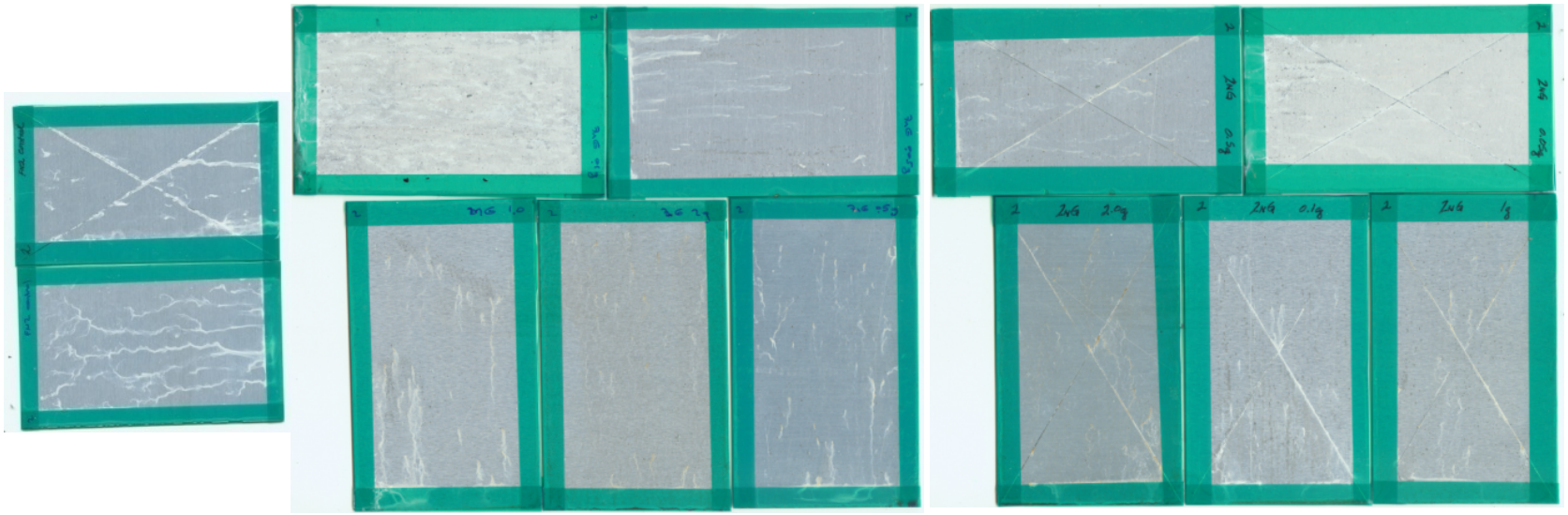

Scribed and unscribed control coupons

On top from left to right: 0.1 g and 0.05 g zinc gallate added coupons, respectively.
At the bottom from left to right: 1 g, 2 g, and 0.5 g zinc gallate added coupons, respectively.

On top from left to right: 0.5 g and 0.05 g zinc gallate added coupons, respectively.
At the bottom from left to right: 2 g, 0.1 g, and 1 g zinc gallate added coupons, respectively.

Figure 5-3 Scans of Sol-gel Coated Control Coupons, Unscribed Zinc Gallate Added Sol-gel Coated Coupons, and Scribed Zinc Gallate Added Sol-gel Coated Coupons Immersed in Salt Fog Chamber for 2 weeks; respectively.

5.6.3 Chromium Gluconate Borate Derivatives

$CrBO_3$

$Cr(gluconate)_3$ and $Cr(gluconate)_3$borates were too soluble to be added to solgel, while $CrBO_3$ and CrO(OH) were only very little soluble making them appropriate to be added to solgel yielding very promising results as shown in Figure 5.4.

In an additional attempt, the product was sieved using a sieve with a 25 micron mesh opening in addition to standard grinding, which seemed to lead to better results especially in the case of scribed samples as shown in Figure 5.5.

In general, the results were very promising for $CrBO_3$ added solgel coated substrates. Total corrosion inhibition was observed in the case of unscribed samples for concentrations 0.1g/50 ml and up and as for scribed samples the scribes were clear for concentrations 0.5g/50ml and up.

Synthesized CrOOH vs Commercial Grade CrOOH

Compared to the controls and to the commercially available CrO(OH) added sol-gel coated Al 2024 substrates, the synthesized CrO(OH) added sol-gel coated substrates performed very well especially in the case of unscribed substrates and for higher concentrations of the inhibitor as shown in Figure 5.6.

Prolonging the curing times to improve corrosion inhibitive properties of synthesized CrO(OH) added sol-gel coating resulted in agglomeration of CrO(OH) particles leading to negative results as shown in Figure 5.7. CrO(OH) particles settled out from the sol-gel coating, which was evident from the color of sol-gel coated substrates, which were not green unlike prior attempts.

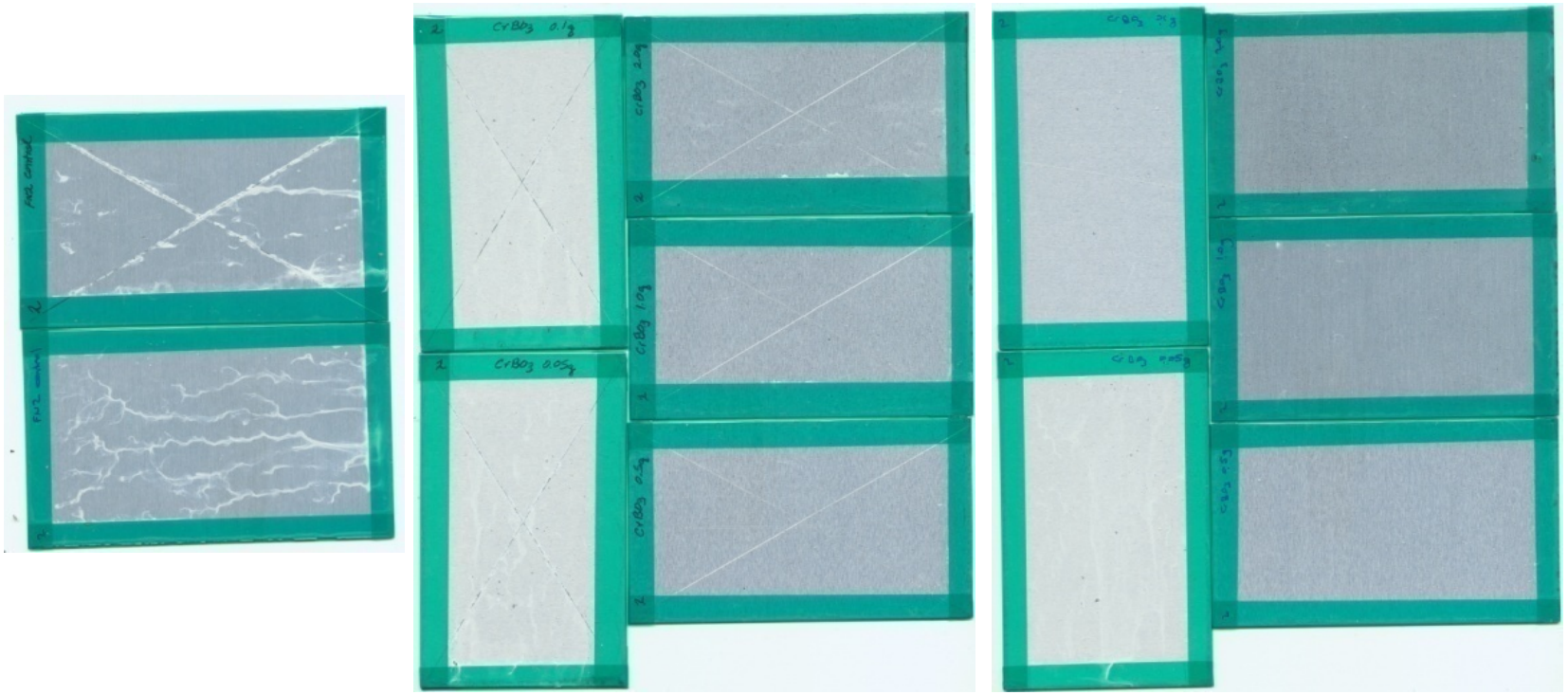

Scribed and unscribed control coupons

On left from top to bottom: 0.1 g and 0.05 g chromium borate added coupons, respectively. On right from top to bottom: 2 g, 1 g, and 0.5 g chromium borate added coupons, respectively.

On left from top to bottom: 0.1 g and 0.05 g chromium borate added coupons, respectively. On right from top to bottom: 2 g, 1 g, and 0.5 g chromium borate added coupons, respectively.

Figure 5-4 Scans of Sol-gel Coated Control Coupons, Scribed Chromium Borate Added Sol-gel Coated Coupons, and Unscribed Chromium Borate Added Sol-gel Coated Coupons Immersed in Salt Fog Chamber for 2 weeks; respectively.

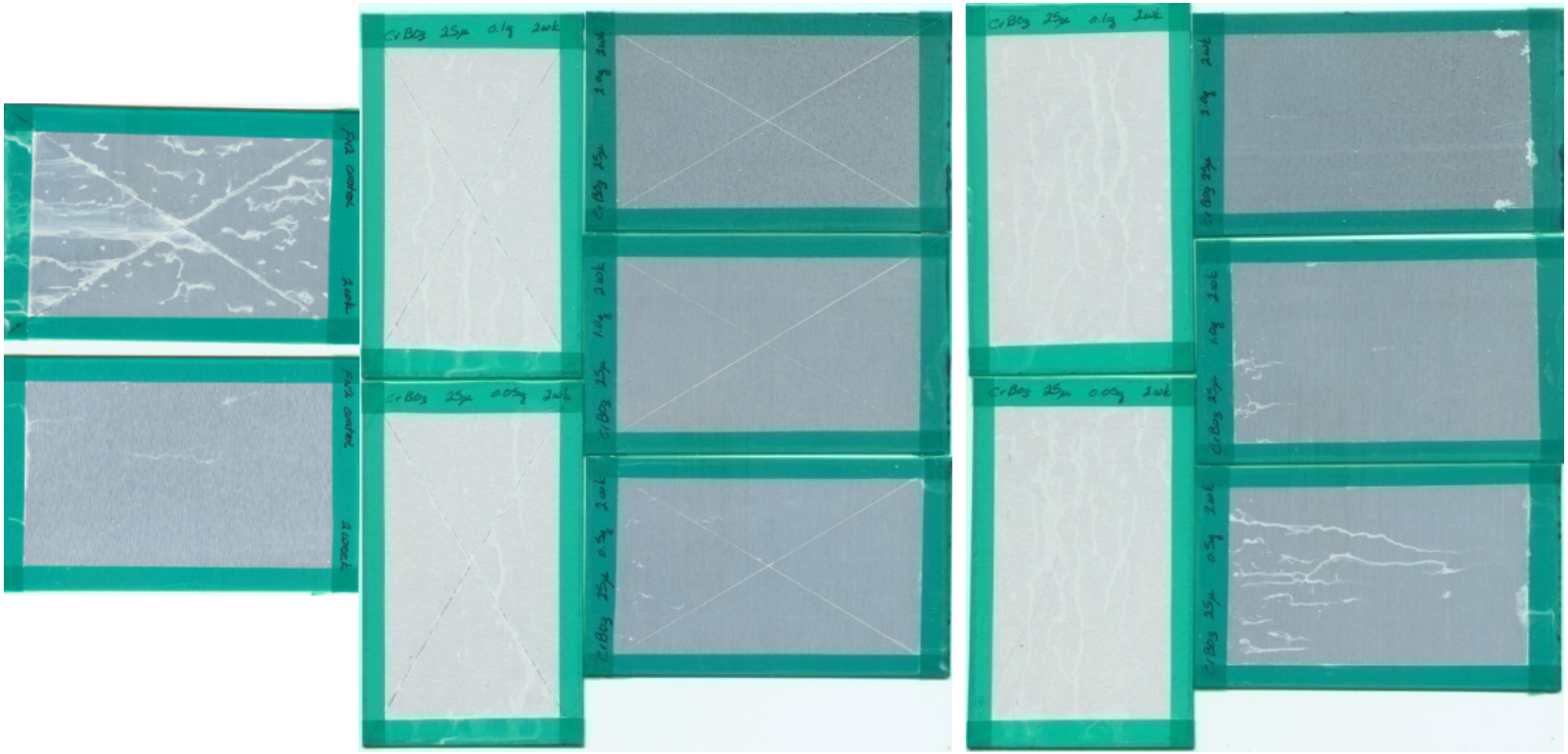

Scribed and unscribed control coupons

On left from top to bottom: 0.1 g and 0.05 g sieved chromium borate added coupons, respectively. On right from top to bottom: 2 g, 1 g, and 0.5 g sieved chromium borate added coupons, respectively.

On left from top to bottom: 0.1 g and 0.05 g sieved chromium borate added coupons, respectively. On right from top to bottom: 2 g, 1 g, and 0.5 g sieved chromium borate added coupons, respectively.

Figure 5-5 Scans of Sol-gel Coated Control Coupons, Scribed Sieved Chromium Borate Added Sol-gel Coated Coupons, and Unscribed Sieved Chromium Borate Added Sol-gel Coated Coupons Immersed in Salt Fog Chamber for 2 weeks; respectively.

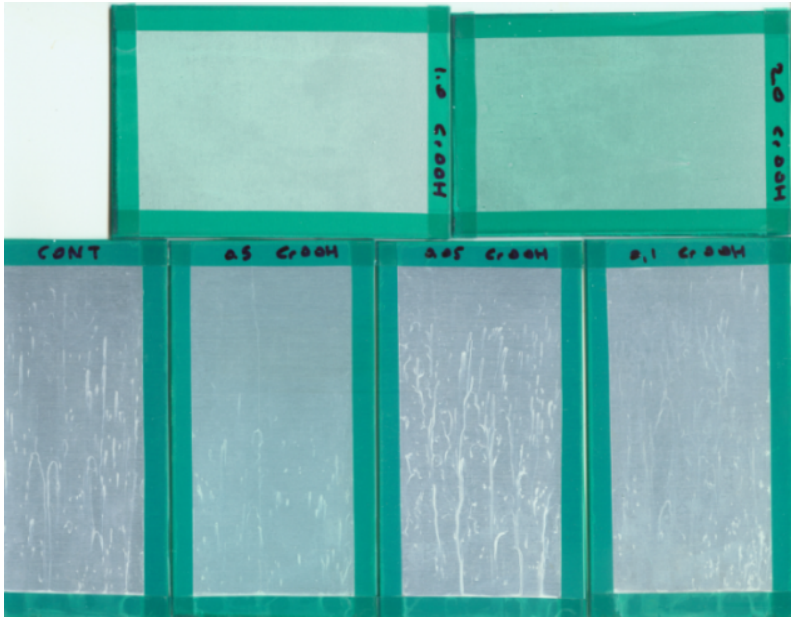

On top from left to right: 1 g and 2 g chromium oxyhydroxide added coupons, respectively.
At the bottom from left to right: control, 0.5 g, 0.05 g, and 0.1 g chromium oxyhydroxide added coupons, respectively.

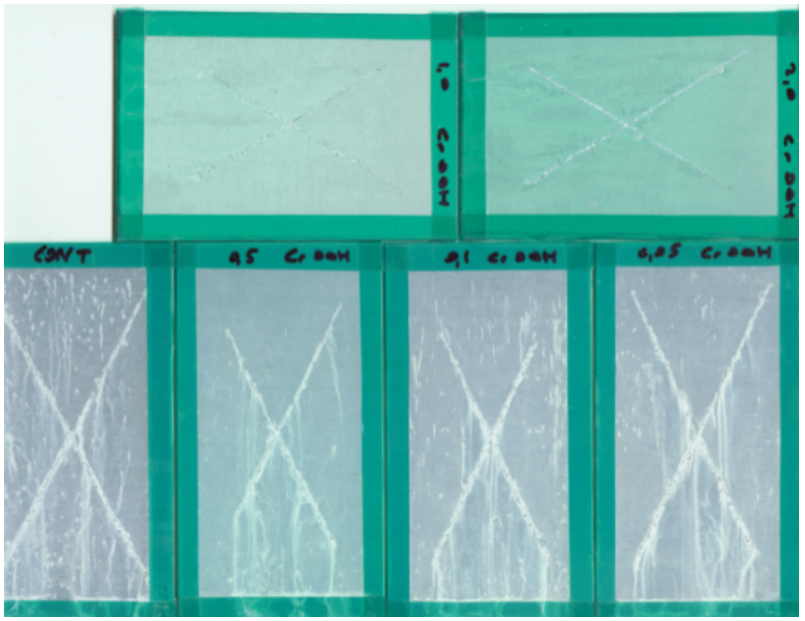

On top from left to right: 1 g and 2 g chromium oxyhydroxide added coupons, respectively.
At the bottom from left to right: control, 0.5 g, 0.05 g, and 0.1 g chromium oxyhydroxide added coupons, respectively.

Figure 5-6 Scans of Sol-gel Coated Control Coupons Together with Unscribed Chromium Oxyhydroxide Added Sol-gel Coated Coupons, and Scribed Chromium Oxyhydroxide Added Sol-gel Coated Coupons Immersed in Salt Fog Chamber for 2 weeks; respectively.

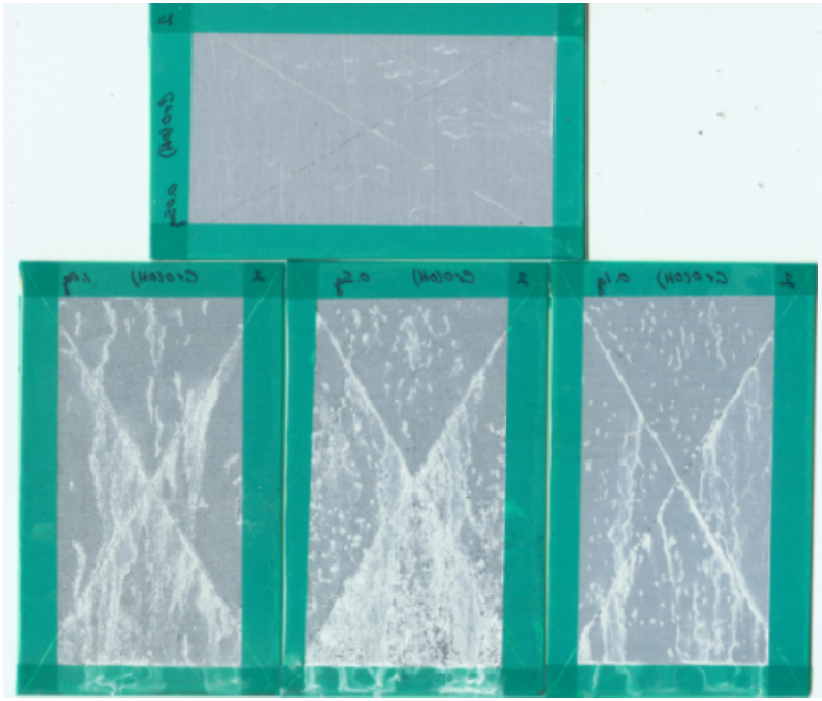

On top 0.05 g chromium oxyhydroxide added coupon.
At the bottom from left to right: control, 0.1 g, 2 g, and 1 g chromium oxyhydroxide added coupons, respectively.

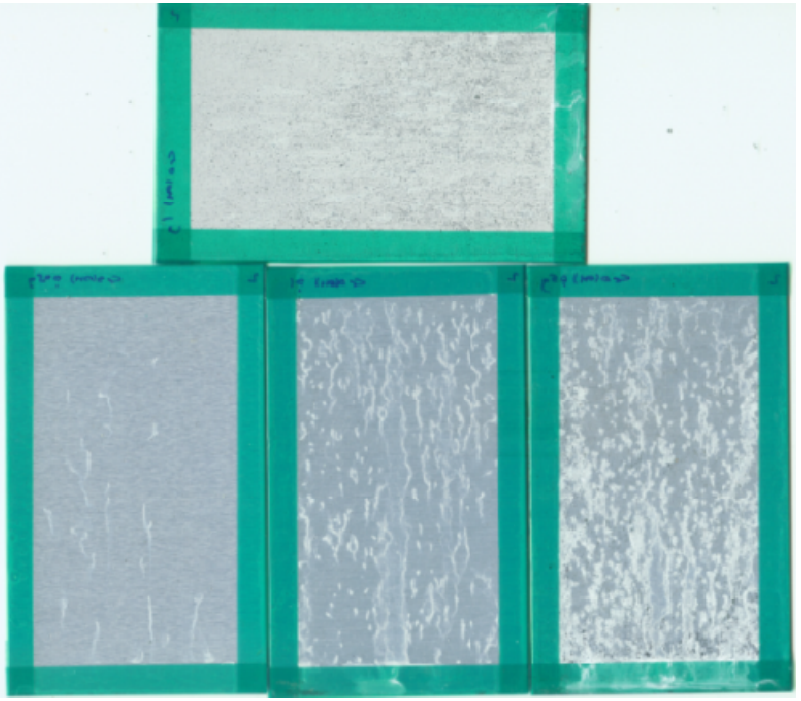

On top 0.1 g chromium oxyhydroxide added coupon.
At the bottom from left to right: control, 0.05 g, 1 g, and 2 g chromium oxyhydroxide added coupons, respectively.

Figure 5-7 Scans of Unscribed and Scribed Chromium Oxyhydroxide Added Sol-gel Coated Coupons (Prepared via an Alternative Method), Immersed in Salt Fog Chamber for 2 weeks; respectively.

Control samples for this figure are the same controls in Figure 5.7.

Shortening the stirring time of the sol mixture from one hour plus half an hour with the pigment down to one hour total revealed negative results as shown in Figure 5.8, presumably resulting in sol particles not to be able to chemically bond with each other due to the presence of CrO(OH) pigments in the sol mixture from the beginning.

Sonicating CrO(OH) particles overnight in 0.05M HNO_3, which is a component of the sol mixture again resulted the sol mixture gelling after half an hour of stirring with the inhibitor despite the seemingly reduced size of CrO(OH) particles. Mixing the inhibitor with the sol-gel mixture only for 3 minutes after one hour mixing of sol-gel mixture however, yielded better results as shown in Figures 5.8 and 5.9. No clogging of nozzles of the sprayer also implied better coating properties. Additionally, for high concentrations the sol-gel could be easily brushed with no evidence of different textures observed on the substrate.

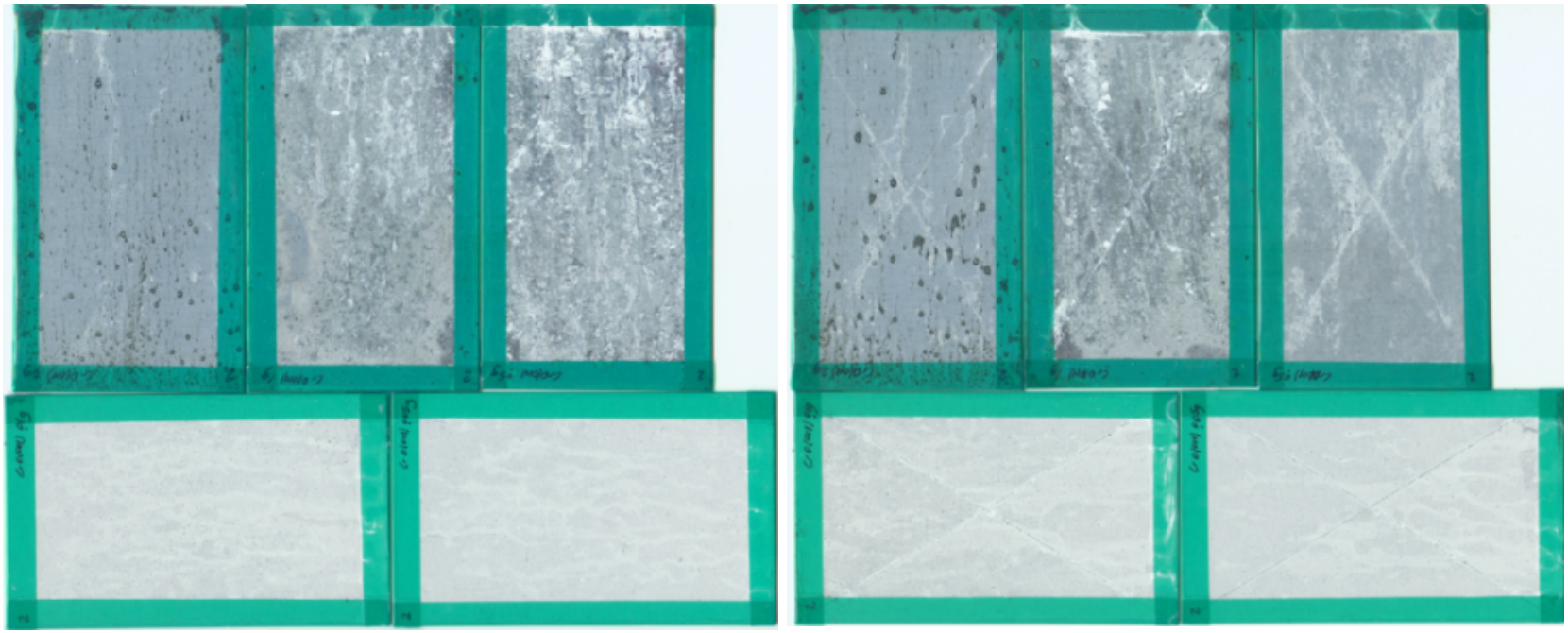

On top from left to right: 2 g, 1 g, and 0.5 g chromium oxyhydroxide added coupons, respectively.
At the bottom from left to right: control, 0.1 g, and 0.05 g chromium oxyhydroxide added coupons, respectively.

On top from left to right: 2 g, 1 g, and 0.5 g chromium oxyhydroxide added coupons, respectively.
At the bottom from left to right: control, 0.1 g, and 0.05 g chromium oxyhydroxide added coupons, respectively.

Figure 5-8 Scans of Unscribed and Scribed Chromium Oxyhydroxide Added Sol-gel Coated Coupons (Prepared via a 3rd Alternative Method), Immersed in Salt Fog Chamber for 2 weeks; respectively.

Control samples for this figure are the same controls in Figure 5.7.

one week test

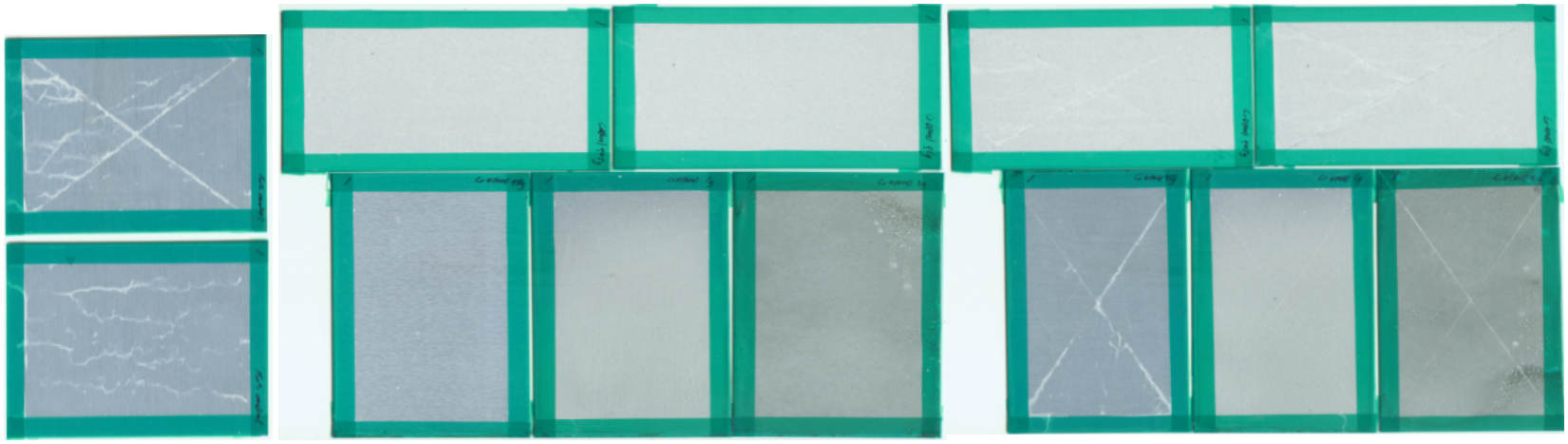

Scribed and unscribed control coupons

On top from left to right: 0.05 g and 0.1 g chromium oxyhydroxide added coupons, respectively.
At the bottom from left to right: 0.5 g, 1 g, and 2 g chromium oxyhydroxide added coupons, respectively.

On top from left to right: 0.05 g and 0.1 g chromium oxyhydroxide added coupons, respectively.
At the bottom from left to right: 0.5 g, 1 g, and 2 g chromium oxyhydroxide added coupons, respectively.

Figure 5-9 1 Week Scans of Sol-gel Coated Control Coupons Along with Unscribed and Scribed Chromium oxyhydroxide Added Sol-gel Coated Coupons (prepared via a 4th alternative method)

Immersed in Salt Fog Chamber for 2 weeks, respectively.

two week test

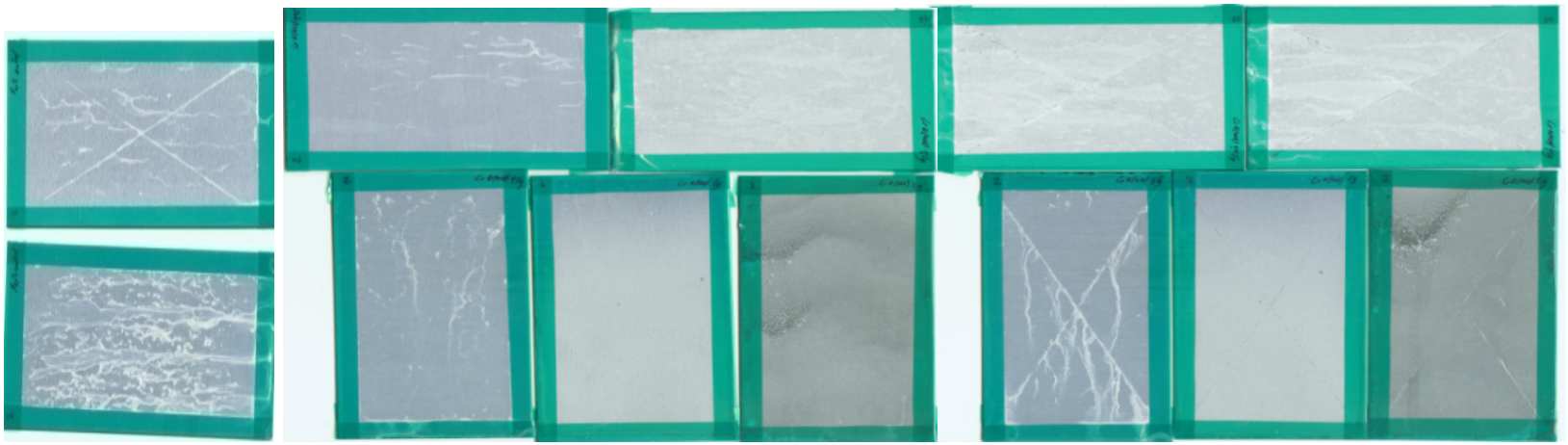

Scribed and unscribed control coupons

On top from left to right: 0.05 g and 0.1 g chromium oxyhydroxide added coupons, respectively.
At the bottom from left to right: 0.5 g, 1 g, and 2 g chromium oxyhydroxide added coupons, respectively.

On top from left to right: 0.05 g and 0.1 g chromium oxyhydroxide added coupons, respectively.
At the bottom from left to right: 0.5 g, 1 g, and 2 g chromium oxyhydroxide added coupons, respectively.

Figure 5-10 2 Week Scans of Sol-gel Coated Control Coupons Along with Unscribed and Scribed Chromium oxyhydroxide (synthesized via a 4th alternative method) Added Sol-gel Coated Coupons Immersed in Salt Fog Chamber for 2 weeks; respectively.

5.6.4 Chromium Carboxylates

Chromium Octanoate

Positive results were obtained for $Cr(octanoate)_3$ containing sol-gel coated Al 2024 substrates especially for the inhibitor concentration of 2.0g/50ml for scribed samples and of 1.0g/50ml for unscribed samples as shown in Figure 5.11. The fine texture of the coating with $Cr(octanoate)_3$ was likely due to its relatively longer alkyl chain. However inhibitor concentration of 2.0g/50 ml seemed to be the upper limit due to formation of different textures on the substrate surface over that amount.

Chromium Caproate

Unlike $Cr(octanoate)_3$, $Cr(caproate)_3$ revealed negative results as shown in Figure 5.12.

Chromium Butyrate, Chromium Propionate, and Chromium Methoxyacetate

Chromium butyrate was dispersible in water although not soluble, while chromium propionate was only slightly soluble and chromium methoxyacetate was highly soluble. All three inhibitors yielded negative corrosion inhibition results when incorporated to sol-gel coating as shown in Figures 5.13, 5.14, and 5.15.

Chromium Acetate

Despite being highly soluble, higher concentrations of 2.0g/50 ml in case of scribed samples and both 1.0g/50 ml and 2.0g/50ml concentrations for unscribed samples revealed positive results as shown in Figure 5.16.

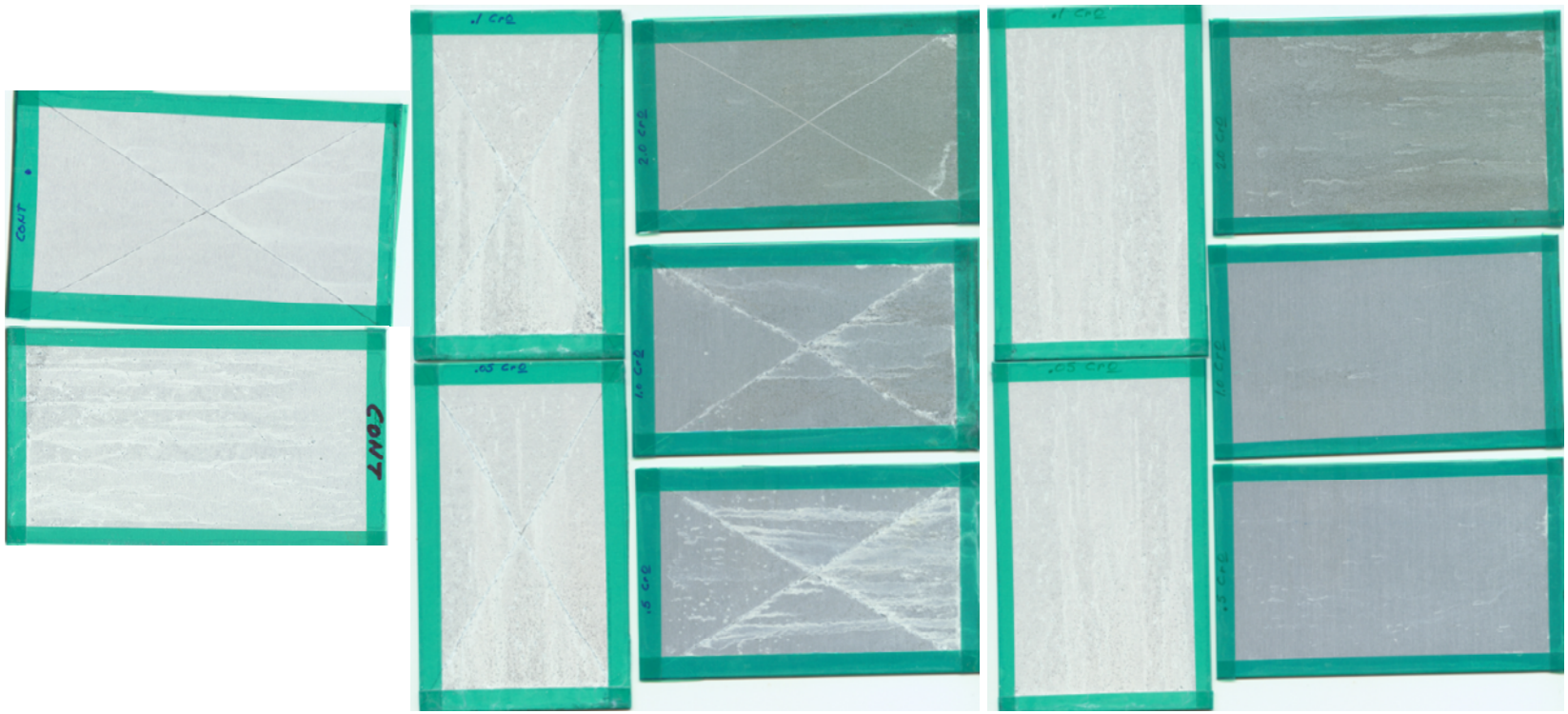

Scribed and unscribed control coupons

On left from top to bottom: 0.1 g and 0.05 g sieved chromium octanoate added coupons, respectively. On right from top to bottom: 2 g, 1 g, and 0.5 g sieved chromium octanoate added coupons, respectively.

On left from top to bottom: 0.1 g and 0.05 g sieved chromium octanoate added coupons, respectively. On right from top to bottom: 2 g, 1 g, and 0.5 g sieved chromium octanoate added coupons, respectively.

Figure 5-11 Scans of Sol-gel Coated Control Coupons, Scribed and Unscribed Chromium Octanoate Added Sol-gel Coated Coupons Immersed in Salt Fog Chamber for 2 weeks, respectively.

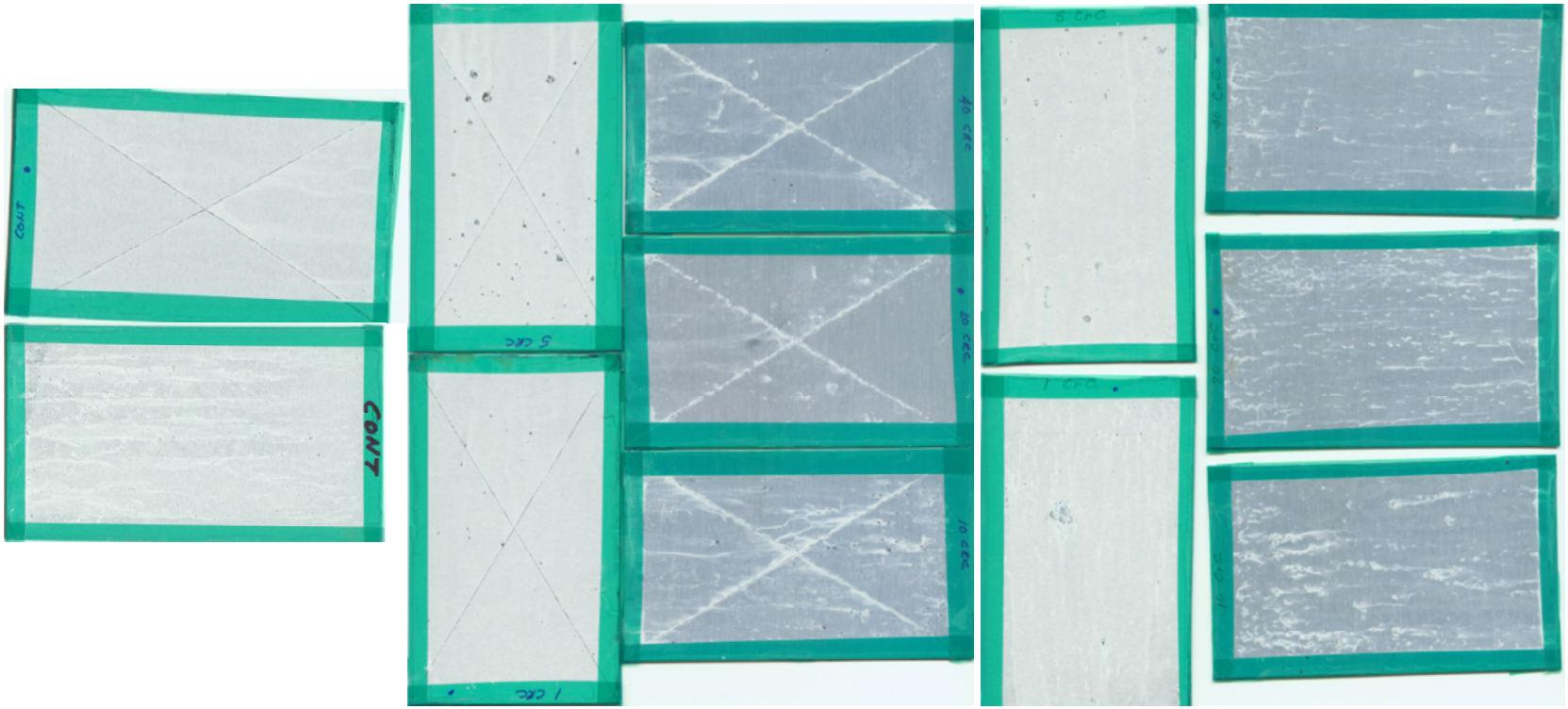

Scribed and unscribed control coupons	On left from top to bottom: 0.1 g and 0.05 g sieved chromium caproate added coupons, respectively. On right from top to bottom: 2 g, 1 g, and 0.5 g sieved chromium caproate added coupons, respectively.	On left from top to bottom: 0.1 g and 0.05 g sieved chromium caproate added coupons, respectively. On right from top to bottom: 2 g, 1 g, and 0.5 g sieved chromium caproate added coupons, respectively.

Figure 5-12 Scans of Sol-gel Coated Control Coupons, Scribed and Unscribed Chromium Caproate Added Sol-gel Coated Coupons Immersed in Salt Fog Chamber for 2 weeks, respectively.

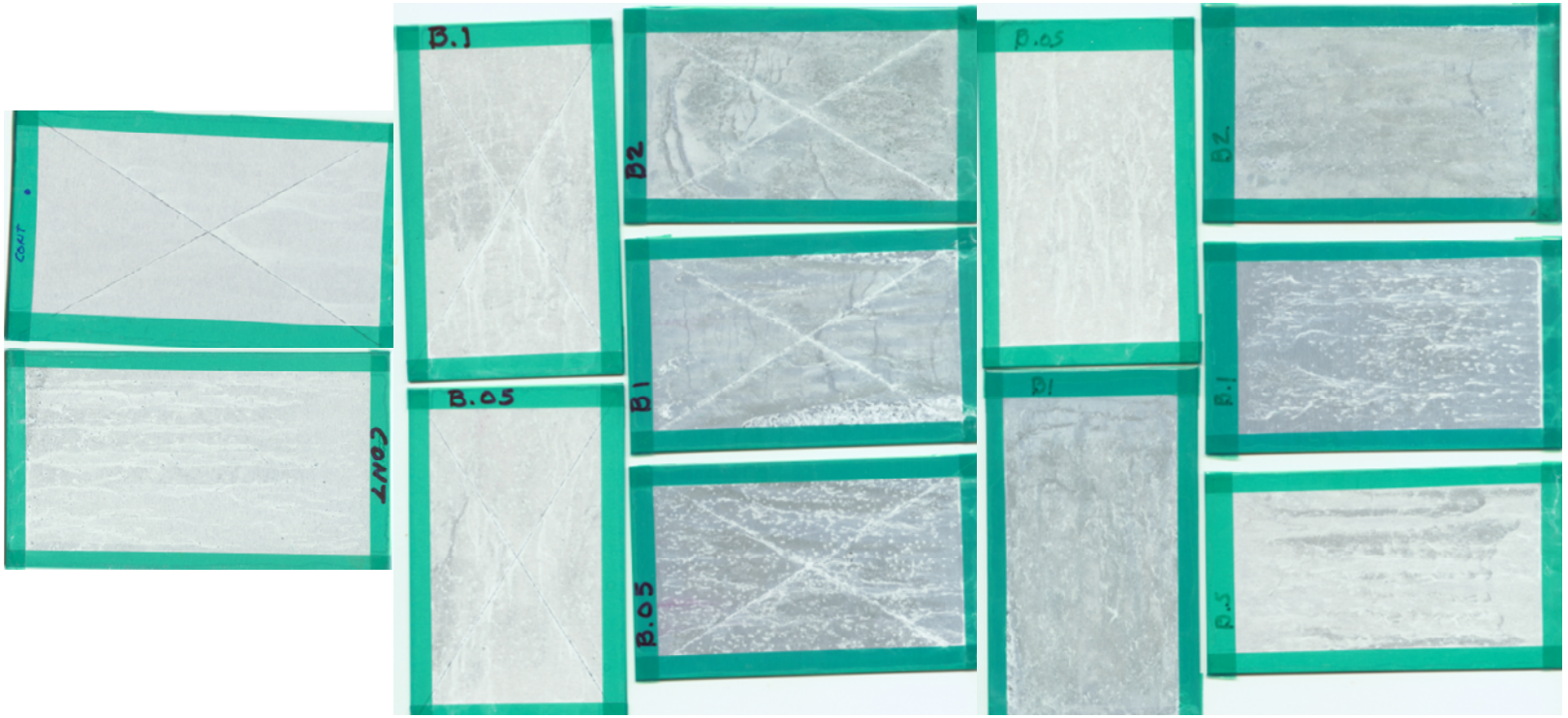

Scribed and unscribed control coupons

On left from top to bottom: 0.1 g and 0.05 g sieved chromium caproate added coupons, respectively. On right from top to bottom: 2 g, 1 g, and 0.5 g sieved chromium caproate added coupons, respectively.

On left from top to bottom: 0.05 g and 1 g sieved chromium caproate added coupons, respectively. On right from top to bottom: 2 g, 0.1 g, and 0.5 g sieved chromium caproate added coupons,

Figure 5-13 Scans of Sol-gel Coated Control Coupons, Scribed and Unscribed Chromium Butyrate Added Sol-gel Coated Coupons Immersed in Salt Fog Chamber for 2 weeks, respectively.

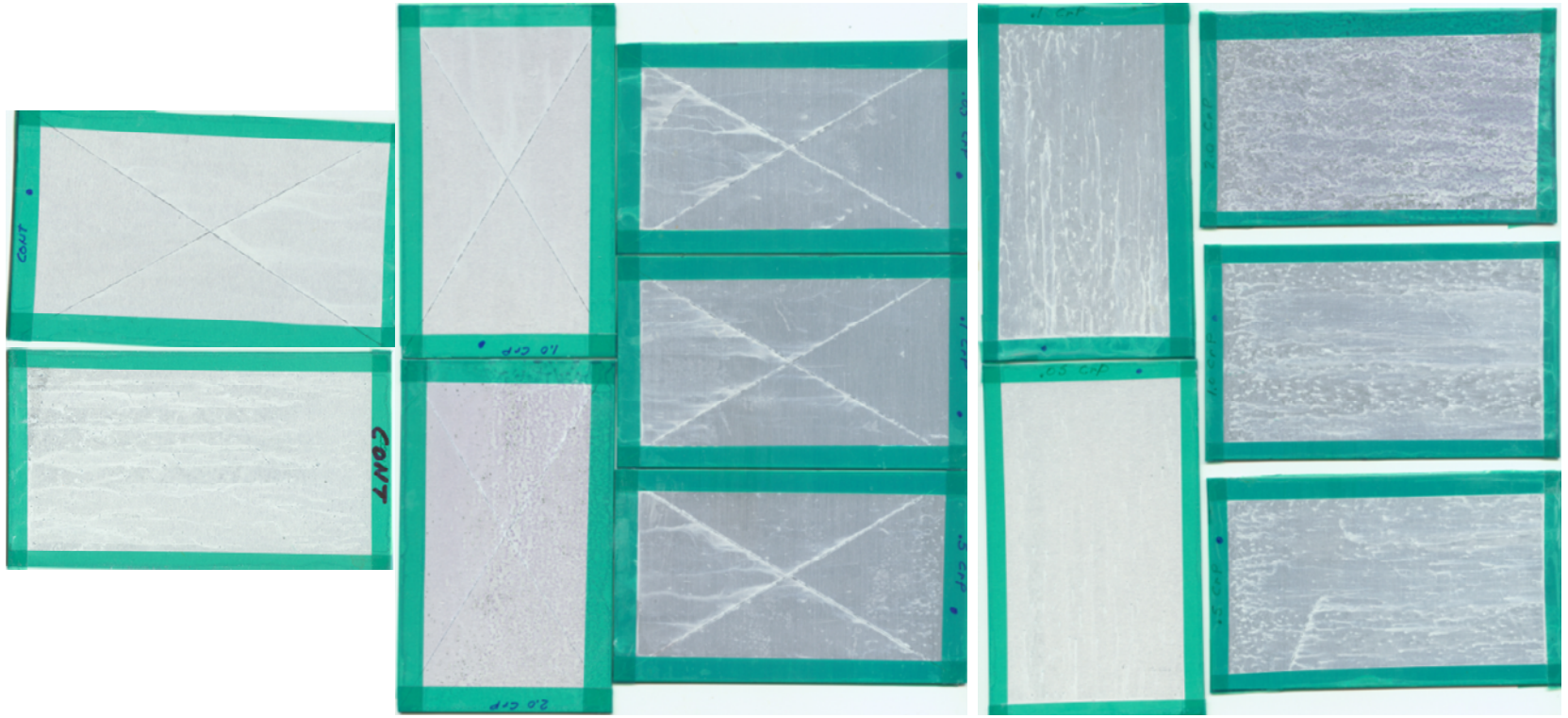

Scribed and unscribed control coupons

On left from top to bottom: 1 g and 2 g sieved chromium propionate added coupons, respectively. On right from top to bottom: 0.05 g, 0.1 g, and 0.5 g sieved chromium propionate added coupons,

On left from top to bottom: 0.1 g and 0.05 g sieved chromium propionate added coupons, respectively. On right from top to bottom: 2 g, 1 g, and 0.5 g sieved chromium propionate added coupons, respectively.

Figure 5-6 Scans of Sol-gel Coated Control Coupons, Scribed and Unscribed Chromium Propionate Added Sol-gel Coated Coupons Immersed in Salt Fog Chamber for 2 weeks, respectively.

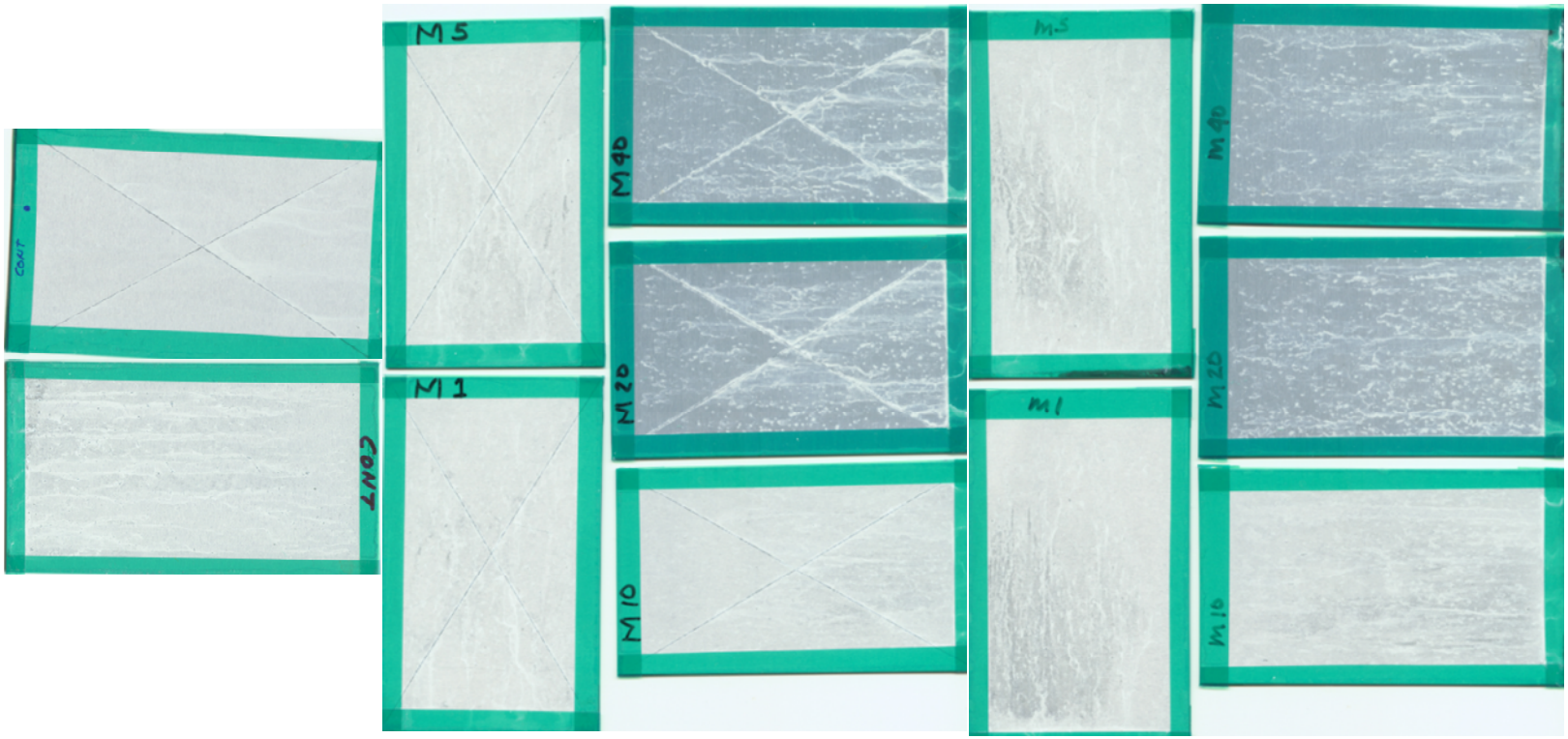

Scribed and unscribed control coupons	On left from top to bottom: 0.1 g and 0.05 g sieved chromium methoxyacetate added coupons, respectively. On right from top to bottom: 2 g, 1 g, and 0.5 g sieved chromium methoxyacetate added coupons, respectively.	On left from top to bottom: 0.1 g and 0.05 g sieved chromium methoxyacetate added coupons, respectively. On right from top to bottom: 2 g, 1 g, and 0.5 g sieved chromium methoxyacetate added coupons, respectively.

Figure 5-7 Scans of Sol-gel Coated Control Coupons, Scribed and Unscribed Chromium Methoxyacetate Added Sol-gel Coated Coupons Immersed in Salt Fog Chamber for 2 weeks, respectively.

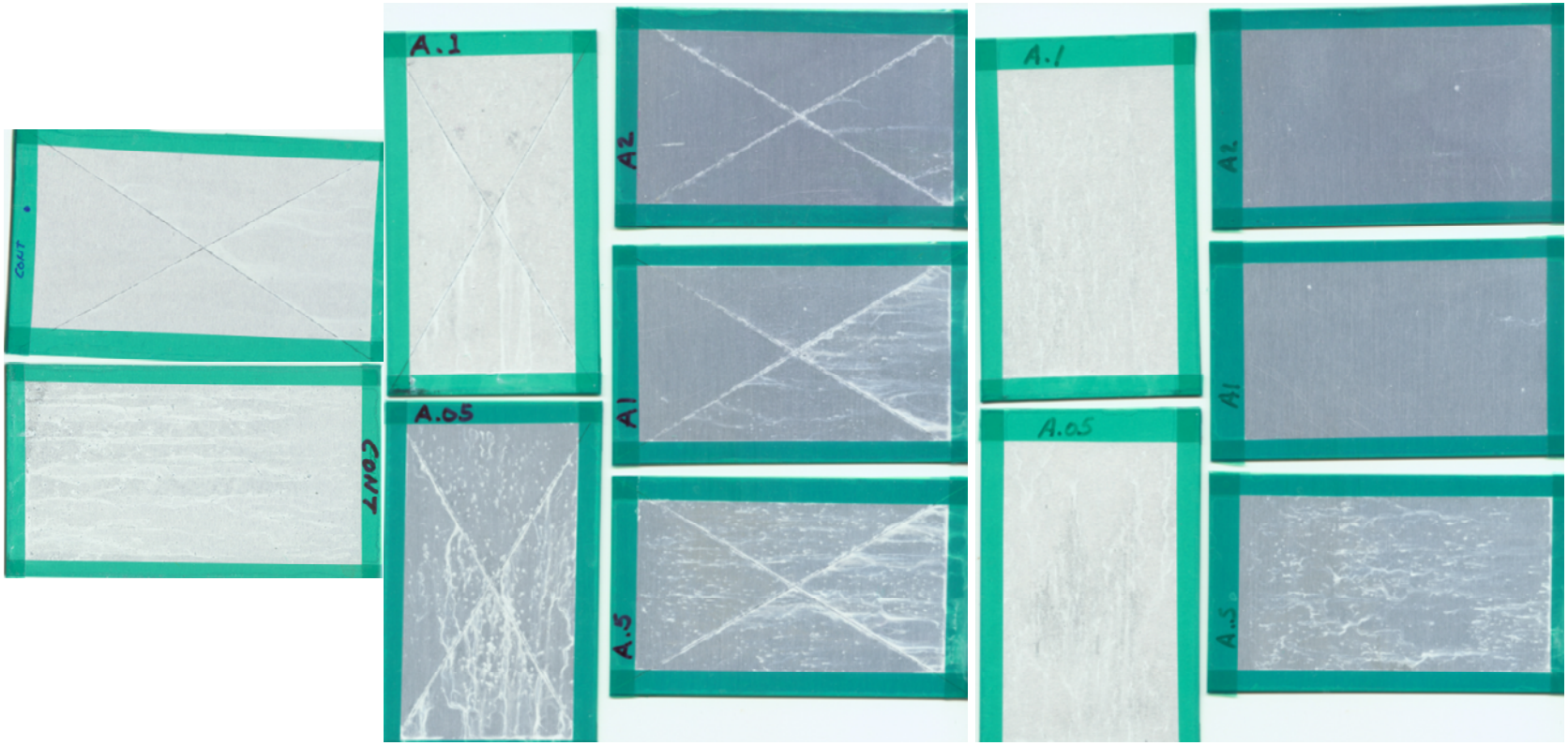

Scribed and unscribed control coupons

On left from top to bottom: 0.1 g and 0.05 g sieved chromium acetate added coupons, respectively. On right from top to bottom: 2 g, 1 g, and 0.5 g sieved chromium acetate added coupons, respectively.

On left from top to bottom: 0.1 g and 0.05 g sieved chromium acetate added coupons, respectively. On right from top to bottom: 2 g, 1 g, and 0.5 g sieved chromium acetate added coupons, respectively.

Figure 5-8 Scans of Sol-gel Coated Control Coupons, Scribed and Unscribed Chromium Acetate Added Sol-gel Coated Coupons Immersed in Salt Fog Chamber for 2 weeks, respectively.

5.6.5 Various Trivalent Chromium Compounds

Results were in general negative for tested chromium (III) compounds, among them were $Cr_2(B_4O_7)_3$, $Cr(acetate)_2OH$ and $Cr(OH)_3$ as shown in Figures 5.17, 5.18, and 5.19. $Cr(acetate)_2OH$ added sol-gel coated substrates performed worse than the controls.

Incorporation of 2.0g/50ml $Cr(OH)_3$, which was synthesized using nanoparticulate chromium hydroxide synthesis method from chromium chloride and ammonium hydroxide, to the sol-gel coating stood out particularly for the unscribed samples in contrast to negative results obtained with other concentrations as shown in Figure 5.19.

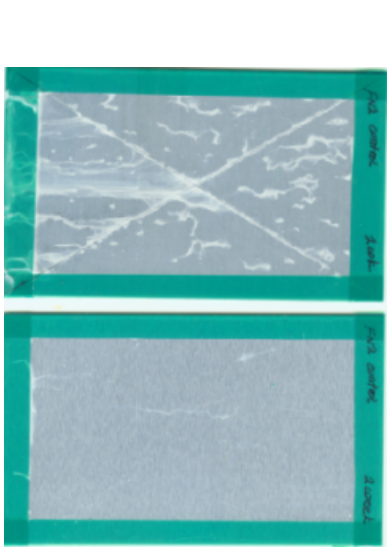

Scribed and unscribed control coupons

On left from top to bottom: 0.1 g and 0.05 g sieved chromium tetraborate added coupons, respectively. On right from top to bottom: 2 g, 1 g, and 0.5 g sieved chromium tetraborate added coupons, respectively.

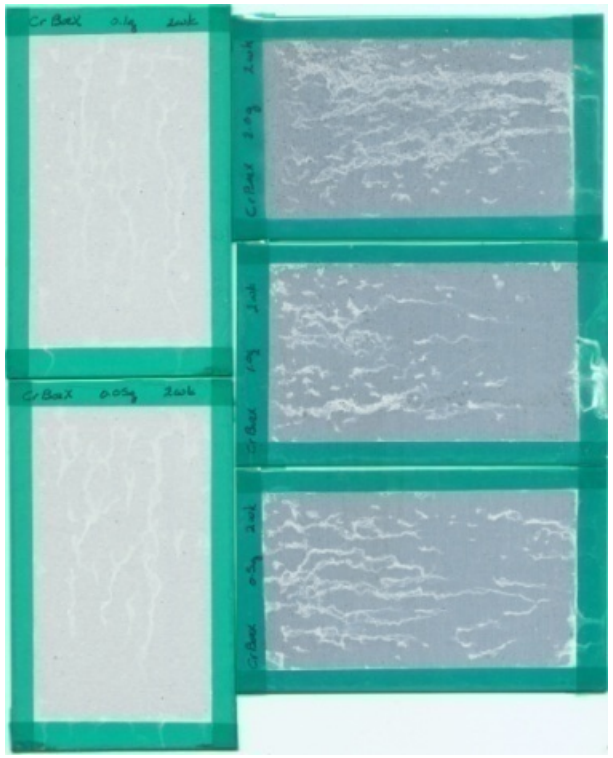

On left from top to bottom: 0.1 g and 0.05 g sieved chromium tetraborate added coupons, respectively. On right from top to bottom: 2 g, 1 g, and 0.5 g sieved chromium tetraborate added coupons, respectively.

Figure 5-17 Scans of Sol-gel Coated Control Coupons, Scribed and Unscribed Chromium Tetraborate Added Sol-gel Coated Coupons Immersed in Salt Fog Chamber for 2 weeks, respectively.

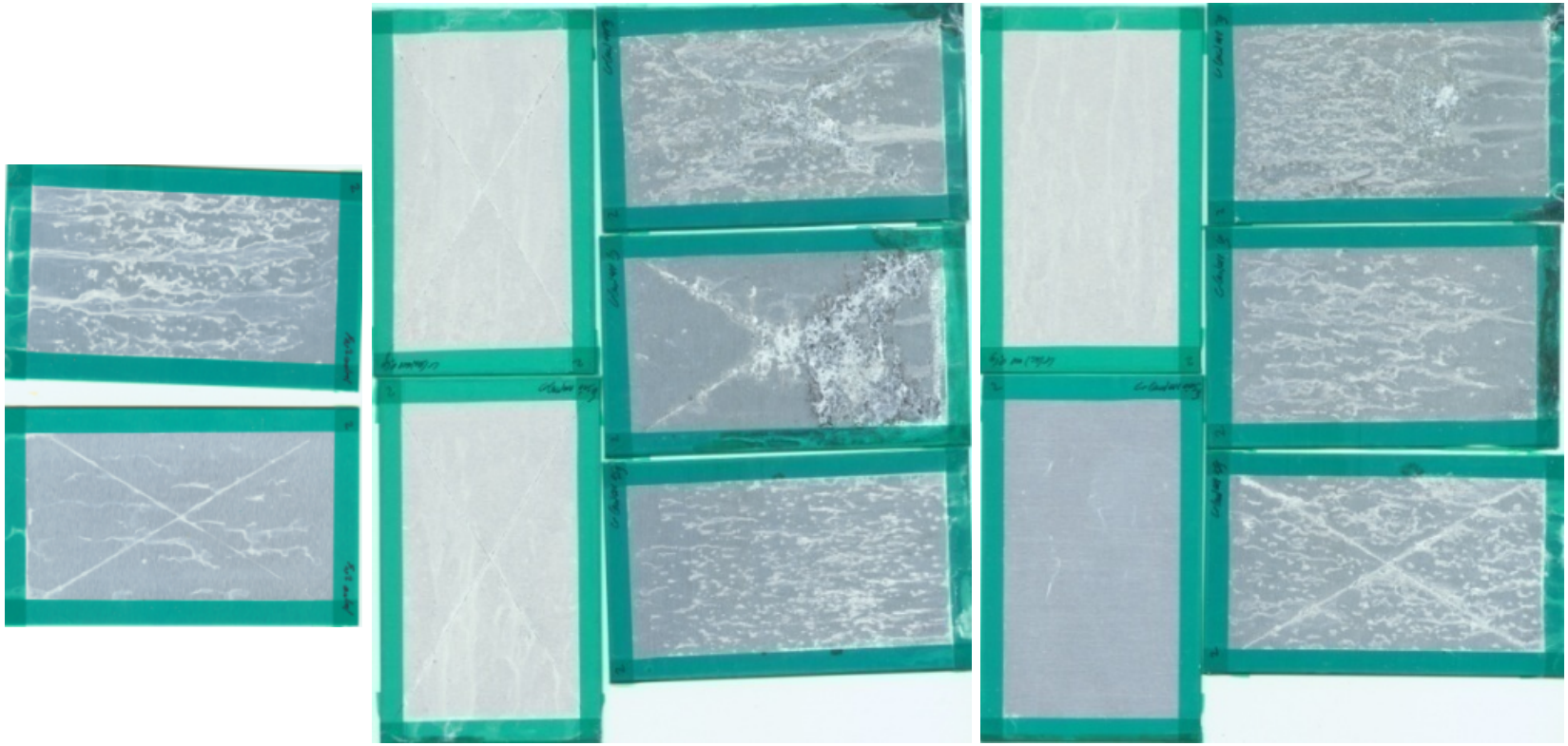

Unscribed and Scribed control coupons	On left from top to bottom: 0.1 g and 0.05 g sieved chromium acetate hydroxide added coupons, respectively. On right from top to bottom: 2 g, 1 g, and 0.5 g sieved chromium acetate hydroxide added coupons, respectively.	On left from top to bottom: 0.1 g and 0.05 g sieved chromium acetate hydroxide added coupons, respectively. On right from top to bottom: 2 g, 1 g, and 0.5 g sieved chromium acetate hydroxide added coupons, respectively.

Figure 5-18 Scans of Sol-gel Coated Control Coupons, Scribed and Unscribed Chromium Acetate Hydroxide Added Sol-gel Coated Coupons Immersed in Salt Fog Chamber for 2 weeks, respectively.

On top from left to right: 2 g chromium hydroxide added coupon and control, respectively.
At the bottom from left to right: 0.05 g, 0.1 g, 0.5 g, and 1 g chromium hydroxide added coupons, respectively.

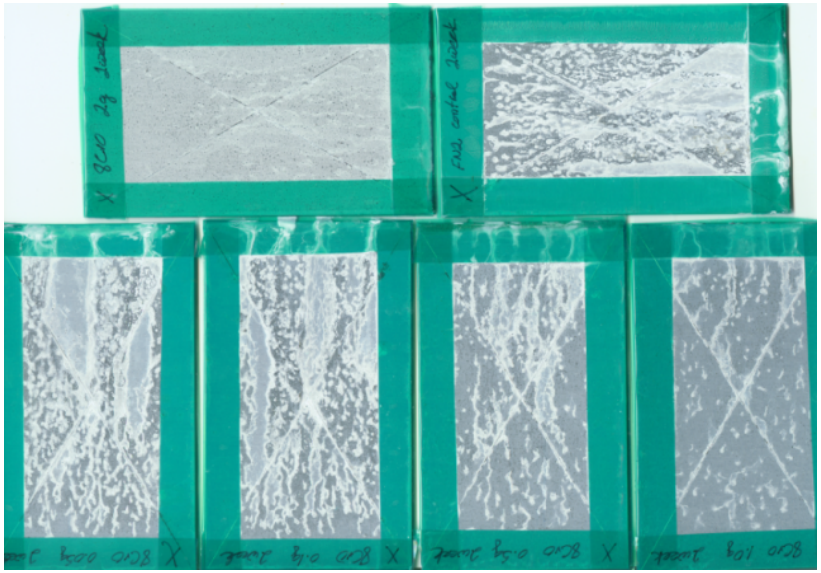

On top from left to right: 2 g chromium hydroxide added coupon and control, respectively.
At the bottom from left to right: 0.05 g, 0.1 g, 0.5 g, and 1 g chromium hydroxide added coupons, respectively.

Figure 5-19 Scans of Sol-gel Coated Control Coupons, Scribed and Unscribed Chromium Hydroxide Added Sol-gel Coated Coupons Immersed in Salt Fog Chamber for 2 weeks, respectively.

5.7 Conclusions

Several inhibitors, that were initially tested for corrosion inhibition of Aluminum 2024 alloy in aqueous solutions, revealed success when incorporated into the sol-gel coating including chromium borate, chromium oxyhydroxide and chromium octanoate. Specific concentrations of chromium acetate and chromium hydroxide also revealed positive results. With the addition of these inhibitors, corrosion resistance properties of the sol-gel coating increased not only against uniform corrosion demonstrated by the unscribed samples but also against crevice corrosion, that is filiform corrosion, and against pitting corrosion demonstrated by the scribed samples.

The most successful inhibitor pigments, chromium borate, chromium oxyhydroxide, and chromium octanoate, were primarily insoluble in water. Based on the weight-loss tests in aqueous solutions, 200 ppm solubility for an inhibitor pigment seemed to be an optimal solubility value to be incorporated in sol-gel coatings. Thus chromium propionate, then chromium butyrate and other tested chemicals, which have window of solubilities in that range, were expected to yield better results than others. Results contradicting this hypothesis indicated that the upper solubility limit for this type of sol-gel coating may not exceed even 20 ppm, since successful inhibitor pigments have less solubility than that. The least soluble chemical that is chromium octanoate yielded very good results, which suggests other factors such as successful incorporation into the sol-gel network are also very important, since there was no phase separation observed with the addition of chromium octanoate to the sol-gel. On the other hand, very aggressive environments such as salt fog chamber may have consumed all the inhibitor pigments, which have solubility values over 20 ppm due to rapid leaching.

5.8 References

1. Kasten, L. S.; Grant, J. T.; Grebasch, N.; Voevodin, N.; Arnold, F. E.; Donley, M. S.; XPS Study of Cerium Dopants in Sol-Gel Coatings for Aluminum 2024-T3, **2001**, 140, 11-15.
2. Ooij, W. J.; Child, T.; Protecting Metals with Silane Coupling Agents, *Chemtech*, **1998**, 26-35.
3. Metroke, T. L.; Kachurina, O.; Knobbe, E. T.; Electrochemical and Salt Spray Analysis of Multilayer Ormosil/Conversion Coating Systems for the Corrosion Resistance of 2024-T3 Aluminum Alloys, *Journal of Coatings Technology*, **2002**, 74, 927, 53-61.
4. Carey, F. A.; Sundberg, R. J.; *Advanced Organic Chemistry*, Plenum Press, New York, **1977**, 540.
5. Sugama, T.; Taylor, C.; Pyrolysis-Induced Polymetallosiloxane Coatings for Aluminum Substrates, *J. Mater. Sci.*, **1992**, 27, 1723.
6. Leidheiser, H.; *Corrosion Mechanism*, Chemical Industries Series 28, Marcel Dekker, New York, **1987**.
7. Smith, C. J. E.; Baldwin, K. R.; Garrett, S. A.; Gibson, M. C.; Hewins, M. A. H.; Lane, P. L.; The Development of Chromate-Free Treatments for the Protection of Aerospace Aluminum Alloys, *ATB Metallurgie*, **1997**, 37, 266.
8. Twite, R.L.; Bierwagen, G.P.; Review of Alternatives to Chromate for Corrosion Protection of Aluminum Aerospace Alloys, *Prog. Org. Coat.*, **1998**, 33, 91.

9. ASTM (American Society for Testing and Materials) Designation, G1–90, Undergone editorial change, Standard Practice for Preparing, Cleaning, and Evaluating Corrosion Test Specimens, **1999**.
10. ASTM Designation, G31-72, Undergone editorial change, Standard Practice Test for Laboratory Immersion Corrosion Testing of Metals, based upon NACE Standard TM-01-69, Test Method-Laboratory Corrosion Testing of Metals for the Process Industries, **1995**.
11. Blue Ribbon Advisory Report, Wright Laboratory, Wright Patterson Airforce Base, Dayton, OH, **1995**.
12. Nylund, A.; Chromium-Free Conversion Coatings for Aluminum Surfaces, *Aluminum Transactions*, **2000**, 2, 121.
13. Forsgren, A.; *Corrosion Control through Organic Coatings*, CRC Press, Boca Raton, FL, **2006**, 115.
14. Forsgren, A.; *Corrosion Control through Organic Coatings*, CRC Press, Boca Raton, FL, **2006**, 121.
15. ASTM B117, Standard Method of Salt Spray (Fog) Testing, ASTM, Philadelphia, PA, **1990**.
16. Forsgren, A.; *Corrosion Control through Organic Coatings*, CRC Press, Boca Raton, FL, **2006**, 134.
17. Buchheit, R. G.; Drewien, C. A.; Martinez, M. A.; Chromate-Free Corrosion Resistant Conversion Coatings for Aluminum Alloys, *Advances in Coatings Technologies for Corrosion and Wear Resistant Coatings*, The Minerals, Metals&Materials Society, **1995**, 173-182.

CHAPTER VI

CONCLUSIONS

6.1 Synthesis and Characterization

A new group of novel metallo-organic compounds were synthesized and tested for use as chromate replacements in corrosion inhibition applications of mild steel and aluminum alloys. For this reason, certain anions and cations that are well-known for their corrosion inhibiting properties were combined under one formulation with the general formula of $(M)_x(\text{hydroxyacid})_y(M'_aO_b)_z$. M denotes the metallic cationic constituent; among them zinc and calcium cations are well established cathodic inhibitors. The second component is the anion of a hydroxy acid or more specifically an α-hydroxy acid such as gluconic acid, which was also recently established as an environmentally friendly corrosion inhibitor for iron and steel. In this investigation benzilic acid was also tested extensively along with other hydroxy-acids such as tartaric, mandelic, gallic, and lactic acids and other carboxylic acids, such as octanoic acid, caproic acid, butyric acid, and propionic acid. Gluconate salts were especially effective in corrosion inhibition of mild steel, while benzilic acid yielded synergistic results particularly with metal oxyanions such as vanadates. Both trivalent chromium and zinc carboxylates revealed almost perfect corrosion inhibition efficiency results for aluminum alloys.

The third component of the formulation, that is metal oxyanions, were selected among well-established corrosion inhibitors such as molybdates, vanadates, and borates. Molybdates, for instance, are very common corrosion inhibitors for mild steel. These metal oxyanions usually inhibit corrosion by forming lower oxidation state oxides and hydroxides repairing the passive oxide film on the metal substrates. However this was not necessarily the case when combined under one formulation with other components. For instance, metal oxyanions initially formed complexes when combined with gluconate salts, which as a result limited inhibitive activity of the gluconates for mild steel corrosion. In the case of aluminum alloys however, a similar tendency to form complexes with hydroxy-acids this time increased the inhibition efficiency of the combined formula, since hydroxy-acid salts such as gluconates were observed to accelerate aluminum corrosion. Notably, while limiting hydroxy-acid salts' negative effects on aluminum corrosion inhibition, metal oxyanions also seemed to form their lower oxidation state oxides and hydroxides preventing further corrosion successfully.

In addition to synergistic formulations of hydroxy-acids and metal oxyanions; a second group of compounds have been derived from chromium gluconates and chromium gluconate borates. Chromium borate obtained via firing chromium gluconate borate, and chromium oxyhydroxide obtained from alkali-treated chromium borate were noted for their interesting physical properties such as high surface areas and nanometer particle sizes. Similar compounds to these trivalent chromium compounds have also been synthesized; among them were nanoparticulate chromium hydroxide, chromium tetraborate, and spinel type iron chromium tetraborate.

6.2 Corrosion Inhibition of Mild Steel in Aqueous Solutions

Developing environmentally friendly effective corrosion inhibitors to replace carcinogenic inhibitors based on chromates is a problem that needs to be addressed in the very near future. Iron and steel are the major components of artificial structures. Thus, increasing their lifetime by limiting the corrosion to lowest possible rates is of utmost importance. Structures in aqueous environments are very common, so effective and environmentally friendly inhibitors specifically designed for mild steel corrosion in aqueous environments are needed. Corrosion of steel is commonly faced in areas such as the oil/petroleum industry, cooling water systems, mine water systems, in soils of marine environments, etc. Gluconates have become well-established corrosion inhibitors of mild steel in the last decade. In addition to their high inhibition efficiencies, the fact that they are even used as medicine for various mineral deficiencies as health supplements is a characteristic that is not common among corrosion inhibitors, which are usually based on toxic materials such as hexavalent chromium, nitrites, phosphates, etc. In this investigation, weight-loss tests with various salts have been repeated and results supporting the literature have been observed. Secondly, synergistic formulations of gluconates along with benzilates and other carboxylates such as lactate, and acetate were put into test and as a result, borate esters of hydroxy-acids, namely, calcium and zinc gluconate borates were observed as very successful inhibitors of mild steel corrosion along with zinc and calcium gluconates. Additionally, evidence supporting conversion coating formation on mild steel substrate by aluminum gluconate hydroxide was realized through weight-loss tests, infrared spectra, X-ray photo electron spectroscopy and digital imaging. Aluminum gluconate hydroxide is one of the gluconate salts and like other

gluconate salts had high inhibition efficiency during regular immersion periods. However, substrates that were dipped into aluminum gluconate hydroxide solutions during first immersion periods were resistant against corrosion during additional immersions of similar or longer periods even when there was no aluminum gluconate hydroxide present in the solution.

Infrared spectra, scanning electron microscopy, X-ray diffraction and X-ray photoelectron spectroscopy, and digital imaging of the substrates as well as the oxidation-reduction potential, pH, and conductivity measurements of immersion solutions before and after completion of immersions revealed valuable characterization results supplementary to weight-loss test results.

In the light of these characterizations, the proposed inhibition mechanism of the synergistic formulations of hydroxy-acids and metal oxyanions was based on the repair of the protective oxide films on the metal substrate. Successful inhibitors such as gluconates and borates repaired the protective oxide film on mild steel substrates either by adsorbing onto the substrate surface and preventing aggressive anions to be adsorbed via competitive adsorption mechanism or by forming mild strength complexes with iron cations leading to an incomplete corrosion cell thus preventing further corrosion or by incorporating into the protective oxide film and repairing defective sites.

However, a mechanism favored by several authors in the literature, that is formation of insoluble iron gluconate complexes on the metal substrate did not seem to be possible at least not for a considerable period of time given the aggressive conditions of the media. On the other hand, supportive results were obtained concerning the proposed inhibition mechanisms of zinc, calcium, and magnesium via weight-loss tests.

These cations inhibit corrosion by forming insoluble hydroxides at cathodic sites. However, no evidence was obtained by X-ray powder diffraction or infrared spectroscopy for the existence of these hydroxide phases.

6.3 Corrosion Inhibition of Aluminum Alloys in Aqueous Solutions

Weight-loss tests of the inhibitors for corrosion of aluminum alloys revealed quite different results than those for mild steel. For instance hydroxy-acid salts performed poorly with the exception of zinc gluconate, which was attributed to the cathodic inhibitive activity of zinc cation. Another example was the metal oxyanion esters of hydroxy-acids; molybdate and vanadate esters of hydroxy-acids performed well but borate esters that performed well in the case of mild steel performed poorly for aluminum alloys. Trivalent chromium compounds performed very well in the case of aluminum alloys. Several inhibitors that were not initially tested for mild steel corrosion were also tested for aluminum corrosion; among them were zinc and trivalent chromium carboxylates, which all performed very well in aqueous solutions provided that the inhibitor is water soluble.

Aluminum gluconate hydroxide was not observed to form a protective coating on aluminum substrates, instead hydroxy-acid esters of molybdates and vanadates seemed to form protective coatings consisting of their lower oxidation state oxides and hydroxides. This was demonstrated by characterization studies via infrared spectra, X-ray fluorescence, and digital imaging. Vanadate esters and benzilate vanadate ester in particular seemed to perform more lasting protective coatings than others.

Based on characterization studies using infrared spectra, scanning electron microscopy, X-ray diffraction, X-ray flourescence spectroscopy, and digital imaging of the substrates as well as the oxidation-reduction potential, and pH measurements of immersion solutions before and after completion of immersions; it was concluded that hydroxy-acid salts, gluconates in particular, slightly damaged the naturally protective aluminum oxide film on the substrate surface by forming complexes with aluminum cations leading to their dissolution. This effect has been minimized when hydroxy-acid salts were complexed with metal oxyanions. Instead, these complexes reacted with aluminum surface to deposit lower oxidation state oxides and hydroxides of the metal oxyanions.

Trivalent chromium compounds performed very well, possibly via a similar mechanism inhibition mechanism of hexavalent chromium forming insoluble oxides and hydroxides of trivalent chromium, only this time there was no hexavalent chromium present in the media.

6.4 Corrosion Inhibition of Sol-gel Coated Al 2024-T3 Alloy via Inhibitor Pigment Enrichment

Inhibitors with not too high water solubilities that successfully inhibited aluminum 2024 alloy corrosion in aqueous solutions have been incorporated into sol-gel coatings on aluminum 2024 substrates. Designed specially for aluminum 2024 alloy in Dr. Allen Apblett's corrosion protective coatings research laboratory, sol-gel coatings have already proven to inhibit corrosion very well. However problems arise when there is a coating failure from which corrosive chemicals can enter and initiate extensive

corrosion since sol-gel coatings do not possess self-healing properties as chromate coatings do and hence they cannot inhibit corrosion by chemically reacting with corrosive agents. This result is very clear when scribed samples of sol-gel coated aluminum substrates are tested. From the scribes, which are artificial coating failures, corrosive chemicals initiate corrosion from underneath the sol-gel coating. Thus, incorporation of corrosion inhibitive pigments that can stop corrosion by chemically reacting with corrosive chemicals is of utmost importance. Several aspects of the pigments come into matter at this point. First, their successful incorporation to the sol-gel coating preventing blistering and coating degradation issues; second sufficient corrosion inhibitive properties either to prevent corrosive chemicals from initiating corrosion or to repassivate metal surface after initiation of corrosion, third their durability based on their solubilities and other chemical properties.

Among tested inhibitor pigments, which were selected based on their corrosion inhibition efficiency for aluminum 2024 alloy in aqueous solutions and their solubilities, chromium borate, chromium oxyhydroxide, and chromium octanoate stood out amongst others. All these three inhibitor pigments were successfully incorporated into the sol-gel coating; chromium oxyhydroxide's army green color was incorporated throughout the sol-gel coating evenly and chromium octanoate and chromium borate could be incorporated into the coating very well with no separate phases forming. The long alkyl chain seemed to cause chromium octanoate to fit in better compared to other tested chromium carboxylates with shorter alkyl chains, such as chromium butyrate and chromium propionate despite their solubility values that were thought to be optimum

initially. Secondly, all three inhibitors successfully inhibited corrosion even at scribes, where there are coating failures.

6.5 Future Work

The synthesis part of the research could be enhanced with more characterization work that would deduce the structural formulas of the synthesized products. Successful syntheses of crystalline products instead of the current amorphous ones could lead to the structural identification of these products using techniques such as X-ray diffraction.

Among other techniques used for characterization, solubility data could be enhanced using another technique in addition to colorimeter and flame atomic absorption spectroscopy.

Thirdly, inhibitors that can form conversion coatings, such as aluminum gluconate hydroxide in the case of mild steel and potassium benzilate vanadate in the case of aluminum alloys, could be deposited on the substrate using layer by layer method. If successful, physical properties of the coating could be measured in addition to the tests to measure the corrosion inhibitive properties.

Surface characterization techniques, X-ray fluorescence, X-ray photoelectron spectroscopy and scanning electron microscopy could be used more for characterization of the substrate surfaces after treating them with inhibitors.

Inhibitor pigment enriched sol-gel coatings' physical and corrosion resistive properties could be measured by means of electrochemical techniques such as electrochemical impedance spectroscopy.

VITA

Volkan Cicek

Candidate for the Degree of

Doctor of Philosophy

Thesis: NOVEL METALLO-ORGANIC CORROSION INHIBITORS FOR MILD STEEL AND ALUMINUM ALLOYS IN AQUEOUS SOLUTIONS AND SOL-GEL COATINGS

Major Field: Chemistry

Biographical:

Personal data: Born in Munchen, Germany on January 28, 1977.

Education: Received Bachelor of Science in general chemistry from Bogazici University, Istanbul, Turkey in July, 2001. Completed the requirements for the Doctor of Philosophy degree in Chemistry at Oklahoma State University in July, 2008.

Experience: Taught chemistry in high schools in Istanbul/Turkey, Kishinev/Moldova, Hong Kong/China, and in Oklahoma City, US in chronological order. Also trained special teams to chemistry Olympiad and project competitions in different schools. Employed by Oklahoma State University, Department of Chemistry as a graduate research/teaching assistant between January, 2002 and December, 2006.

Publications: Presented his work in several national, regional, and pentasectional A.C.S. conferences, and EPSCOR conferences at OSU.

Professional Memberships:

Name: Volkan Cicek Date of Degree: July, 2008

Institution: Oklahoma State University Location: Stillwater, Oklahoma

Title of Study: NOVEL METALLO-ORGANIC CORROSION INHIBITORS FOR MILD STEEL AND ALUMINUM ALLOYS IN AQUEOUS SOLUTIONS AND SOL-GEL COATINGS

Pages in the Study: 319 Candidate for the Degree of Doctor of Philosophy

Major Field: Chemistry

Scope and Method of Study: The objective of this research was to develop novel metallo-organic corrosion inhibitors for mild steel and aluminum alloys to be employed in aqueous solutions and sol-gel coatings. For this reason, inhibitors that are commonly used for corrosion inhibition of mild steel and aluminum alloys were combined under one formulation in order to result in synergism. Among chosen inhibitor constituents were α-hydroxyacids and other hydroxy-acids and their salts along with metal oxyanions. Occasionally, these inhibitor constituents had to be synthesized as well if none available commercially. Gluconates and benzilates were the most commonly used hydroxy-acid salts, while molybdates, vanadates, and borates were the most commonly used metal oxyanions. As for cationic constituents, zinc, trivalent chromium, and calcium cations were used the most. Synthesized compounds were then characterized by means of different techniques and were put into test later for their corrosion inhibition efficiencies. First, corrosion inhibition efficiencies in aqueous solutions were measured by weight-loss tests. If any indication of a conversion coating formation on the substrate surface was present, it was characterized using different surface techniques. Immersion solutions before and after completion of weight-loss tests were also characterized for the common solution properties using a variety of probes. Secondly, inhibitors with optimal water solubilities that successfully inhibited aluminum corrosion in aqueous solution were incorporated into sol-gel coating. Aluminum 2024 substrates coated with sol-gel enriched with inhibitor pigments then were tested in a salt-fog chamber in accordance with ASTM methods.

Findings and Conclusion: Novel metallo-organic corrosion inhibitors were synthesized and a considerable number of them were found to successfully inhibit mild steel and aluminum corrosion in aqueous solutions and sol-gel coatings.

ADVISER'S APROVAL: _____ **Dr. Allen Apblett**: _____